

Use of Laser Capture Microdissection to generate a translational map of gene expression patterns in the liver

Inauguraldissertation

Zur

Erlangung der Würde eines Doktors der Philosophie
vorgelegt der
Philosophisch-Naturwissenschaftlichen Fakultät
Der Universität Basel

von

Diego Calabrese

aus Italien, Napoli

Basel, 2018

Originaldokument gespeichert auf dem Dokumentenserver der Universität Basel
edoc.unibas.ch



Dieses Werk ist unter dem Vertrag "Creative Commons Namensnennung-Keine kommerzielle Nutzung-Keine Bearbeitung 2.5 Schweiz" lizenziert. Die vollständige Lizenz kann unter www.creativecommons.org/licenses/by-nc-nd/2.5/ch eingesehen werden.

Genehmigt von der Philosophisch-
Naturwissenschaftlichen Fakultät

auf Antrag von

Prof. Dr. Alex Odermatt

Dr. med. Pierre Moulin

Prof. Dr. med. Luigi Terracciano

Prof. Dr. med. Stephan Krähenbühl

Basel, 21.06.2016

Prof. Dr. J Schibler

Dekan

During my PhD training I have extensively investigated the applications of the Laser Capture Microdissection associated with the transcriptomic profiling in the context of toxicology studies.

This thesis consists of an **introduction** briefly describing the histology of liver, the pathologies affecting the organ and the drug induced injuries, focusing on the importance of having tools for the early detection of drug driven molecular alterations. It follows a deep description of the state of art in the field of the laser capture microdissection, the high-throughput methodologies for the transcriptomic profiling and their applications in the context of a toxicology study. A complete description of **methods** used and **results** obtained is then included. Finally, major findings and their implications are reviewed in the **discussion**.

The results of this study will be included in a manuscript currently under preparation.

Beside my main research project, I have also been involved in additional projects addressing several aspects of liver biology, viral and non-viral liver pathologies and liver regeneration. A list of publications resulting from these studies is included in the **appendix**.

Introduction.....	6
Liver, histopathology and toxicology.....	6
Histology	6
Pathologies	9
Drug induced liver injury (DILI)	10
Introduction	10
Patterns of injury of DILI.....	11
Mechanisms of injury in DILI.....	12
Cholestatic DILI	16
Hepatotoxicity induced by Herbal and Dietary Supplements.....	18
Toxicology study: state of the art of in vitro systems, regulations for in vivo studies and limitations of the experimental models.....	19
Toxicogenomics and transcriptomic.....	22
Aim of the project and methodological approach to resolve the tissue heterogeneity.....	22
Laser capture microdissection	25
Gene expression profile	31
Affymetrix Gene Chip platform.....	31
Data pre-processing	32
The statistical approach to the tissue deconvolution	33
Tool compound: Methapyrilene.....	34
N,N-dimethyl-N'-pyridin-2-yl-N'-(2-thienylmethyl)ethane-1,2-diamine.....	34
Background	34
Material and Methods.....	36
Animals and necropsy	36
Fixation methods for immuno-LCM	36
RNase inhibitors efficacy	38
Immunofluorescence for laser capture microdissection (immuno-LCM)	39
Laser capture microdissection	40
RNA purification and quality assessment.....	40
Total RNA amplification and Affymetrix array hybridization	41
Methapyrilene study	42
Immunohistochemistry (IHC).....	43
Isotype controls	44
Image analysis	45
Results.....	46
Effect of tissue fixation on RNA quality	46
Effect of RNase inhibitors use on RNA quality.....	47
Laser capture microdissection (LCM) and Immuno-LCM.....	49
Transcriptomic analysis	52
Pre-processing algorithms	52
Quality controls and PCA.....	54
Comparative gene expression analysis.....	56
Unbiased approach for designing structure specific gene signatures.....	56
Liver zonation	58
Gender differences and Liver zonation	62
Cross species comparison	64
Affymetrix expression flag pre-filtering.....	65
Validation of bile duct gene signatures by immunohistochemistry.....	67

Genes and protein selectively expressed in liver zone I or zone III	72
Methapyrilene study: transcriptomic analysis based on data generated by independent LCM experiment	75
Immunohistochemistry and image analysis on methapyrilene treated samples .	82
Validation of gene regulation in bile ducts	82
Discussion	86
Intellectual and practical contribution	99
Summary	100
Supplementary data	103
Supplementary table 1: Morphological Patterns of Injury Observed in DILI (mod. from [72])	104
Supplementary table 2: Main types of drug-induced vascular injury	106
Supplementary table 3: Drugs involved in cholestatic DILI	107
Supplementary table 4: Selected Herbals and Dietary Supplements Causing Hepatotoxicity	109
Bibliography	111
Gene signatures	123
Rat bile duct signature	123
Rat liver zone I signature	129
Rat liver zone III signature	131
Male rat liver zone I signature	135
Female rat liver zone I signature	136
Male rat liver zone III signature	136
Female rat liver zone III signature	138
Dog bile duct signature	138
Dog liver zone I signature	145
Dog liver zone III signature	148
Monkey bile duct signature	152
Monkey liver zone I signature	158
Monkey liver zone III signature	159
Methapyrilene induced genes	161
Bile duct genes induced in treated animals vs. untreated animals at day 3	161
Bile duct genes induced in treated animals vs. untreated animals at day 7	162
Bile duct genes induced in treated animals vs. untreated animals at day 14 ...	164
Appendix	167
Curriculum Vitae	167

Introduction

Liver, histopathology and toxicology

Histology

The liver plays very important roles in mammals, as center of many metabolic reactions, as a gland, as a blood reservoir, and takes part in the modulation of immune reactions.

From the histological point of view, the liver parenchyma has a significant complexity, even though it comprises a limited number of cell types.

Hepatocytes, which represent the majority of cells (60% by number and 80% by volume) are spatially organized in the parenchyma in rows (one or two composing the hepatocytes plate), and are surrounded by 4 types of non-parenchymal cells (35% by number and 17% by volume): endothelial cells lined along the sinusoids and forming the vascular walls; resident macrophages (also called Kupffer cells); perisinusoidal cells (also known as stellate cells or Ito cells) and large granular lymphocytes [1].

Hepatocytes are large polygonal cells. In adult rats, up to 40% of hepatocytes are tetraploid but only 20% out of them are binucleated [2]. In human the frequency of binucleated cells is approximately 10% [3]. Each nucleus has two or more nucleoli. The average life span of hepatocytes is five months. They contain abundant rough endoplasmic reticulum and mitochondria, large stores of glycogen, lipid droplets of various sizes, and several small elaborate Golgi complexes. They also contain many peroxisomes, a variable amount of smooth endoplasmic reticulum and lysosomes.

Hepatocytes are organized in trabeculae separated by a vascular space: the sinusoid. In the sinusoids, the blood flows towards the central vein which drains into the sub-hepatic veins, then further in the vena cava. At the distal end of the sinusoid, there is the portal space or triad. The “portal triad” is a key element of liver architecture: it contains the intra-hepatic bile ducts, and the terminal branch of hepatic arteries and portal veins, delimited by connective tissue. It represents the major element of discontinuity in the liver parenchyma. Vessels and bile ducts are responsible for transportation and distribution of fluids (blood and bile) through the organ.

The liver receives blood from the hepatic artery and from the portal vein, which represents about 60% of the incoming blood. The blood from the hepatic artery supplies the liver with oxygen. The blood from the portal vein has already supplied

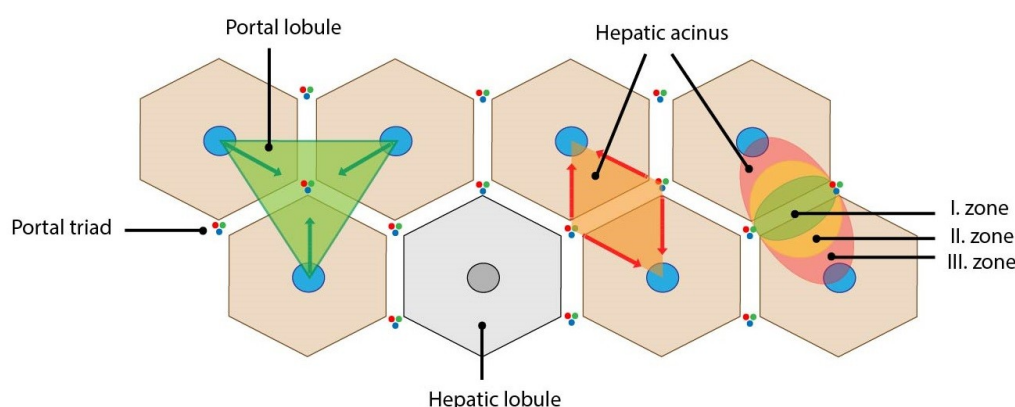
the small intestine, pancreas and spleen, and is largely deoxygenated when it reaches the liver. It contains nutrients and noxious substances absorbed in the intestine, blood cells and their breakdown products from the spleen, and endocrine secretions from the pancreas. Because blood from these two sources intermingles as it perfuse the hepatocytes, it is less saturated in O_2 compared to arterial blood found elsewhere in the body. This means that hepatocytes carry out their many activities under low oxygen conditions that most other cells could not tolerate [4]. The oxygen deficit of portal blood in the liver is compensated by an higher O_2 extraction capacity compared to other organs (e.g. intestine) [5].

Bile ducts are tubular structures arranged in a branching tree carrying the bile from the hepatocytes down to the intestine. They are covered by a monolayer of cubical or columnar epithelial tissue. The bile is produced by the hepatocytes and flows in between hepatocytes, through bile canaliculi delimited by a specialized portion of the plasma membrane of adjacent hepatocytes. At the end of this canaliculi, the bile is collected by intrahepatic bile ducts sitting in the portal spaces and; and flows towards the larger – extrahepatic – bile ducts. The bile is then drained into the gall bladder where it is concentrated. The bile function is to help the elimination of unsuitable metabolites and to solubilize fats present in food to facilitate their absorption [4].

Hepatocytes have a remarkable metabolic diversity. Many functional models for this organ have been proposed based on metabolic differences between hepatocytes spatially distributed along the periportal-pericentral axis [6] (Fig. 1). The first model was proposed by Kiernan in 1833, and was based on “Lobule” structure, which is the polygonal structure, composed of parenchymal cells surrounding the central vein. This structure is delimited by connective tissue and the corners are represented by the portal spaces, containing the terminal branches of portal vein, hepatic artery and bile duct.

A second model was proposed by Matsumoto in 1979, and was based on the “portal unit” or “sickle zone”: it differs from the previous anatomical model on that it represents a functional model based on microcirculation. In this latter case, the functional unit is composed by the polygonal structure between three central veins surrounding one portal space.

Earlier in the 1960, Rappaport described the “liver acinus”: in this structure, three different regions can be delimited on the base of their spatial distribution and of their specific metabolisms. The zone I or periportal, composed by the hepatocytes surrounding the portal space, the zone III or perivenous, composed by the hepatocytes surrounding the central vein and, ultimately, the zone II, a transition zone between the zone I and III. Rappaport’s model is, currently, the most accredited liver functional model.



<http://fbt.cz/wp-content/uploads/2013/12/jaterni-acinus-a-portalni-lalucek-ENG-01.jpg>

Schematic representation of liver functional models

Models based on microcirculation, as the latter two cases, take into account the distribution and availability of substrates and products, which can influence the enzymatic distribution and the consequent metabolic activity.

Many liver specific enzymes have been studied in the years and their activity and localization within the liver parenchyma have been described [7, 8].

The gene expression of these enzymes and their metabolic functions in the liver are strictly and precisely regulated. A key regulator of the metabolic zonation of the liver seems to be the interplay between the WNT/ β Catenin pathway and Hedgehog (Hh) signaling. The two pathways create opposite gradients and play their roles by mutual inhibition, depending on the strength of their activity gradients. Hh signaling appears to be an important regulator of lipid metabolism (lipogenesis, cholesterol synthesis, VLDL formation) in the Zone I - periportal area. Contrarily, WNT/ β Catenin appears to control ammonia production, bile acid synthesis and xenobiotic

metabolism in the Zone III - centro-lobular area [9-12]. Unfortunately, this mechanism was not totally proven and it was, in part, built on indirect evidences and speculations.

Pathologies

The liver is vulnerable to wide variety of metabolic, infectious and circulatory insults. The major causes of liver diseases are hepatitis viruses, alcohol or other drugs, and metabolic or cryptogenic causes.

Liver diseases are generally insidious and do not produce evident symptoms until cirrhosis and hepatic decompensation, which may occur long time after the onset of disease. The major causes of chronic liver injury are hepatitis C virus (HCV), alcohol, and metabolic abnormalities typically leading to non-alcoholic fatty liver disease (NAFLD).

Acute liver injury may also occur and is clinically more apparent as it can lead rapidly to liver failure. The major causes of acute liver injury are viruses (HBV and HAV, and others), and drug induced liver injury (DILI).

The cellular responses to liver injury are limited in number: hepatocytes or cholangiocytes degeneration or intracellular accumulation, apoptosis or necrosis, inflammation, and fibrosis.

Clinically, responses to many different diseases correspond two major syndromes: cirrhosis and hepatic failure.

Cirrhosis represents the end stage of chronic liver diseases irrespectively of their causes. Cirrhosis is defined histologically as diffuse fibrosis coexisting with hepatocellular 'Regenerative' nodules resulting into abnormal liver architecture. The consequences of cirrhosis are related to the increase in resistance to the blood flow caused by fibrosis, and include portal hypertension and ascites. On the long term, cirrhosis is complicated by the development on hepatocellular carcinoma (HCC).

Hepatic failure corresponds to the impossibility for the liver to fulfill its functions: production and elimination of bile, metabolism of ammonia, and synthesis of circulating proteins. The failure of these functions results into cholestasis and jaundice, encephalopathy, and coagulation abnormalities, respectively. [13]. In the next section we will focus mainly on the pathological stage resulting from the exposure to xenobiotic.

Drug induced liver injury (DILI)

Introduction

Drug-induced liver injury (DILI) is a broad term applied to any injury to the liver by a prescribed medication, over-the-counter medication, herb, or dietary supplement, manifesting as a spectrum from asymptomatic liver test elevations, to acute liver failure (ALF). DILI can lead to clinically significant acute and chronic liver disease in both children and adults. Drug-induced liver injury remains the leading cause of ALF in western countries and the most common reason for withdrawal of approved medications from the marketplace [14]. Limited data exist on the incidence of DILI in the population, and some recent epidemiologic data indicate an annual crude incidence rate of approximately 20 new cases of DILI per 100,000 inhabitants per year [15]. However, these numbers may be much higher, because of underreporting, difficulties in detection or diagnosis, and incomplete observation of persons exposed.

The lack of objective diagnostic tests, the lack of specificity of clinical presentations and idiosyncratic nature of most cases makes DILI a significant challenge for the gastroenterologist. As reported by the U.S. Drug Induced Liver Injury Network (DILIN), the initial symptoms and signs of DILI are often non-specific and include fatigue, nausea and abdominal pain. The onset of clinical symptoms can be important in determining the latency of a possible DILI episode. Liver specific symptoms as pruritus, jaundice, ascites and encephalopathy are usually reported only in patients with more severe DILI; jaundice in the setting of an acute one. Drugs and herbal dietary supplements often cause subclinical liver injury as mild serum alanine aminotransferase (ALT) elevations or slight unconjugated hyperbilirubinemia.

Getting accurate timing of medication start and stop dates, onset of symptoms, liver biochemistry abnormalities and liver recovery are of importance in order to reach a proper diagnosis of DILI. The pattern of liver biochemistry elevations at presentation is second only to a good anamnesis in diagnostic importance. The type of liver injury can be inferred by elevations of liver enzymes, and they are categorized by the *R* value ($R = [\text{ALT value} / \text{ALT upper limit of normal}] \div [\text{alkaline}$

phosphatase (AP) value /AP upper limit normal]). R values of >5 are considered as hepatocellular, <2 cholestatic and 2-5 as mixed [17]. Although many medications responsible for DILI produce stereotypical biochemical signatures, it should be noted that different biochemical patterns could be caused by the same medication. Serious DILI is usually characterized by the 'Hy's law', a combination of hepatocellular injury (AST elevation) and jaundice, and is associated with a mortality of 10% [16].

The diagnosis of DILI usually does not always require a liver biopsy, however the collection of a biopsy sample might be necessary in case of clinical situation complicated by concurrent medical conditions (e.g. autoimmune hepatitis) or multiple potential drug candidates. The liver biopsy serves multiple purposes in the evaluation of DILI, as the identification of morphological pattern of liver injury, to include or exclude DILI in the differential diagnosis, by matching reported patterns of injury, to unravel the mechanisms of injury, and to assess the degree of injury as evaluation of liver fibrosis in chronic methotrexate therapy.

The evaluation of liver biopsy in a case of suspected DILI is challenging because of several reasons, including: 1) Drug-related injury can mimic any pattern of primary liver disease, 2) an unequivocal histological diagnosis is not possible in many cases 3) inadequate clinical history and/or multiple drugs being taken simultaneously often confound the problem, 4) it can be difficult to obtain information about herbal agents, over-the-counter medications and exposure to household or industrial toxins.

Occasionally a liver biopsy may be necessary for continued use or contemplated rechallenge with medication such as a chemotherapeutic drug for advanced malignancy.

Patterns of injury of DILI

Although the pathological changes in DILI can mimic essentially every nontoxic liver disease, the patterns associated with one agent are limited, and sometimes drugs in the same class will cause similar patterns of injury. The observed injury pattern also narrows the pathological differential diagnosis. Injury patterns may be broadly categorized as hepatitic (necroinflammatory), cholestatic, steatotic, vascular and neoplastic, whereas necroinflammatory and cholestatic injuries account for around

80% of cases [18]. Major morphological patterns of injury observed in DILI are summarized in the supplementary table 1.

Mechanisms of injury in DILI

Etiologically, DILI can be roughly divided in two broad categories [19]:

Direct (intrinsic) hepatotoxic

- Dose-dependent
- Relatively rare
- Predictable

Idiosyncratic

- Dose-independent
- Relatively frequent
- Unpredictable

Injuries belonging to the latter category can be classified as host-dependent (genetic, metabolic) or host-independent (immunologic), although this distinction is somehow not precise [20], as for instance immunologic responses can have also a genetic or a metabolic basis, or metabolic mechanisms can elicit inflammatory responses.

The role of the liver in the coordination of the metabolism of the whole body cannot be underestimated. In particular, the liver is essential for xenobiotic metabolism and detoxification, is a mediator of innate immune response and it is involved in the regulation of the immune system [21]. It is therefore also morphologically, biochemically and functionally heterogeneous [22, 23]. That means that the capacity of the liver to react to drugs is different in the different zones of the parenchyma.

In general, the aim of drug metabolism is the biotransformation of a nonpolar compound in a polar one (Phase I) and subsequent conjugation with a hydrophilic component (Phase II) to facilitate the excretion [24]. These reactions take place in several subcellular compartments (smooth endoplasmic reticulum - SER, mitochondria, lysosomes, etc.). The Phase I can be achieved by [25, 26]:

1. Oxidation: loss of electrons. Generally involves cytochromes (CYP).
2. Reduction: gain of electrons. Generally involves GSH, FADH, FMNH and NAD[P]H.

3. Hydrolysis: production of two molecules or opening a ring in a molecule.
Involves different enzymes.

Phase II can be glucuronidation, sulfation, amino acid conjugation, acetylation, methylation or GSH conjugation and takes generally place in the cytosol [20, 27].

The final step of the biotransformation in the liver (so-called phase III) is the transmembrane transport to the blood or to the bile. Molecular transporters are generally found on the canalicular or sinusoidal membranes of the hepatocytes and are important for the clearance of xenobiotic. The most important transporters are the ABCC (ATP-binding cassette transporter family, subfamily C) efflux proteins and the multidrug resistance proteins (MDRs). They can be found on the sinusoidal and/or the canalicular membrane of hepatocytes [28].

During biotransformation short-lived intermediates are produced, and they may be very reactive and therefore harmful. They include [29-32]:

1. Electrophiles (the vast majority): produced by redox reactions. The compound loses electrons and is charged positively. Examples: aromatic compounds, like epoxides, quinone imines (paracetamol, diclofenac)
2. Nucleophiles (a small number): produced by redox reactions. The compound is charged negatively. Example: hydrazines (isoniazide, rifampicin)
3. Free radicals: molecule containing one or more unpaired electrons. They are formed when a compound loses or acquires an electron. Examples: metabolism of aromatic substances, quinones, etc. They can extract electrons from other substances, forming new free radicals (cisplatin)
4. Reactive Oxygen Species (ROS): Produced during the metabolism of xenobiotics and drugs, in particular when the CYP450 system is impaired. Examples: Superoxide ($O_2^{\bullet-}$), Hydroxyl (OH^{\bullet}), Peroxyl (RO_2^{\bullet}). When produced in excessive amounts, ROS are harmful because they saturate GSH, inducing then oxidative modifications of macromolecules (azathioprine, cyclosporine A).

On the other hand, drugs or their reactive metabolites can exert their effect on the hepatocyte by three different mechanisms [33-39]:

1. Direct injury to the hepatocyte impairing critical cellular functions.
 - a. Paracetamol, Diclofenac: the reactive intermediate (quinone imine) binds covalently to glutathione (GSH). The antioxidative capacity of

the liver is thus impaired, with the consequence of a diffuse oxidative damage (stress) of the cell and subsequent necrosis.

- b. Azathioprine: the free radicals saturate the GSH with mitochondrial damage and necrosis
 - c. Cisplatin: the formation of ROS induces mainly a mitochondrial damage that leads to apoptosis
2. Sensitization to cytokine-induced effect.
- a. Diclofenac, Chlorpromazine, Amiodarone: a single dose of drug can induce hepatocellular necrosis through a mechanism similar to bacterial lipopolysaccharide
3. Covalent modification of proteins (so-called haptization) with triggering of immune response similar to autoimmune reaction
- a. Halothane, dicloxacillin, nitrofurantoin, methyldopa.

In summary, when endogenous biomolecules are permanently damaged or the cell cannot react adequately to the damage induced by reactive species, subcellular structures and/or essential metabolic pathways can be affected, leading to cell death and eventually to clinical manifestations [24].

Possible mechanisms at subcellular/cellular level are:

Mitochondrial dysfunction: the enhanced membrane permeability induced by drugs can activate the intrinsic pathway of apoptosis by release of cytochromes in the cytosol. More serious damage can lead to rupture of the mitochondrion, with subsequent hepatocyte necrosis. These mechanisms are well known in the case of paracetamol, where the formation of a highly reactive intermediate, *N*-acetyl-*p*-benzoquinone imine (NAPQI) leads to saturation of GSH and subsequent accumulation of toxic compounds [40-43]. Moreover, the overwhelming redox changes induced by NAPQI may activate of the janus-kinase (JNK) pathway thus leading to proapoptotic signaling and inhibition of the respiratory chain with subsequent cell death [44].

Some drugs (e.g. valproate, alcohol, tetracycline, amiodarone, antiviral drugs) can directly or indirectly inhibit beta-oxidation of fat acids, leading to micro- or macrovesicular steatosis that can progress to steatohepatitis and cirrhosis [45-47]. Mutations and or inactivation of genes such as mitochondrial DNA polymerase gamma (POLG) or superoxide dismutase 2 (SOD2) are involved in this metabolic

effect [46, 48]. Valproate can also impair the respiratory chain leading to depletion of ATP and finally to activation of programmed cell death [49].

Activation of the liver immune system: it is clear that several instances of DILI involve immune mechanisms, including innate and adaptive processes [50]. Haptenization, i.e. covalent binding of the drug or its metabolite(s) to proteins can create neoantigens, that trigger an autoimmune-like response (halothane, diclofenac) [20, 39]. An alternative mechanism is the possibility of an immune reaction against the drug itself by direct stimulation of the T-Cell receptor (sulfomethoxazol, carbamazepine) [51, 52].

Release of apoptotic bodies or cellular fragments from necrotic hepatocytes can elicit the immune response with release of proinflammatory molecules, such as high mobility group box 1, heat shock proteins, hyaluronate, beta-defensin (so-called damage-associated molecular pattern, DAMP) [50]. Additionally, cytokines released during the inflammatory response may enhance the toxic effect of drugs. Examples are Interferon-gamma, MIF, IL-1 and TNF-alpha in paracetamol toxicity [50].

Intrahepatic cholestasis: it is characterized by impaired bile flow, with subsequent cytotoxic damage of hepatocytes and cholangiocytes. The final effect can be liver fibrosis and/or cirrhosis [53]. As recalled above, functional impairment of the membrane transporters (ABC superfamily, MDR2 and MDR3 and bile salt pump, BSEP) can lead to accumulation of bile compounds and xenobiotics in the liver, with cholestatic liver damage (ciclosporin, rifampicin, estradiol) [54, 55]. Variation in the expression of the corresponding genes may explain the different sensitivity to drugs in different individuals as well as the susceptibility to progressive liver disease [55, 56]. Another possibility is triggering of immune-mediated damage to biliary epithelium [28, 57, 58].

Vascular abnormalities: chemicals and their metabolites can damage hepatic sinusoids, portal venules, arterioles and hepatic veins. The resultant lesions produce a range of liver diseases, including non-cirrhotic portal hypertension, sinusoidal dilatation, peliosis hepatis, nodular regenerative hyperplasia, occlusion of portal veins and sinusoidal obstruction syndrome (veno-occlusive syndrome) including large vein obstruction and thrombosis, obstruction of small hepatic veins and sinusoids. In addition, vascular tumors, especially angiosarcoma, have been associated with agents as arsenic and monovinyl chloride that more often cause

non-cirrhotic portal hypertension. Individual drugs have been associated with more than one type of hepatic vascular injury. It seems likely, therefore that these disorders are inter-related and represent varying manifestations of damage to the vascular endothelium

Many vascular alterations are associated with drug intake, with distinctive morphological features.

Sinusoidal obstruction syndrome (SOS): Sinusoidal endothelial cells (SECs), may be more susceptible to toxic injury than hepatocytes themselves [59]. As for hepatocytes, the CYP450 system plays a crucial role, probably together with nitric oxide (NO) depletion, metalloproteinases (MMPs) and clotting factors [60]. Drugs associated with SOS are metabolized by the CYP450 system. Metabolites are then detoxified by GSH as in the hepatocytes. Severe depletion of GSH due to overload of metabolites leads to mitochondrial damage, apoptosis and necrosis, as described above [61, 62]. Experimentally, it has been shown that inhibition of NO synthesis and administration of MMP can exacerbate SOS [63, 64]. SOS is associated to:

1. Conditioning before bone marrow transplantation: cyclophosphamide together with busulfan and total body irradiation. In this case probably an additional effect is due to the irradiation effect on bone marrow stem cell repair of SECs [65].
2. Cytoreductive therapy of metastatic colorectal cancer: oxaliplatin may cause SOS [66].
3. Chemotherapy for AML: gemtuzumab ozogamicin (GO). SOS is described in ca. 9% of cases [67].

Peliosis hepatis: This phenomenon is related, like SOS, to an intrinsic toxicity effect of drugs against SECs, through the CYP450 system. Drugs causing peliosis are androgens, contraceptive, thiopurine-derivatives.

Major morphological patterns of vascular injury are summarized in Supplementary Table 2

Cholestatic DILI

Cholestatic damage to the liver, characterized by elevation of alkaline phosphatase (AP) levels in serum, represents the second most frequent type of DILI (30%). In general, symptoms resolve with withdrawal of the drug, but in some cases, if there

is significant loss of bile duct, damage can become chronic.

Drugs can impair bile excretion by directly or indirectly interfering with membrane transporter such as BSEP, ABC superfamily, MDRs [54, 55, 68]. Interestingly, also nuclear receptors such as FXR, RXR, LXR, are involved in the regulation of bile acid homeostasis. Therefore drugs or metabolites that act on such receptors (rifampicin, dexamethasone phenobarbital), can influence cholestasis [68-70]. Another mechanism is the obstruction to bile flow after secretion, following damage to cholangiocytes/bile ducts [68, 71].

Histology of cholestatic DILI

In summary, cholestatic damage to the liver can be classified as follows [68]:

1. Acute Drug-Induced Cholestasis without Hepatitis (bland cholestasis).
2. Acute Drug-Induced Cholestasis with Hepatitis (Cholestatic Hepatitis).
Canalicular and hepatocellular cholestasis with lobular and portal inflammation and hepatocellular necrosis.
3. Chronic Drug-Induced Cholangiopathies. A variable pattern, from mild duct injury to vanishing bile duct syndrome and/or sclerosing cholangitis.

Acute drug-induced cholestasis without hepatitis (bland cholestasis).

Bile plugs are seen in hepatocytes and/or canaliculi, without inflammation, prevalently in zone 3 of the hepatic lobule. This is the typical reaction to anabolic steroids or contraceptives. Other possible causes are prochlorperazine, thiabendazole and warfarin [72, 73]. The differential diagnosis is essentially with sepsis, shock, cardiac failure, acute large duct obstruction and benign recurrent intrahepatic cholestasis (BRIC) [72].

Acute Drug-Induced Cholestasis with Hepatitis (Cholestatic Hepatitis).

Characterized by neutrophilic and eosinophilic inflammation, canalicular and liver cell cholestasis and/or cholestasis. Many antibiotics can be associated with such damage: erythromycin, tetracyclines, ciprofloxacin, cephalosporines. Other drugs associated with cholestatic hepatitis are chlorpromazine, risperidone, amitriptyline, azathioprine [71, 73, 74]. The differential diagnosis is with acute viral hepatitis, autoimmune hepatitis, and acute large duct obstruction. In general, it can be said that localization of the damage in zone 3 of the hepatic lobule is more likely to be due to drug injury [73-75].

Chronic drug-induced Cholangiopathies.

Chronic drug-induced cholestasis is defined as a cholestasis lasting more than three months [73]. The cholestasis induces a necroinflammatory portal and lobular necrosis, leading to duct sclerosis and loss, periportal cholestasis, portal fibrosis, and copper accumulation in periportal hepatocytes (orcein or rodhamin staining). Hepatocytes often show a clear aspect, due to accumulation of bile salts. Bile duct hyperplasia ('neoductulation') may also be observed. If the damage is very severe, it can progress to liver fibrosis and, very rarely, to cirrhosis. The continuous inflammation eventually leads to vanishing bile duct syndrome (VBDS, > 50% of portal fields lacking bile ducts). Drugs involved in chronic cholestasis are the association amoxicillin-clavulanic acid, flucloxacillin, terbinafine (an antifungine) amiodarone. VBDS can be associated with carbamazepine and zonisamide, antipsychotics such as chlorpromazine and sulpiride, NSAIDs such as ibuprofen and tenoxicam, and antibiotics such as amoxicillin, flucloxacillin, clindamycin and trimethoprim-sulfamethoxazole [71, 73, 74]. The differential diagnosis is with PBC or obstructive biliary diseases rely also on clinical and imaging data (AMA determination, biliary tree imaging).

Major morphological patterns of cholestatic DILI are summarized in supplementary table 3

Prognosis.

As mentioned above, most cholestatic DILIs resolve after withdrawal of the causative drug. However, in recent series, cases with severe/chronic cholestatic injuries are associated with a mortality rate from 5% to 14% [74, 76, 77]. A chronic evolution, defined as above, was observed in roughly 5% of cases, whereas the development of cirrhosis is very rare [78].

Hepatotoxicity induced by Herbal and Dietary Supplements

Herbal and dietary supplements (HDS) are emerging as a major cause of DILI worldwide.

The incidence of DILI from HDS varies by geography and patterns HDS use. It accounts for approximately 9% of the cases of DILI in United States and up to 19% to 63% of the cases of DILI in Asian Countries [79-81]. These numbers however are probably underestimated because the widespread availability of HDS and the low frequency, with which patients report their use, means that the true frequency of

attributable hepatotoxicity is unknown. The clinical as well as the morphological presentation of HDS-associated hepatotoxicity is similar to that of DILI. The general patterns of presentation are either predominantly hepatocellular or predominantly cholestatic. However, vascular lesions are also rather frequently observed.

Major herbals and dietary supplements causing hepatotoxicity are summarized in supplementary table 4

Toxicology study: state of the art of in vitro systems, regulations for in vivo studies and limitations of the experimental models

Toxicology studies are performed in order to predict adverse reaction in response to a specific compound.

These studies can be performed in vitro or in vivo, although the current regulation imposes the safety assessment in animal, to support the first clinical trial in human, and registration of new medicines.

In vitro studies are performed on live material out of its biological context. In fundamental research, cell culture is one of the most common and widely used experimental approaches. It allows the reduction of the biological complexity (organism/organ/tissue/cells) in order to better understand basic mechanisms.

The need of an unlimited source of biological material, led to the established of many organ-specific cell lines. These cell lines derived from neoplastic tissues through a clonal expansion, resulting in a monoclonal cell lineage with specific genotypic and phenotypic features. Unfortunately being derived from neoplastic material, the cell lines also carry many specific aberrations (e.g. in the liver cell lines, alteration in the innate immunity attitudes [82], lack of gene/proteins expression [83], several biologically relevant SNPs, lack of the metabolic genes' expression). Despite the large use of cell lines in the basic research, the translatability of many findings and, consequently, their usefulness for toxicology assessment, are limited.

Primary human hepatocytes (PHH) are still the state of art in the study of phenomena related with liver toxicity in vitro. In optimized conditions those cells preserve the liver metabolic enzymes (CYPs) and most of the liver specific functions. Unfortunately, PHH availability is limited from the liver explants and organ donation shortage. The cells have a high batch-to-batch variability and even if

cultured in optimized conditions, they tend to de-differentiate towards a mesenchymal phenotype within few days/weeks, losing liver specific functions. Specific culturing system, such as co-culture with non-parenchymal cells[84], use of specific substrates and specific media, 3D printing/culturing, microfluidic perfusion systems [84] and bioreactor-assisted culturing [85], helped in preserving the liver specific phenotype, but the improvements are limited and these modifications increased the handling costs of several folds.

Given the limitations of in vitro models, one can understand the need of a more reliable system for drug safety assessment. Thus, experiments performed on animal models are, not only a legal requirement for the submission of new drugs, but they are also justified scientifically.

The Declaration of Helsinki imposes the need for a preclinical safety testing before the introduction of new drugs into human beings. Regulatory approval is required prior to the first clinical trial and this is contingent on the assessment of potential risks through preclinical safety studies. Currently, these studies must be performed on animal models in order to identify the safe dose for human, and the potential target organs of toxicity. This has a huge economic and emotional impact on society, raising also significant ethical questions.

A toxicological study should be designed to obtain the following information, with the minimal use of model animals: target organ(s) of toxicity, relationship between dose/exposure (Pharmacokinetics-PK) and response (Pharmacodynamics-PD), potential reversibility of any adverse effect, relevance to human and potential parameters for identification and monitoring of adverse event in clinical studies.

Another crucial parameter to be determined in toxicological studies is the relationship between dose, exposure and effectiveness. The legislation requires that a drug must be safe after repeated dosing to a specific exposure [86]. This needs the assessment, during the animal studies, of a maximum exposure dosage and minimum exposure dosage.

The maximum exposure determines toxicity and target organ damage. The induction and the identification of tissue damage are, therefore, critical, although it should be minimized to reduce the animal suffering.

The minimum exposure, vice versa, represents the condition that causes no tangible effect and no toxicity.

Regulatory authorities suggest designing toxicological studies including repeated exposure at high, medium and low dosages.

The highest dose at which no overt toxicity occurs in a 90-day study (the *maximum tolerated dose*), is generally used to establish animal dosing levels for chronic assays that provide insight into potential latent effects [86].

Reversibility of damage can be assessed by introducing recovering time, aimed at providing to the animals the time to excrete the toxins and recover from adverse event.

Relevance for human safety is, indeed, one of goals of the toxicological studies and it is the most difficult result to achieve. This implies a deep knowledge of the species specificities, leading to the selection of the correct animal model.

Toxicology tests are fairly standardized and outlined in the ICH guidance documents (S1-5, S7-8). In general, two animal species are used to maximize the chance of detecting toxicity, a rodent and non-rodent species [87].

It is currently well known that animal models differ from human for the genes and the proteins involved in drug metabolism, and ultimately in the production of catabolites. Rodents have a peculiar hepatic xenobiotic metabolism regulation, operated through the Growth Hormone (GH), which generates strong sexual dimorphism and differences in the circadian cycle. Contrarily, other animal models are less affected by this dimorphism.

Considerations for species selection also include: pharmacokinetics, metabolites, activity/affinity of the molecule at the target and at related targets, and non-sensitive vs too-sensitive species [87].

Nowadays many databases reporting the species-specificities toxicity of some compound have been published online and represent a useful source of information for researcher and regulatory authorities [88].

However, for new compounds the identification of the most appropriate species for toxicological studies is still crucial. Economical and ethical reasons do not allow to run systematically those studies on non-human primates (NHP), closer to human, however, a deep knowledge of species (and tissue) specificities might drastically reduce, in the future, the risk of drug induced adverse events, and drastically reduce the use of irrelevant animal models, thus reducing the economic impact of the safety assessment for new drugs.

In common practice, animal studies start with rodents, but genetic and metabolic differences with human, or susceptibility to specific pathologies, may reduce drastically the relevance of those experiments. The dog is generally the non-rodent species of choice.

Toxins do not target in same way all the tissues/organs in the body. The target organ is determined by the capacity of the tissue to absorb the xenobiotic itself or, produce or absorb metabolites thereof. The route of administration also determines the target organ. Oral administration is adsorbed by the intestine and reaches the liver through the portal vein, where most of drugs are metabolized. Drug administered intravenously reaches rapidly the heart and the lung.

Liver is the organ exposed to the highest risk of drug toxicity. However, due to the differential metabolic functions and capacity to break down drugs and metabolites between the hepatocytes spatially distributed along the periportal-pericentral area, the concept of target organ should be further extended to a cell specific resolution in this organ.

Toxicogenomics and transcriptomic

Toxicology aims at understanding the effects of acute, prolonged or repeated exposure to a compound. It makes use of all the basic research tools for understanding when, where and how a compound may injury a tissue.

Transcriptomics is the study of gene transcripts (mRNA), made by different technologies (i.e. oligonucleotide chips or RNAseq).

Toxicogenomics is transcriptomics applied to toxicology.

The basic assumption is that the transcriptome reflects the metabolic state of a cell and the changes from a baseline can be used for the study of the drug-induced alterations.

The obvious advantage is to be able to observe changes in wide spectrum and not only in pathways conceivably involved in the metabolism of a compound. This allows the identification of previously unknown mechanisms of toxicity.

Aim of the project and methodological approach to resolve the tissue heterogeneity.

Several factors, related to the individual genetic background and the intrinsic characteristics of the organs involved in drug metabolism, contribute to the toxicity

of compounds. This makes the prediction of adverse events induced by drugs in the patients (the ultimate goal of toxicology), a challenging task.

The technological advances have improved predictive capabilities by providing more sensitive methodologies, able to perceive minor molecular changes in the target organ.

However, more efforts are required in order to achieve the ambitious goal of early prediction of drug induced adverse event. For these, two points are crucial:

- Sensitivity: methods must be capable of identifying phenomena that occur at the single cell level.
- Reference data for qualification: reference values must be in order to provide the necessary basis for interpretation of subsequent experiments (e.g. baseline, or typical changes).

Nowadays, the technologies are so sensitive that in most of cases they have a resolving power sufficient to detect small phenomena. However, the most sensitive technique still requires some criteria for the discrimination between relevant variations, though minor, and random variations (noise). This is particularly problematic in the field of the transcriptomic analysis, for genes with low expression values [89]. The new -omics technologies are in general very sensitive to minor phenomena, but the interpretation and the discrimination of (non)relevant noise, is sometimes the major issue limiting the understanding of such phenomena. This limitation is amplified when transcriptomics are applied to the study of heterogeneous tissues, where all the cells concur to the transcriptomic profile. Variation of gene expression values between experimental conditions are proportional, not only to the magnitude of a molecular phenomenon in cells (up- or down-regulation), but also, and in big extent, to the change of this cell population in the whole tissue. In other words, the transcriptomic profile of a single cell population is averaged by those of the other cells composing the tissue, and a gene highly expressed in a small subset of cells can have a low expression value when estimated from the expression profile of the entire tissue.

In this respect, it is often difficult to deconvolve whole tissue transcriptomic data and identify changes in a rare cell population with optimal specificity and sensitivity, mostly because the apparent expression value of specific genes is difficult to distinguish from the background noise. To help overcome this issue, a

detailed transcriptomic profile of the cell types that compose the tissue in a homeostatic state could be useful, but is in most of cases missing.

The untreated controls included in all the studies, while providing global information on the tissue in analysis, fail to provide information at single cell resolution, because of their own heterogeneous composition. Moreover, traditional analysis of large sets of gene expression data make extensive use of statistical filtering in order to reduce the likelihood of false discovery. In this scenario, minor events, as well as big events occurring at a minor cell population, are systematically underestimated due to the precedence given to statistical significance.

As previously discussed, the liver is one of the organs mainly affected by the drug induced injury. The understanding of the molecular mechanisms leading to the injury in this organ is challenging due to its histological and functional complexity.

For this reason, we undertook the creation of a transcriptomic map of the major histological components of the normal liver from the species usually used for preclinical safety assessment of drug candidates.

We decided to approach the creation of this detailed gene expression map by a technique, the Laser Capture Microdissection (LCM), able to isolate cell populations from heterogeneous tissues, based on a morphological anchor. Specifically, we aim at profiling the functional areas of the liver parenchyma (liver zone I and zone III), the bile ducts and the blood vessels, all potential target organs for several compounds.

We have chosen to combine the LCM and the immuno-LCM, the laser capture microdissection guided by immunolabeling of target cells, with the oligonucleotide technology for profiling the transcriptome of those tissues.

The resulting data will serve as a comparative tool in prospective and retrospective studies in drug safety investigations.

Here we will also use this data, as tool for the early detection of the morphological and molecular changes occurring in rats, upon the administration of a reference compound: Methapyrilene. We explored how minimal molecular changes, which would have not been taken into account using traditional filtering because of their limited statistical value in the pool of a transcriptomic analysis, might indeed be indicative of morphological changes in the liver, which would have been diagnosed only at a later time-point by a standard approach.

Laser capture microdissection

Many groups attempted, over the years, to profile the liver gene expression: in preclinical studies, where transcriptomics has become a fundamental tool for screening early toxicity [90-95], and in clinical study for identification of mechanisms in liver diseases [96-99]. In most of cases, the studies relied on usual statistical filtering of expression data generated from whole liver tissue or small tissue biopsies, underestimating the importance of the tissue heterogeneity and its impact on the gene expression profiling.

Beside specific methods based on tissue digestion and cell sorting (e.g. the fluorescence-activated cell sorting or the immuno-magnetic separation), the possibility to analyze the gene expression in situ, in ex-vivo liver tissues, is limited to few options. While in situ PCR based methods (i.e. target amplification) are very sensitive, they are targeting a single transcript per assay and are prone to false positive signals due to contamination and/or insufficient primer specificity [100].

Modern multiplex in situ hybridization systems allows the localization in situ of only some transcripts.

Both these approaches are not any close to the power of transcriptome-wide profiling to help generate hypotheses.

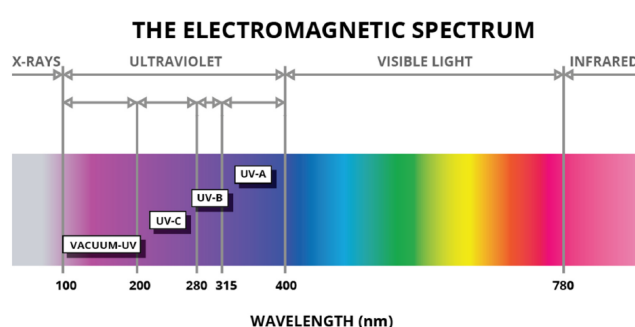
Laser capture microdissection (LCM) is a technique to isolate microscopic samples, using pulsed lasers technology, which makes possible dissection and collection of small portion of tissue, under the direct operator control, from frozen or formalin fixed paraffin embedded (FFPE) tissue sections. The technique, introduced in 1976 [101], has had extensive development and improvement by the late years 90s onwards to date, and can be considered a well-established methodology, commonly used in the molecular pathology field [102-105].

In general, a laser capture microdissector consists of a microscope (working with transmitted and reflected light), a computer controlled stage, a laser unit, and a tissue collector. Current technology allows isolating samples as small as single cell, or even smaller sub-cellular structures (e.g. metaphasic chromosomes) [106]. LCM derived samples can be used for protein [107] and nucleic acid purification [108, 109], and also for single live cell collection [110-112].

Currently, two technologies are available, which differ for the method of tissue collection and for the physical features of the laser used to cut and collect the tissues.

All the equipment so far available makes use of UV-A (349 nm) laser, and, in one case, of an additional infrared (IR) laser.

The UV light is the only one fulfilling the requirement of a sufficient energy for vaporizing and cutting the tissues. However, the energy transferred to tissue during the laser capture microdissection may easily lead to the degradation of the nucleic acid, due to the transformation of the energy in heat.



<http://marktechopto.com/img/uv-color-spectrum.png>

There is an inverse relationship between the wave length and the energy of light. Therefore, within the UV spectrum, the UV-A, located at the top of the wave length range, is the one, among the UV classes, with the lowest energy, and represents the best compromise between the need of energy for cutting and the preservation of biological molecules.

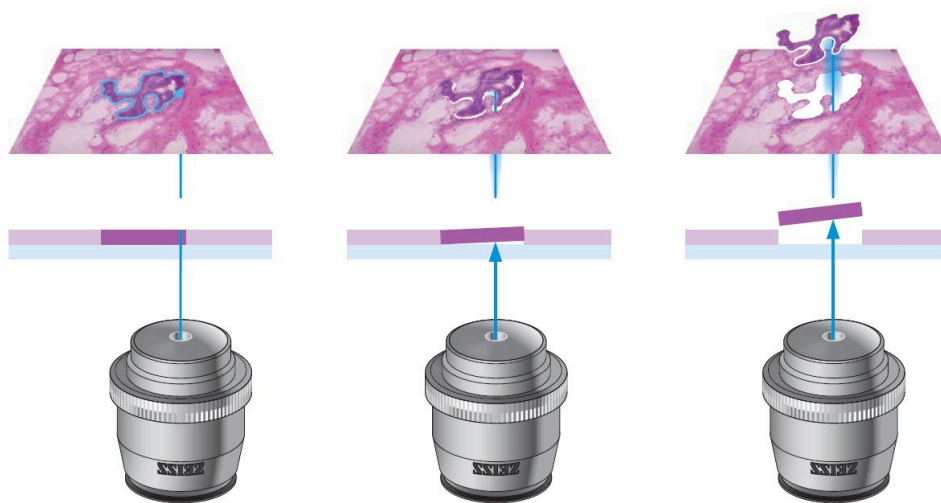
Differently, the use of the IR laser does not impact the organic molecules, due to its high frequency and low energy.

Beyond the physical properties of laser beams, additional precautions are necessary for avoiding the excessive irradiation of the tissues during the laser capturing. For instance, pulse-width modulation (PWM) is mechanism commonly used in LCM applications to modulated the laser energy.

The use of different lasers influences the precision of the systems: the UV-A (only) based systems resulted generally more precise than the one using a combination of UV-A and IR. This is due to intrinsic characteristic of the light frequency and also to the collection method associated with the different lasers. That is, if the UV-A based systems are able to reach a minimal laser spot diameter as small as 0.5 μ m, and they

have an estimated precision of $1\mu\text{m}$ [113], the system using a combination of UV-A and IR laser can reach only a precision of $7.5\mu\text{m}$ (spot diameter) [114].

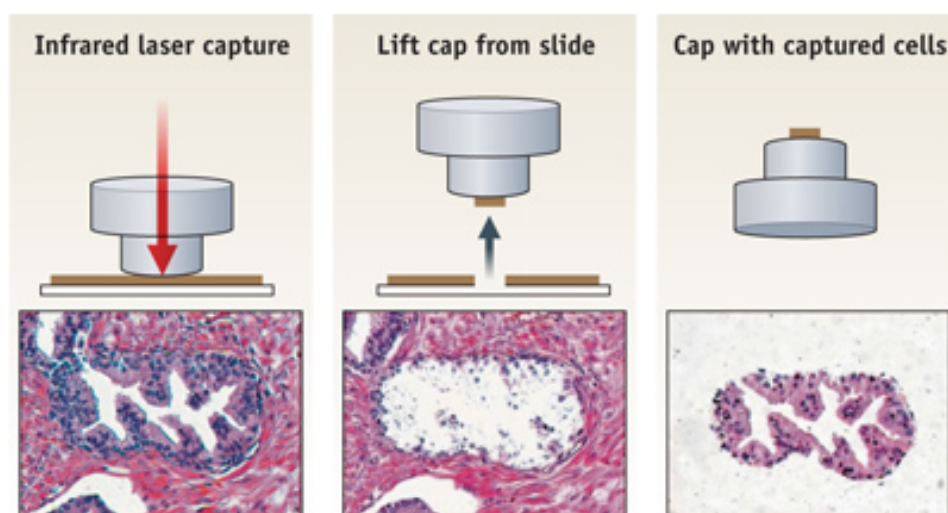
The collection of dissected tissue samples is operated in different ways. The systems based on UV-A use two different approaches: the laser pressure catapult (LPC) in which, after the cutting phase, the laser is refocused at a lower plane than that of the tissue. A single laser shot is then used for generating pressure wave, able to catapult the cut tissue up in the tissue collector. This system is effective, but it is affected by the size and the weight of the microdissected area (representative picture below).



https://lookfordiagnosis.com/mesh_info.php?term=laser%20capture%20microdissection&lang=1

The second approach to the tissue collection is a gravity assisted system, in which the tissue collector has been moved below the tissue and the dissected area is catapulted down with the help of the gravity force.

The last approach to the tissue collection is typical of the hybrid systems (UV-A/IR). It makes use of a plastic device covered by a plastic microfilm. The IR light is then used to melt and fuse together the microdissected area and the plastic device. As this system is the less affected by the size of the microdissected tissue are, it is intuitively the best one for applications that are aiming at large lesions and do not require very high topographical precision (representative picture below).



https://lookfordiagnosis.com/mesh_info.php?term=laser%20capture%20microdissection&lang=1

In terms of sample purity, the first approach allows better results, since there is no physical interaction with the tissue, which is, instead, necessary by using the plastic devices for the collection.

In this project we had the possibility to use two different systems, taking advantage from their collecting system, in order to achieve the best results with samples differing by sizes.

The combination of laser microdissection techniques with those of oligonucleotide array technology has revolutionized the molecular analysis of heterogeneous tissues. Nevertheless, many drawbacks have limited the use of LCM to specific fields.

As general observation, the generation of the transcriptomic profile and the analysis of LCM derived samples is time consuming and extremely expensive.

The LCM involves complex and lengthy procedures that may negatively affect the RNA integrity.

The choice of the right starting material is crucial for the final results. Despite the plethora of protocols for extracting RNA from FFPE tissues [108, 109, 115, 116], the resulting RNA quality is generally poor, due to degradation by endogenous ribonucleases (RNAses), or cross-links between nucleic acids and proteins, which results in a massive RNA fragmentation and a lower yield of the purification procedure.

Tissue collection, embedding and freezing, sectioning, fixation, staining, and microdissection are the common preparation phases of LCM samples: each of them may hide potential risks for the RNA integrity.

The tissue should be quickly resected, embedded and kept at low temperature until the sectioning and fixation.

The fixatives can be divided into two major categories: the precipitating fixatives (alcohol) and the cross linking fixatives (aldehydes).

Several authors have investigated the capacity of different fixatives to preserve nucleic acids, concluding that the precipitating fixatives were more effective to preserve RNA than the cross linking ones [117, 118].

The aldehydes form covalent crosslinks between nucleic acids and proteins, and their penetration in the tissues is slower than alcoholic fixatives. Both factors contribute to the poor yield and quality of the RNA purified out of FFPE samples.

The denaturation operated by the alcohol is based on removal of water from specimen and is far less effective as fixation method compare to cross-linking. The RNases can return to their native conformation and activity during sample processing, where water or water-based buffers are necessary. Therefore, the use of alcohol fixatives imposes a fast processing in order to limit the re-activation of endogenous RNases.

The isolation of specific tissue structures from the surrounding using LCM is possible from unstained sections or from sections stained by chemical dyes (e.g. hematoxylin-eosin, cresyl violet, etc) [113, 119, 120]. Such staining is fast, and therefore does not strongly affect the RNA quality. However, they are often inadequate for the isolation of specific structures or single cells, due to the low specificity of the stains.

The use of specific immuno-staining is strongly recommended in order to selectively highlight structures of interest and, thus, limit the possible cross contamination from surrounding cells or tissues [121-127].

The introduction of immunohistochemical technique in the LCM workflow, however, greatly complicates the entire procedure, because it generally requires a longer processing time than the chemical dye.

Tissue exposure to water-based solution is detrimental for the RNA quality because chemical RNA hydrolysis may occur in certain conditions, and, most importantly, it

allows the reactivation of endogenous RNases. Fend *et al.* have shown that it is possible to minimize the immunohistochemistry processing time, thus preserving the RNA quality, however, the interaction antigen-antibody requires time and during this time the endogenous RNase, reactivated, can freely operate [122].

The use of enzymatic RNase inhibitors, to limit the RNase activity, is controversial: some authors, such as Kube *et al.* believe that the RNase inhibitors may improve the RNA quality [105], some other authors, such as Zhou *et al.*, argue that the use of inhibitors does not result in any improvement [102].

Tissue dehydration and the lack of coverslip, due to the need to have free access to tissues for microdissection, represent further difficulties, because they reduce drastically the morphology and make difficult to discern different cell types. A fluid cover medium, specifically designed for this purpose seems to improve both the morphology and the capturing, but may reduce the catapulting efficiency in the LPC system [128].

Over all, the processing optimization and the time reduction are of primary importance.

Laser microdissection has been used by several groups for the study of liver malignancies and bile ducts diseases [104, 129-135]. While the use of chemical dyes in these studies has allowed the identification and isolation of regions of interest with sufficient precision, the dissection of bile ducts might have been greatly improved by immunofluorescence due to the direct and the unambiguous labeling of these tissues.

The use of immunostaining to guide LCM have greatly increased the accuracy of the identification of specific structures, and has to some extent allowed operators less trained in histology or pathology to perform adequate LCM. The resulting increase in dissection accuracy improves the precision of the resulting gene expression profile by reducing the likelihood and the amount of contamination of the sample by surrounding tissues.

Finally, RNA purification from LCM samples is a challenging activity because of the limited abundance and the inherent fragility of this type of nuclei acids.

The amount of RNA obtained from LCM derived samples is usually insufficient for array-based methods of gene expression analysis. Sample pooling from serial sections appears to be the only solution to solve this issue [127].

The classical approach for nucleic acid purification is not able to provide a sufficient yield and the use of specific kits is most recommended.

RNAs quality should be preserved as much as possible, due to the necessity of preserving full-length RNAs for an effective hybridization with the oligonucleotides spotted on the chips.

RNAseq methodologies may greatly overcome the current challenges associated with LCM and gene expression profiling, as they are less sensitive to partial RNA degradation and could allow molecular profiling from FFPE samples. This may represent in the future, an important step forward in the field, allowing the use of the huge amount of samples stored in the tissue bio banks of pathology institutes all around the world.

Gene expression profile

Affymetrix Gene Chip platform

The study of gene expression by oligonucleotide array (Affymetrix GeneChip 3'IVT) has become a very common practice in last years, thanks to the lowering of costs and the standardization of some processes of analysis, which have made this approach accessible to a wide audience of researchers. This approach will be, likely, eclipsed in the next years, by the RNAseq technology, more powerful and less sensitive to partial RNA degradation, but oligonucleotide arrays still represent a good and reliable option for high-throughput gene expression profiling.

The success of these platforms, was based on the multi-probes system, which make them very reliable and reproducible.

The technology is based on synthetic supports spotted, through lithography process, with many hundred thousand of short oligonucleotide (21 bases each), complementary to species-specific gene sequences. In brief, the entire transcriptome contained in a sample is retrotranscribed and the resulting cDNAs are hybridized onto the spotted probe set arrays. The hybridization results into a fluorescence signal the intensity of which is thought to be linearly proportional to the abundance each single transcript [136]. Additionally, each probe set includes a mismatched nucleotide probe. Those probes are intended to provide an estimation of the fluorescence background, versus the actual signal determined by the perfect matched probes [137].

Data pre-processing

Fluorescence raw data require pre-processing in order to make them reliable and comparable with data from other sources (data from the same array type can be compared upon pre-processing and normalization). Pre-processing includes several steps: raw data quality control, background reduction, summarization and normalization, transformation in logarithmic scale.

The raw data quality control addresses the quality of the samples and the correct hybridization on the array surface [138].

Nowadays the summarization algorithms more widely used for the Affymetrix platform 3'IVT are the Robust Multi-array Average (RMA) [139] and the Affymetrix Micro Array Suite rel. 5.0 (MAS5) [140]. Additional algorithms are modified and optimized variants of these basic algorithms (GC-RMA, PLIER, etc.).

An alternative and uncommon approach to the analysis of the Affymetrix GeneChip was the one proposed by Li and Wong, based on the identification of single-probe outliers within the probe sets targeting a single transcript [141].

The choice of the right algorithm may influence in some extent the data distribution, thus it is important to know the peculiar characteristics of each approach and choose the algorithm which best fit to the experimental design.

Algorithms differ in the approach to data summarization and the background correction: MAS5 fully utilizes the characteristics of the Affymetrix chips, using the perfect match probes (PM) and the mismatch ones (MM) for the reduction of background ($PM-MM = \text{raw signal}$). MAS5 has been further improved to avoid attributing negative values, if the intensity of a MM probe exceeds that of the corresponding PM, generating a negative value.

A further peculiarity of the algorithm MAS5 is represented by the call flag (Present, Marginal or Absent, P, M, A) attributed to each probe set by the analysis software. This flag represents an indication of how reliable the expression measurement is. In other words, the MAS5 algorithm not only provides a measure of the gene expression, but also an additional parameter on the reliability of such a measurement.

The use of call flag as pre-filtering tool allows a high correspondence between data pre-processed by MAS5 or RMA algorithm. However, this strategy may results, in

specific cases, in a too stringent filtering [140, 142]. In our study we will show how the application of this filter may result in the exclusion of relevant biological information.

The RMA and GCRMA have a completely different approach to data summarization and background correction: they do not take advantage of the MM probes, but perform a normalization of the data across chips: in brief data are sorted in a table; values are then distributed in descending order in the columns, according to raw intensity values. Then, the expression values in each row are replaced by the median value of that row. Finally, the data are re-sorted according to the original order. By this, the data frequency distribution is identical in all the chips and the data will be perfectly comparable. This system, although theoretically more solid and less prone to give false positives, showed a major issue, introducing a nonexistent correlation between samples, in specific experimental conditions, such as low expressed genes and few replicates [143].

The algorithm developed by Li and Wong takes into account the variation of signal within the single probe set, assuming that variability between probes, belonging to the same probe set and targeting the same transcript, should be minimal. This algorithm, tries to overcome an off-target bias (probe targeting random transcripts, different from the probe set target) common in the Affymetrix platform [141]

The discussion on which algorithm returns the best results is still ongoing. All these methods have weaknesses. It is common opinion that the increased accuracy of the algorithms, which do not take into account the MM probes, is obtained, in most of cases, at the expense of sensitivity.

The MAS5 has been much criticized over the years for its tendency to return false positives, but it remains a valid algorithm.

Here we will also explore the possible differences between the two major algorithms applied at our data set.

The statistical approach to the tissue deconvolution

In the past decade, gene expression profiling has demonstrated an amazing potential for identifying disease biomarkers and improving our understanding of cellular processes. Several groups have attempted to resolve the issue derived from the tissue heterogeneity and the derived variability in the transcriptomic analysis

by statistical methods [144-147]. Although those studies look promising and the possibility to deconvolve the histological complexity of tissues, by just applying statistical methods sounds very appealing, the reality is that these approaches require at least a validation phase, based on experimental data, derived by pure tissues or cells.

The most significant current limitation of these statistical methods, and indeed of all signature gene-based methods, is the robustness of reference profiles.

In our study, therefore, instead of approaching this issue from the computational and analytical point of view, we decided to first generate tissue and cell-type specific profiles, necessary for the deconvolution of whole tissue profiles, and then apply that knowledge to analyses focusing on biologically relevant questions.

Tool compound: Methapyrilene

N,N-dimethyl-N'-pyridin-2-yl-N'-(2-thienylmethyl)ethane-1,2-diamine

Background

Methapyrilene (MP) is an antihistaminic compound once used as sleep-aid component and also used in cold and allergy medications. It was found to induce hepatocellular carcinomas and cholangiocellular carcinomas in rats [148-150], and was subsequently withdrawn from the market. However, its carcinogenicity appears to be species-specific because no evidence has been found of MP-associated carcinogenesis in mice [150, 151] guinea pigs, hamsters [152] or human [153]. Methapyrilene was negative in a series of assays, performed by independent groups all around the world, aimed at understanding if the drug was mutagenic, an inducer of DNA synthesis, or a cause of sister-chromatin exchange [154-158]. However, despite the number of studies performed, there is not so far a clear explanation on how this compound induces the liver cancers. The most accredited theory is that the carcinogenicity of this drug is played during the phase I of the drug metabolism; theory endorsed also by the evidence that CYP450 inhibitors protect from the toxicity [159]. It is therefore possible that, in rat, the catabolites derived from the metabolism phase I cause oxidative stress and cell proliferation, both contributing to the development of the hepatocellular carcinoma and cholangiocellular carcinoma [160, 161]. Despite these extensive studies, there has been limited

characterization of the relationship between molecular changes and microscopic observations resulting from MP exposure.

Hamadeh et al., have tried to correlate the molecular changes and the histopathological alteration observed in the liver of SD rats treated with MP at different doses [162], showing a high correlation between gene expression patterns and histopathological findings.

Material and Methods

Animals and necropsy

Wistar Han (WH) and Sprague Dawley (SD) adult healthy rats (3+3 males and 3+3 females) were provided from Harlan Laboratories.

Canis lupus familiaris liver samples (3 males and 3 females), as well as Macaca fascicularis liver (3 males and 3 females) were collected from healthy control animals enrolled in other Novartis studies, performed according with the local Country animal protection laws. Specifically rat and dog samples were collected in Switzerland (Basel) and monkey tissues were collected in USA and then transferred to Switzerland in line with the current regulations.

For the rodent experiments, the study was performed in conformity with the Swiss Animal Welfare Law (Tierschutzgesetz, 1978, 1981).

Specifically, rats were euthanized by CO₂ during necropsy under the Animal License No. 5109 by 'Kantonales Veterinäramt Basel Land' (Cantonal Veterinary Office, Basel Land).

Liver tissues were rapidly dissected, embedded in OCT and then frozen by the immersion in liquid nitrogen chilled methylbutane. The tissues were stored at -80°C until the use.

Liver portions from additional male Wistar Han rats were snap frozen in liquid nitrogen and stored at -80°C until the use for RNA purification.

Fixation methods for immuno-LCM

The fixation methods could strongly impact the RNAs quality and yield, and this is especially true in case of LCM samples. Several fixation conditions were tested, in order to identify the one associated with the best preservation of RNAs during the immuno-LCM procedures.

Sections (8 µm thick) from Wistar Han control rat livers were mounted onto polyethylene naphthalate (PEN) membrane glass slides (Arcturus, Mountain View, CA USA).

To assess the ability of fixative to preserve the RNA, two groups of sections were fixed by five different protocols as following: 30 seconds in ethanol 75% at room temperature (RT) as described by the HistoGene LCM Frozen Section Staining Kit protocol (Arcturus, Mountain View, CA USA); 5 minutes in ethanol 75% RT; 5

minutes in ethanol 100% RT; 5 minutes in methanol 100% at -20°C; and 10 minutes in 10 % buffered formalin RT. The sections were, then, immersed in water to allow the reactivation of endogenous RNase and check the fixation protection. Exposure to an aqueous environment is what normally occurs during the immuno-staining. For this reason, upon fixation, the tissue slices were exposed to water for a period of 5 or 15 minutes, corresponding to immuno-LCM staining times. The slides were, then, dehydrated in RNase free ethanol ascending scale and clarified by Xylene (Arcturus, Mountain View, CA USA). After additional 10 minutes of exposure to air, the PEN membrane was cut and sections were removed from the slides, collected in microcentrifuge tubes containing 50 μ L of extraction buffer (PicoPure RNA Isolation Kit, Arcturus, Mountain View, CA USA), and placed at 42°C for 30 minutes according with the manufacturer's protocol. The samples were then stored at -80°C until the RNA purification.

To assess the initial RNA quality, one additional section of tissue was collected in a microcentrifuge tube during the sectioning session, 50 μ L of extraction buffer were added, and subsequently it was incubated at 42°C.

The RNA was purified using the PicoPure RNA Isolation Kit (Arcturus, Mountain View, CA USA), according with the manufacturer's protocol, including on-column DNase treatment (Qiagen, Valencia, CA USA) and eluted in (20 μ L) elution buffer (Arcturus, Mountain View, CA). The sections fixed by 10% buffered formalin were additionally treated with proteinase K (Qiagen 19131, Valencia, CA USA) as follow: after the DNase digestion and following rinse in wash buffer 1 (W1, Arcturus, Mountain View, CA USA), 75 μ L of proteinase K (Qiagen, Valencia, CA USA) were applied to the RNA purification columns, in order to break the fixative induced cross-links. The columns were incubated at 55°C for 15 minutes and then at 80°C for 15 minutes. The RNA purification columns were then rinsed by 100 μ L of W1 buffer (Arcturus, Mountain View, CA USA). The RNA purification was, then, carried out according with the kit manufacturer's protocol.

RNA quality was assessed using an Agilent 2100 bioanalyzer, RNA 6000 Pico Chips and Agilent 2100 Expert software (Agilent Technologies, Palo Alto, CA USA).

All the conditions were tested in triplicate (Figure 1, A).

RNase inhibitors efficacy

To evaluate the usefulness of RNase inhibitors in the context of the immuno-LCM experiment, Wistar Han rat liver sections were fixed in methanol at -20 ° C, and then, treated using the HistoGene LCM Frozen Section Staining Kit (Arcturus, Mountain View, CA USA) according to the manufacturer's protocol, with the following modifications.

Protector RNase Inhibitor (0 U/ μ L, 4 U/ μ L, 8 U/ μ L final concentrations; 03335402001, Roche Applied Science, Mannheim, DE) was added to the staining solutions (composed by Antibody Diluent, S3022, Dako, Baar CH and normal rabbit polyclonal IgG 2 μ g/mL, ab27478, Abcam, Cambridge UK). 50 μ L of solution were added to each section. Tissue sections were incubated for 5 and 15 minutes at room temperature (RT) to emulate the experimental condition of the immuno-LCM.

According to the manufacturer's protocol the slides were, then, rinsed in RNase free water, dehydrated in RNase free ethanol ascending scale and clarified by Xylene.

The microdissection was performed by the Arcturus Veritas (Arcturus, Mountain View, CA USA) system, using the CapSure Macro LCM caps (Arcturus, Mountain View, CA USA), within a time of 15 (\pm 10) minutes (power 90mW, pulse 3000 μ s). One square millimeter (\pm 0.1mm²) of liver parenchyma was captured from each slide.

After the dissection, the plastic membrane caps with the microdissected tissue were transferred to microcentrifuge tubes containing 50 μ L of extraction buffer (PicoPure RNA Isolation Kit, Arcturus, Mountain View, CA) and put up side down at 42°C for 30 minutes according with the manufacturer's protocol. The samples were then stored at -80°C until the RNA purification.

To assess the starting RNA quality, one section of untreated tissue was collected in a microcentrifuge tube during the sectioning session. The RNA was purified according with the manufacturer's instruction.

The RNA was purified using the PicoPure RNA Isolation Kit (Arcturus, Mountain View, CA), according to the manufacturer's protocol, including on-column DNase treatment (Qiagen, Valencia, CA) and eluted in (11 μ L) elution buffer (20 μ L for the control section [Arcturus, Mountain View, CA USA]).

RNA quality was assessed using an Agilent 2100 bioanalyzer, RNA 6000 Pico Chips and Agilent 2100 Expert software (Agilent Technologies, Palo Alto, CA USA).

All the conditions were tested in triplicate.

For each single group of samples, the average RIN score was recorded and the RNA degradation percentage was expressed in absolute terms (absolute degradation, AD: tested condition RIN/10*100), assuming the highest RIN score (10) and the relative RNA degradation (relative degradation, RD: tested condition RIN/untreated tissue RIN*100), assuming the unfixed section RIN as highest value. T-tests was used to assess significant differences between treated and untreated samples pairs (Figure 1, B-C).

Immunofluorescence for laser capture microdissection (immuno-LCM)

Frozen liver was sectioned by cryostat (Hyrax C50, Carl Zeiss, Oberkochen, DE). Sections (8 µm thick) were mounted onto polyethylene naphthalate (PEN) membrane glass slides (Arcturus, Mountain View, CA USA), and kept at -20°C until the tissue fixation to prevent RNA degradation.

Tissue sections were fixed in absolute methanol (-20°C for 5 minutes) and then rapidly rinsed in RNase free water.

The excess of water was drained from the slide. Tissues were stained by immunofluorescence (IF), using a mix of mouse monoclonal antibodies against Cytokeratin 19 and Cytokeratin 7 for bile ducts labeling, and a mouse monoclonal antibody against Alpha 2 Actin (Alpha 2 Smooth Muscle Actin, αSMA) conjugated to Cy3 for the vessels labelling (antibodies details in Table 1). The antibody solution (50 µL, composed of antibody at experimental established titer, diluted in Antibody Diluent, S3022, Dako, Baar CH + Protector RNase Inhibitor, 8 U/µL final concentration, 03335402001, Roche Applied Science, Mannheim, DE) was applied on the tissue.

For detection of antibodies targeting the cytokeratins, after 8 minutes of primary antibody incubation, a secondary antibody solution (10ul, goat anti mouse Alexa Fluor 546) was added on the slide and incubated for additional 7 minutes. This step was not necessary for vessel labeling. The sections, then, were rinsed in RNase free water, dehydrated in ascending scale RNase free ethanol and clarified in RNase free xylene, according with HistoGene LCM Frozen Section Staining Kit protocol (Arcturus, Mountain View, CA USA). The tissues then were used for laser capture microdissection.

Laser capture microdissection

The Palm MicroBeam (Carl Zeiss, Oberkochen, DE) was used for the laser capture microdissection of intrahepatic bile ducts, liver parenchyma zone I and zone III (according with Rappaport liver model description) and the isolation of vein and artery from the portal space. All the slides were processed within 30 ± 15 minutes. The Carl Zeiss LD Planar Neofluor 20X objective was used for the in situ observation and selection of the tissues. The laser energy power and focus parameters were set at 46 ± 2 and 72 ± 2 respectively. Two consecutive cutting cycles were used to avoid high laser power and, consequently, an extensive UV-A tissue irradiation.

The RNase free AdhesiveCap tubes (415101-4400-250, Carl Zeiss, Oberkochen, DE) were used as microdissected tissue collector.

Total microdissected surface area was used as quantitative parameter, at least 0.5-0.7 mm² were collected to obtain sufficient RNA for the further analysis. An average of 25 bile ducts was isolated from each liver section. Pooling of bile ducts from 5 to 8 serial sections was necessary (figure 2, A-C).

Similarly, 0.7-1 mm² of microdissected tissue from liver parenchyma zone I and zone III were isolated from liver sections, previously stained by Mayer's hematoxylin and water based eosin. The RNAs from each single area were isolated and subsequently analyzed for gene expression in biological triplicates and technical duplicates (zone I and III) per each single animal (Figure 2, D-I).

In a similar way, portal vein and hepatic artery were isolated and collected using a multi collector tube holder, by immune-LCM using the anti- α SMA antibody conjugated with Cy3 (Sigma Aldrich) (Figure 2, J-N).

RNA purification and quality assessment

RNA from laser-captured tissues was purified using the PicoPure RNA Isolation Kit (Arcturus, Mountain View, CA USA), according to the manufacturer's protocol, including on-column DNase treatment (Qiagen, Valencia, CA USA) and eluted in (11 μ L) elution buffer.

RNA from snap frozen liver (200-400 micrograms of tissue) was purified using Trizol solution (Invitrogen, Carlsbad, CA, USA) in combination with RNeasy (Qiagen, Valencia, CA USA) kit, according with manufacturer's protocols.

RNA quality was assessed using an Agilent 2100 bioanalyzer and RNA 6000 Pico Chips according to the manufacturer's protocol (Agilent Technologies, Palo Alto, CA USA). RNA Integrity Number (RIN) score and electropherogram were used as reference qualitative parameters (figure 2, O).

Total RNA amplification and Affymetrix array hybridization

Total RNA, from LCM derived samples, as well as, from liver section scraped off from glass slides, were amplified by a RNA-dependent DNA polymerase reaction (Ovation Pico WTA System, NuGEN, AC Bemmell, Netherlands). Total RNA was pre-amplified according to the manufacturer's protocol and 4.55 µg of SPIA cDNA targets from previous step were used for the hybridization on GeneChip platform.

RNA from snap frozen tissues was not pre-amplified.

Hybridization mixtures were prepared according to Affymetrix procedures. The Affymetrix Rat Genome 230 2.0, Canine Genome 2.0 and Human Genome U133 Plus 2.0 3' IVT chips were used respectively for rat, dog and monkey tissues (Macaca f. chip was not available).

Affymetrix arrays were hybridized, washed and revealed according to the manufacturer's protocol. GeneChips were scanned using a 7 G scanner (Affymetrix) and images (DAT files) were converted to .CEL files. Data analysis was performed using Agilent Gene Spring GX 11.5.1, Tibco Spotfire and GraphPad Prism software.

Using Gene Spring GX, raw data were pre-processed by Robust Multi-array Analysis (RMA) algorithm (including quantile normalization). Alternatively, raw data were pre-processed by Microarray Suite 5.0 (MAS5) algorithm. Where not differently specified, data were, then, Log transformed and pre filtered within the 20-100 percentile assuming the median as baseline (RAW data). Spearman rank correlation factor and Bland-Altman plot were used to explore the agreement between the two Pre-processing algorithms (Figure 3).

Quality controls, including correlation analysis across arrays and Affymetrix chips internal quality control showed any abnormalities in the hybridization processes (data not shown).

Principal component analysis (PCA) was used as unsupervised approach to explore sample variance (PCA on sample groups, number of principal components=2).

Linear regression analysis on fold change (FC) frequency distribution was used to identify best fitting FC value for gene signature definition.

Differential gene expression was assessed by volcano plot and asymptotic unpaired T-test with Benjamini-Hochberg false discovery rate (FDR; p value ≤ 0.05 where not differently specified).

Impact of Affymetrix expression call flag pre-filtering (agreement in at least 80% of samples in analysis) on low or specifically expressed genes was evaluated by Venn diagram based on the expression call flags assigned by MAS5 algorithm (Figure 11).

Methapyrilene study

A total of 96 Sprague Dawley rats have been enrolled in a past study aiming at qualifying biomarkers of renal damage. Methapyrilene was used as control compound devoid of renal effects, but causing clear hepatic effects [163]. Animals have been treated with the drug at different concentrations and for different time, according with the following table. Animals were sacrificed at the specific time-point unless clear evidences of sufferance emerged earlier during the treatment, in which case the subject have been excluded from the following analysis.

Day 1	Day 3	Day 7	Day 14
Controls*	Controls*	Controls*	Controls*
15mg/kg/day*	15mg/kg/day*	15mg/kg/day*	15mg/kg/day*
30mg/kg/day*	30mg/kg/day*	30mg/kg/day*	30mg/kg/day*
60mg/kg/day*	60mg/kg/day*	60mg/kg/day*	60mg/kg/day*

Scheme of the Methapyrilene study (* daily oral administration, controls treated with vehicle, H₂O).

At time-points the animals have been euthanized by CO₂ and all the organs have been collected during the necropsy. In the specific liver was divided and collected in order to have snap frozen samples for molecular biology applications (lateral left lobe allocated for gene expression profiling) and samples for the histopathological analysis (caudate lobes and papillary process, allocated for histology), these latter were fixed in 10% buffered formalin for 48 hours and then dehydrated and embedded in paraffin.

Total RNA from whole liver tissue was purified and processed for the hybridization on Affymetrix Rat Genome 230 2.0, as previously described, without pre-amplification step. Raw data were pre-processed by Microarray Suite 5.0 (MAS5) algorithm, including Log transformation and pre-filtering on 20-100 percentile assuming the median as baseline (RAW data). The standard internal controls have been verified.

Immunohistochemistry (IHC)

Immunohistochemistry was performed using the fully automated instrument Ventana Discovery (Roche Diagnostics AG, Rotkreuz, CH). All chemicals were provided by Roche Diagnostics Schweiz AG. See detailed conditions used for each antibody in (table 1)

Briefly, formalin fixed paraffin embedded sections (3µm) were de-paraffinized and re-hydrated under solvent-free conditions (EZprep solution) followed by antigen retrieval pretreatment performed by heat retrieval cycles in a Tris-EDTA based buffer (CC1 solution – option Mild) or by enzymatic digestion (Protease 1 for 6min). Subsequently slides were blocked using 1x Casein solution in PBS (PBSC-0100-5x, BioFX laboratories, Owing Mills, MD, USA). Endogenous avidin/biotin activity was quenched in all cases secondary antibody to be used was not UltraMap anti-rabbit HRP (direct peroxydase detection). Next 100 µL of diluted primary antibody were added to each slide and incubated at room temperature. A short post-fixation (glutaraldehyde at 0.05%) was performed before applying conjugated secondary antibody.

Detection was performed using either a streptavidin-biotin peroxydase detection system (DABMap Kit), streptavidin-biotin AP conjugated (RedMap Kit), or direct peroxydase detection (ChromoMap kit) when using UltraMap anti-rabbit HRP; in all cases manufacturer recommendations were followed. Slides were counter stained with hematoxylin and bluing reagent and finally dehydrated and mounted using Pertex (00814, Histolab Products, Gothenburg, SE).

Table 1

Antibody	Application	Antigen Retrieval Treatment	Primary AB working dilution	Primary AB incubation time	Secondary antibody	Secondary AB working dilution	Secondary AB incubation time
anti-Krt7 (Abcam ab9021)	IF-LCM	None	1/50 Eq. 20µg/mL	8 min	Goat anti-mouse Alexa Fluor 546 (Invitrogen, A11030)	1/25 Eq. 80µg/mL	7 min
Anti-Actin, α -Smooth Muscle - Cy3	IF-LCM	None	1/50	8 min	None	NA	NA
anti-Krt7 (Dako M7018)	IHC	Protease	1/50 Eq. 5µg/mL	6 h	Donkey anti-mouse biotin-conjugated (Jackson ImmunoResearch)	1/500 Eq. ~ 3µg/mL	16 min
anti-Krt19 (Bioss B08029M)	IF-LCM	None	1/50 Eq. 1µg/mL	8 min	Goat anti-mouse Alexa Fluor 546 (Invitrogen, A11030)	1/25 Eq. 80µg/mL	7 min
anti-Krt19 (Novocastra NCL-CK19)	IHC	Protease	1/200	6 h	Donkey anti-mouse biotin-conjugated (Jackson ImmunoResearch)	1/500 Eq. ~ 3µg/mL	16 min
anti-Krt20 (Dako M7019)	IHC	Protease	1/100 Eq. 0.5µg/mL	6 h	Donkey anti-mouse biotin-conjugated (Jackson ImmunoResearch)	1/500 Eq. ~ 3µg/mL	16 min
anti-Claudin6 (Abcam ab107059)	IHC	Heat	1/200	6 h	UltraMap® anti-rabbit HRP-conjugated (Ventana)	Ready to use	16 min
anti-Claudin7 (Abcam ab27487)	IHC	Heat	1/200 Eq. 1µg/mL	6 h	UltraMap® anti-rabbit HRP-conjugated (Ventana)	Ready to use	16 min
Anti-LOX (Novus Bio NB100-2530)	IHC	None (frozen sections)	1/100	ON 4°C	Donkey anti-rabbit biotin conjugated (Jackson ImmunoResearch)	1/500 Eq. ~ 3µg/mL	1hr RT
Anti-Col1A1 (ABonline ABIN97475)	IHC	Heat	1/200 Eq. 1µg/mL	3 h	Donkey anti-rabbit biotin conjugated (Jackson ImmunoResearch)	1/500 Eq. ~ 3µg/mL	16 min
Muc1 (Abcam ab15481)	IHC	Heat	1/200 Eq. 1µg/mL	3 h	Donkey anti-rabbit biotin conjugated (Jackson ImmunoResearch)	1/500 Eq. ~ 3µg/mL	16 min

Antibodies and experimental conditions for protein localization

Isotype controls

All the histological assays have been run on paired sections with mouse or rabbit anti-target antibodies and normal mouse or rabbit isotype controls to prove the specificity of the primary antibody. All the antibodies, used in the conditions previously described, did not show any non-specific binding in the liver tissues of the 3 species analyzed (representative picture in the Supplementary Data, Supplementary Picture 1)

Image analysis

Immunohistochemistry stained slides (controls vs. 60mg/Kg/day at time-point day 3, day 7 and day 14) were scanned by Hamamatsu Nanozoomer 2.0 HT. RAW data (.ndpi files) were converted in Tiff RGB files.

RGB tiff files were deconvolved for the isolation of the signal revealed by 3,3'-Diaminobenzidine (DAB). The pictures were then converted in binary and the positive area has been quantified in pixels by ImageJ software. Numerical data have been exported to GraphPad Prism software for the statistical analysis.

Results

Effect of tissue fixation on RNA quality

RIN score has been used as a qualitative parameter for the evaluation of RNA integrity. The RIN is a numeric score in the range from 1 to 10, provided by the Agilent 2100 expert software, and it is calculated based on a complex algorithm taking into account many characteristics recorded during a gel filled capillaries RNA electrophoresis. The RIN has proved to be a valid indicator of RNA quality (62). Nevertheless, the Agilent 2100 expert software has failed several times in the LCM derived samples RIN allocation. This issue could be due to the low RNA concentration, which was at limit of the detection threshold.

Five different fixation procedures were tested to identify the one that provides the best results in experiments of immuno-LCM. The fixation in 75% ethanol for 30 seconds, suggested by HistoGene LCM Frozen Section Staining Kit protocol, has been compared with other methods.

The tissue sections were, then, exposed to an aqueous environment in order to reproduce the conditions occurring during the immuno-staining. The qualitative assessment was performed for two time-points (5 minutes and 15 minutes) to verify to which extent the fixative protective effect can be considered.

The graph in Fig 1A shows the RIN scores found after RNA purification from samples exposed to water for 5 and 15 minutes. After 5 minutes, the embedding and cryo-sectioning processes lead to RNA deterioration estimable by around 20% (AD 17%) as detectable in untreated section. As expected, exposure to water for short time does not lead to massive RNA degradation: all sections fixed with precipitating fixatives reached a detectable RIN scores as shown, the software was not repeatedly able to assign a correct RIN score to formalin fixed sample, probably due to the low RNA concentration.

The data analysis did not show significant differences between the precipitating fixation methods at this time-point.

Data previously observed were confirmed by exposing the tissue sections to water for 15 minutes. No significant difference between precipitating fixation methods was found. The RNA quality and quantity from formalin fixed sections was not sufficient for the RIN allocation. As in the previous test, the highest RIN score was

obtained with 5 minutes ethanol 75% fixation, followed by cold methanol, 30 seconds ethanol 75%, and ultimately, 5 minutes absolute ethanol.

We therefore conclude that the exposure to water based solution, like during an immune-staining, is detrimental for the RNA. The contribution of fixatives for the RNA preservation is minimal. For the specific application, the use of alcoholic fixative is recommended, although we could not appreciate differences between the alcoholic fixatives in analysis. Contrarily, the use of aldehydes, should be discouraged due to the low yield obtained in the RNA purification.

Effect of RNase inhibitors use on RNA quality

In order to ascertain the real usefulness of the RNase inhibitors in LCM protocols development, we used a similar experimental approach to the fixatives test, based on the exposure of tissue to different conditions and evaluating the RIN after the RNA extraction. Methanol fixed sections were rinsed and exposed to water based solution in presence and absence of RNase inhibitors for different time (5 or 15 minutes). The RNA purified from RNase inhibitors treated and untreated sections, as well as RNA from a single unfixed section collected during the cryo-sectioning session, were compared by the RIN scores (average \pm SD).

Absolute RNA degradation and relative RNA degradation were calculated, as described in material and methods and shown in Fig1 B and C.

Similarly, to what we described in the previous paragraph, freezing, embedding, and cryo-sectioning processes lead to an absolute RNA degradation estimable, in this case, by around 40% in the untreated section.

The entire staining procedure leads to a further degradation in the section exposed to water solution not containing RNase inhibitors (0U/ μ l).

RNase inhibitors concentrations up to 4 U/ μ L have limited protection effect on section exposed to water for 5 minutes. Contrarily, the use of 8 U/ μ L is able to completely inhibit the endogenous RNases effect. In fact, there were not significant differences between the starting tissues (RIN score) and sections treated with the highest RNase inhibitor dose Fig 1B.

RIN scores recorded from sections exposed for 15 minutes to water confirmed previous data, emphasizing the usefulness of RNA protectors in these experimental

conditions. The RNA quality of the unprotected sections (0 U/ μ L) was very low (average RIN = 2.73), the use of inhibitors at concentrations of 4 U/ μ L blocks the endogenous RNase only partially. A significant improvement is achieved by raising the inhibitors concentration up to 8 U/ μ L Fig1C.

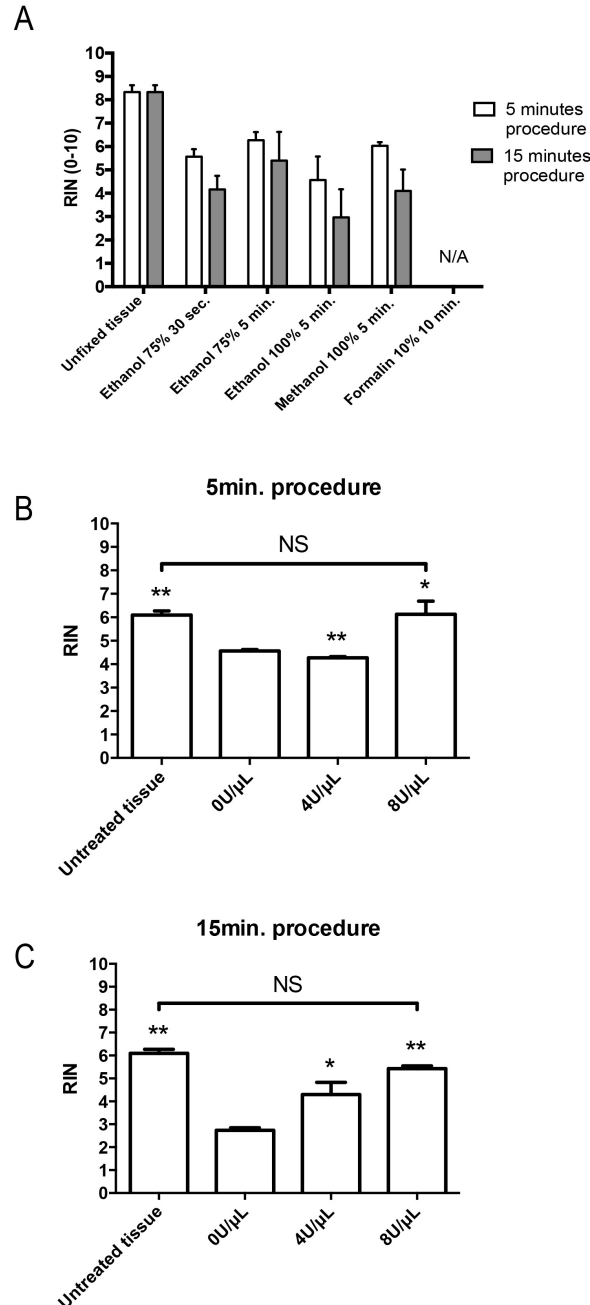


Figure 1: The use of different fixatives does not significantly improve the RNA quality for immuno-LCM applications: alcohol fixed tissues yielded comparable RNA quality compared to an unfixed section (in A) collected in RNA extraction buffer during cryosectioning. Formaldehyde did not allow recovering a sufficient amount of RNA for the analysis.

Contrarily, the use of RNase inhibitors at certain concentrations showed to be very effective in preserving the RNA quality. Indeed, while the absence or the use of insufficient RNase inhibitors (up

to 4U/ μ l) lead to RNA degradation already after 5 minutes (B) and more after 15 minutes (C) of exposure to a water based solution, tissues treated with 8U/ μ l of RNase inhibitors showed no difference compared with a reference tissue collected in RNA extraction buffer during the cryosectioning, neither after 5 minutes, nor after 15 minutes (C).

In summary the use of the RNase inhibitors is strongly recommended for immuno-LCM experiments, due to their beneficial effects. However, we should note that the amount of enzymes used for this kind of experiment is extremely high and above the doses suggested for other kind of experiments (i.e. RT-PCR). In this concern, beside the economical factor resulting from the huge use of reagent, it should be taken into account also the composition of the RNases inhibitor buffer. Specifically, it contains glycerol, which at high concentration might inhibit the interaction antigen-antibody during the immunolabeling reaction. We then discourage the use of concentration above the ones used in this test, because the buffer composition might impact the sensitivity and specificity of the antibody.

Laser capture microdissection (LCM) and Immuno-LCM

The laser microdissection is a complex and time consuming activity.

The isolation of liver parenchyma's regions (zone I and zone III) was possible using a chemical dye (eosin), which allowed enough resolution for the correct identification of the periportal-pericentral axis and, therefore, the identification of the 3 liver zones. Hepatocytes lying between adjacent portal fields were selected and isolated as zone I (Fig 2 D, E, F). A round area composed of few hepatocytes layers surrounding the central veins was identified and isolated as zone III (Fig 2 G, H, I). Tissues isolated from a single liver section were normally enough (roughly 1mm²) for providing sufficient total RNA upon purification.

Despite that the recognition of the parenchymal areas was possible using the eosin staining, this approach was not as good enough for the identification and isolation of bile ducts and vessels from the portal area. Additionally, due to the small size of these structures, a possible contamination derived from an approximate histological identification, with surrounding stromal cells, would have resulted in a contaminated RNA samples and a transcriptome not representative of the original tissues.

Thus we decided to implement the method with an immune-detection of the tissue of interest (Immuno-LCM).

The immuno-LCM, however is very demanding due to the fast RNA degradation and the need for very specific and reactive antibodies, targeting the markers for cell discrimination. The labeling of the bile ducts (Fig 2 A, B, C) and vessels (Fig 2 J, K, M) by immunofluorescence, substantially improved the detection quality and strongly increases the laser microdissection precision.

Due to the small size of bile ducts and vessels, the pooling of samples obtained in many experiments was necessary in order to reach a tissue amount sufficient for RNA purification. Consistency of selection, dissection and collection processes was visually inspected after each experiment, double-checking the collector tube. The number of bile ducts and vessels collected was compared with the collected area by the software. The entire process of staining and microdissection was performed in an average time of 45 minutes.

Bile ducts were stained with a monoclonal antibody against cytokeratins (7 and 19), allowing the selection and isolation.

For the isolation of vessels, we used an antibody against the smooth muscle actin. This antibody marks the smooth muscle cells resident in the vessels wall (Tunica Media). We did not observe other cells labeled by this antibody in the liver.

However, as we used smooth muscle actin staining for immuno-LCM approach, the discrimination between hepatic arteries and portal veins was based mainly on the experience and knowledge of the operator and on the histological features of the tissues (thickness of tunica media and elastic lamina).

Overall, the optimization of tissue fixation, the use of RNase inhibitors and the processing time reduction allowed the collection of samples with good RNA quality and quantity for this kind of samples (Fig 2 O, RIN ranging between 5 and 7).

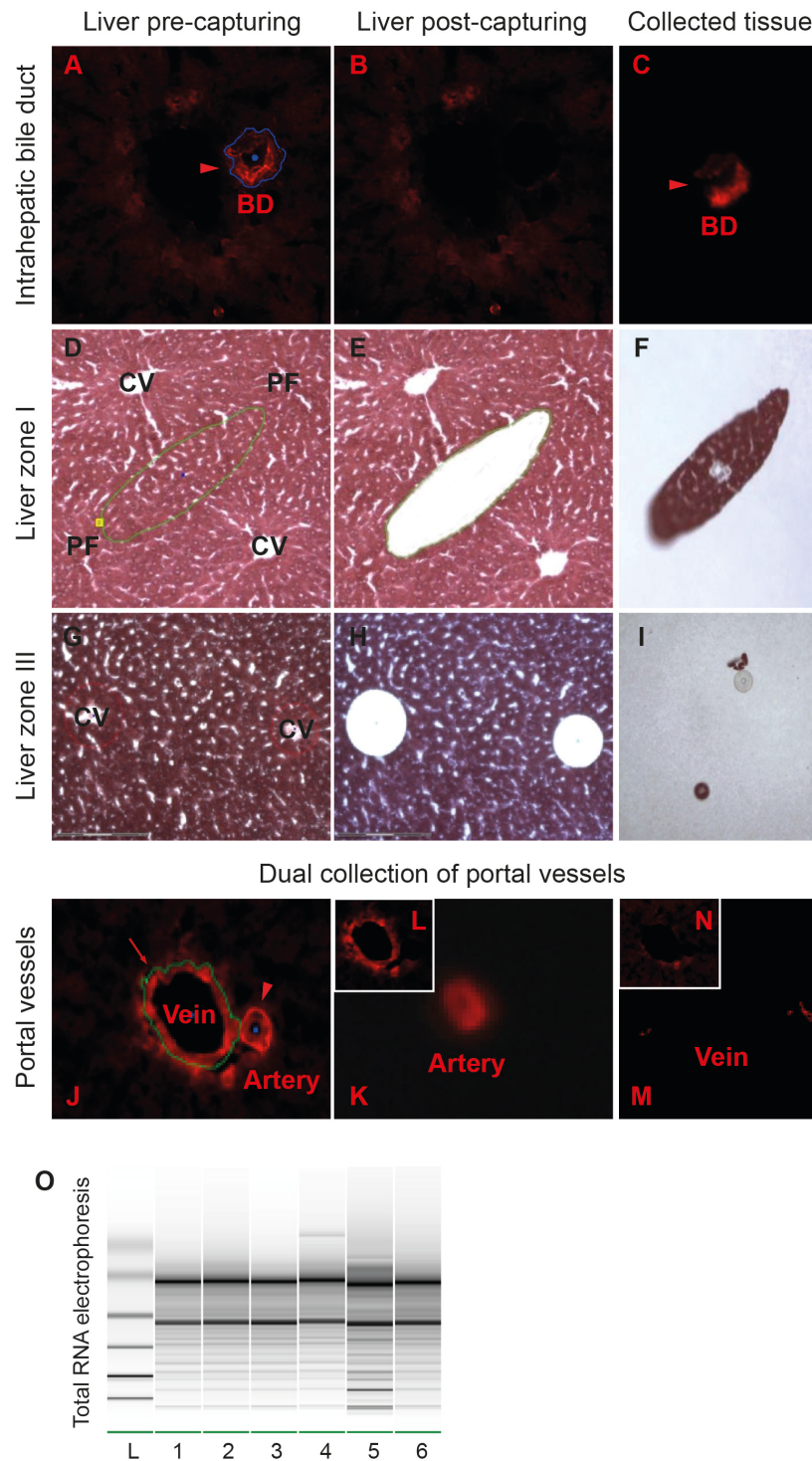


Figure 2: representative isolation of liver tissue by laser capture microdissection (LCM). Picture are representative of the whole tissue before and after the dissection and of the isolated tissue, upon collection. Immuno-LCM has been used for the isolation of intrahepatic bile ducts and blood vessels from the portal area (A-C and J-N). Liver zone I and liver zone III have been recognized by eosin staining, based on the tissue morphological features (D-I). RNA was purified and its integrity has been verified by micro-capillary electrophoresis (Agilent Bioanalyser). The presence of both the ribosomal RNA bands is indicative of good quality and low degradation (L, ladders; 1, liver zone I; 2, liver zone III; 3, hepatic artery; 4, portal vein; 5, liver bile duct; 6, whole liver scrape).

Transcriptomic analysis

Total RNA were amplified and hybridized on the species-specific Affymetrix GeneChip platforms (GeneChip®Rat Genome 230 2.0, GeneChip® Canine Genome 2.0), except for the samples from *Macaca fascicularis*, which was hybridized on the Human Genome U133 Plus 2.0 Array.

Pre-processing algorithms

Rat samples were used as pilot study with the aim to identify the best pre-processing procedure. RMA and MAS5 pre-processing algorithms were compared. Transcriptomic raw data have been pre-processed by the software Agilent GeneSpring (ver.11.5.1), as described in materials and methods, using the RMA and the MAS5 algorithms. To assess the agreement between the data pre-processed by the two algorithms, the average expression values from whole rat liver were compared by Spearman rank correlation and, visualized by Bland-Altman plot. The analysis revealed a high correlation, with a value of rank R squared of 0.90 (rank R 0.95, p value <0.001) (Fig 3 A). Rank R squared reached 0.95 (rank R 0.97, p value <0.001) if the analysis was limited to the probe set receiving Affymetrix expression flag “present” in 80% of samples in analysis (Fig 3 B). Recently, some groups have proposed such a method for increasing the correlation between pre-processing algorithms and to increase the statistical power of the results. In our data set, the improvement determined by the pre-filtering on present calls was limited. We have analyzed the effects of this pre-filtering procedure on transcriptomic analysis of heterogeneous tissue samples and our findings will be further described in the next chapter.

According with previous data, the Bland-Altman graph also showed that there is an agreement of 94.7% between the two algorithms (number of probe sets comprised within the interval of Average $\pm 1.96 \times \text{SD}$ [Fig 3 C]).

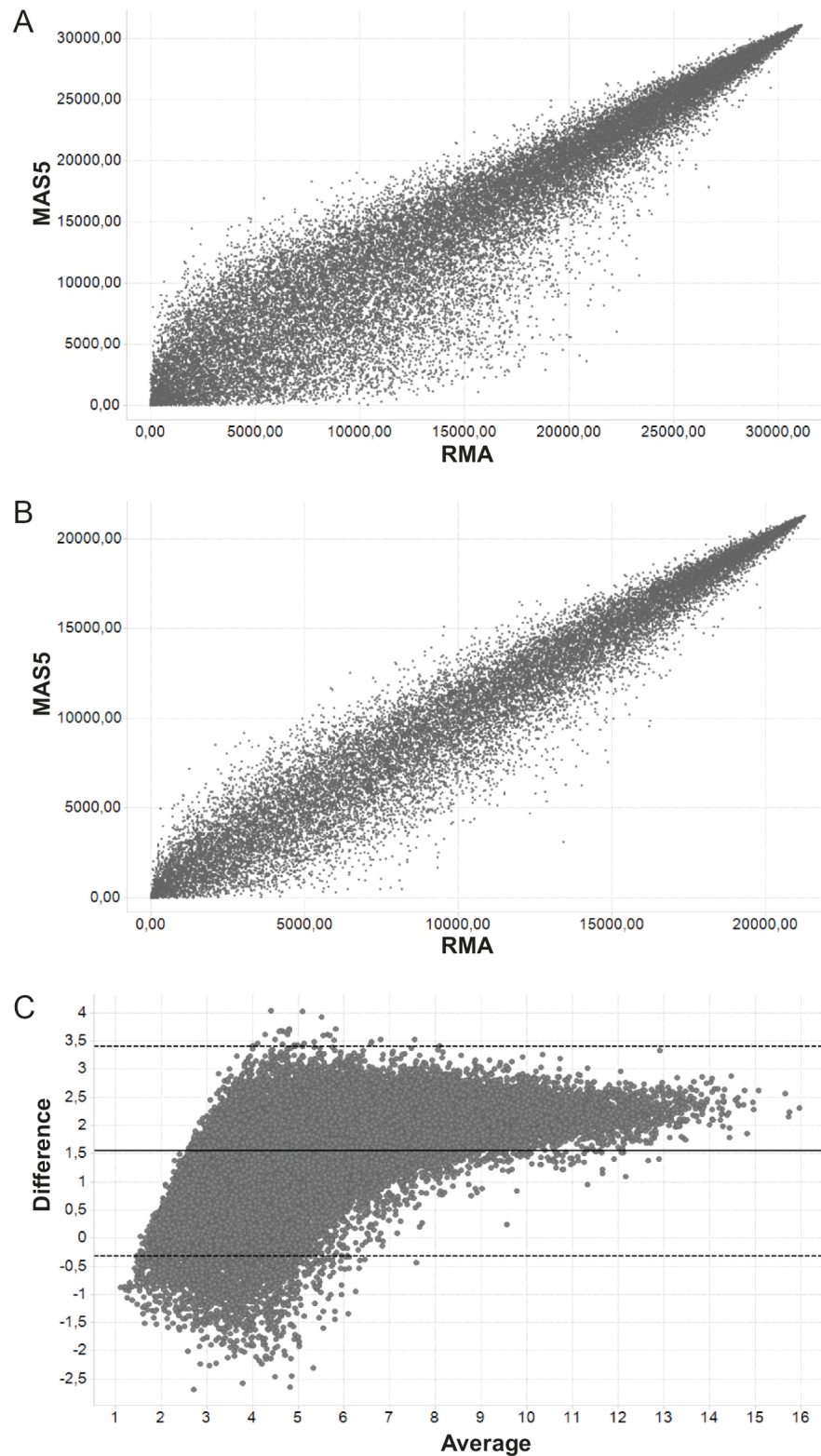


Figure 3: The correlation between different pre-processing (MAS5 and RMA) approaches has been tested comparing the gene expression profiles of rat whole liver. We performed a Spearman rank correlation of the whole data set and of the data set pre filtered by the presence call flag parameter (respectively A and B) and, alternatively, a Bland-Altman distribution graph (whole data set; C). In all the tests, the data sets showed a good correlations degree. MAS 5 algorithm has been used for the following analysis.

As previously described, some groups have demonstrated an algorithm driven artifact in the RMA, inducing an artificial correlation between samples, in specific experimental conditions, including a limited sample number and low expressed genes. Our experimental system was characterized by a restricted number of samples, due to the difficulties of obtaining LCM enriched tissues, and many genes showed a low expression. Although the high correlation between data preprocessed with the two algorithms suggests comparable results, our dataset is characterized by those peculiarities by which the RMA algorithm may incur in the artifact described previously. Therefore, we decided to use only the MAS5 preprocessing for the following analysis.

Quality controls and PCA

Common quality controls like 3'/5' ratio, internal Affymetrix hybridization controls, inter-assays correlation plot (Pearson's correlation) showed no abnormalities in any of the species-specific platform, upon data pre-processing and normalization.

In order to visualize, in an unbiased way, the inherent characteristics of LCM samples, a Principal Component Analysis was run (PCA on sample groups, 2 principal components). In all the species (Figure 4. A, Rat; B, Dog; C, Monkey), liver scrape, liver zone I and liver zone III, always clustered together, likely due to the sample compositions, mostly hepatocytes. Similarly, portal vein and hepatic arteries clustered together, far from the previous group. Finally, bile ducts represented an independent group in all the species. The analysis showed a good separation between samples, indicating good cell phenotype enrichment obtained by LCM.

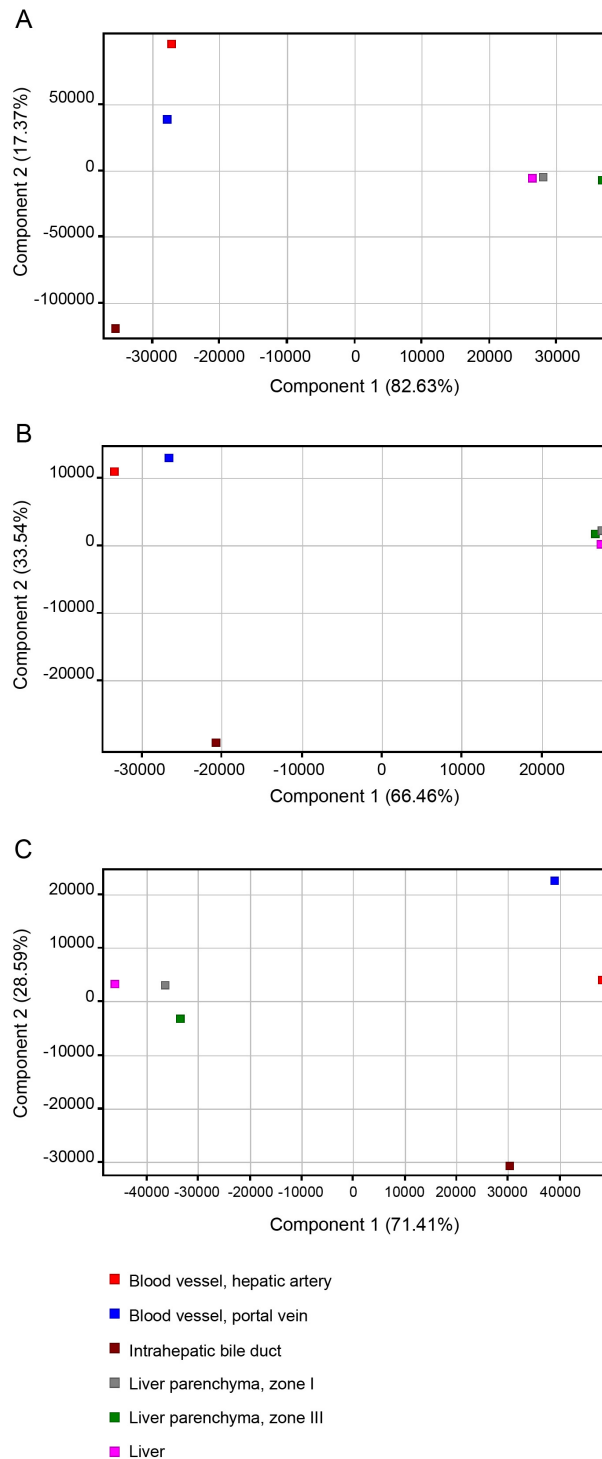


Figure 4: The principal component analysis (PCA) performed on all the data sets from the 3 animal species. In all the graphs, the tissues clustered according with their characteristic: whole liver scrapes clustered with liver zone I and liver zone III samples, based on their cellular composition. Arteries and veins also clustered close to each other. Finally, intrahepatic bile ducts were separated from all the other samples. This unbiased analysis revealed the good tissue enrichment obtained by LCM.

Comparative gene expression analysis

Unbiased approach for designing structure specific gene signatures

Potentially pure samples, isolated by LCM, provided the possibility to identify genes selectively expressed in some cells among a heterogeneous tissue. Of particular interest, the possibility to analyze the transcriptome from the bile ducts, isolated from the whole liver, offered the unique possibility to delineate a gene signature specific for those structures and a physiological baseline for comparative studies. Nevertheless, the definition of a specific signature is a challenging exercise. Given the peculiarities of samples isolated by LCM and the experimental approach chosen, we attempted to identify a methodology, based on comparative approach, able to discriminate with maximum sensitivity and specificity, genes strongly enriched and/or selectively expressed in bile duct. We have therefore generated a binned fold change frequency histogram, in an interval between 0 and 50 fold changes (FC; Figure 5 A). An exponential shape characterizes the histogram; however, two linear stages (Figure 5B and 5C), defined by linear regression analysis, can be identified. Interestingly these two linear phases intersected at value of 9.2 FC (in rat data set). In fact, this cutoff value determines the best compromise in the R square value of the two linear phases ($FC \leq 9.2$ $r^2 = 0.974$; $9.2 < FC \leq 50$ $r^2 = 0.928$). Under the biological point of view, this intersection represents the joint point between two different trends: below 9.2 FC, small variation determines a significant increase in the number of probe sets selected, likely associated with a decrease in specificity. Above this FC value, vice versa, small variation does not determine massive changes in the number of probe sets selected. We therefore decided to use this value of 9.2 as a cutoff value ($p \leq 0.05$, Student's t-test unpaired, multiple testing correction Benjamini-Hochberg [164]) for the selection of genes enriched in bile ducts (Figure 6). According with this parameter, 767 probe sets, out of 31099 probe sets present on Rat Genome 230 2.0 chips, were selected as significantly increased in the bile duct, in comparison with whole liver (liver scrape).

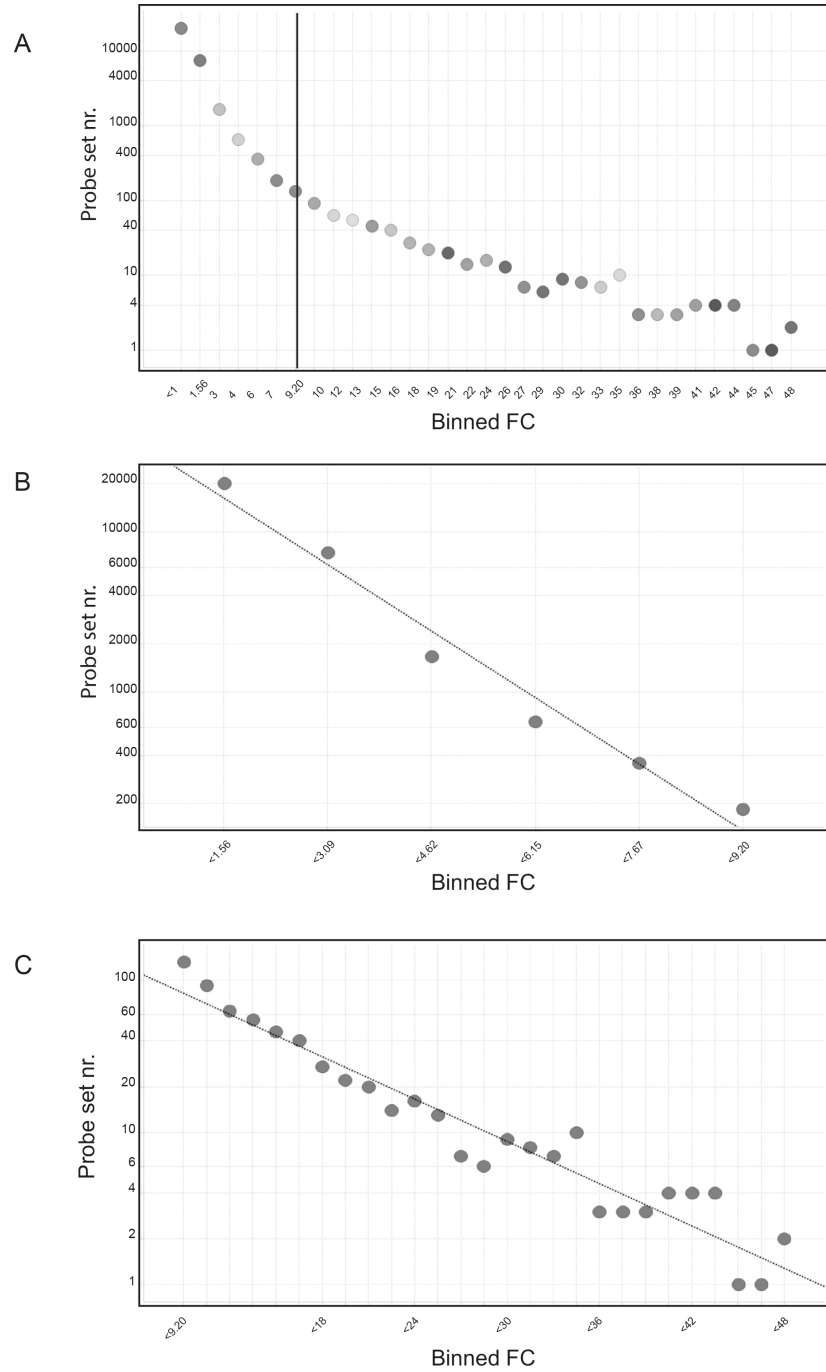


Figure 5: The approach used for the selection of genes enriched and/or selectively expressed in rat bile ducts. The whole data set has been ranked according with the fold change (FC) in gene expression, in bile ducts vs. whole liver scrape. The FC values were then classified in categories between 1 and 50 (binned FC, Fig 5A, X axis). Those values have been plotted together with the number of genes selected as enriched in bile duct, by the corresponding FC value (Fig 5A, Y axis). The resulting distribution describes an exponential curve, characterized by two major linear phases, identified by linear regression analysis (Fig 5B and 5C). The intersection point of the two best fitting linear phases ($FC \leq 9.2$ $r^2 = 0.974$; $9.2 < FC \leq 50$ $r^2 = 0.928$), determines the best cut-off value for the selection of genes enriched in the bile ducts.

In a similar manner, based on the same selection criterion, we have chosen the FC cutoff for selection of bile ducts specific signatures also in the other 2 species, obtaining values close to that obtained in rats (dog FC cutoff 8.17, 765 probe sets; monkey FC cutoff 9.14, 709 probe sets).

Based on the success of the empirical definition of criteria, it might be interesting to pursue the development of an algorithmic method, able to adjust the cutoff according with our experimental observations.

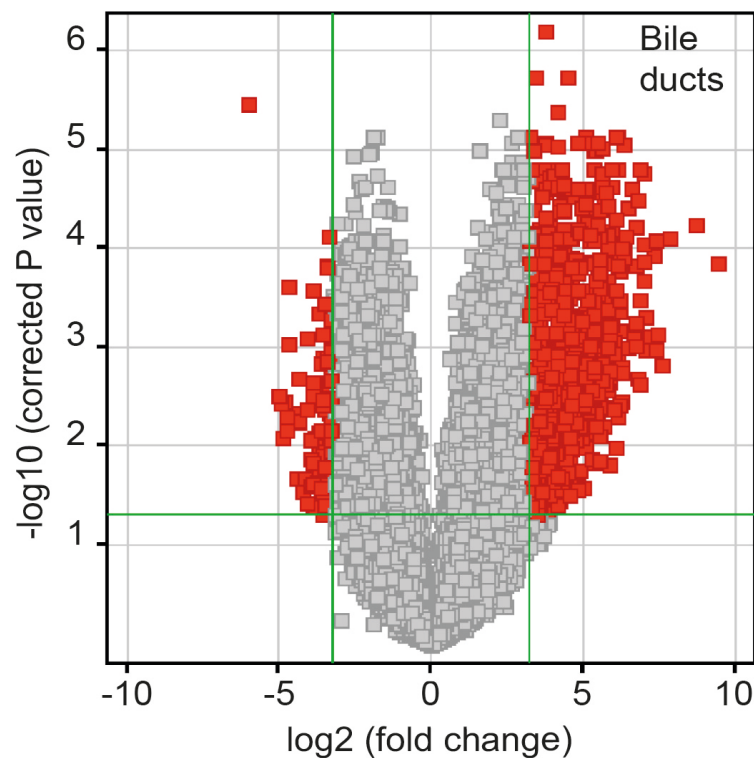


Figure 6: a volcano plot showing genes selected by using a FC cut-off of 9.2 (bile duct vs. whole liver scrape. $p \leq 0.05$, Mann-Whitney unpaired test, multiple testing correction Benjamini-Hochberg). The genes up regulated in right hand side of the graph represent our gene signature for bile ducts.

Liver zonation

For the selection of liver parenchymal zone I and zone III gene signatures, we used a different comparative approach. Specifically, assuming that the comparison was made between two similar cell populations (mostly composed by hepatocytes), a very high FC cutoff would have not been biologically meaningful, unless to highlight genes selectively expressed in one rather than in the other zone. We have, therefore, used as an arbitrary FC cutoff of 2 in a volcano plot ($p \leq 0.05$) to identify genes enriched, as well as selectively expressed, either in zone I or zone III (Figure 7).

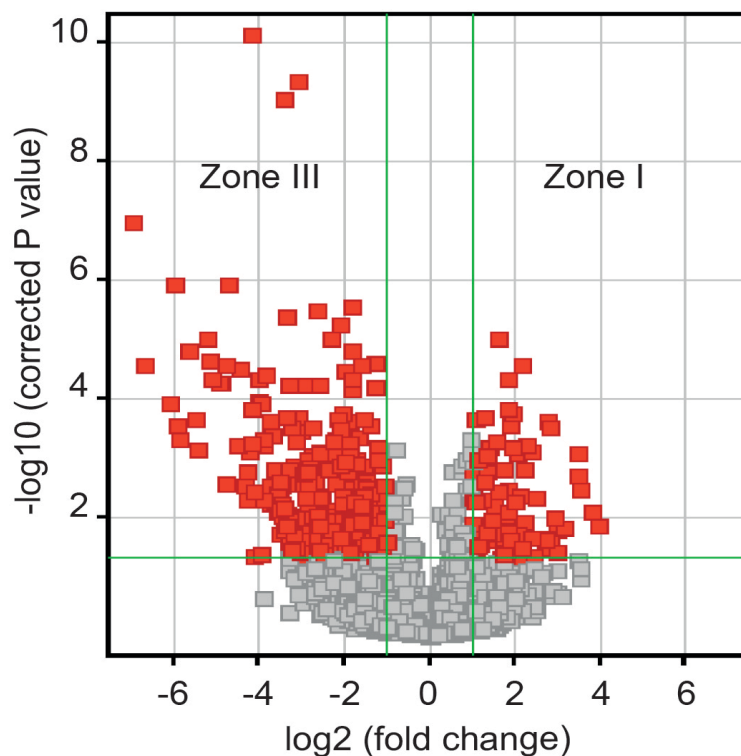


Figure 7: a volcano plot showing the selection of genes enriched either in liver zone I or in liver zone III in rat (rat liver zone I vs. zone III, $p \leq 0.05$, Mann-Whitney unpaired test, multiple testing correction Benjamini-Hochberg). The same approach has been used for the selection of enriched genes in dog and in monkey.

The comparison showed 631 probe sets differentially expressed in rat liver zone I vs. liver zone III ($p \leq 0.05$, Mann-Whitney unpaired test, multiple testing correction Benjamini-Hochberg). Out of this number, 130 probe sets were differentially expressed in zone I and 501 in zone III.

Similarly, 709 probe sets were differentially expressed in dog liver zone I vs. liver zone III. Out of this number, 305 probe sets were up regulated in zone I and 404 were up regulated in zone III.

Ultimately, the comparison in monkey liver revealed 242 probe sets differentially expressed in liver zone I vs. liver zone III: 91 probe sets were up regulated in zone I and 151 were up regulated in zone III.

We then investigated selectively the expression of Wnt genes (19 members from Wnt1 to Wnt16), the major driver of liver zonation. Interestingly, most of those genes resulted not significantly regulated. A focused analysis, however, revealed that in rat and monkey liver zone III, Wnt2 was significantly up regulated, in

comparison to liver zone I (Figure 8A and 8C). In dog, none of the annotated genes belonging to the WNT family reached the statistical significance in the comparative analysis. However, WNT5B was the only one member of the family enriched in liver zone III ($p=0.03$, corrected $p=0.2$, Figure 8B) although its profile was rather flat, showing limited differences between the tissues in analysis.

In order to verify the effect of the Wnt expression, we have selected as reporter gene of the Wnt pathway, Axin2 and Glul. The 2 genes were also enriched in the liver zone III of rats and monkey (Figure 8A and 8C). In dog, according with the lack of a significant driver gene, Axin2 was equally expressed in most of the liver tissues. GLUL gene, however, conserved its pericentral expression (Figure 8B). We might speculate on a different mechanisms regulating the liver zonation, which might not be unique across species. Additionally, the preservation of the GLUL expression in the pericentral area in dog (together with many other zone III specific genes), might be indicative of a different mechanism driving the liver zonation, independent from the postulated WNT gradient. An alternative explanation might also be that, additional WNT genes, not annotated in dog platform, may play a role in driving the liver zonation in this species, although this would not explain the lack of the up regulation of AXIN2 in the same area.

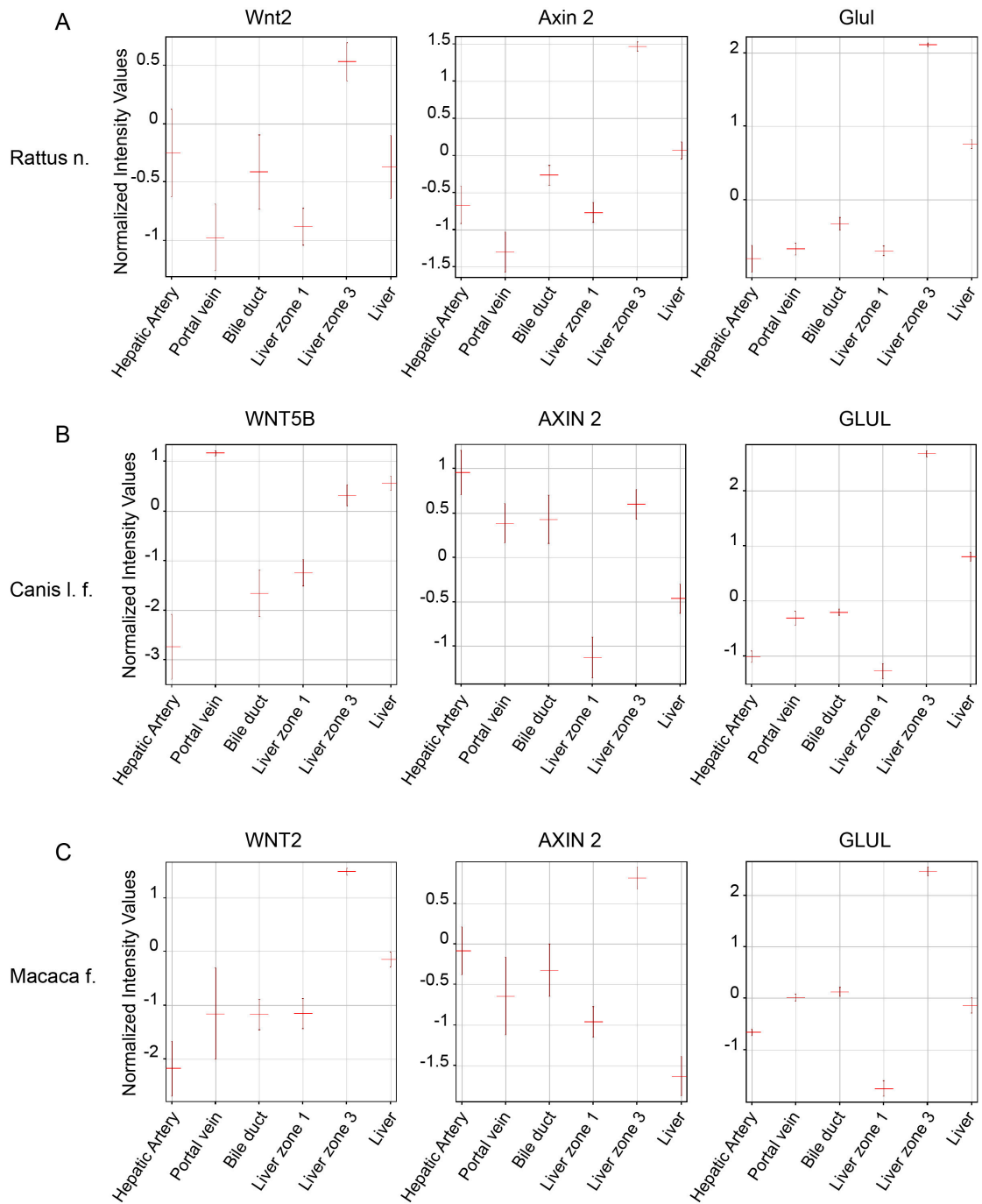


Figure 8: The gene expression profile of the liver zonation driver genes WNT2(rat and monkey) and WNT5B (dog), and genes down-stream in the WNT pathway (AXIN 2 and GLUL). Interestingly, while in rat and monkey we were able to identify WNT2 as the only member of the WNT family significantly up regulated in the liver zone III vs. all the other liver samples, in dog, none of the WNT genes was up regulated in the same area. Accordingly, AXIN2 and GLUL were up regulated in liver zone III in rat and monkey. In dog, only the GLUL preserved its enrichment in liver zone III (Normalized expression data in log scale).

Gender differences and Liver zonation

In order to assess the presence a sexual dimorphism in the liver gene expression, we compared, in first instance, the gene expression profile of the whole liver tissues derived from male and female animals. We then used the LCM derived tissues (liver zone I and liver zone III) and we compared the expression profiles of male animals to those of the female animals in those specific areas, in order to highlight a gender specific mechanism orchestrating the gene expression, in the liver zones.

Interestingly, the direct comparison of whole liver tissues from male and female animals yielded only a limited number of gender specific genes. In the specific, in rats we obtained a total of 76 probe set significantly differentially regulated between males and females (Volcano plot, Mann-Whitney unpaired test, $p \leq 0.05$, FC cutoff 2, multiple testing correction Benjamini-Hochberg; 34 probe sets enriched in females, and 42 enriched in the males). In dog and monkey only one probe set reached the statistical significance (Volcano plot, Mann-Whitney unpaired test, $p \leq 0.05$, FC cutoff 2, multiple testing correction Benjamini-Hochberg; MYNN transcript up regulated in female dogs, TSIX transcript up regulated in female monkeys).

We then compared the LCM liver zone I and liver zone III, in male vs. female (Volcano plot, Mann-Whitney unpaired test, $p \leq 0.05$, FC cutoff 2, multiple testing correction Benjamini-Hochberg) in all the species.

In rat liver zone I the comparison revealed 130 probe sets with an absolute FC greater than 2 in male vs. female, but only 27 were statistically significant (14 probe sets enriched in male animals and 13 enriched in female animals).

Similarly, in rat liver zone III, we found 501 regulated probe sets, 218 with statistical significance (male vs. female, 194 enriched in male animals and 24 enriched in female animals) (Figure 9).

Any probe set reached the statistical relevance in neither liver zone I nor zone III in dog and monkey samples (Figure 9B & 9C).

The results are consistent with the literature describing a strong sexual dimorphism in rodents, which resulted much less evident in other mammals [165, 166].

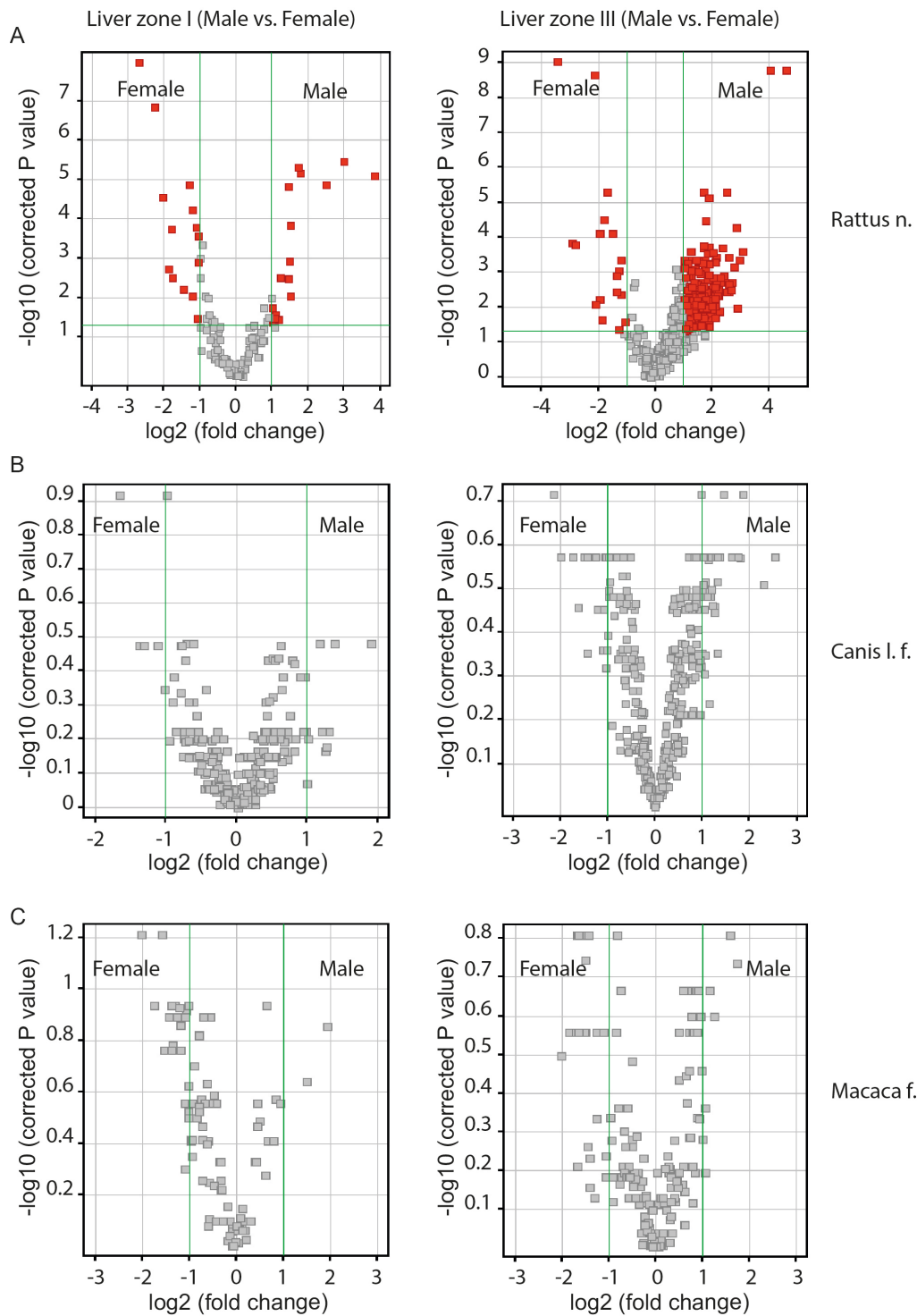


Figure 9: The genes enriched in liver zone I and liver zone III have been screened to verify the existence of a gender specific gene expression regulation. In rats, many genes involved in the liver zonation, were also regulated in different way, in male animals than in female ones. This phenomenon was however not detectable in the other two species (Volcano plot, Mann-Whitney unpaired test, $p \leq 0.05$, FC cutoff 2, multiple testing correction Benjamini-Hochberg).

Cross species comparison

A reliable comparison of genes enriched in specific cell phenotypes across different species is challenging. There are some limitations linked to the technology used in this project and in general to our knowledge of the gene ontology. The annotation of Affymetrix probe sets is regularly updated. Nevertheless, a relative high number of probe sets are not annotated or generically annotated as putative transcript. In a similar manner, the species-specific platforms have different transcript libraries, therefore, genes present on one platform may be absent on another platform. Furthermore, the gene nomenclature is sometime not consistent across the species: orthologous transcripts do not necessarily have the same name in the different species. All this factors are strongly affecting the possibility to compare gene signatures for different species, especially using the GeneChip technology.

We limited our analysis to the transcripts correctly annotated by Affymetrix and which were recognized as orthologous genes by the Agilent software. In order to achieve this result, the software used the human annotation as reference. Rat and dog genes, included in the tissue signatures, were translated to the orthologous human genes and, finally, the resulting lists were compared by a Venn diagram.

Venn diagram in Figure 10 showed the number of genes shared between the species based on their localization.

The analysis revealed only a limited number of shared transcripts enriched or selectively expressed in the bile ducts of all the species (Fig 10A). In some cases this was clearly due to the absence of some transcript in one or some of the gene libraries of the chips (e.g. Krt19 in dog platform) in some other it might be due to an annotation discrepancy, which the software was not able to resolve. We further tried to investigate more in detail this issue of species-specificities providing some examples of genes identified in the bile ducts of some species and absent in the others, validating the transcriptomic data by protein localization.

Similarly, we investigated the similarities in the gene signature for liver zone I (Fig 10B) and liver zone III (Fig 10C).

In all the cases, the number of common genes between species was very limited. Based on this result, it is not clear so far if the data we were able to obtain by this approach and software reflects the reality. Indeed, a so small overlap in the gene expression of the same organ, in mammals, is quite surprising, but the explanation

may be linked to technical limitations more than in a so striking biological diversity between species.

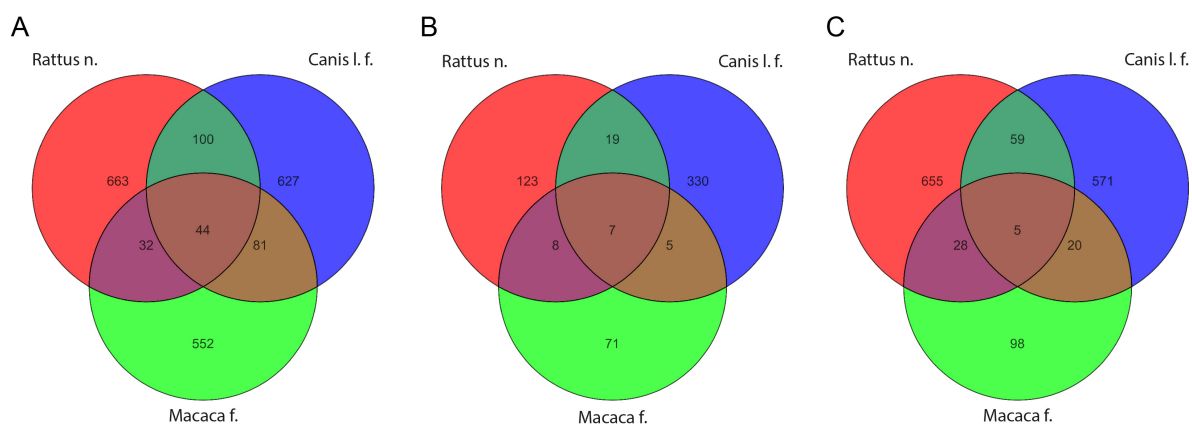


Figure 10: A cross-species comparison of the gene signature identified (A, bile duct signature; B, liver zone I; C, liver zone III) has been performed. Surprisingly, the number of common probe sets across the species resulted very limited. Intrinsic limitations (e.g. gene annotation or orthologous nomenclature) of the technology used in this study might be responsible for the low amount of common genes in same tissues of different species.

Affymetrix expression flag pre-filtering

Affymetrix gene chips are on the market since long time and can be considered a reliable method for the gene expression profiling. One commonly used feature of this platform is the Affymetrix expression flag, introduced with the MAS5 algorithm. This parameter provides an estimation of reliability of the expression data. The use of this parameter improves the specificity of the assay at the expense of the sensitivity, reducing the false positive near or just above the background threshold. However, the use of this pre-filtering methodology, without any consideration of the tissue composition, may result in a loss of precious information. Indeed, low abundant cell phenotypes and their biological processes can be mostly filtered out by this approach.

Taking advantage from the LCM samples, we tried to evaluate the impact of the expression flag pre-filtering on the expression analysis of the whole liver. In the specific, we screened the assignment of the “present” flag within the whole liver transcriptome. We have then evaluated the presence of genes, belonging to the bile duct signature obtained by LCM, in those that received the “present” flag in the whole liver data set. Cholangiocytes represent less than 10% of the total amount of

cells in the liver. Their specific transcriptome is weakly represented in the whole liver transcriptome, due to their low abundance.

The analysis revealed that the application of expression flag pre-filtering on whole liver, resulted in the inclusion of only a limited number of genes, ranging between 2% and 60% (between species), of those genes enriched or selectively expressed in bile ducts (Figure 11; 38 probe sets included, out of 815 probe sets included in bile duct signature for rat; similarly, in dog 412/731 and in monkey 487/800).

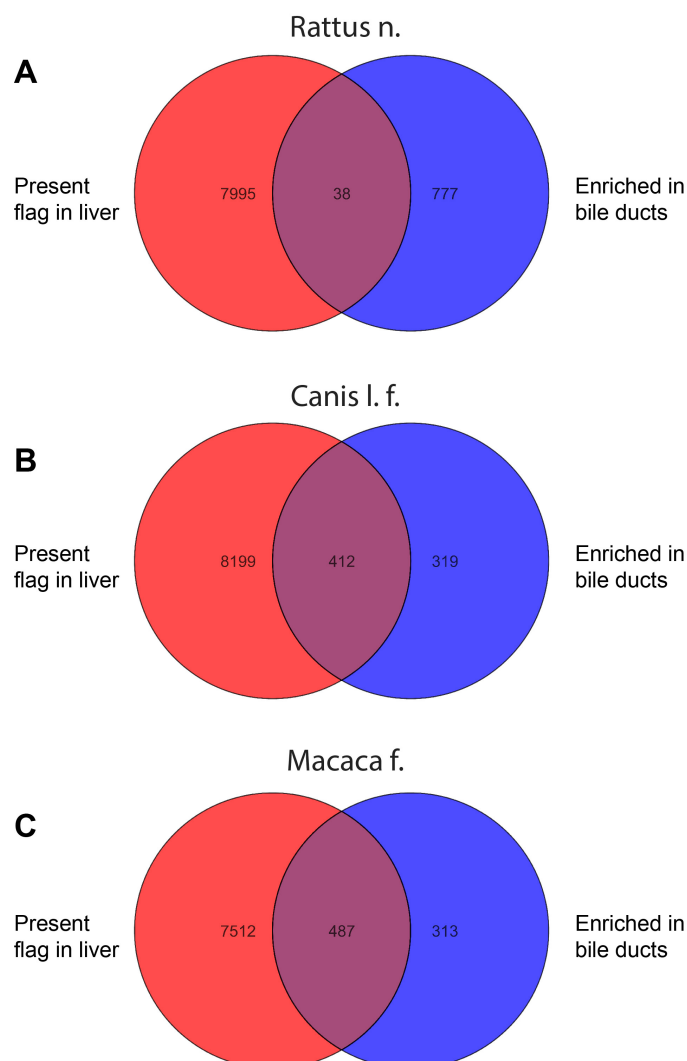


Figure 11: the impact of a pre-filtering based on Affymetrix call flag on the analysis of heterogeneous tissues, and specifically on the expression profile of low represented cell populations. In this example, we analyzed the whole liver scrape data set, excluding from the analysis the probe set which received in 80% of whole liver samples the call flags “marginal and absents”. We then compared the resulting data set with the gene signature of bile ducts. Not surprisingly, the pre-filtering strategy excluded from the analysis a relevant number of those genes. The use of this strategy irrespectively of the tissue composition, may, therefore, lead to the exclusion of relevant

data and consequently to the miss interpretation of biological phenomena affecting low represented cell populations.

These results showed that the application of this pre-filtering excludes data representative of a liver cell sub-population, thus excluding a priori biologically relevant data.

By this way, we showed the massive impact that this approach might have in the study of tissue specificities and the importance to evaluate correctly the sample composition for a correct pre-processing and interpretation of transcriptomic data.

Validation of bile duct gene signatures by immunohistochemistry

Amongst the genes included in the bile duct signatures, according with the criteria described, we identified some genes, expressed in all the species, to validate our gene expression profiles. Considering the low RNA yield obtained by LCM, we decided to validate the signature specificity by immunohistochemistry and not by real time PCR.

However, the number of antibodies commercially available, with a cross-species reactivity, drastically limited the number of candidate target proteins.

We have identified some candidates (keratin 7, 19 and 20, mucin 1 and claudin 6 and 7), we have exported the expression values from the transcriptomic data sets and verified their statistical significance (BD vs whole liver). Finally, we have localized the corresponding proteins in situ.

We have localized keratin 7, keratin 19 and keratin 20 in FFPE liver sections of control animals by immunohistochemistry (Figure 12, gene expression profile for each single marker, gene enrichment in bile ducts vs. whole liver, multiple t-test analysis corrected for multiple comparisons with Bonferroni-Dunn method).

Keratin 7 is a well-known marker of epithelial tissues. Indeed, our IHC confirmed the localization of this protein in the bile ducts of all the species, in agreement with the expression data.

Similarly, also keratin 19 is a marker of epithelium and this protein was expressed in intrahepatic cholangiocytes in all the 3 species. Interestingly, the Canine chip from Affymetrix lacks the probe set for this specific transcript, so we were not aware of the gene expression profile relative to the keratin 19 in dog livers.

Keratin 20, as the previous ones, is a marker of epithelium, but the localization of this protein revealed some differences across the species in analysis. Indeed, while the gene and protein were expressed in the cholangiocytes in rat, the transcriptomic data revealed no significant differences between bile ducts and whole liver in dog. Accordingly, the protein was not detectable in dog liver.

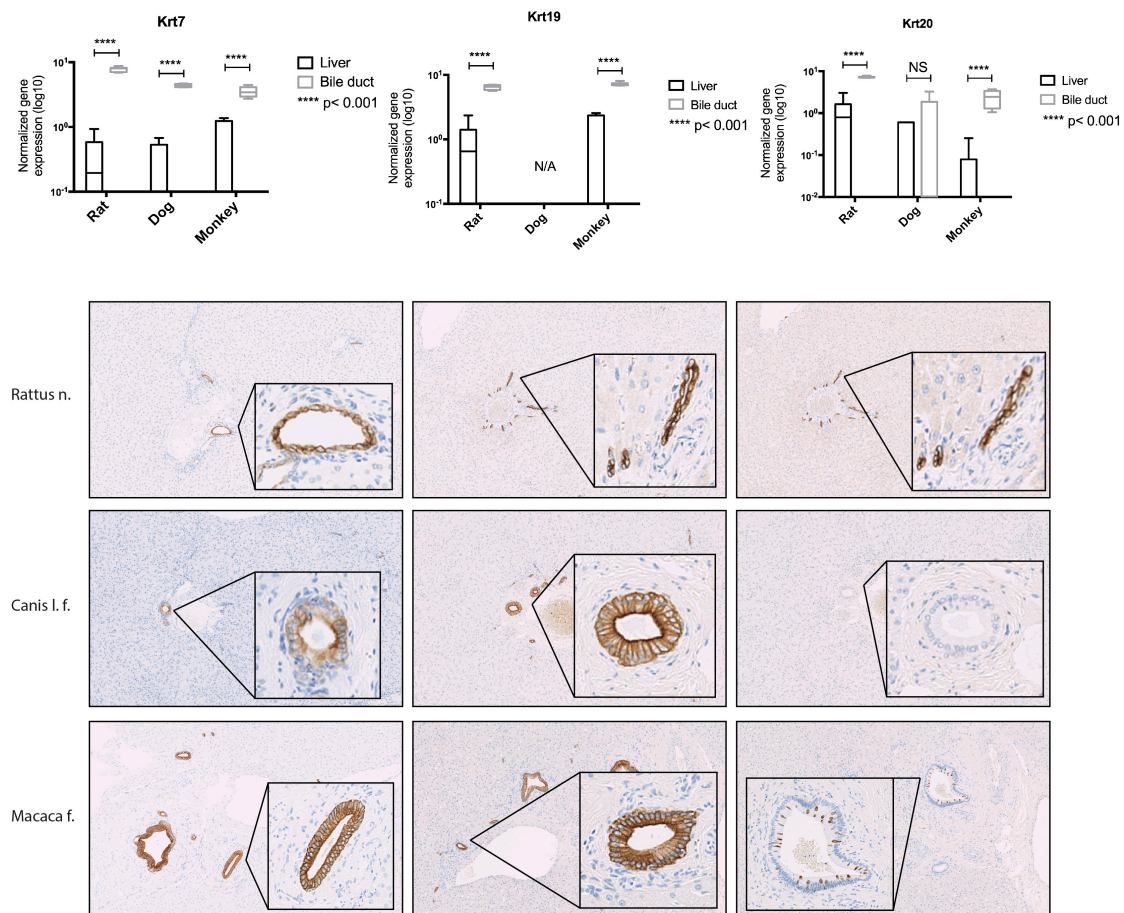


Figure 12: Validation of the bile duct signature specificity. Three genes (Keratin 7, Keratin 19 and Keratin 20) have been selected among the genes included in the bile duct signature. A significant enrichment has been shown in LCM samples vs whole liver (t-test, corrected for multiple comparisons with Bonferroni-Dunn method; **** p<0.001). To validate the signature, the corresponding proteins have been localized in the livers of the 3 species. Accordingly, with the expression data, proteins have been found only in the bile ducts in all the species.

Ultimately, transcriptomic data showed a significant enrichment of keratin 20 in the bile ducts of Macaca f, however, in our first analysis we observed only a limited number of bile ducts positive for this protein. A more accurate analysis revealed that terminal branches of bile ducts (Figure 13A), in Cyno monkey liver, resulted

negative for the Keratin 20, but the frequency of positive cells increased together with the size of bile ducts (Figure 13B). This gradient of expression reached the gall bladder, which was completely positive for keratin 20 (Figure 13C) and represent one of the species specificities we wanted to explore by this project.

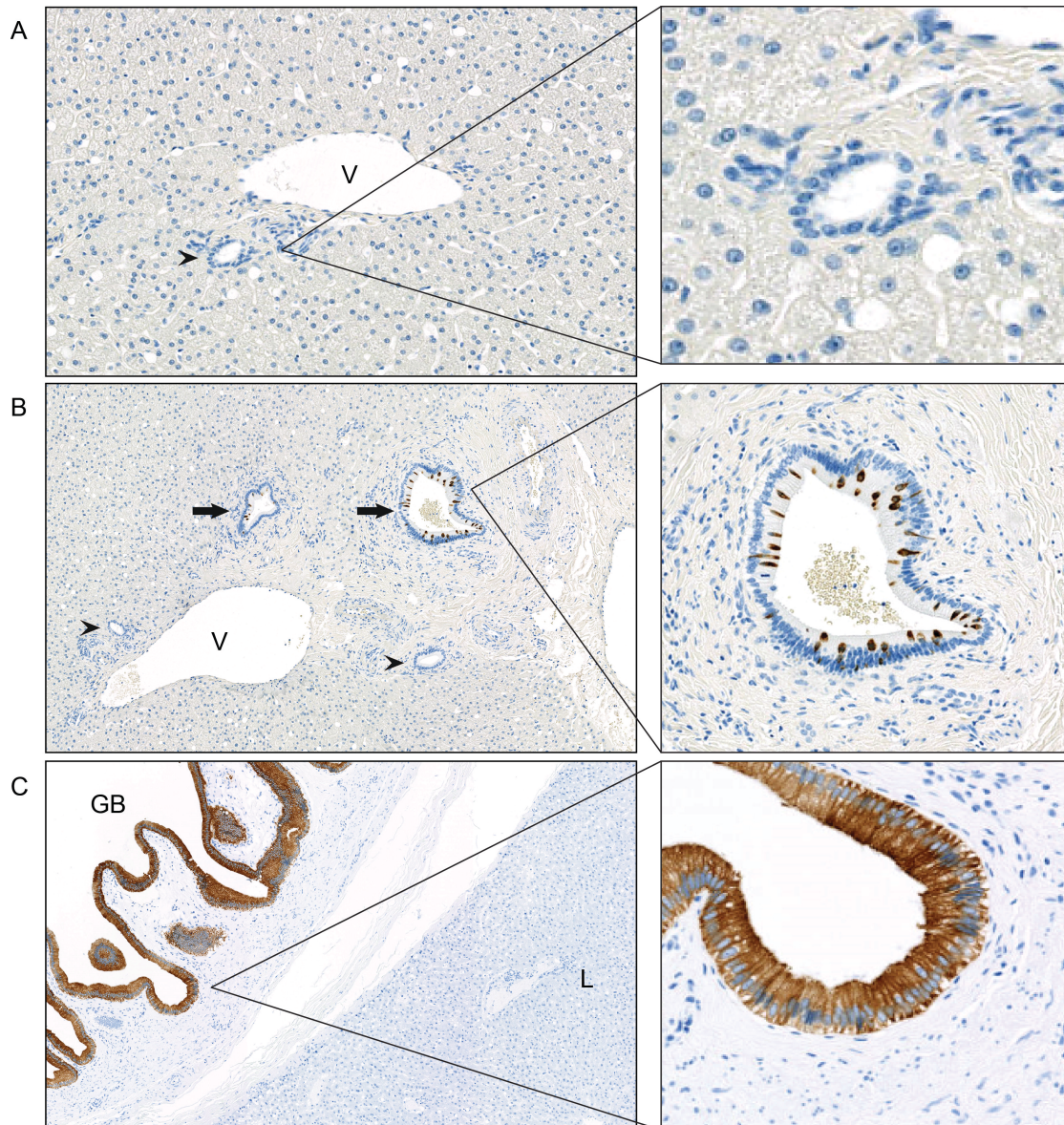


Figure 13: the peculiar Keratin 20 gene/protein expression in the monkey liver (labeled as L) and in the gall bladder (labeled as GB). In these pictures we have shown the absence of the protein in the small terminal branches of bile duct (A), the expression in few cells in the bigger intra hepatic bile ducts (B) and finally, the expression in all the cells in the gall bladder (C). This peculiarity has been never described so far and was observed only in monkey in this study.

Similarly, we localized also protein poorly described in the liver: Mucin 1, Claudin 6 and Claudin 7 (Figure 14).

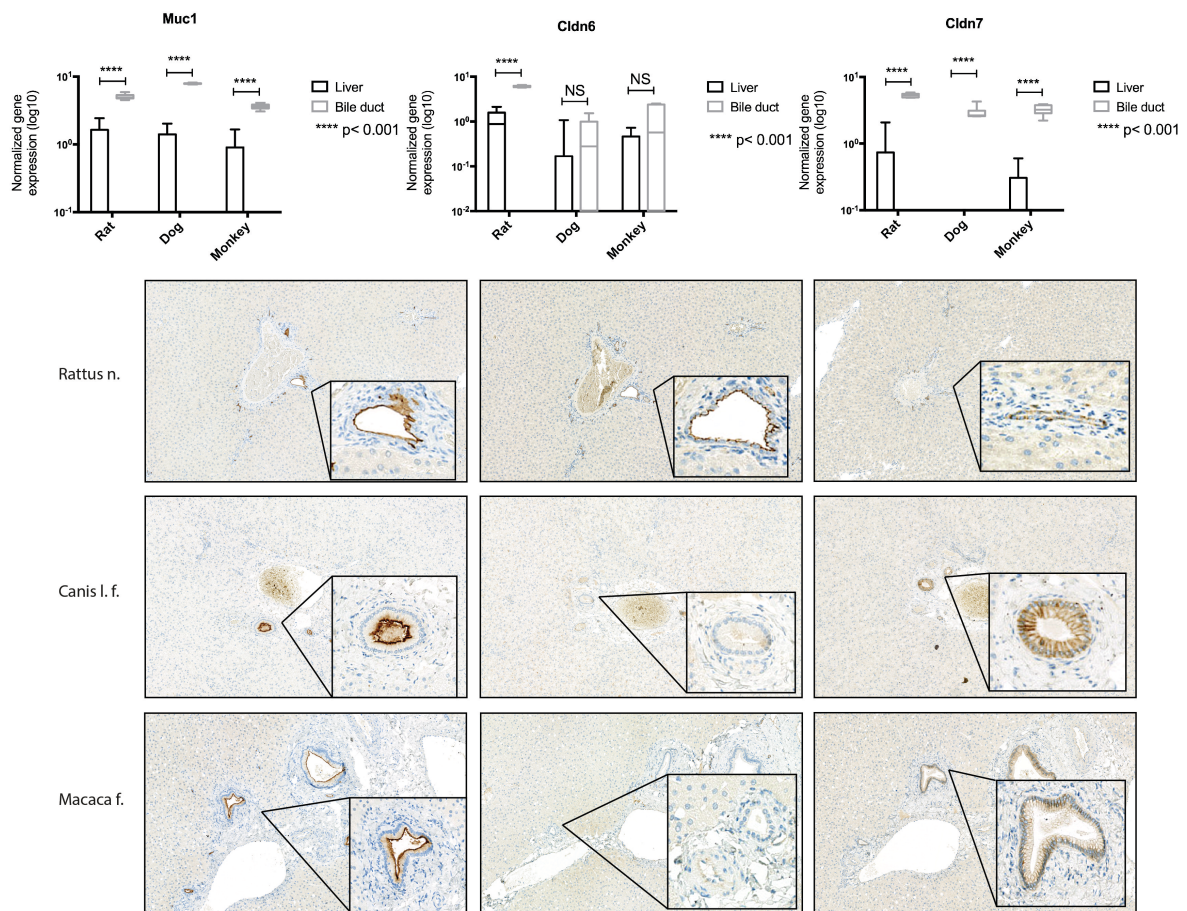


Figure 14: Additional three genes (Mucin 1, Claudin 6 and Claudin 7) have also been selected among the genes included in the bile duct signature. A significant enrichment has been shown in LCM samples vs whole liver (t-test, corrected for multiple comparisons with Bonferroni-Dunn method; **** $p < 0.001$). Mucin 1 and Claudin 7 were expressed in the bile ducts in all the species, confirming the expression data. Claudin 6 was significantly enriched only in rat bile ducts. The protein localization confirmed also this data, showing a strong specificity of the expression profiling in LCM samples.

Mucin 1 gene was strongly enriched in all the species in the cholangiocytes derived by LCM. The protein localization confirmed the transcriptomic data. The protein showed also a peculiar apical expression in the bile ducts.

Claudins are a family of proteins present in the tight junction of epithelia. In the liver Claudin 1 has been extensively studied, due to its function as HCV receptor and entry factor, but the function and the specific localization of other members of this family is rather unknown.

LCM data showed an enrichment of Claudin 6 in rat bile ducts, while in dog and monkey we did not observe significant differences.

The protein localization indeed revealed that Claudin 6 is expressed only in rat bile ducts. A minimal expression however was also observed in small artery endothelium and this faint positivity was common in all the species. A deeper investigation revealed that this species specificity was not limited to rat cholangiocytes, while also other rat cubic epitheliums (i.e. thyroid epithelium, Fig 15) showed Claudin 6 expression.

Claudin 7 belongs to the same protein family of Claudin 6, however, this gene showed a different profile. The gene was enriched in bile ducts of all the species and the protein was localized according with the gene expression profile.

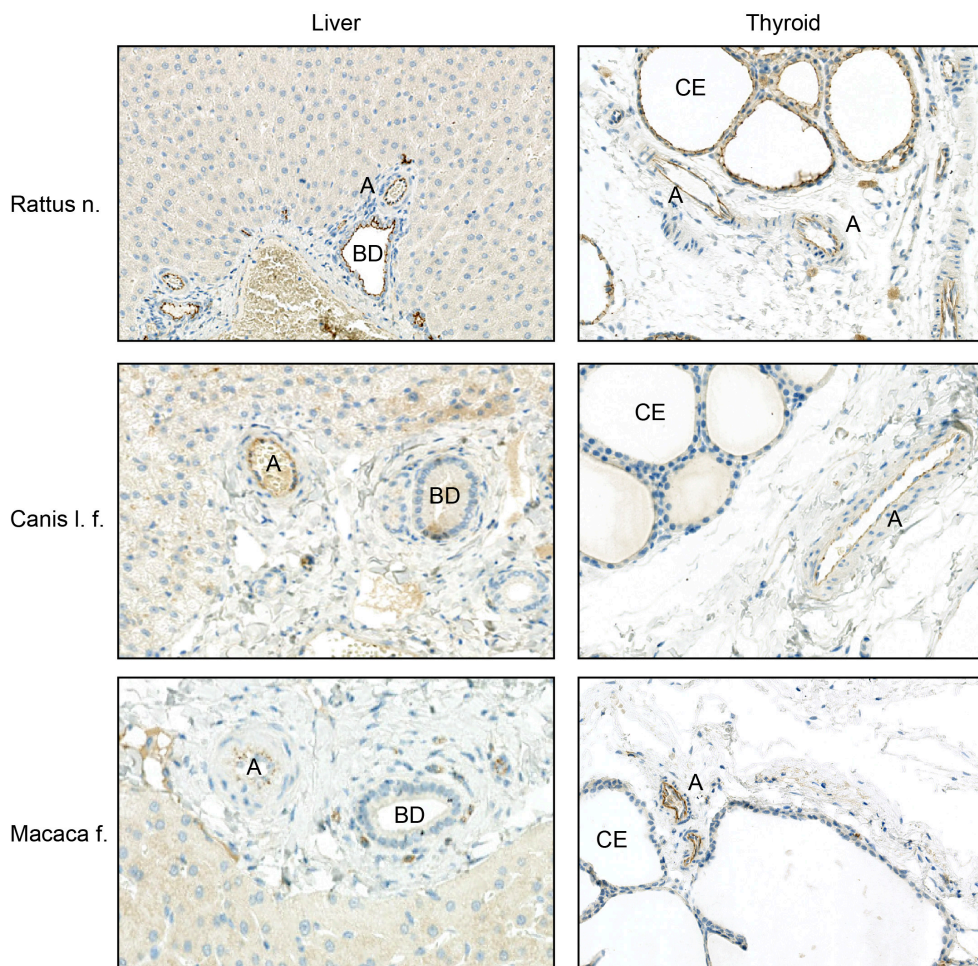


Figure 15: The Claudin 6 has been identified as a gene enriched in bile ducts (BD) in rats. In this species its expression is common in all the cubic epithelia (CE), like the thyroid epithelium, as shown in these pictures. Surprisingly, in the other two species, both the bile duct and the thyroid epithelia

resulted negative for this protein, which is indeed expressed from smooth muscle cells in the tunica media of the small arteries (A).

Genes and protein selectively expressed in liver zone I or zone III

The liver zonation is a phenomenon well known for many years, therefore it is not surprising that many genes and proteins have been described as expressed in a specific location in the liver parenchyma. We have mentioned in the introduction some of the pathway involved in the establishment of the liver zonation. One gene downstream in the WNT pathway is the glutamine synthetase (GLUL). The localization of the corresponding protein is used as diagnostic tool for some liver malignancies. Indeed in most of the hepatocellular carcinomas, the WNT/ β Catenin pathway is strongly altered, which results in the perturbation of the liver zonation. In those cases, the Glutamine synthetase, which is normally expressed in a tiny layer of hepatocytes around the central vein, will then be expressed from most of cells in the parenchyma. Here we have localized the Glutamine synthetase in all the 3 species in normal livers, and the localization, as expected, was in a limited number of pericentral hepatocytes (Figure 16A, rat liver; B, dog liver; C, monkey liver).

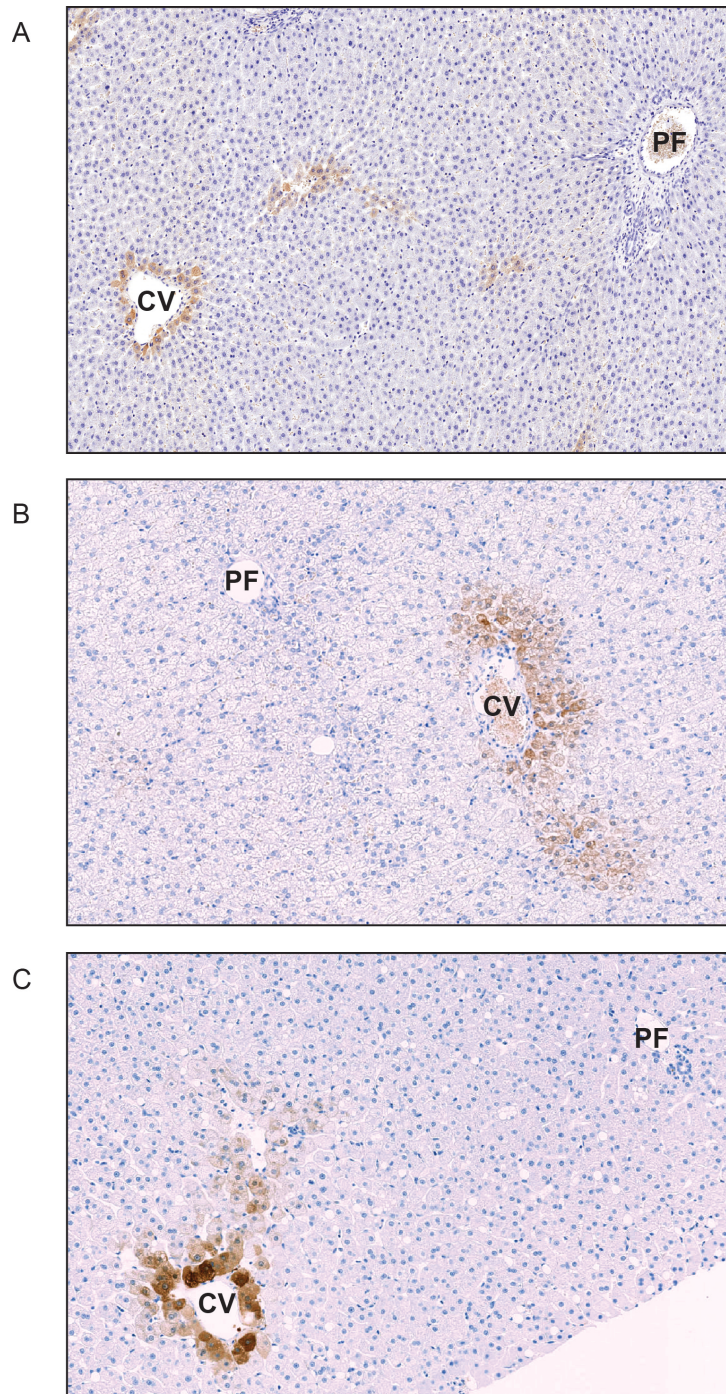


Figure 16: Glutamine synthetase localization in normal livers of the 3 species (A, rat; B, dog; C, monkey)

It is not in the aim of this study to describe all the genes/protein expressed selectively in only one area of liver parenchyma, but we found one gene in the analysis of gender and zone specific expression, which showed a very characteristic profiles. The Lysyl oxidase (LOX), also known as protein-lysine 6-oxidase resulted selectively expressed in liver zone III of only male rats.

We therefore wanted to localize the corresponding protein, in order to validate its peculiar profile. In Figure 17 A we can observe the localization of this protein in a male rat liver. In agreement with the transcriptomic data (data not shown), the protein was expressed only in pericentral area. In female rat liver, indeed, the protein was almost not expressed. Lysyl oxidase is an extracellular copper enzyme that catalyzes formation of aldehydes from lysine residues in collagen and elastin precursors. The protein localization was mainly extracellular, which match perfectly with the biological function of this enzyme.

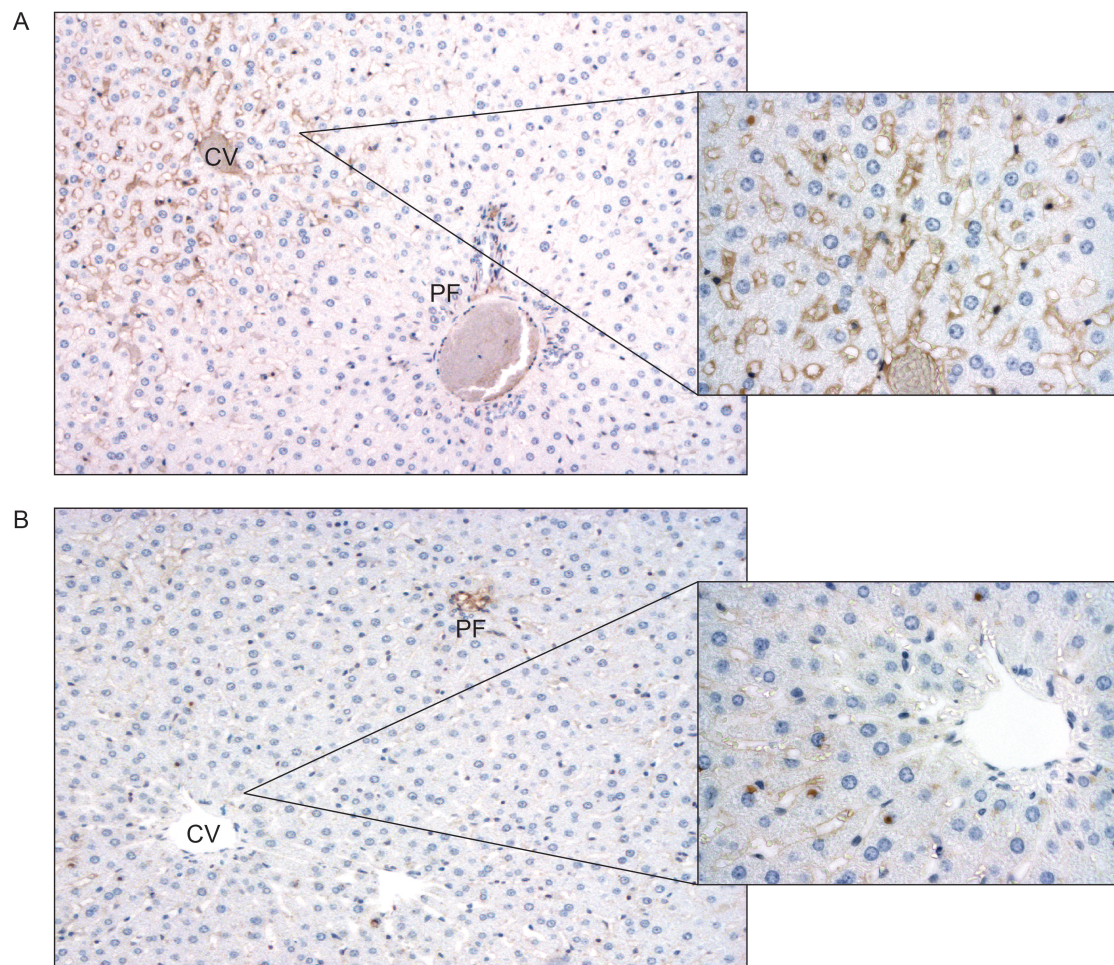


Figure 17: The Lysyl oxidase localization in male (A) and female (B) rat livers. Signal was detectable only around the central veins (CV) in male rats and, sometimes, within the portal fields (PF).

Based on the peculiar localization of the Lox protein, we investigated the presence of a substrate for this enzyme, which might have had the same peculiar localization in rat liver. Indeed, we found that the Collagen 1A1 also showed a zone and gender

specific profile, thus we decided to validate the transcriptomic data by localizing the corresponding protein.

In Figure 18 we showed the localization of the Collagen 1A1 protein in male (A) rat liver and in female (B) rat liver. Similarly to the Lox protein, also in this case, accordingly with the biological function of this protein, its localization was exclusively extracellular.

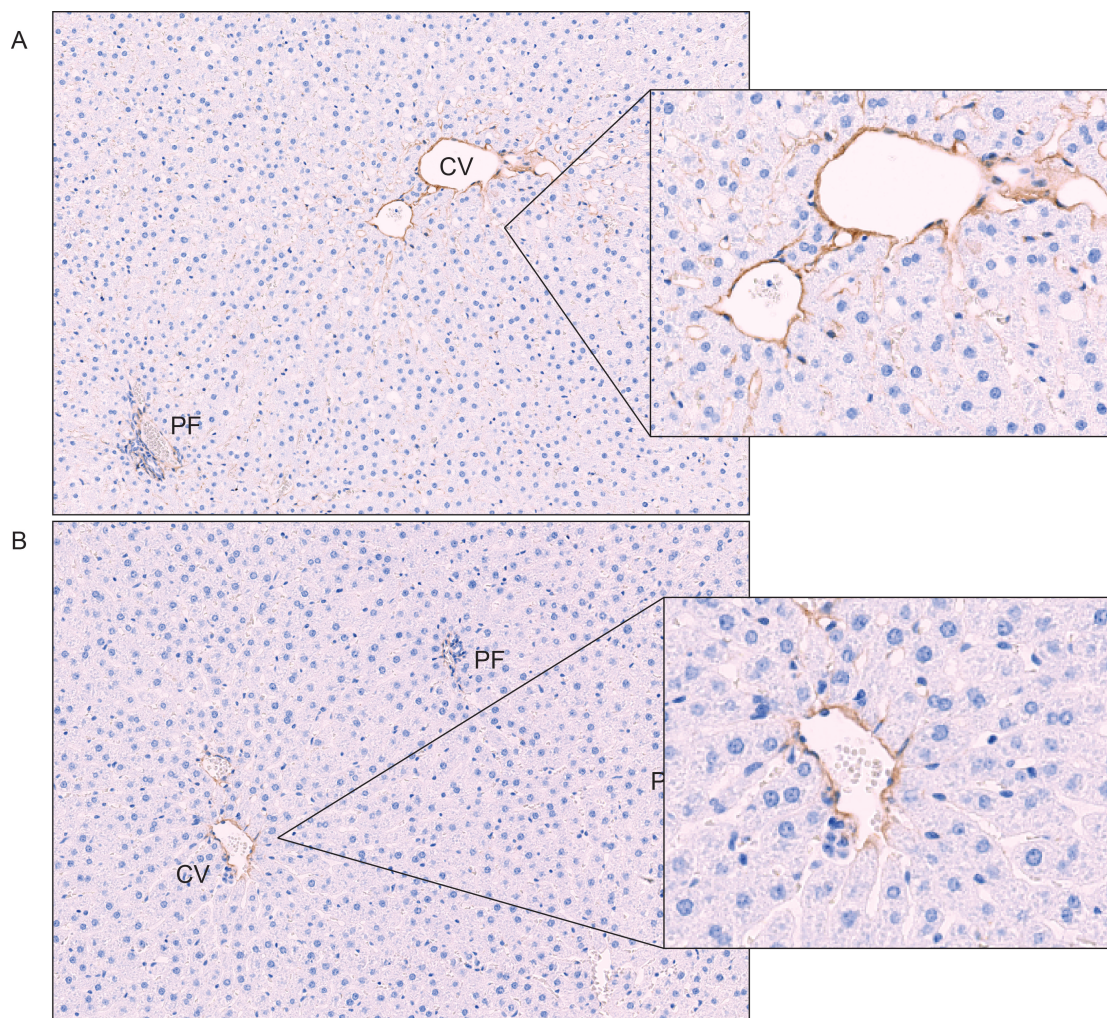


Figure 17: The Collagen 1A1 localization in male (A) and female (B) rat livers. Collagen 1A1 was more abundant in male rats than in female rats, and in both the cases, the protein was localized in the pericentral area (CV, central vein; PF, portal field).

Methapyrilene study: transcriptomic analysis based on data generated by independent LCM experiment

As a case study for the application of the knowledge generated from the analysis of the LCM samples, we retrospectively analyzed a study performed on a reference compound withdrawn from the market due to its carcinogenicity in rodents:

Methapyrilene. We performed an analysis of the whole liver transcriptomic profiles using the various structure-specific gene signatures established previously. We wanted to prove that making use of the knowledge generated by LCM, we may identify the cell type affected by the toxicity, based on whole tissue transcriptomic profiles. Conceptually, the use of LCM profiles, allows a “conscious” analysis of whole tissue transcriptomes, allowing the identification of phenomena occurring at the level of different cell populations. Thus, the (comparative) analysis is not strictly dependent on the statistical significance anymore. In this respect, changes in the expression of groups of genes belonging to a specific gene signature, although not statistically significant, can give indications on the target site of toxicity. The validation of these findings, then, is no longer delegated (only) to statistical significance of the transcriptomic profile, but to further in situ investigations.

The study included 96 SD rats, treated daily by oral administration of the drug or vehicle (H₂O).

The drug administration lead to no unscheduled death and only thin appearance of sufferance were detectable in 2 of the 6 animals treated with 60mg/kg/day for 14 days.

The histopathological analysis revealed minimal histological changes in all the treated groups, including increase of mitotic figures, minimal single cell necrosis, and a dose and time dependent bile duct hyperplasia (ductal reaction), detectable in all the conditions, but graded as minimal by the pathologist. None of the animals developed neoplasia.

The initial study design included 4 time-points, as described in material & methods: day 1, day 3, day 7 and day 14. However, during the quality control of the transcriptomic data, the principal component analysis revealed that the samples collected at the first time-point clustered all together, but they showed massive differences in comparison with the other groups (Figure 18).

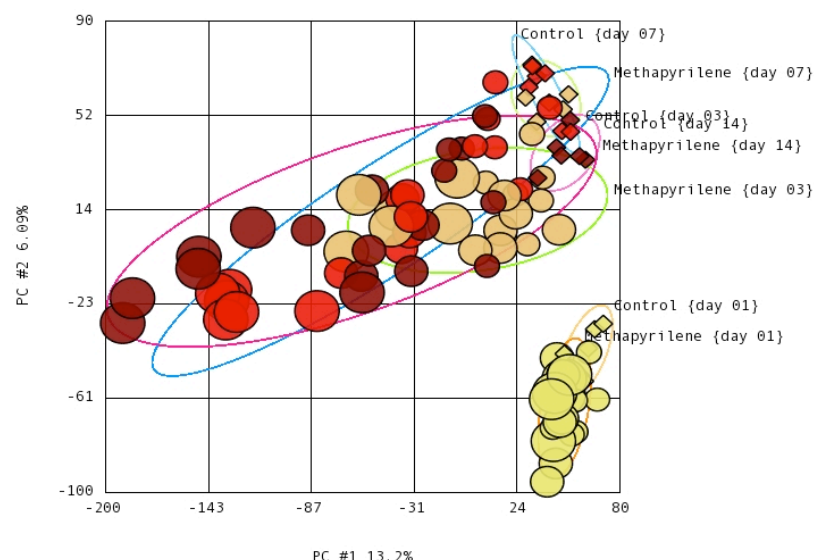


Figure 18: Principal Component Analysis of all samples included in the Methapyrilene study. The sample collected at first time-point showed clear dissimilarities compared to the rest of samples (PCA performed by Dr.. Eleine Tritto).

A deeper analysis revealed, indeed, big differences within the controls (266 genes differentially expressed between the controls at day 1 and the controls at the other time-points, data not shown). Thus, due to the high variations within the controls, we considered the samples of the first time-point as not reliable and we excluded them from the following analysis.

The transcriptomic data were pre-processed as described in material and methods and analyzed by Agilent Gene Spring software.

In order to understand if the drug treatment induced a specific pattern of expression, with one or more pathways involved, we performed a gene and sample clustering analysis (Hierarchical clustering, Euclidean distance metric and complete linkage).

The analysis revealed the absence of specific pattern of gene expression, highlighted by a random and non-patterned distribution of genes and sample in the heat map (Figure 19A).

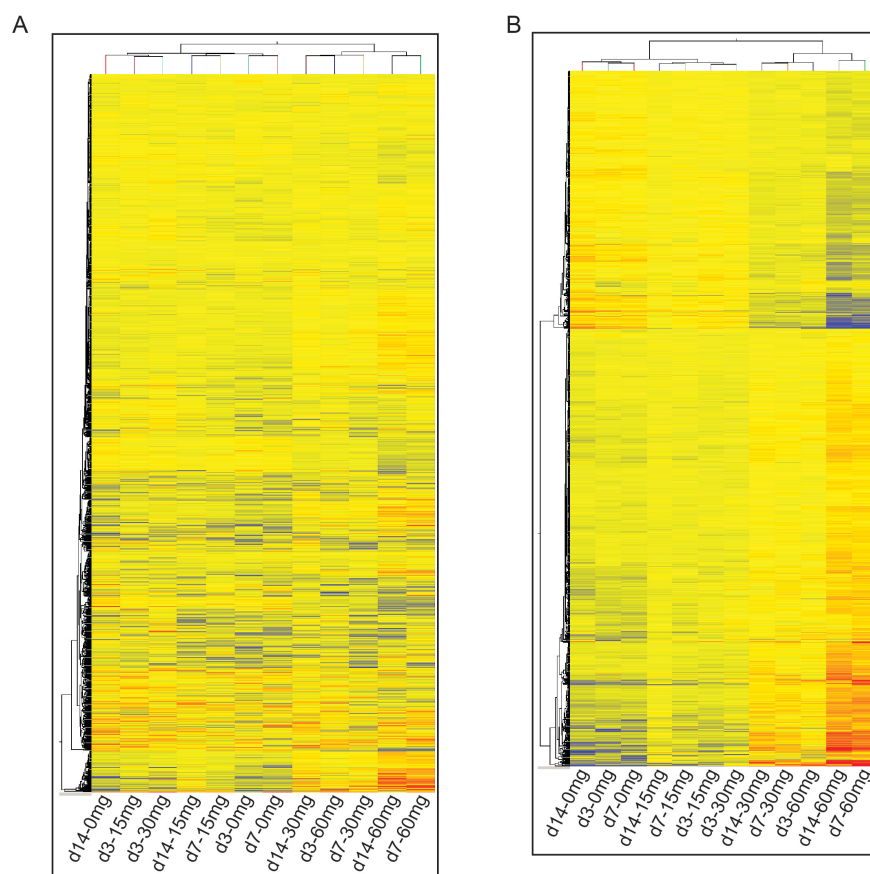


Figure 19: Clustering analysis of the transcriptomic data set from controls and Methapyrilene treated samples (A). Gene differentially expressed (controls vs. treated) were identified by an ANOVA test. However, also restricting the clustering analysis to the differentially expressed genes, it did not emerge any specific pattern of expression (as demonstrated by the short metrical distance in the hierarchical tree) (B). This is indicative that the drug induced only subtle molecular changes and did not massively impact the gene expression profile.

To reveal changes with a statistical relevance we performed an ANOVA analysis, comparing all the treated samples with the corresponding control (per each time-point, controls vs. 60 mg treated; one way ANOVA, $p \leq 0.05$, Tukey honest significant difference [HSD] post-hoc test, Benjamini-Hochberg multiple test correction), which identified 8608 probe sets with a significant differential expression. We then repeated the clustering analysis on this significant sub set of probes (Figure 19B). Despite the reduction of the probe set number and their significant regulation, the clustering revealed again the lack of a driving pathway. A very general increase in the gene expression value was observable in the samples treated with the highest dose at day 7 and day 14 (Figure 19B).

The principal component analysis confirmed the absence of a driving force regulating the gene expression. Indeed, samples did not cluster together, but they were rather randomly distributed in the plane (Figure 20).

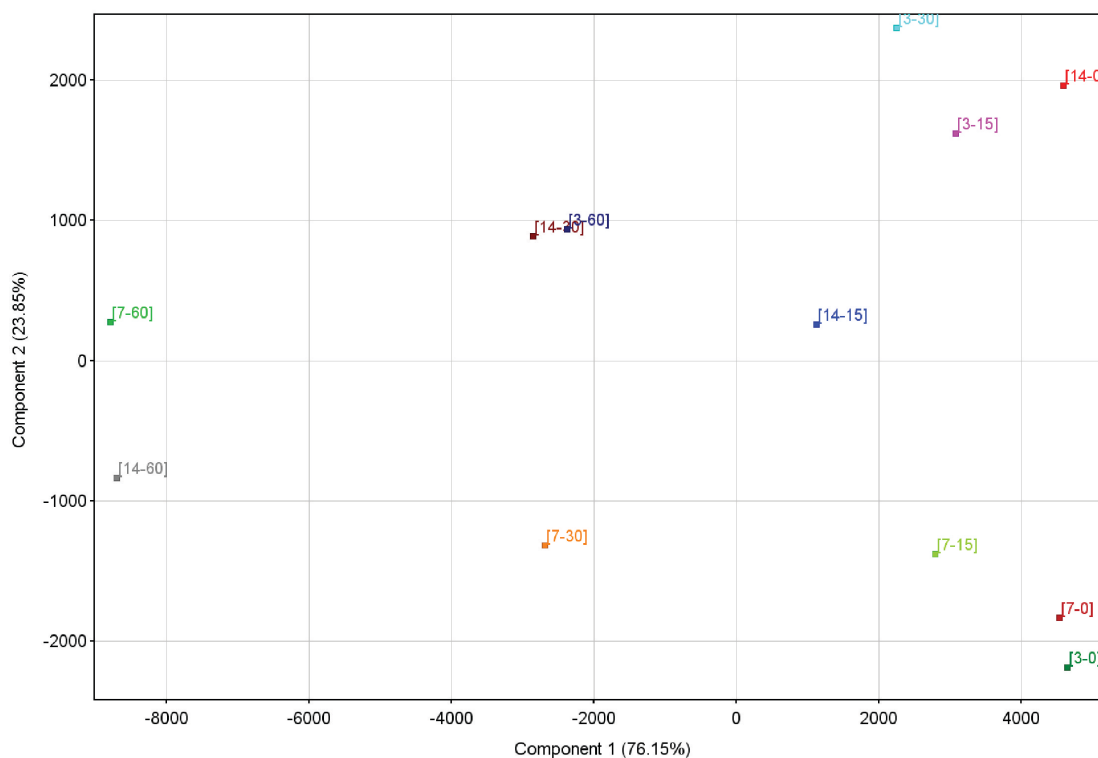


Figure 20: The principal component analysis revealed a dose-dependent distribution of samples in the plane. However, the lack of clusters containing samples with similar features is, again, indicative of small molecular changes and the lack of any driving pathway induced by the drug (index structure: [time-point-dose (mg/kg/day)]).

In our analysis, we were interested in understanding if the knowledge generated by the laser capture microdissection on normal liver might have been useful for addressing a specific tissue, impacted by the drug treatment. We therefore identified the genes induced by the drug and verified their link with a specific liver tissue, by using the gene signature generated by our LCM sample analysis.

We therefore selected the genes up regulated ($>2FC$, from those resulted significant in the previous ANOVA test) at all the time-points, in the animals treated with the highest drug dose, in comparison with their corresponding controls (Figure 21), generating gene lists specific per each time-point.

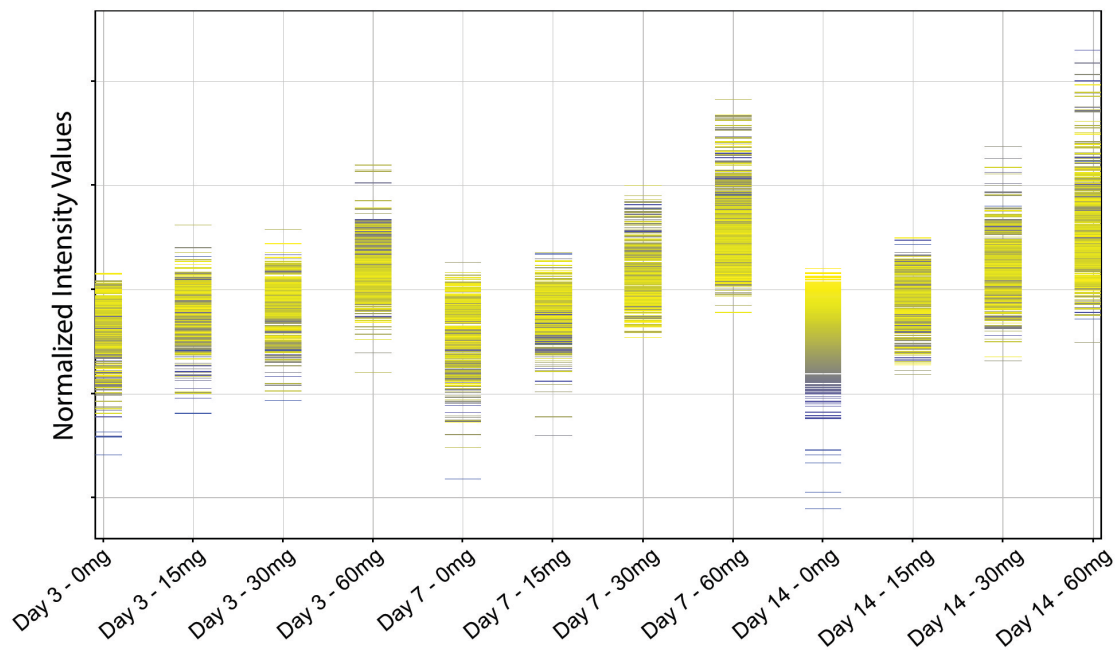


Figure 21: bar plot showing all the genes up regulated upon the drug administration (FC>2 in controls vs. treated with 60mg/kg/day, at all time-points).

We then compared together those gene lists by a Venn diagram. Beside few genes expressed selectively in one or few conditions, most of them (1561 transcripts) were common in all the 3 time-points. They represented the transcripts up regulated by the treatment with Methapyrilene (Figure 22).

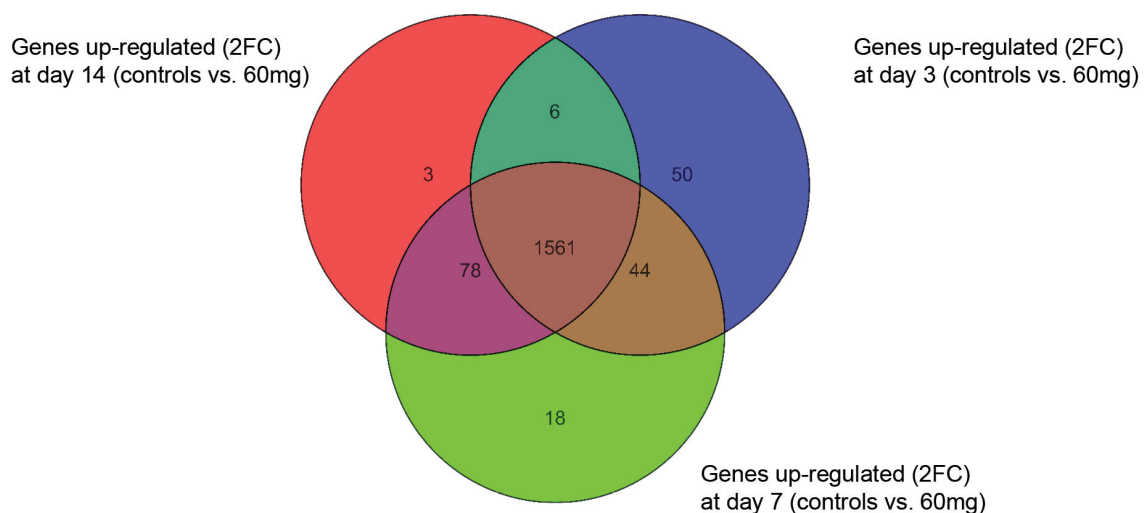


Figure 22: using a Venn diagram we compared the list of genes up regulated at different time-points. 1561 transcripts were up regulated in all the time-points.

We then compared those 1561 genes with the genes included in the bile duct signature, generated from the LCM samples. This comparison revealed an abundant number of common genes (Figure 23 A).

More in detail, we analyzed the number of genes present in the bile duct signature and up regulated at the different time-points of the treatment. Indeed the number of those genes was almost constant in all the time-points (120 at day 3, Figure 23B; 131 at day 7, Figure 23C; and 132 at day 14, Fig 23D). Despite the need for a validation of these findings, this approach provided a specific indication of the cell type interested by the drug induced molecular changes, supporting the histopathological analysis and predicting this finding at an earlier time-point.

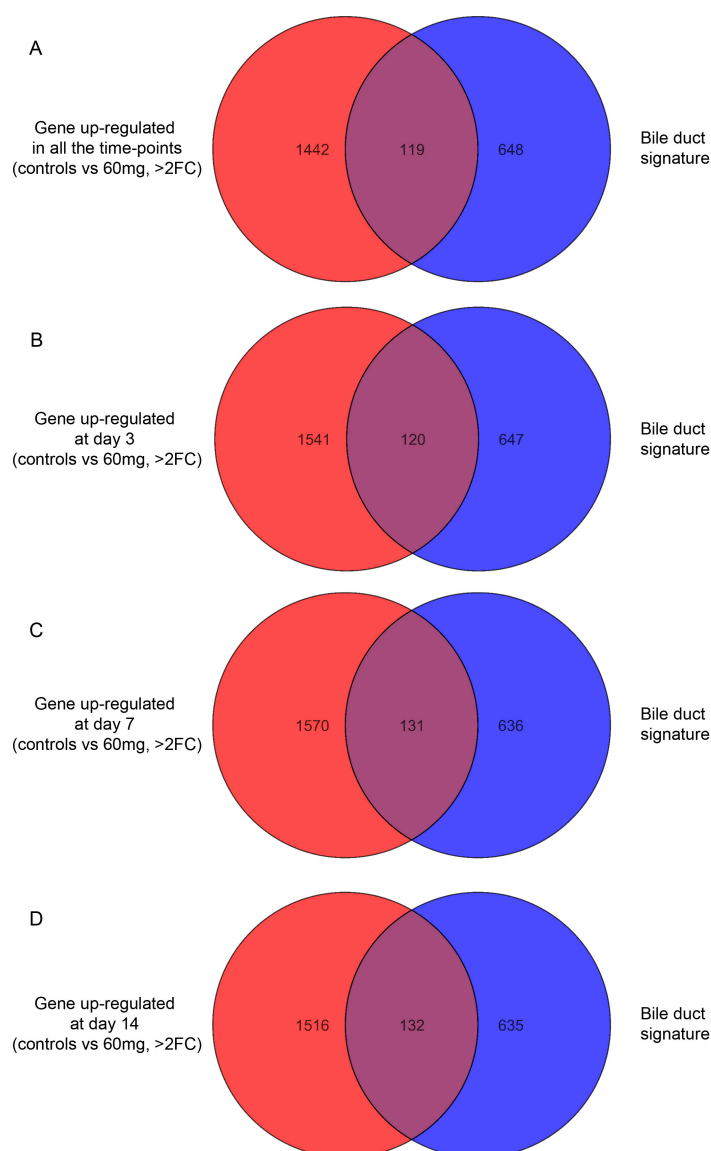


Figure 23: genes belonging to the bile ducts signature, up regulated in animals, treated with Methapyrilene, at different time-points.

Immunohistochemistry and image analysis on methapyrilene treated samples

Validation of gene regulation in bile ducts

In order to validate the involvement of bile ducts, predicted from the metadata analysis, in the phenomena induced by the drug treatment, we performed the immunolocalization (IHC) of some validated marker of bile ducts.

Specifically, we used antibodies against Keratin 19 and Claudin 7. As previously described, both the genes, and the derived proteins, are selectively expressed in the liver bile ducts. Indeed, also in the animals included in this study those markers showed their specificity as shown in the Figure 24 and 25.

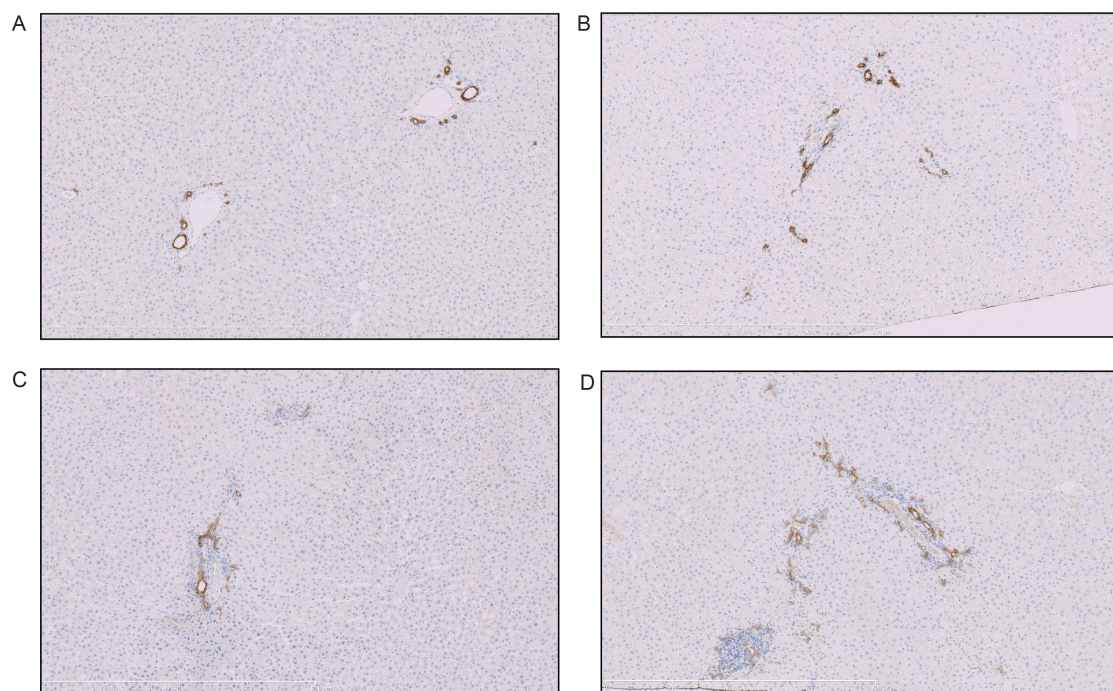


Figure 24: Keratin 19 localization in control (A) and treated animals (60mg/kg/day) at day 3 (B), day 7 (C) and day 14 (D)

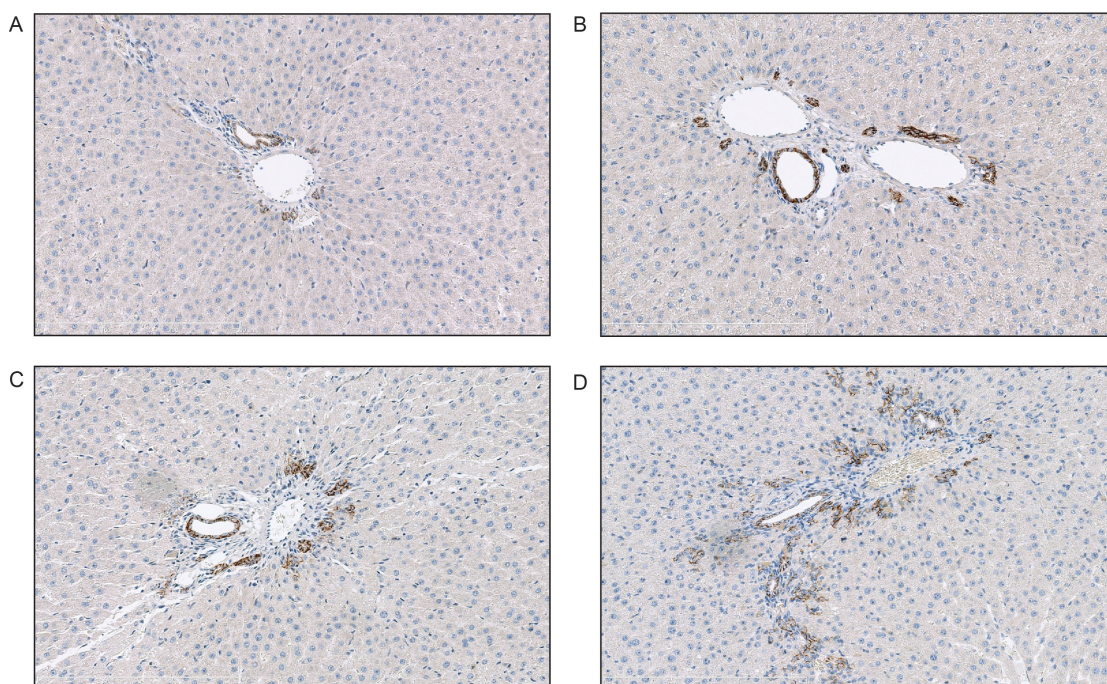


Figure 25: Claudin 7 localization in control (A) and treated animals (60mg/kg/day) at day 3 (B), day 7 (C) and day 14 (D)

To quantitatively evaluate the increase of the proteins in the treated animals, we performed an image analysis on the IHC pictures acquired in bright field microscopy. In order to isolate the signal from the RGB images, we applied an algorithm for color deconvolution (Figure 26). This step allowed the isolation of the signal derived for the chromogenic staining. The signal has been then converted in binary pictures and therefore we quantified the area covered from the cells labeled with the specific marker.

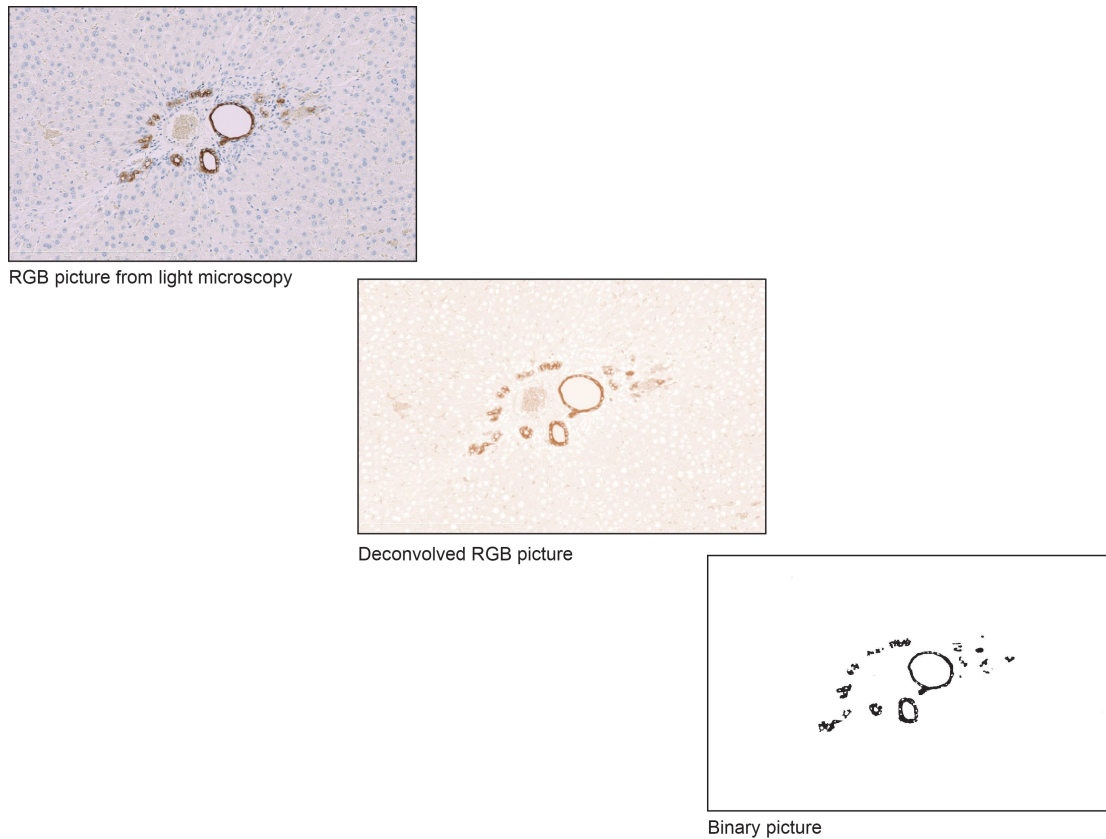


Figure 26: the image analysis steps, leading from an RGB picture acquired at brightfield microscope, through the color deconvolution, for the isolation of the region of interest (ROI) and finally to the binary conversion. This process allowed the quantification of the area covered by bile ducts in controls and in treated animals.

The image analysis revealed an increase of both the proteins at all the time-points. This increase was statistically not significant at day 3, neither for Keratin19, nor for Claudin7, however, it was significant at day 7 and day 14 (Fig 27, average of 3 fields per each time-point, \pm SD; multiple t-test, significance corrected for multiple comparison by Holm-Sidak method, $p \leq 0.05$).

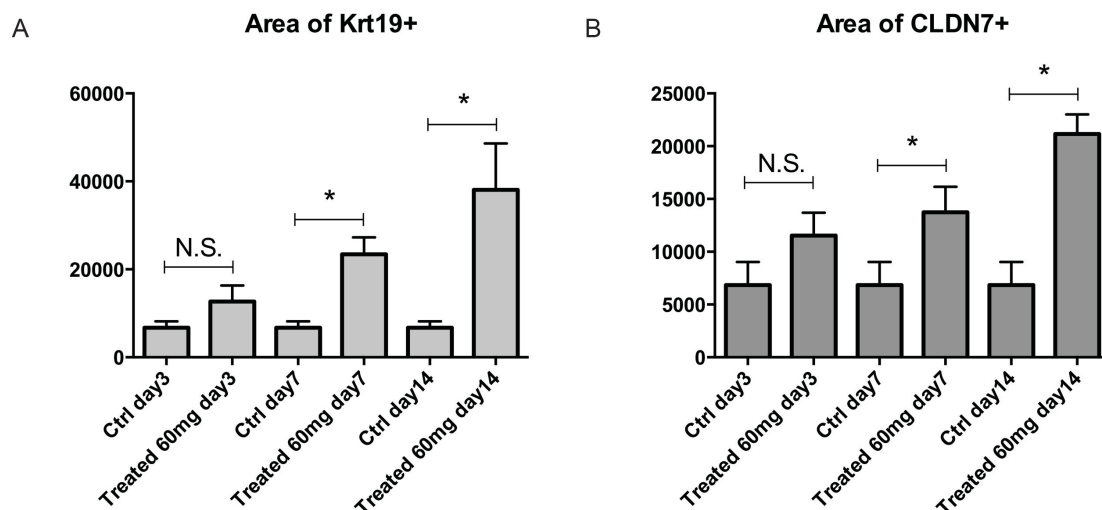


Figure 27: the graphs represented the area (average of 3 fields per each time-point, \pm SD) covered by the cells labeled with the respective antibodies against the Krt19 and Cldn7 (multiple t-test, significance corrected for multiple comparison by Holm-Sidak method, $p \leq 0.05$).

This data confirmed the involvement of the bile duct in the phenomena induced by the drug. Indeed, the drug is inducing a ductal reaction, a proliferation of biliary epithelial tissues outside the portal tract. This hyperplasia was correctly detected by the increase of the area corresponding to the cells labeled by both the antibodies at all the time-points. Despite this data validated the histopathological analysis and, most important, our findings from the transcriptomic metadata analysis, due to the lack of significance at day 3, we can conclude that the predictive power derived from the IHC investigation was limited to conditions in which the phenomena were likely detectable by a trained veterinary pathologist, thus resulting less sensitive than the metadata analysis, which, using the bile duct signature, identified comparable molecular changes in all the time-points.

Discussion

Nowadays, the pharmaceutical companies invest conspicuous capitals in the development of new compounds. This is a long process (one decade in average), which rarely (less than 10% of the compounds) leads to the commercialization of a new drug [167].

As largely discussed, preclinical toxicological studies are routinely performed in order to explore all the possible risks associated with new compounds. In this respect, all the drugs on the market have a well-defined safety profile, considered as acceptable for a given indication.

The general improvement of the investigative methodologies has led to an increase of the drug safety (and also a corresponding decrease of the drugs reaching advanced preclinical phases and/or on the market) [168].

The introduction of high-throughput screening methods allowed the simultaneous detection of thousand parameters in one single assay.

The use of those technologies for exploring the genomic, transcriptomic, proteomic and phosphoproteomic aspects of biological samples, in the context of a toxicology study, is frequent (reviewed in [169-171] and in [172-174]). Intuitively, the reason is that the possibility to explore the state of a tissue from multiple angles increases the likelihood of understanding the effects of a compound.

However, the interpretation of such a multi-modal picture might not be so immediate if the sample in analysis is not pure.

Indeed, while those methods provide insight about the transcriptomic and/or the proteomic of the sample in analysis, the data they produce is not usually used to infer information about cellular composition of the sample and the contribution of each single cell type in the global picture.

In the context of the -omic data analysis, the tissue deconvolution, meant as an analytical process able to decompose a tissue in its components, attributing to each of them a fraction of the total, in a proportional manner to the relative abundance of the components and/or to the magnitude of a phenomenon, is a very challenging activity that researchers are called to sort out.

Despite that many groups have attempted to approach this issue *a posteriori*, using statistical and mathematical methods [144-147], the reality is that those

approaches require at least a validation phase, based on experimental data derived by pure tissues or cells.

On the other hand, the use of in vitro systems or the collection of pure cell populations from tissue, with some available methods, is controversial, if the aim is to reproduce the features of the original organ.

The use of in vitro system, based on primary cells or on immortalized cell lines, has shown significant limitations in resembling normal tissues. Essentially, primary cell lines are low representative of the derivative tissues due to the batch-to-batch variations, and their availability is determined by the organ donations. Immortalized cell lines derive, in most of the cases, by tumor tissue, and, in the time (decades), they became monoclonal, losing in fact the cell heterogeneity, typical of the heterogeneous tissues. Additionally, the culturing conditions strongly influence the cell phenotype.

The isolation of cells from tissue by enzymatic methods may by itself induce changes in the gene expression profile and in the phosphorylation state of many proteins, resulting therefore low representative of the tissue physiological steady state.

This aim of this study was to generate the knowledge necessary to operate the tissue deconvolution of the liver.

To achieve this objective, we created a map of gene expression of the liver.

This map can be considered as a primordial and essential step to further understand mechanisms of drug injury.

Other authors have described the gene expression in the liver, but in most of the cases they have made use of whole liver tissues [98, 175-177].

We decided to isolate metabolic relevant area of liver (zone I and zone III), representative of those areas where the drug metabolism happens; and the bile duct and the blood vessels, also as possible target tissues of some drugs.

We took advantage of the laser capture microdissection, for the isolation of those areas, directly from frozen tissue.

The laser capture microdissection, however, is a demanding activity. It is expensive, time consuming and requires a long process optimization, in order to provide reliable results.

One of first issue we were called to solve was the intrinsic RNA instability and its degradation during the sample processing and the microdissection.

RNA degradation in tissue sections is primarily due to endogenous RNases, which are activated in an aqueous medium.

The addition of RNase inhibitors is generally accepted as necessary to prevent endogenous RNases reactivation during the staining process, and reduce RNA degradation [105, 122]. In only one study, it was mentioned that their role was uncertain, reporting no improvement in RNA quantity and even a decreased in RNA quality [102]. In previous LCM protocols discussion, authors also recommended to cool all reagents for fixation, staining and dehydration at 4°C and to carry on the staining on ice. This could preserve the RNA integrity, but, on the other hand, is generally not applicable when an immunohistochemical staining is required, because the low temperature slows down the enzymatic activity of RNases, but also the kinetic of the antibody binding to the epitopes.

The fixatives used and the staining time are also crucial factors determining RNA quality. The ethanol fixation was shown to improve RNA quality and quantity compared to unfixed sections [102]. Moreover, cross-linking reagents such as paraformaldehyde was reported to decline the amplifiable RNA on the contrary to precipitating agents (acetone, methanol or ethanol) which gave superior performance in downstream RNA analysis [122].

An essential property of fixatives is to preserve tissue and an optimal compromise should be found to maximize the balance between RNA integrity and tissue morphology. In our study, we adopt an iced-cooled methanol fixation step, although we did not observe significant differences between the precipitating fixatives. Additionally, in agreement with literature, we were not able to collect RNA of good quality upon the fixation with formaldehyde.

To determine the RNA quality, we used the Agilent 2100 Bioanalyzer able to assign integrity score from a software algorithm. This method is considered by some authors as a reliable, reproducible and standardized approach to classify the quality of RNA samples [102]. According to some other authors, determination of RNA quality using the Agilent Bioanalyzer lacks reproducibility [105]. In our study, we encountered some technical difficulties with the Bioanalyzer because of the very

small amounts of RNA, often a second run of analysis has been necessary, in few instances the software failed in assigning the RIN score.

The precision of microdissection is generally limited by the difficulty to identify cell types by morphology alone, mainly because of staining and dehydration process, which deeply alter tissue quality [122]. The use of frozen sections and the absence of the final mounting with a coverslip are also necessary for microdissection but reduce cellular details, further diminishing the ability to isolate a specific cell population. In our study the main challenge remained the identification of small portal structures since HE staining did not allow to distinguish small biliary ducts from portal vessels with a sufficient confidence. To solve this problem, we developed a rapid immunostaining procedure, similar to those described in the literature [122, 127, 178]. The immuno-LCM technique allows the isolation of specific cell populations according to their immunophenotype, even if they are of similar morphology. The specificity and precision of microdissection is greatly increased by the ease of identification of labeled cells.

As regarding RNA quality with immuno-LCM, the RNA extracted from immunostained tissue was of equal quality compared to unstained (control - scrape) or quick HE stained sections.

For the gene expression profiling we used the GeneChip platform from Affymetrix. They are oligonucleotide chips able to quantitatively evaluate the gene expression transcriptome-wide. The GeneChip are species-specific platform, however at time of this study, there was not a specific assay designed for *Macaca fascicularis*. To overcome this limitation, we used the Human Genome U133 plus 2.0. One group have shown the feasibility of this approach, demonstrating an average consistency of 85.78% between human and rhesus monkey, indicating that a human microarray might provide a part of the information for monkey sample testing (Illumina Chips) [179]. We did not perform specific investigations for assessing the level of sensitivity and specificity achievable in this hybrid experimental condition; however, we were able to validate the presence of genes detected as low expressed. The use of different algorithm for pre-processing the raw expression data is still controversial.

Affymetrix provided its own solution with the MAS5 algorithm, which use all the technical specifications of the GeneChip platform (PM and MM probe set). This results in reliable results, but at the expense of a reduced sensitivity.

Many independent groups have provided their alternative solution to improve the data pre-processing.

In our project we have compared data pre-processed with the MAS5 and RMA algorithms.

Our correlation analysis revealed a high agreement between the two data sets in our LCM experimental conditions. From the practical point of view, we did not observe differences between the two algorithms. However one group have described an algorithm driven artifact affecting the RMA algorithm, which would overestimate the similarities between samples in specific conditions [180].

Assuming the absence of a real advantage in using the RMA algorithm vs. the MAS5 in our data set, and the possibility to incur in this artificial correlation, we decided to proceed with only the MAS5 algorithm.

Upon the pre-processing and normalization of the data, we proceeded with the analysis.

We approached the analysis in a first instance in an unsupervised manner.

We analyzed all the data sets from the 3 species using a Principal Component Analysis, to highlight the intrinsic characteristic of our samples.

In all the species we obtained an optimal distribution of the samples, according with their cellular composition.

Indeed, the clustering together of the liver zone I, zone III and whole liver tissue can be easily explained by the major cell composition of those samples. The hepatocytes represent the majority of cells in those samples, and their expression profile influenced in large extent the variance and the distribution of samples in the PCA analysis.

Similarly, the clustering of arteries and veins can be explained by the similar cellular composition, although the greater distance between these samples, compared with the samples in the previous group, is likely determined by the difference between the artery and vein tissues (e.g. the more abundant presence of smooth muscle cells in the tunica media of arteries).

The isolation of the bile duct sample is, as well, a sign of a successful enrichment process.

The graph in Figure 4 represents alone the proof that it is possible to isolate and profile histological elements from a heterogeneous tissue like the liver.

For the selection of genes enriched in the bile ducts, we tried to identify a method with the highest sensitivity and specificity.

The selection of gene signature is based on a comparative process. Here we compared the whole liver samples with the LCM bile ducts, using the fold change value as selection and cut off parameter.

Generally, the selection of a cut off parameter is arbitrary, but we tried to identify universal criteria applicable in all the species in analysis.

Our analysis revealed that a unique cut off value could be identified in order to achieve the best compromise between sensitivity and specificity.

Indeed, in our explorative analysis on rat tissue, the intersection of the two best fitting linear phases, identified in the global exponential curve of the FC frequency distribution, corresponded to the best compromise in sensitivity and specificity for the selection of genes specific for bile ducts.

An increase of the FC value from 0 to 9.2 leads to an exclusion of roughly 20000 probe sets. This of course increases the specificity of our signature. Above this value, a further increase of the FC cut off, would result in a minimal increase of the specificity. Indeed, a further increase from a FC 9 to FC 18, would result in the exclusion of only 80 probe sets, a very minimal increase of the specificity at the expense of sensitivity.

Although this approach is empirical in some extent and arbitrary, it allowed the selection of bile duct gene signatures in all the species. Interestingly enough, the cut off values resulted quite similar in all the species, possibly due to a common tissue specific expression pattern.

As expected, the signatures included well-known epithelial markers, functional markers (e.g. bile carriers) and metabolic elements.

Our gene expression analysis has been followed by a validation step. Due to the limited amount of RNA we obtained from the LCM samples, it has not been possible to validate directly the expression profiles by real-time PCR.

On the other hand, the validation of oligonucleotide array data by real time PCR is controversial. Several authors have shown a good agreement between real time PCR data and oligonucleotide array data in many different applications [181-183], others have shown significant differences [184], which can be corrected by using specific algorithms for the pre-processing of the chip data .

We decided then to validate some of our markers by protein localization.

The validation has been performed cross-species and this limited the number of targets we could localize. Indeed, the number of antibodies recognizing epitopes from different species with comparable efficiency is very restricted.

We could localize 6 markers of bile ducts: keratin7, keratin19 and keratin20, mucin 1, claudin 6, and claudin 7.

We found those proteins expressed in the bile ducts, according with the gene expression profiles, in which we observed a strong enrichment of the gene in the LCM bile duct versus the whole liver.

Interestingly we were able to find the keratin 19 also in dog, an unpredicted data, due to the lack of the specific probe set in the dog Chip.

We were also capable to show, for the first time, in best of our knowledge, a gradient of expression of keratin 20 in the biliary tree, inside the liver and in the gall bladder of monkey.

Furthermore, we discovered an additional specie-specificity relative to the claudin 6, expressed in the bile duct only in rat.

Although the number of protein localized was not very high, based on these results, we were very optimistic about the specificity of our gene signature.

For the gene signature relative to the liver zone I and zone III, we did not perform specific analysis, for the selection of a specific FC value. The cellular composition of those samples was very similar, therefore we used a FC 2 in order to identify most of the metabolic specificities of each zone, without the need to highlight genes selectively expressed in one area.

We validated transcriptomic data for some gene expressed in the liver zone III. We localized the Glutamine synthetase as a marker of the liver zone III. This marker is well known to be expressed in a tiny layer of hepatocytes in the pericentral area, and it has a biological and diagnostic relevance [185, 186]. According to

transcriptomic data, the Glutamine synthetase was localized in all the species around the central vein.

Recently, we have contributed to show that RSPO-LGR4/5-ZNRF3/RNF43 module controls metabolic liver zonation and is a hepatic growth/size rheostat during development, homeostasis and regeneration [187], providing evidences that both, Wnt ligand and the entire system of receptors and enhancer are necessary for the activation of β Catenin and the establishment of the liver zonation in mice.

Based on these evidences, the Rappaport's model could be revised: if the driving forces of liver zonation are actually two (the Wnt pathway as we have shown and Hedgehog as shown by other authors [10]), and the mechanism is based on gradients' opposition, the intermediate area, defined by Rappaport as zone II, could be, not only topographically, but also from the metabolic point of view, just a transition area, where none of the two pathways is strong enough to overwhelm the other. In this respect the zone II assumes less importance because it actually suffers the influence of both the driving forces without, apparently, having an active role in the liver zonation.

Despite all the species showed a number of genes regulated either in zone I or in zone III, we managed to identify only in rat and in monkey the putative drivers of the liver zonation. The gene WNT2 indeed, was differentially expressed in liver zone III, in these two species. Other two genes downstream in β Catenin pathway were up regulated as well (AXIN2 and GLUG).

Moreover, the absence of a significantly regulated WNT gene in the zone III in dog is very surprising. Despite this absence, we were able to distinguish a liver zonation in this species, highlighted also by the GLUL expression profile and protein localization. The explanation of this might be either technical or biological. The GeneChip technology relies on the gene annotation, therefore some genes might not be annotated or not present at all on the hybridization platform. Indeed, we observed a similar issue with the KRT19 transcript, not present at all on the dog chip. A second explanation could be that the mechanism leading to the establishment of liver zonation in dog differs substantially from the other species. This might be corroborated also by the lack of induction of the AXIN 2, although requires additional investigation.

Next, we wanted to verify the influence of the sexual dimorphism on the liver zonation. Not surprisingly, this phenomenon interested only the rodent. In rat we were able to detect a conspicuous number of genes regulated in different manner in male or female animals, both in the zone I and in the zone III.

This finding is in agreement with a recent publication, in which the authors, using a similar approach, isolated by LCM the zone I and zone III from mouse livers [188].

Within the genes with a gender and zone specific profile, we localized the lysyl oxidase (Lox). Lysyl Oxidase, also known as protein-lysine 6-oxidase, is an extracellular copper enzyme that catalyzes formation of aldehydes from lysine residues in collagen and elastin precursors.

The Lox transcript has been found, in rats only, in the liver zone III of male subjects. The protein localization confirmed this specific pattern of expression. Indeed, the protein was localized in the extracellular space in the pericentral area in male rat livers. It remains unclear why an enzyme playing an important role in the stabilization of the extracellular matrix is expressed only in male animals and in a limited region of the organ.

Moreover, we were also capable to confirm the same pattern of expression in one of the substrate of this enzyme: the collagen 1A1, at transcriptional and protein level.

One of the most critical analysis performed in this study, is the one comparing the tissue specific gene signatures previously identified, across the 3 species in analysis. We approached this comparison, using the same software we used for the expression analysis, GeneSpring from Agilent.

This software can compare cross-species platform, operating a series of translations, to convert gene signatures from one species to another. Intuitively, the software makes use of the orthologous databases, and operates in order to finally obtain lists with comparable names/data.

Unfortunately, in this multistep process there are some limitations, which indeed reduced the efficacy of the entire analysis. The first issue is the detail of the GeneChip annotation: although Affymetrix tried in the years to keep up to date the gene annotation on its platforms, all of them have a conspicuous number of probes annotated as putative genes, genes of uncertain function (LOC sites), and probes not annotated at all. Intuitively those probes cannot be translated and will be lost in the cross-species comparison. Additionally, we have found several transcripts for which

there was not a corresponding probe set on the Chip for one species (e.g. KRT19 in dog).

Second limitation is not related to the technology, but might be related to the annotation of the genes in the global databases. Gene orthologues might have different names and the recognition by the software might not be perfect.

In this context, we tried to run our cross-species analysis, but the results were not very convincing. The number of genes common between species in zone I, zone III or bile ducts results very limited. In our opinion it is unlikely that tissues with so close biological functions can share so few genes. We are rather convinced that this analysis was strongly impacted by the approach and by the limitation dictated by the technical characteristics of Chips and databases.

In the future a more accurate analysis might be performed based on the sequence homology, making use of the modern algorithm optimized for the alignment of the RNAseq data, and remapping the oligonucleotide sequences and therefore the target transcripts. A sequence based comparison across species might provide more reliable results. This approach, anyhow would require a bigger computational effort in order to remap the 600000-1 mio of probes spotted on the chip of different species.

Our final analysis on the gene expression data set was focalized in understanding the impact of the call flag pre-filtering strategy, in order to increase the global statistical power of the analysis.

As described, Affymetrix introduced this parameter in its MAS5 algorithm, in order to provide estimation about reliability of the gene expression data.

However, the use of this pre-filtering strategy might result too stringent and lead to the loss of biologically relevant data.

We analyzed the gene expression profile from the whole liver scrape, pre-filtering all the genes labeled as present in at least 80% of the samples in analysis. We then evaluated the impact of this filtering on genes representing a small cell population in the liver, as the bile duct. To do this we calculated how many genes present in the bile duct signature were excluded by the pre-filtering.

Whole liver data set, pre-filtered by the “present” flag included only between 2% and 60% of the bile duct genes in the different species. In other words, an analysis performed on a data set pre-filtered on “present” flag, may strongly underestimate

biological phenomena happening in the bile ducts, masked by the dilution effect operated by the sample composition on the transcriptomic data.

With the validation of the specificity of our signatures, we concluded the first phase of our project, consisting of generating the tissue specific knowledge relative to liver sub-units.

We selected a restricted number of proteins belonging to the gene signature of bile ducts and liver zones. In this we focused more on the validation of the bile duct signature than on the others. The reason was that for bile duct genes we used a very high FC cut off and we wanted to be sure that also genes with a very low expression, selected by our empirical approach, were actually expressed in this tissue. The selection of the candidate proteins was in large extent dictated by the antibodies availability, therefore the selection of Keratin 7 and 19 is, overall not surprising. For those two markers very good antibodies are commercially available for diagnostic purpose. Nevertheless, we also included proteins poorly described like the Claudins. In this we wanted to include markers with a low gene expression and not homogeneously distributed across the species, like the Claudin 6.

The immunohistochemistry analysis validated all the transcriptomic findings, reflecting perfectly the gene expression profiles in all the species, and leading to the description of species specificities (e.g. the peculiar gene expression profile and protein localization of KRT20 in monkey, the Claudin6, expressed only only in rat bile ducts, the Lox and the Col1A1).

All this, made us very confident of the profiles derived by the LCM experiments, but we wanted to challenge these findings in the context of a real toxicology study, to assess the value of the data set for drug safety.

We wanted to assess if, based on our molecular profiling (LCM), we would have been able to address the drug toxicity to a specific tissue structure within the liver.

We decided to retrospectively analyze a study on the effect of Methapyrilene on SD rat.

We approached the study in an unsupervised way, although the molecular and morphological alterations induced by this drug have been largely explored in the past from other groups (e.g. in [162]).

The evaluation of drug safety has been based on whole liver transcriptomic data, the histopathological report of the study and the IHC analysis.

As our standard we performed first an unsupervised analysis of the whole data set of transcriptomic data relative to this study.

The Principle Component Analysis revealed an unusual sample segregation. Indeed, the animal (controls and treated) belonging to the first time-point, showed a significant divergence versus all the other groups. From a deeper analysis we discovered that there was a difference in terms of global gene expression in this sample group, which interested many genes involved in the circadian cycle (data not shown). Not being able to assess if this phenomenon was relevant or not for the following analysis, we decided to exclude this sample group.

We then clustered genes and samples in an unsupervised gene clustering analysis. In line with previous report [162], this analysis revealed just minimal variations, dose and time dependently, and highlighted the lack of driving pathways.

The gene expression variations were mainly subtle and isolated. Other authors also found the absence of driving mechanisms. This might explain why, so far, nobody could identify a unique drug induced mechanism driving the liver cancer in rats.

In summary, the unsupervised analysis showed a minimal impact of the drug in all tested conditions.

The lack of gene expression pattern in this study represents, however, the perfect condition for testing our approach, making use of the knowledge generated by LCM samples.

The histopathological analysis, in agreement with the literature, and consistently with the lack of a gene expression pattern observed, described single cell necrosis and a general increase of mitotic figures, associated with a minimal bile duct hyperplasia.

All this morphological changes, were however, reported as mild.

In this context, if bile ducts were affected by the drug toxicity, there should have been molecular alterations, even though minimal. Now, if these signals were not perceptible due to the dilution effect in the pool of the whole tissue transcriptome, then, we should be able to observe them by applying the bile duct-specific gene signature generated by LCM.

Indeed, upon a statistical analysis aimed at identifying the significant gene variations, we evaluated the overlap between the regulated genes and our bile duct signature.

A conspicuous amount of genes (120 transcripts at day 3, 131 at day 7 and 132 at day 14) from the bile duct signature were indeed induced by the drug, providing a strong evidence that the drug impacted bile ducts.

Interestingly, the number of genes interested was almost constant at all time-point, showing a precise pattern of toxicology, onset from the earliest time-point on.

To validate this observation, we performed the localization of the bile duct markers (keratin 19 and claudin7) and we quantified the bile duct area by image analysis.

This analysis confirmed the bile duct area enlargement, in agreement with the increase in expression of bile duct markers and in agreement with the observed and reported bile duct hyperplasia.

The image analysis, however, did not produce statistically significant results at first time-point, showing in this, a lower predictive and diagnostic power compared to the molecular profiling of tissues.

Similarly, and more striking, the morphological alterations were classified only as mild in the literature and in the histopathological report.

Therefore, this analysis revealed that it was possible to identify the specific structures targeted by toxicity in a complex tissue, by analyzing the whole tissue transcriptomic data, with the help of a molecular signature generated by LCM on independent 'reference' samples. It also shows that the deconvolution of the transcriptomic data from a heterogeneous tissue, like the liver, is possible, provided that the adequate reference data are available.

The transcriptomic data were more sensitive and reliable than the histopathological analysis, based on the critical observation of the hematoxylin and eosin staining, and also of the IHC data, not enough sensitive at an early time-point, to reach a significant evaluation of the phenomena.

This study was not aimed at identifying the molecular mechanism of the Methapyrilene toxicity, which were so far still unclear and subject of speculation from several groups. Our aim was to show that, in the analysis of new drug, the transcriptomic data could provide precious insight in the molecular alteration, responsible for morphological alterations. Moreover, the use of molecular signature, like the one generated by LCM, could increase the predictive value and analytical power of the transcriptomic data, by several folds.

Indeed, the general level of expression of the genes used for the retrospective diagnosis of the bile duct hyperplasia, was very low in the data set from the Methapyrilene treated animals. However, with the support of our LCM data, we were able to approach to this analysis, without the strict necessity of the statistical power, corroborated by the certainty of the specificity of our markers. Our study is in full agreement with another report about the Methapyrilene treatment [162]. This study introduces the concept of functional toxicogenomic. Functional toxicogenomic is the study of the biological activities of genes in the context of effects of a compound on an organism and or on a specific target organ. Gene expression changes can be analyzed for information that might provide insight into specific mechanistic pathways driving morphological changes.

These observations are of importance because they suggest that molecular changes in genes associated with specific histological structure are predictive of morphological alteration and can be measured with more sensitivity than microscopic observation.

Here we showed that our approach, although time consuming and expensive, may provide the knowledge to improve and increase the predictive power of toxicogenomic studies, both, retrospectively and prospectively.

However, our methods resulted still arbitrary and basic in the gene selection criteria and in the application of the knowledge generated, to new studies.

In both these contexts, we performed a simple comparative analysis, which provided solid evidences, but not supported by any statistical validation.

They then required an additional experimental validation.

In the future it would be valuable to explore mathematical models for selection of tissue specific genes, able to describe what we were only able to assess empirically and based on our experience.

Intellectual and practical contribution

This work was developed under the supervision of MD PhD Pierre Moulin at the Preclinical Safety unit of the Novartis Institute for BioMedical Research, and was completely founded by Novartis Pharma AG.

Diego Calabrese performed all the experiments and the analysis for this project, as described in the manuscript, with the following exceptions.

Fannie Baudimont performed the LCM from dog livers. She performed the experiments and a basic analysis, writing a short descriptive report on the contribution of Laser Capture Microdissection in the modern molecular pathology, the report has been submitted for her board certification in Veterinary Pathology (Fr). She was tutored during her fellowship at NIBR from Diego Calabrese and Pierre Moulin.

Andr  Cordier, Elaine Tritto and Carlo Ravagli introduced me to the molecular profiling and transcriptomic data analysis.

Katy Darribat and Serafino Pantano provided technical advices for the LCM execution and troubleshooting.

Valerie Dubost, Geraldine Wacker, Brigitte Greiner and Magali Jivkov provided technical advices for the immunohistochemistry and in situ hybridization assays.

Methapyrilene study was performed at Novartis Pharma. Tissue sampling and transcriptomic analysis (GeneChip hybridization only) were previously performed. Metadata analysis, histopathological assays and image analysis were performed by Diego Calabrese.

Diego Calabrese wrote this manuscript. Pierre Moulin and Luigi Terracciano revised it, providing critical suggestions for the manuscript improving.

The data in this manuscript are in large extent still unpublished; therefore a delayed publication will be requested at time of the submission to the University office.

Summary

Animal models are widely used in toxicology studies of new chemical compounds. The metabolism of drugs occurs largely in the liver, but interspecies differences in the molecular mechanisms at the basis of drug metabolism have been widely demonstrated. These differences may limit the translatability of the results to human, and compromise the safety assessment for new compounds. Urge therefore a more in-depth understanding of the molecular mechanisms of liver for the selection of suitable animal models, which are the most representative for the

human. In addition an in-depth knowledge of the cells specific transcriptome may drastically improve the identification of the target organ of toxicity.

Accordingly, in this experimental work we focused our attention in generating a molecular map of liver gene expression for different animal models, taking advantage from the use of laser capture microdissection for obtaining cell-specific transcriptomes, from rat, dog and monkey liver slices.

We developed LCM and immuno-LCM protocols for liver zone I, liver zone III, bile ducts, hepatic arteries and portal veins specimen collection and we profiled the transcriptomes of these samples by oligonucleotide arrays.

The analysis confirmed the enrichment of specific cells/tissues and allowed the identification of known and unknown tissue-specific genes.

We have then investigated the impact of sexual dimorphism on the expression of zone specific genes. We showed that sexual dimorphism in liver zonation is a phenomenon interesting only rats and we couldn't observe any significant differentially expressed gene in other species.

The cross species comparison of gene signature for liver zone I, III and bile ducts, revealed a surprising low number of common genes. However this data might be dependent from technical limitations more than from actual biological diversity of similar tissues in different species.

The specificity of our gene signatures has been proved, at protein level, by IHC, resulting in all the cases valid and revealing additional species specificities unknown so far.

We have applied the knowledge generated in the first phase of this project to a retrospective case study on toxic effects of Methapyrilene in rat liver.

The histopathology report described minimal histological changes in treated animals, including single cell necrosis, increase of mitotic figures and bile duct hyperplasia.

At transcriptomic level, the exposure to Methapyrilene induced a mild impact on the global liver gene expression, and a specific gene expression pattern of toxicity was not detectable.

The analysis of differentially expressed genes, revealed 1500 up regulated genes in treated animals vs. controls and the comparison of those genes with the bile duct

gene signature revealed a constant number (120-130) of common genes at all the time points.

Using two markers belonging to rat bile duct signature (Cldn7 and Krt19), we were able to quantitatively evaluate the bile duct hyperplasia, by measuring the area covered by labeled cells. However the revealed differences were statistically significant at day 7 and 14, but not at day 3.

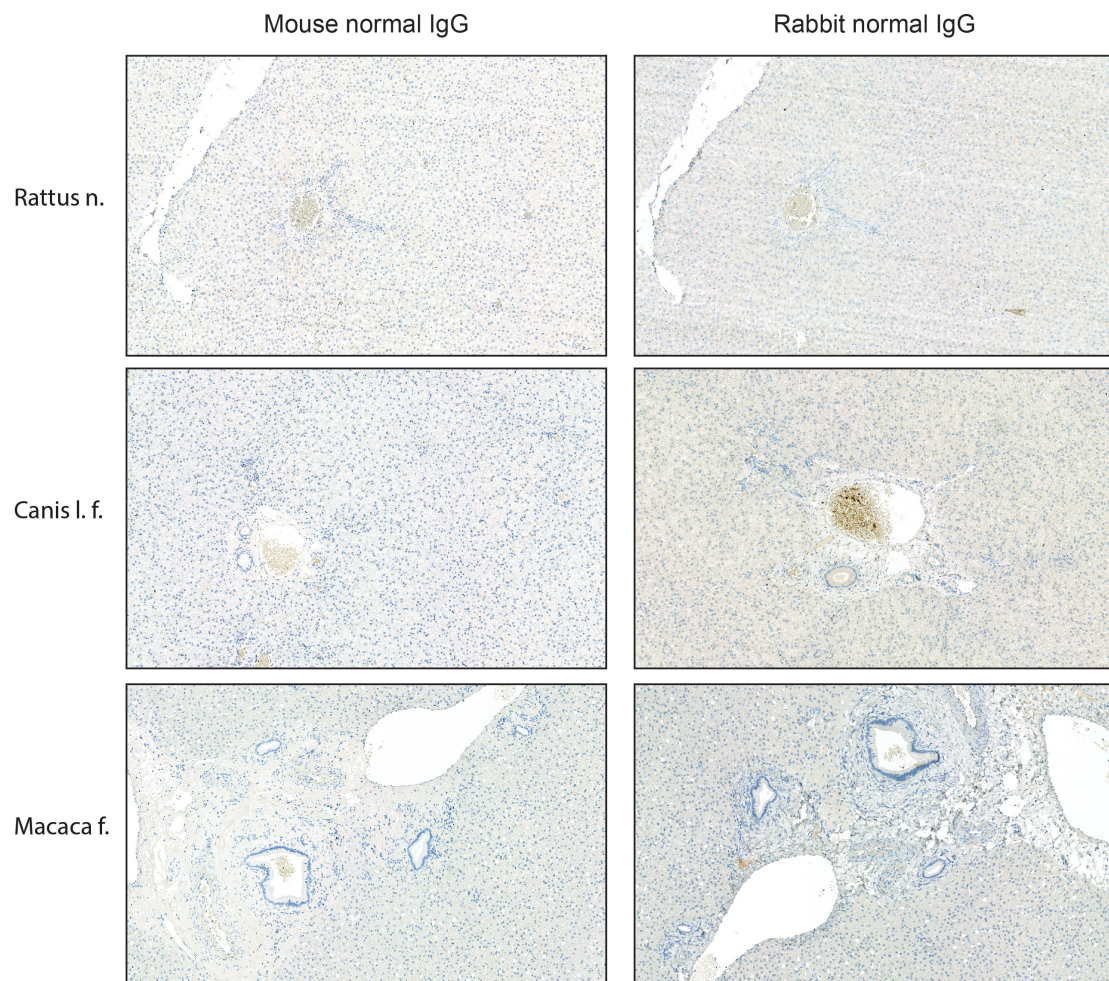
The generation of a liver gene expression map and of tissue specific signatures allowed an “informed” whole liver transcriptome analysis. This uncommon approach revealed subtle drug induced molecular changes and histological alterations, otherwise difficult to identify.

Interestingly, the transcriptomic profiling resulted more sensitive and statistically powerful than the histological approach.

We can then conclude that, although a mathematical model describing the empirical approach used in this project is still missing, the knowledge generated by our work improved the interpretation of a retrospective case study, allowing the identification of a specific toxicity pattern.

Additionally, the possibility to apply the same approach in prospective studies and to different species, represents a powerful contribution for the understanding of liver pathophysiology and DILI.

Supplementary data



Supplementary Figure 1: Paired liver sections incubated with normal Mouse or Rabbit IgG. as negative controls in the immunohistochemical assays.

Supplementary table 1: Morphological Patterns of Injury Observed in DILI (mod. from [72])

	Exemplary drugs	Pattern	Characteristic features	Main differential diagnoses
Necroinflammatory	Isoniazid, Niacin, phenylbutazone, sulphasalazine, phenytoin	Acute hepatitis	> lobular inflammation with/without confluent or bridging necrosis	Acute viral (including EBV, CMV and HEV !) or autoimmune hepatitis
	a-Methyldopa, nitrofurantoin, minocycline, TNF_α antagonists, vemurafenib, hydralazine, ipilimumab, atorvastatin,	Chronic hepatitis	> Portal inflammation with interface hepatitis	Chronic viral or auto-immune diseases; early PSC /PBC
	Allopurinol, amiodarone, carbamazepine, diltiazem, phenylbutazone,	Granulomatous hepatitis	non-necrotizing granulomas	Sarcoidosis, PBC, fungal and mycobacterial atypical bacterial infections
	Acetaminophen, halotane, carbon tetrachloride	Zonal coagulative necrosis	Zone 3 or 1 coagulative necrosis, usually without significant inflammation	Hypoxic-ischemic injury, necrotizing viral infections
Cholestatic	Anabolic and contraceptive steroids, cyclosporine A	Acute intrahepatic cholestasis	Hepatocellular and /or canalicular bilirubinostasis in zone 3; minimal /no inflammation (“pure cholestasis”)	Benign Familial Intrahepatic cholestasis (M. Sommerskill-Tygstrup) Sepsis, acute large duct obstruction, cholestasis of pregnancy
	Sulfonamides, beta-lactams, chlorpromazine, thiabendazole	Chronic cholestasis (vanishing bile duct syndrome)	Duct sclerosis and loss; periportal cholate stasis	Primary sclerosing cholangitis
	Amoxicillin/clavulanate, carbamazepine	Chronic cholestasis (PBC-like cholangiodestructive)	Florid duct injury; periportal cholate stasis	Primary biliary cirrhosis, autoimmune cholangitis,

	Phenytoin, chlorpromazine, tricyclic antidepressant	Mixed hepatocellular-cholestatic injury (cholestatic hepatitis)	Acute or chronic hepatitis + zone 3 cholestasis	chronic large duct obstruction Viral hepatitis
Steatotic	Didanosine, Fialuridine, Valporate	Microvesicular steatosis	> microvesicular steatosis	Alcohol, fatty liver of pregnancy, metabolic diseases
	Steroids, Methotrexate	Macrovesicular steatosis	macrovesicular steatosis without significant inflammation; no cholestasis	Alcohol, obesity, metabolic syndrome
	Tamoxifen, perhexiline maleate, amiodarone, nifedipine	Steatohepatitis	Zone 3 ballooning; sinusoidal fibrosis; mallory-Denk bodies, variable inflammation and steatosis	Alcohol, obesity, metabolic syndrome
Vascular	Busulfan, azathioprine, danazol, androgenic-anabolic steroids	Sinusoidal dilatation/peliosis	Sinusoidal dilatation / peliosis	Artifactual; acute congestion; bacillary angiomatosis; nearby mass lesions
	Oxaliplatin, azathioprine; Vitamin A, pyrrolizidine alkaloids	Sinusoidal obstruction syndrome /Veno occlusive disease /Budd-Chiari	Occlusion or loss of central veins/thrombosis	
	Inorganic arsenicals. Vinyl chloride	Hepatoportal sclerosis	Disappearance of portal veins	Arteriohepatic dysplasia
	Azathioprine, busulphan	Nodular regenerative hyperplasia	Diffuse nodular transformation	Collagen-vascular diseases; lymphoproliferative diseases
Neoplastic	Oral contraceptive steroids, anabolic steroids, Thorotrast, Vinyl chloride	Hepatocellular adenoma and carcinoma, cholangiocarcinoma and angiosarcoma	Standard features of neoplastic liver disease	Other causes of chronic liver disease and cirrhosis, PSC, and parasitic infection

Supplementary table 2: Main types of drug-induced vascular injury

Condition	Clinical features	Diagnosis	Causative Agents
Nodular regenerative hyperplasia	Portal hypertension; rarely hepatic encephalopathy, especially after variceal bleed	Liver histology	Azathioprine; oxaliplatin; busulfan; doxorubicin, cyclophosphamide, bleomycin, carmustine, 6-thioguanine
Non-cirrhotic portal hypertension (perisinusoidal fibrosis)	Portal hypertension, splenomegaly, hypersplenism	Doppler ultrasonography; liver biopsy	Vitamin A; cytotoxic agents; methotrexate; azathioprine; vinyl chloride; arsenic
Sinusoidal dilatation	Hepatomegaly, abdominal pain	Imaging; incidental histology	Oral contraceptives (sex steroids)
Peliosis hepatis	Hepatomegaly; portal hypertension	Imaging; appearance at surgery; avoid liver biopsy	Anabolic steroids; azathioprine; oestrogens; 6-thioguanine
Budd-Chiari syndrome	Abdominal pain, tender hepatomegaly, ascites; liver failure; portal hypertension	Doppler ultrasonography; MRI; hepatic venography; liver biopsy	Oestrogens; dacarbazine
Sinusoidal obstruction syndrome (veno-occlusive syndrome)	Abdominal pain, tender hepatomegaly, ascites; liver failure;	Imaging similar to Budd-Chiari syndrome, except large hepatic veins patent	Pyrrolizidine and other plant alkaloids; azathioprine; oxaliplatin, carmustine, busulfan; cyclophosphamide; Cytosine arabinoside

Supplementary table 3: Drugs involved in cholestatic DILI

Drug	Histology	Remarks
Amoxicillin/clavulanic acid	Bland cholestasis, cholestatic hepatitis or (rarely) VBDS	Age > 65, sex (F), repeated courses higher risk
Flucloxacillin	Cholestatic hepatitis, VBDS, biliary cirrhosis	Age > 65, sex (F), high doses higher risk
Cloxacillin	Cholestatic hepatitis	
Dicloxacillin	Cholestatic hepatitis	
Oxacillin	Cholestatic hepatitis	
Amoxicillin	Severe cholestatic hepatitis, VBDS	
Ciprofloxacin	Cholestatic hepatitis	
Benzympenicillin	Severe cholestasis	
Cephalosporin	Cholestatic hepatitis	Relatively rare; 1 case with liver failure
Erithromycin	Cholestasis, cholestatic hepatitis	
Clarithromycin	Cholestatic hepatitis	
Azithromycin	Cholestatic hepatitis	
Clindamycin	Cholestatic hepatitis, VBDS	
Trimethoprim/sulfamethoxazole	Cholestasis, cholestatic hepatitis with cholangiolitis, VBDS	Cholestasis due to sulfamethoxazole
Tetracyclines	Cholestatic hepatitis	
Thiabendazole	Cholestatic hepatitis	May progress to cirrhosis
Terbinafine	Severe cholestatic hepatitis, acute liver failure	

Chlorpromazine	Cholestatic hepatitis, VBDS	May progress to biliary cirrhosis
Risperidone	Cholestatic hepatitis	
Sulpiride	VBDS	
Imipramine	Cholestatic hepatitis	
Amitriptyline	Cholestatic hepatitis	
Duloxetine	Cholestatic hepatitis	Dose-dependent?
Carbamazepine	VBDS	
Zonisamide	VBDS	Complete restitutio after drug withdrawal
Amiodarone	Cholestatic hepatitis	May become chronic
5-FU	PSC-like	
Azathioprine	Severe cholestatic hepatitis	Sometimes associated with NRH [189]
Diclofenac	Cholestasis, cholestatic hepatitis	
Ibuprofen	Cholestatic hepatitis	VBDS in pediatric age [74]
Nimesulide	Cholestatic hepatitis	
Tenoxicam	VBDS	
Sulindac	Cholestasis, cholestatic hepatitis	
Nevirapine	Cholestatic Hepatitis	May develop portal hypertension
Didanosine	Cholestatic hepatitis	May develop portal hypertension
Oral contraceptives	Canalicular cholestasis	
Anabolic steroids	Canalicular cholestasis	
Warfarin	Canalicular cholestasis	
Rivaroxaban	Canalicular cholestasis, severe	

Supplementary table 4: Selected Herbs and Dietary Supplements Causing Hepatotoxicity

Herbals & Dietary Supplements	Common use	Phenotype / Liver histology
Aloe vera	Gastrointestinal ailments / topical emollient	Acute hepatocellular injury; portal/ lobular inflammation with eosinophilic infiltrates and acidophilic bodies
Atractylis gummifera (Disthaff thistle, African remedy)	Multiple uses: Antipyretic, antiemetic, abortifacient	Acute liver failure; diffuse hepatic necrosis
Ayurvedic herbs : Psoralea corylifolia, Acacia catechu, Eclipta alba, Bacopa monnieri	Miscellaneous purposes	Acute and chronic hepatitis; granulomatous hepatitis, cirrhosis
Black cohosh (Cimicifuga racemosa)	Ameliorating menopausal vasomotor symptoms	Autoimmune features
Callilepis laureola (Impila, Zulu remedy)	Gastric problems, tapeworm infestations, cough	Acute liver and renal failure, diffuse hepatic necrosis
Cascara sagrada (Rhamnus purshiana)	Constipation	Cholestatic hepatitis, bile duct injury, portal inflammation, intrahepatic bile stasis
Camphor oil (Cinnamomum camphora)	Rubefacient, mucolytic	Acute hepatitis, mimics Reye syndrome
Centella asiatica	Wound healing, psychophysical regenerator and blood purifier	Autoimmune features, cellular necrosis, apoptosis and lymphoplasmacytic infiltrate
Chaparral (Larrea tridentate, Larrea divaricata)	Bronchitis, rheumatic pain, weight loss, stomach pain	Cholestatic hepatitis, biliary changes, cirrhosis, massive necrosis
Jin Bu Huan (Lycopodium serratum)	Sedation	Chronic hepatitis, portal fibrosis, steatosis, cholestatic hepatitis
Ma-Huang (Ephedra sinensis)	Weight loss	Hepatocellular damage with autoimmune features; massive necrosis

Dai-saiko-to	Hypertension; shoulder stiffness; insomnia; anxiety;	Autoimmune features
Germander (Teucrium chamaedrys)	Weight loss; tonic	Acute and chronic hepatitis, massive necrosis. cirrhosis,
Green tea (Camellia sinensis)	Weight loss	Acute hepatocellular injury, cholestasis, steatosis
Herbalife; nutritional supplements	Weight loss, nutritional supplementation	Acute and chronic lobular and portal hepatitis,with eosinophilic infiltrates
Kava Kava (piper methysticum)	Anxiety; depressive symptoms	Acute cholestatic hepatitis; bile duct injury, hepatic necrosis
Pennyroyal (Mentha pulegium) Hedeoma pulegoides)	Abortifacient; menses induction	Acute liver failure; centrilobular degeneration and massive necrosis

Bibliography

1. Vidal-Vanaclocha F: **Functional heterogeneity of liver tissue: from cell lineage diversity to sublobular compartment-specific pathogenesis**. Austin, New York: Landes; Distributed by Chapman & Hall; 1997.
2. Guidotti JE, Bregerie O, Robert A, Debey P, Brechot C, Desdouets C: **Liver cell polyploidization: a pivotal role for binuclear hepatocytes**. *The Journal of biological chemistry* 2003, **278**(21):19095-19101.
3. Kudriavtsev BN, Kudriavtseva MV, Zavadskaia EE, Smirnova SA, Skorina AD: **[Polyploidy in the human liver normally and in hepatitis]**. *Tsitologiya* 1982, **24**(4):436-444.
4. **Histology course for medicine school** [<http://www.courseweb.uottawa.ca/medicine-histology/English/Gastrointestinal/Liver.htm>]
5. Lutz J, Henrich H, Bauereisen E: **Oxygen supply and uptake in the liver and the intestine**. *Pflugers Arch* 1975, **360**(1):7-15.
6. Torre C, Perret C, Colnot S: **Molecular determinants of liver zonation**. *Prog Mol Biol Transl Sci* 2010, **97**:127-150.
7. Wang J, Olin M, Rozell B, Bjorkhem I, Einarsson C, Eggertsen G, Gafvels M: **Differential hepatocellular zonation pattern of cholesterol 7alpha-hydroxylase (Cyp7a1) and sterol 12alpha-hydroxylase (Cyp8b1) in the mouse**. *Histochem Cell Biol* 2007, **127**(3):253-261.
8. Gebhardt R, Gaunitz F: **Cell-cell interactions in the regulation of the expression of hepatic enzymes**. *Cell Biol Toxicol* 1997, **13**(4-5):263-273.
9. Gebhardt R, Matz-Soja M: **Liver zonation: Novel aspects of its regulation and its impact on homeostasis**. *World J Gastroenterol* 2014, **20**(26):8491-8504.
10. Matz-Soja M, Hovhannisyan A, Gebhardt R: **Hedgehog signalling pathway in adult liver: a major new player in hepatocyte metabolism and zonation?** *Med Hypotheses* 2013, **80**(5):589-594.
11. Benhamouche S, Decaens T, Godard C, Chambrey R, Rickman DS, Moinard C, Vasseur-Cognet M, Kuo CJ, Kahn A, Perret C *et al*: **Apc tumor suppressor gene is the "zonation-keeper" of mouse liver**. *Dev Cell* 2006, **10**(6):759-770.
12. Loeppen S, Schneider D, Gaunitz F, Gebhardt R, Kurek R, Buchmann A, Schwarz M: **Overexpression of glutamine synthetase is associated with beta-catenin-mutations in mouse liver tumors during promotion of hepatocarcinogenesis by phenobarbital**. *Cancer research* 2002, **62**(20):5685-5688.
13. Kumar V, Abbas AK, Fausto N, Robbins SL, Cotran RS: **Robbins and Cotran pathologic basis of disease**, 7th edn. Philadelphia: Elsevier Saunders; 2005.
14. Hayashi PH, Fontana RJ: **Clinical features, diagnosis, and natural history of drug-induced liver injury**. *Seminars in liver disease* 2014, **34**(2):134-144.
15. Sgro C, Clinard F, Ouazir K, Chanay H, Allard C, Guilleminet C, Lenoir C, Lemoine A, Hillon P: **Incidence of drug-induced hepatic injuries: a French population-based study**. *Hepatology (Baltimore, Md)* 2002, **36**(2):451-455.
16. Robles-Diaz M, Lucena MI, Kaplowitz N, Stephens C, Medina-Caliz I, Gonzalez-Jimenez A, Ulzurrin E, Gonzalez AF, Fernandez MC, Romero-Gomez M *et al*: **Use of Hy's law and a new composite algorithm to predict acute liver failure in patients with drug-induced liver injury**. *Gastroenterology* 2014, **147**(1):109-118.e105.

17. Chalasani NP, Hayashi PH, Bonkovsky HL, Navarro VJ, Lee WM, Fontana RJ: **ACG Clinical Guideline: the diagnosis and management of idiosyncratic drug-induced liver injury.** *The American journal of gastroenterology* 2014, **109**(7):950-966; quiz 967.
18. Kleiner DE, Chalasani NP, Lee WM, Fontana RJ, Bonkovsky HL, Watkins PB, Hayashi PH, Davern TJ, Navarro V, Reddy R *et al*: **Hepatic histological findings in suspected drug-induced liver injury: systematic evaluation and clinical associations.** *Hepatology (Baltimore, Md)* 2014, **59**(2):661-670.
19. Tujios S, Fontana RJ: **Mechanisms of drug-induced liver injury: from bedside to bench.** *Nature reviews Gastroenterology & hepatology* 2011, **8**(4):202-211.
20. Njoku DB: **Drug-induced hepatotoxicity: metabolic, genetic and immunological basis.** *International journal of molecular sciences* 2014, **15**(4):6990-7003.
21. Nemeth E, Baird AW, O'Farrelly C: **Microanatomy of the liver immune system.** *Seminars in immunopathology* 2009, **31**(3):333-343.
22. Gebhardt R: **Metabolic zonation of the liver: regulation and implications for liver function.** *Pharmacology & therapeutics* 1992, **53**(3):275-354.
23. Jungermann K, Kietzmann T: **Zonation of parenchymal and nonparenchymal metabolism in liver.** *Annual review of nutrition* 1996, **16**:179-203.
24. Gu X, Manautou JE: **Molecular mechanisms underlying chemical liver injury.** *Expert reviews in molecular medicine* 2012, **14**:e4.
25. Testa B, Kramer SD: **The biochemistry of drug metabolism--an introduction: part 3. Reactions of hydrolysis and their enzymes.** *Chemistry & biodiversity* 2007, **4**(9):2031-2122.
26. Testa B, Kramer SD: **The biochemistry of drug metabolism--an introduction: Part 2. Redox reactions and their enzymes.** *Chemistry & biodiversity* 2007, **4**(3):257-405.
27. Testa B, Kramer SD: **The biochemistry of drug metabolism--an introduction: part 4. reactions of conjugation and their enzymes.** *Chemistry & biodiversity* 2008, **5**(11):2171-2336.
28. Kusters A, Karpen SJ: **The role of inflammation in cholestasis: clinical and basic aspects.** *Seminars in liver disease* 2010, **30**(2):186-194.
29. Brabec V, Kasparkova J: **Modifications of DNA by platinum complexes. Relation to resistance of tumors to platinum antitumor drugs.** *Drug resistance updates : reviews and commentaries in antimicrobial and anticancer chemotherapy* 2005, **8**(3):131-146.
30. Mason RP, Chignell CF: **Free radicals in pharmacology and toxicology--selected topics.** *Pharmacological reviews* 1981, **33**(4):189-211.
31. Saad EI, El-Gowilly SM, Sherhaa MO, Bistawroos AE: **Role of oxidative stress and nitric oxide in the protective effects of alpha-lipoic acid and aminoguanidine against isoniazid-rifampicin-induced hepatotoxicity in rats.** *Food and chemical toxicology : an international journal published for the British Industrial Biological Research Association* 2010, **48**(7):1869-1875.
32. Testa B, Kramer SD: **The biochemistry of drug metabolism--an introduction: part 5. Metabolism and bioactivity.** *Chemistry & biodiversity* 2009, **6**(5):591-684.
33. Buchweitz JP, Ganey PE, Bursian SJ, Roth RA: **Underlying endotoxemia augments toxic responses to chlorpromazine: is there a relationship to drug idiosyncrasy?** *The Journal of pharmacology and experimental therapeutics* 2002, **300**(2):460-467.

34. Deng X, Stachlewitz RF, Liguori MJ, Blomme EA, Waring JF, Luyendyk JP, Maddox JF, Ganey PE, Roth RA: **Modest inflammation enhances diclofenac hepatotoxicity in rats: role of neutrophils and bacterial translocation.** *The Journal of pharmacology and experimental therapeutics* 2006, **319**(3):1191-1199.
35. Donaldson PT, Daly AK, Henderson J, Graham J, Pirmohamed M, Bernal W, Day CP, Aithal GP: **Human leucocyte antigen class II genotype in susceptibility and resistance to co-amoxiclav-induced liver injury.** *Journal of hepatology* 2010, **53**(6):1049-1053.
36. Dugan CM, MacDonald AE, Roth RA, Ganey PE: **A mouse model of severe halothane hepatitis based on human risk factors.** *The Journal of pharmacology and experimental therapeutics* 2010, **333**(2):364-372.
37. Jaeschke H, Knight TR, Bajt ML: **The role of oxidant stress and reactive nitrogen species in acetaminophen hepatotoxicity.** *Toxicology letters* 2003, **144**(3):279-288.
38. Lu J, Jones AD, Harkema JR, Roth RA, Ganey PE: **Amiodarone exposure during modest inflammation induces idiosyncrasy-like liver injury in rats: role of tumor necrosis factor-alpha.** *Toxicological sciences : an official journal of the Society of Toxicology* 2012, **125**(1):126-133.
39. Pohl LR, Satoh H, Christ DD, Kenna JG: **The immunologic and metabolic basis of drug hypersensitivities.** *Annual review of pharmacology and toxicology* 1988, **28**:367-387.
40. Nelson SD: **Molecular mechanisms of the hepatotoxicity caused by acetaminophen.** *Seminars in liver disease* 1990, **10**(4):267-278.
41. Fromenty B, Pessayre D: **Inhibition of mitochondrial beta-oxidation as a mechanism of hepatotoxicity.** *Pharmacology & therapeutics* 1995, **67**(1):101-154.
42. Jones BE, Lo CR, Liu H, Srinivasan A, Streetz K, Valentino KL, Czaja MJ: **Hepatocytes sensitized to tumor necrosis factor-alpha cytotoxicity undergo apoptosis through caspase-dependent and caspase-independent pathways.** *The Journal of biological chemistry* 2000, **275**(1):705-712.
43. Joza N, Susin SA, Daugas E, Stanford WL, Cho SK, Li CY, Sasaki T, Elia AJ, Cheng HY, Ravagnan L *et al*: **Essential role of the mitochondrial apoptosis-inducing factor in programmed cell death.** *Nature* 2001, **410**(6828):549-554.
44. Han D, Shinohara M, Ybanez MD, Saberi B, Kaplowitz N: **Signal transduction pathways involved in drug-induced liver injury.** *Handbook of experimental pharmacology* 2010(196):267-310.
45. Bissell DM, Gores GJ, Laskin DL, Hoofnagle JH: **Drug-induced liver injury: mechanisms and test systems.** *Hepatology (Baltimore, Md)* 2001, **33**(4):1009-1013.
46. Kakuda TN: **Pharmacology of nucleoside and nucleotide reverse transcriptase inhibitor-induced mitochondrial toxicity.** *Clinical therapeutics* 2000, **22**(6):685-708.
47. Silva MF, Ruiter JP, Illst L, Jakobs C, Duran M, de Almeida IT, Wanders RJ: **Valproate inhibits the mitochondrial pyruvate-driven oxidative phosphorylation in vitro.** *Journal of inherited metabolic disease* 1997, **20**(3):397-400.
48. Lucena MI, Andrade RJ, Fernandez MC, Pachkoria K, Pelaez G, Duran JA, Villar M, Rodrigo L, Romero-Gomez M, Planas R *et al*: **Determinants of the clinical expression of amoxicillin-clavulanate hepatotoxicity: a prospective series from Spain.** *Hepatology (Baltimore, Md)* 2006, **44**(4):850-856.

49. Kass GE, Price SC: **Role of mitochondria in drug-induced cholestatic injury.** *Clinics in liver disease* 2008, **12**(1):27-51, vii.
50. Holt M, Ju C: **Drug-induced liver injury.** *Handbook of experimental pharmacology* 2010(196):3-27.
51. Naisbitt DJ, Britschgi M, Wong G, Farrell J, Depta JP, Chadwick DW, Pichler WJ, Pirmohamed M, Park BK: **Hypersensitivity reactions to carbamazepine: characterization of the specificity, phenotype, and cytokine profile of drug-specific T cell clones.** *Molecular pharmacology* 2003, **63**(3):732-741.
52. Pichler WJ: **Direct T-cell stimulations by drugs--bypassing the innate immune system.** *Toxicology* 2005, **209**(2):95-100.
53. Li MK, Crawford JM: **The pathology of cholestasis.** *Seminars in liver disease* 2004, **24**(1):21-42.
54. Pauli-Magnus C, Meier PJ: **Hepatobiliary transporters and drug-induced cholestasis.** *Hepatology (Baltimore, Md)* 2006, **44**(4):778-787.
55. Stapelbroek JM, van Erpecum KJ, Klomp LW, Houwen RH: **Liver disease associated with canalicular transport defects: current and future therapies.** *Journal of hepatology* 2010, **52**(2):258-271.
56. Colombo C, Vajro P, Degiorgio D, Coviello DA, Costantino L, Tornillo L, Motta V, Consonni D, Maggiore G: **Clinical features and genotype-phenotype correlations in children with progressive familial intrahepatic cholestasis type 3 related to ABCB4 mutations.** *Journal of pediatric gastroenterology and nutrition* 2011, **52**(1):73-83.
57. Adams DH, Ju C, Ramaiah SK, Uetrecht J, Jaeschke H: **Mechanisms of immune-mediated liver injury.** *Toxicological sciences : an official journal of the Society of Toxicology* 2010, **115**(2):307-321.
58. Degott C, Feldmann G, Larrey D, Durand-Schneider AM, Grange D, Machayekhi JP, Moreau A, Potet F, Benhamou JP: **Drug-induced prolonged cholestasis in adults: a histological semiquantitative study demonstrating progressive ductopenia.** *Hepatology (Baltimore, Md)* 1992, **15**(2):244-251.
59. Fan CQ, Crawford JM: **Sinusoidal obstruction syndrome (hepatic veno-occlusive disease).** *Journal of clinical and experimental hepatology* 2014, **4**(4):332-346.
60. Helmy A: **Review article: updates in the pathogenesis and therapy of hepatic sinusoidal obstruction syndrome.** *Alimentary pharmacology & therapeutics* 2006, **23**(1):11-25.
61. Srivastava A, Poonkuzhali B, Shaji RV, George B, Mathews V, Chandy M, Krishnamoorthy R: **Glutathione S-transferase M1 polymorphism: a risk factor for hepatic venoocclusive disease in bone marrow transplantation.** *Blood* 2004, **104**(5):1574-1577.
62. Vreuls CP, Olde Damink SW, Koek GH, Winstanley A, Wisse E, Cloots RH, van den Broek MA, Dejong CH, Bosman FT, Driessen A: **Glutathione S-transferase M1-null genotype as risk factor for SOS in oxaliplatin-treated patients with metastatic colorectal cancer.** *British journal of cancer* 2013, **108**(3):676-680.
63. DeLeve LD, Ito Y, Bethea NW, McCuskey MK, Wang X, McCuskey RS: **Embolization by sinusoidal lining cells obstructs the microcirculation in rat sinusoidal obstruction syndrome.** *American journal of physiology Gastrointestinal and liver physiology* 2003, **284**(6):G1045-1052.
64. DeLeve LD, Wang X, Kanel GC, Ito Y, Bethea NW, McCuskey MK, Tokes ZA, Tsai J, McCuskey RS: **Decreased hepatic nitric oxide production contributes**

- to the development of rat sinusoidal obstruction syndrome. *Hepatology (Baltimore, Md)* 2003, **38**(4):900-908.
65. Harb R, Xie G, Lutzko C, Guo Y, Wang X, Hill CK, Kanel GC, DeLeve LD: **Bone marrow progenitor cells repair rat hepatic sinusoidal endothelial cells after liver injury.** *Gastroenterology* 2009, **137**(2):704-712.
 66. Rubbia-Brandt L, Audard V, Sartoretti P, Roth AD, Brezault C, Le Charpentier M, Dousset B, Morel P, Soubrane O, Chaussade S *et al*: **Severe hepatic sinusoidal obstruction associated with oxaliplatin-based chemotherapy in patients with metastatic colorectal cancer.** *Annals of oncology : official journal of the European Society for Medical Oncology / ESMO* 2004, **15**(3):460-466.
 67. Tallman MS, McDonald GB, DeLeve LD, Baer MR, Cook MN, Graepel GJ, Kollmer C: **Incidence of sinusoidal obstruction syndrome following Mylotarg (gemtuzumab ozogamicin): a prospective observational study of 482 patients in routine clinical practice.** *International journal of hematology* 2013, **97**(4):456-464.
 68. Yang K, Kock K, Sedykh A, Tropsha A, Brouwer KL: **An updated review on drug-induced cholestasis: mechanisms and investigation of physicochemical properties and pharmacokinetic parameters.** *Journal of pharmaceutical sciences* 2013, **102**(9):3037-3057.
 69. Geier A, Wagner M, Dietrich CG, Trauner M: **Principles of hepatic organic anion transporter regulation during cholestasis, inflammation and liver regeneration.** *Biochimica et biophysica acta* 2007, **1773**(3):283-308.
 70. Zollner G, Marschall HU, Wagner M, Trauner M: **Role of nuclear receptors in the adaptive response to bile acids and cholestasis: pathogenetic and therapeutic considerations.** *Molecular pharmaceuticals* 2006, **3**(3):231-251.
 71. Nakanishi Y, Saxena R: **Pathophysiology and Diseases of the Proximal Pathways of the Biliary System.** *Archives of pathology & laboratory medicine* 2015, **139**(7):858-866.
 72. Kleiner DE: **The pathology of drug-induced liver injury.** *Seminars in liver disease* 2009, **29**(4):364-372.
 73. Ramachandran R, Kakar S: **Histological patterns in drug-induced liver disease.** *Journal of clinical pathology* 2009, **62**(6):481-492.
 74. Bjornsson ES, Jonasson JG: **Drug-induced cholestasis.** *Clinics in liver disease* 2013, **17**(2):191-209.
 75. Trauner M, Boyer JL: **Bile salt transporters: molecular characterization, function, and regulation.** *Physiological reviews* 2003, **83**(2):633-671.
 76. Bjornsson E, Olsson R: **Outcome and prognostic markers in severe drug-induced liver disease.** *Hepatology (Baltimore, Md)* 2005, **42**(2):481-489.
 77. Chalasani N, Fontana RJ, Bonkovsky HL, Watkins PB, Davern T, Serrano J, Yang H, Rochon J: **Causes, clinical features, and outcomes from a prospective study of drug-induced liver injury in the United States.** *Gastroenterology* 2008, **135**(6):1924-1934, 1934.e1921-1924.
 78. Bjornsson E, Davidsdottir L: **The long-term follow-up after idiosyncratic drug-induced liver injury with jaundice.** *Journal of hepatology* 2009, **50**(3):511-517.
 79. Navarro VJ, Lucena MI: **Hepatotoxicity induced by herbal and dietary supplements.** *Seminars in liver disease* 2014, **34**(2):172-193.
 80. Suk KT, Kim DJ, Kim CH, Park SH, Yoon JH, Kim YS, Baik GH, Kim JB, Kweon YO, Kim BI *et al*: **A prospective nationwide study of drug-induced**

- liver injury in Korea.** *The American journal of gastroenterology* 2012, **107**(9):1380-1387.
81. Zhou Y, Yang L, Liao Z, He X, Zhou Y, Guo H: **Epidemiology of drug-induced liver injury in China: a systematic analysis of the Chinese literature including 21,789 patients.** *European journal of gastroenterology & hepatology* 2013, **25**(7):825-829.
 82. Feigelstock DA, Mihalik KB, Kaplan G, Feinstone SM: **Increased susceptibility of Huh7 cells to HCV replication does not require mutations in RIG-I.** *Virology* 2010, **7**:44.
 83. Humphrey-Johnson A, Abukalam R, Eltom SE: **Stability of the aryl hydrocarbon receptor and its regulated genes in the low activity variant of Hepa-1 cell line.** *Toxicology letters* 2015, **233**(2):59-67.
 84. Kang YB, Sodunke TR, Lamontagne J, Cirillo J, Rajiv C, Bouchard MJ, Noh M: **Liver sinusoid on a chip: Long-term layered co-culture of primary rat hepatocytes and endothelial cells in microfluidic platforms.** *Biotechnol Bioeng* 2015.
 85. Bricks T, Hamon J, Fleury MJ, Jellali R, Merlier F, Herpe YE, Seyer A, Regimbeau JM, Bois F, Leclerc E: **Investigation of omeprazole and phenacetin first-pass metabolism in humans using a microscale bioreactor and pharmacokinetic models.** *Biopharm Drug Dispos* 2015, **36**(5):275-293.
 86. National Research Council (U.S.). Committee on Applications of Toxicogenomic Technologies to Predictive Toxicology.: **Applications of toxicogenomic technologies to predictive toxicology and risk assessment.** Washington, D.C.: National Academies Press; 2007.
 87. Bussiere JL: **Species selection considerations for preclinical toxicology studies for biotherapeutics.** *Expert opinion on drug metabolism & toxicology* 2008, **4**(7):871-877.
 88. Interspecies [<http://www.interspeciesinfo.com/>]
 89. Richard AC, Lyons PA, Peters JE, Biasci D, Flint SM, Lee JC, McKinney EF, Siegel RM, Smith KG: **Comparison of gene expression microarray data with count-based RNA measurements informs microarray interpretation.** *BMC genomics* 2014, **15**:649.
 90. Kulkarni K, Larsen P, Linninger AA: **Assessing chronic liver toxicity based on relative gene expression data.** *J Theor Biol* 2008, **254**(2):308-318.
 91. Heinloth AN, Boorman GA, Foley JF, Flagler ND, Paules RS: **Gene expression analysis offers unique advantages to histopathology in liver biopsy evaluations.** *Toxicologic pathology* 2007, **35**(2):276-283.
 92. Fielden MR, Brennan R, Gollub J: **A gene expression biomarker provides early prediction and mechanistic assessment of hepatic tumor induction by nongenotoxic chemicals.** *Toxicological sciences : an official journal of the Society of Toxicology* 2007, **99**(1):90-100.
 93. Heinloth AN, Irwin RD, Boorman GA, Nettesheim P, Fannin RD, Sieber SO, Snell ML, Tucker CJ, Li L, Travlos GS *et al*: **Gene expression profiling of rat livers reveals indicators of potential adverse effects.** *Toxicological sciences : an official journal of the Society of Toxicology* 2004, **80**(1):193-202.
 94. Nie AY, McMillian M, Parker JB, Leone A, Bryant S, Yieh L, Bittner A, Nelson J, Carmen A, Wan J *et al*: **Predictive toxicogenomics approaches reveal underlying molecular mechanisms of nongenotoxic carcinogenicity.** *Mol Carcinog* 2006, **45**(12):914-933.

95. Van Hummelen P, Sasaki J: **State-of-the-art genomics approaches in toxicology.** *Mutation research* 2010, **705**(3):165-171.
96. Shackel NA, Gorrell MD, McCaughan GW: **Gene array analysis and the liver.** *Hepatology (Baltimore, Md)* 2002, **36**(6):1313-1325.
97. Morgan KT, Jayyosi Z, Hower MA, Pino MV, Connolly TM, Kotlenga K, Lin J, Wang M, Schmidts HL, Bonnefoi MS *et al*: **The hepatic transcriptome as a window on whole-body physiology and pathophysiology.** *Toxicologic pathology* 2005, **33**(1):136-145.
98. Shackel NA, Seth D, Haber PS, Gorrell MD, McCaughan GW: **The hepatic transcriptome in human liver disease.** *Comparative hepatology* 2006, **5**:6.
99. Yano N, Habib NA, Fadden KJ, Yamashita H, Mitry R, Jauregui H, Kane A, Endoh M, Rifai A: **Profiling the adult human liver transcriptome: analysis by cDNA array hybridization.** *Journal of hepatology* 2001, **35**(2):178-186.
100. Shin YJ, Cho SW, Hahm KB, Kim YS, Kim JH, Park KH, Lee SI: **Localization of hepatitis B virus DNA in hepatocellular carcinoma by polymerase chain reaction in situ hybridization.** *J Korean Med Sci* 1998, **13**(4):377-382.
101. Meier-Ruge W, Bielser W, Remy E, Hillenkamp F, Nitsche R, Unsold R: **The laser in the Lowry technique for microdissection of freeze-dried tissue slices.** *Histochem J* 1976, **8**(4):387-401.
102. Wang S, Wang L, Zhu T, Gao X, Li J, Wu Y, Zhu H: **Improvement of tissue preparation for laser capture microdissection: application for cell type-specific miRNA expression profiling in colorectal tumors.** *BMC genomics* 2010, **11**:163.
103. Cerroni L, Minkus G, Putz B, Hofler H, Kerl H: **Laser beam microdissection in the diagnosis of cutaneous B-cell lymphoma.** *Br J Dermatol* 1997, **136**(5):743-746.
104. Yim SH, Ward JM, Dragan Y, Yamada A, Scacheri PC, Kimura S, Gonzalez FJ: **Microarray analysis using amplified mRNA from laser capture microdissection of microscopic hepatocellular precancerous lesions and frozen hepatocellular carcinomas reveals unique and consistent gene expression profiles.** *Toxicologic pathology* 2003, **31**(3):295-303.
105. Kube DM, Savci-Heijink CD, Lamblin AF, Kosari F, Vasmatazis G, Cheville JC, Connelly DP, Klee GG: **Optimization of laser capture microdissection and RNA amplification for gene expression profiling of prostate cancer.** *BMC molecular biology* 2007, **8**:25.
106. Stark RW, Rubio-Sierra FJ, Thalhammer S, Heckl WM: **Combined nanomanipulation by atomic force microscopy and UV-laser ablation for chromosomal dissection.** *Eur Biophys J* 2003, **32**(1):33-39.
107. Mouldous L, Hunt S, Harcourt R, Harry J, Williams KL, Gutstein HB: **Navigated laser capture microdissection as an alternative to direct histological staining for proteomic analysis of brain samples.** *Proteomics* 2003, **3**(5):610-615.
108. Burgemeister R: **Laser capture microdissection of FFPE tissue sections bridging the gap between microscopy and molecular analysis.** *Methods Mol Biol* 2011, **724**:105-115.
109. Burgemeister R: **Nucleic acids extraction from laser microdissected FFPE tissue sections.** *Methods Mol Biol* 2011, **724**:117-129.
110. Stich M, Thalhammer S, Burgemeister R, Friedemann G, Ehnle S, Luthy C, Schutze K: **Live cell catapulting and recultivation.** *Pathol Res Pract* 2003, **199**(6):405-409.

111. Langer S, Geigl JB, Ehnle S, Gangnus R, Speicher MR: **Live cell catapulting and recultivation does not change the karyotype of HCT116 tumor cells.** *Cancer Genet Cytogenet* 2005, **161**(2):174-177.
112. Podgorny OV: **Live cell isolation by laser microdissection with gravity transfer.** *J Biomed Opt* 2013, **18**(5):55002.
113. Lu JX, Szeto CC: **Gene expression using the PALM system.** *Methods Mol Biol* 2011, **755**:47-56.
114. Ladanyi A, Sipos F, Szoke D, Galamb O, Molnar B, Tulassay Z: **Laser microdissection in translational and clinical research.** *Cytometry A* 2006, **69**(9):947-960.
115. Specht K, Richter T, Muller U, Walch A, Werner M, Hofler H: **Quantitative gene expression analysis in microdissected archival formalin-fixed and paraffin-embedded tumor tissue.** *The American journal of pathology* 2001, **158**(2):419-429.
116. Lehmann U, Kreipe H: **Real-time PCR analysis of DNA and RNA extracted from formalin-fixed and paraffin-embedded biopsies.** *Methods (San Diego, Calif)* 2001, **25**(4):409-418.
117. Su JM, Perlaky L, Li XN, Leung HC, Antalffy B, Armstrong D, Lau CC: **Comparison of ethanol versus formalin fixation on preservation of histology and RNA in laser capture microdissected brain tissues.** *Brain Pathol* 2004, **14**(2):175-182.
118. Liu A: **Laser capture microdissection in the tissue biorepository.** *J Biomol Tech* 2010, **21**(3):120-125.
119. Gallagher RI, Blakely SR, Liotta LA, Espina V: **Laser capture microdissection: Arcturus(XT) infrared capture and UV cutting methods.** *Methods Mol Biol* 2012, **823**:157-178.
120. Bevilacqua C, Makhzami S, Helbling JC, Defrenaix P, Martin P: **Maintaining RNA integrity in a homogeneous population of mammary epithelial cells isolated by Laser Capture Microdissection.** *BMC Cell Biol* 2010, **11**:95.
121. Baskin DG, Bastian LS: **Immuno-laser capture microdissection of rat brain neurons for real time quantitative PCR.** *Methods Mol Biol* 2010, **588**:219-230.
122. Fend F, Emmert-Buck MR, Chuaqui R, Cole K, Lee J, Liotta LA, Raffeld M: **Immuno-LCM: laser capture microdissection of immunostained frozen sections for mRNA analysis.** *The American journal of pathology* 1999, **154**(1):61-66.
123. Brown AL, Smith DW: **Improved RNA preservation for immunolabeling and laser microdissection.** *RNA* 2009, **15**(12):2364-2374.
124. Fend F, Kremer M, Quintanilla-Martinez L: **Laser capture microdissection: methodical aspects and applications with emphasis on immuno-laser capture microdissection.** *Pathobiology* 2000, **68**(4-5):209-214.
125. Kaneko T, Okiji T, Kaneko R, Suda H, Nor JE: **Laser-capture microdissection for Factor VIII-expressing endothelial cells in cancer tissues.** *Methods Mol Biol* 2011, **755**:395-403.
126. Gallup JM, Kawashima K, Lucero G, Ackermann MR: **New quick method for isolating RNA from laser captured cells stained by immunofluorescent immunohistochemistry; RNA suitable for direct use in fluorogenic TaqMan one-step real-time RT-PCR.** *Biol Proced Online* 2005, **7**:70-92.
127. Macdonald JA, Murugesan N, Pachter JS: **Validation of immuno-laser capture microdissection coupled with quantitative RT-PCR to probe blood-brain barrier gene expression in situ.** *J Neurosci Methods* 2008, **174**(2):219-226.

128. Micke P, Bjornsen T, Scheidl S, Stromberg S, Demoulin JB, Ponten F, Ostman A, Lindahl P, Busch C: **A fluid cover medium provides superior morphology and preserves RNA integrity in tissue sections for laser microdissection and pressure catapulting.** *J Pathol* 2004, **202**(1):130-138.
129. Blatt R, Srinivasan S: **Defining disease with laser precision: laser capture microdissection in gastroenterology.** *Gastroenterology* 2008, **135**(2):364-369.
130. Honda M, Kawai H, Shiota Y, Yamashita T, Kaneko S: **Differential gene expression profiles in stage I primary biliary cirrhosis.** *The American journal of gastroenterology* 2005, **100**(9):2019-2030.
131. Schulze F, Schardt K, Wedemeyer I, Konze E, Wendland K, Dirsch O, Tox U, Dienes HP, Odenthal M: **[Epithelial-mesenchymal transition of biliary epithelial cells in advanced liver fibrosis].** *Verh Dtsch Ges Pathol* 2007, **91**:250-256.
132. Baba N, Kobashi H, Yamamoto K, Terada R, Suzuki T, Hakoda T, Okano N, Shimada N, Fujioka S, Iwasaki Y *et al*: **Gene expression profiling in biliary epithelial cells of primary biliary cirrhosis using laser capture microdissection and cDNA microarray.** *Transl Res* 2006, **148**(3):103-113.
133. Dos Santos A, Court M, Thiers V, Sar S, Guettier C, Samuel D, Brechot C, Garin J, Demaugre F, Masselon CD: **Identification of cellular targets in human intrahepatic cholangiocarcinoma using laser microdissection and accurate mass and time tag proteomics.** *Mol Cell Proteomics* 2010, **9**(9):1991-2004.
134. Tretiakova M, Hart J: **Laser microdissection for gene expression study of hepatocellular carcinomas arising in cirrhotic and non-cirrhotic livers.** *Methods Mol Biol* 2011, **755**:233-244.
135. Leone F, Cavalloni G, Pignochino Y, Sarotto I, Ferraris R, Piacibello W, Venesio T, Capussotti L, Risio M, Aglietta M: **Somatic mutations of epidermal growth factor receptor in bile duct and gallbladder carcinoma.** *Clin Cancer Res* 2006, **12**(6):1680-1685.
136. Fidanza JA, McGall GH: **High-density nucleoside analog probe arrays for enhanced hybridization.** *Nucleosides Nucleotides* 1999, **18**(6-7):1293-1295.
137. Lipshutz RJ, Fodor SP, Gingeras TR, Lockhart DJ: **High density synthetic oligonucleotide arrays.** *Nat Genet* 1999, **21**(1 Suppl):20-24.
138. Eijssen LM, Jaillard M, Adriaens ME, Gaj S, de Groot PJ, Muller M, Evelo CT: **User-friendly solutions for microarray quality control and pre-processing on ArrayAnalysis.org.** *Nucleic acids research* 2013, **41**(Web Server issue):W71-76.
139. Irizarry RA, Hobbs B, Collin F, Beazer-Barclay YD, Antonellis KJ, Scherf U, Speed TP: **Exploration, normalization, and summaries of high density oligonucleotide array probe level data.** *Biostatistics (Oxford, England)* 2003, **4**(2):249-264.
140. Pepper SD, Saunders EK, Edwards LE, Wilson CL, Miller CJ: **The utility of MAS5 expression summary and detection call algorithms.** *BMC bioinformatics* 2007, **8**:273.
141. Li C, Wong WH: **Model-based analysis of oligonucleotide arrays: expression index computation and outlier detection.** *Proceedings of the National Academy of Sciences of the United States of America* 2001, **98**(1):31-36.
142. McClintick JN, Edenberg HJ: **Effects of filtering by Present call on analysis of microarray experiments.** *BMC bioinformatics* 2006, **7**:49.
143. Lim WK, Wang K, Lefebvre C, Califano A: **Comparative analysis of microarray normalization procedures: effects on reverse engineering gene networks.** *Bioinformatics (Oxford, England)* 2007, **23**(13):i282-288.

144. Clarke J, Seo P, Clarke B: **Statistical expression deconvolution from mixed tissue samples.** *Bioinformatics (Oxford, England)* 2010, **26**(8):1043-1049.
145. Li Y, Xie X: **A mixture model for expression deconvolution from RNA-seq in heterogeneous tissues.** *BMC bioinformatics* 2013, **14** Suppl 5:S11.
146. Gong T, Szustakowski JD: **DeconRNASeq: a statistical framework for deconvolution of heterogeneous tissue samples based on mRNA-Seq data.** *Bioinformatics (Oxford, England)* 2013, **29**(8):1083-1085.
147. Newman AM, Liu CL, Green MR, Gentles AJ, Feng W, Xu Y, Hoang CD, Diehn M, Alizadeh AA: **Robust enumeration of cell subsets from tissue expression profiles.** *Nature methods* 2015, **12**(5):453-457.
148. Habs M, Shubik P, Eisenbrand G: **Carcinogenicity of methapyrilene hydrochloride, mepyramine hydrochloride, thenyldiamine hydrochloride, and pyribenzamine hydrochloride in Sprague-Dawley rats.** *Journal of cancer research and clinical oncology* 1986, **111**(1):71-74.
149. Lijinsky W, Reuber MD, Blackwell BN: **Liver tumors induced in rats by oral administration of the antihistaminic methapyrilene hydrochloride.** *Science (New York, NY)* 1980, **209**(4458):817-819.
150. Lijinsky W: **Chronic toxicity tests of pyrilamine maleate and methapyrilene hydrochloride in F344 rats.** *Food and chemical toxicology : an international journal published for the British Industrial Biological Research Association* 1984, **22**(1):27-30.
151. Brennan LM, Creasia DA: **The effects of methapyrilene hydrochloride on hepatocarcinogenicity and pentobarbital-induced sleeping time in rats and mice.** *Toxicology and applied pharmacology* 1982, **66**(2):252-258.
152. Lijinsky W, Knutsen G, Reuber MD: **Failure of methapyrilene to induce tumors in hamsters or guinea pigs.** *Journal of toxicology and environmental health* 1983, **12**(4-6):653-657.
153. Mirsalis JC: **Genotoxicity, toxicity, and carcinogenicity of the antihistamine methapyrilene.** *Mutation research* 1987, **185**(3):309-317.
154. Casciano DA, Schol HM: **Methapyrilene is inactive in the hepatocyte-mediated Chinese hamster ovary/hypoxanthine-guanine phosphoribosyl transferase mutational assay.** *Cancer letters* 1984, **21**(3):337-341.
155. Casciano DA, Shaddock JG, Talaska G: **The potent hepatocarcinogen methapyrilene does not form DNA adducts in livers of Fischer 344 rats.** *Mutation research* 1988, **208**(3-4):129-135.
156. Casciano DA, Talaska G, Clive D: **The potent hepatocarcinogen methapyrilene induces mutations in L5178Y mouse lymphoma cells in the apparent absence of DNA adduct formation.** *Mutation research* 1991, **263**(2):127-132.
157. Lijinsky W, Yamashita K: **Lack of binding of methapyrilene and similar antihistamines to rat liver DNA examined by 32P postlabeling.** *Cancer research* 1988, **48**(22):6475-6477.
158. Oberly TJ, Scheuring JC, Richardson KA, Richardson FC, Garriott ML: **The evaluation of methapyrilene for bacterial mutation with metabolic activation by Aroclor-induced, methapyrilene-induced and noninduced rat-liver S9.** *Mutation research* 1993, **299**(2):77-84.
159. Ratra GS, Cottrell S, Powell CJ: **Effects of induction and inhibition of cytochromes P450 on the hepatotoxicity of methapyrilene.** *Toxicological sciences : an official journal of the Society of Toxicology* 1998, **46**(1):185-196.

160. Ratra GS, Powell CJ, Park BK, Maggs JL, Cottrell S: **Methapyrilene hepatotoxicity is associated with increased hepatic glutathione, the formation of glucuronide conjugates, and enterohepatic recirculation.** *Chemico-biological interactions* 2000, **129**(3):279-295.
161. Richardson FC, Copple DM, Eacho PI: **Effects of methapyrilene on DNA synthesis in mice and rats following continuous dietary exposure.** *Carcinogenesis* 1992, **13**(12):2453-2457.
162. Hamadeh HK, Knight BL, Haugen AC, Sieber S, Amin RP, Bushel PR, Stoll R, Blanchard K, Jayadev S, Tennant RW *et al*: **Methapyrilene toxicity: anchorage of pathologic observations to gene expression alterations.** *Toxicologic pathology* 2002, **30**(4):470-482.
163. Dieterle F, Perentes E, Cordier A, Roth DR, Verdes P, Grenet O, Pantano S, Moulin P, Wahl D, Mahl A *et al*: **Urinary clusterin, cystatin C, beta2-microglobulin and total protein as markers to detect drug-induced kidney injury.** *Nature biotechnology* 2010, **28**(5):463-469.
164. Ferreira JA: **The Benjamini-Hochberg method in the case of discrete test statistics.** *The international journal of biostatistics* 2007, **3**(1):Article 11.
165. Waxman DJ: **Growth hormone pulse-activated STAT5 signalling: a unique regulatory mechanism governing sexual dimorphism of liver gene expression.** *Novartis Foundation symposium* 2000, **227**:61-74; discussion 75-81.
166. Roy AK, Chatterjee B: **Sexual dimorphism in the liver.** *Annual review of physiology* 1983, **45**:37-50.
167. DiMasi JA, Hansen RW, Grabowski HG: **The price of innovation: new estimates of drug development costs.** *Journal of health economics* 2003, **22**(2):151-185.
168. Hay M, Thomas DW, Craighead JL, Economides C, Rosenthal J: **Clinical development success rates for investigational drugs.** *Nature biotechnology* 2014, **32**(1):40-51.
169. Kennedy S: **The role of proteomics in toxicology: identification of biomarkers of toxicity by protein expression analysis.** *Biomarkers : biochemical indicators of exposure, response, and susceptibility to chemicals* 2002, **7**(4):269-290.
170. Miller I, Serchi T, Murk AJ, Gutleb AC: **The added value of proteomics for toxicological studies.** *Journal of toxicology and environmental health Part B, Critical reviews* 2014, **17**(4):225-246.
171. Cui Y, Paules RS: **Use of transcriptomics in understanding mechanisms of drug-induced toxicity.** *Pharmacogenomics* 2010, **11**(4):573-585.
172. Ren X, Li J, Xia B, Liu W, Yang X, Hong WX, Huang P, Wang Y, Li S, Zou F *et al*: **Phosphoproteomic analyses of L-02 liver cells exposed to trichloroethylene.** *Toxicology mechanisms and methods* 2015, **25**(6):459-466.
173. Pan X, Whitten DA, Wu M, Chan C, Wilkerson CG, Pestka JJ: **Early phosphoproteomic changes in the mouse spleen during deoxynivalenol-induced ribotoxic stress.** *Toxicological sciences : an official journal of the Society of Toxicology* 2013, **135**(1):129-143.
174. Williams TD, Mirbahai L, Chipman JK: **The toxicological application of transcriptomics and epigenomics in zebrafish and other teleosts.** *Briefings in functional genomics* 2014, **13**(2):157-171.
175. Boorman GA, Irwin RD, Vallant MK, Gerken DK, Lobenhofer EK, Hejtmancik MR, Hurban P, Brys AM, Travlos GS, Parker JS *et al*: **Variation in the hepatic gene expression in individual male Fischer rats.** *Toxicologic pathology* 2005, **33**(1):102-110.

176. Minami K, Saito T, Narahara M, Tomita H, Kato H, Sugiyama H, Katoh M, Nakajima M, Yokoi T: **Relationship between hepatic gene expression profiles and hepatotoxicity in five typical hepatotoxicant-administered rats.** *Toxicological sciences : an official journal of the Society of Toxicology* 2005, **87**(1):296-305.
177. Seth D, Leo MA, McGuinness PH, Lieber CS, Brennan Y, Williams R, Wang XM, McCaughan GW, Gorrell MD, Haber PS: **Gene expression profiling of alcoholic liver disease in the baboon (*Papio hamadryas*) and human liver.** *The American journal of pathology* 2003, **163**(6):2303-2317.
178. Murakami H, Liotta L, Star RA: **IF-LCM: laser capture microdissection of immunofluorescently defined cells for mRNA analysis rapid communication.** *Kidney international* 2000, **58**(3):1346-1353.
179. Lu YR, Wang LN, Jin X, Chen YN, Cong C, Yuan Y, Li YC, Tang WD, Li HX, Wu XT *et al*: **A preliminary study on the feasibility of gene expression profile of rhesus monkey detected with human microarray.** *Transplantation proceedings* 2008, **40**(2):598-602.
180. Giorgi FM, Bolger AM, Lohse M, Usadel B: **Algorithm-driven artifacts in median polish summarization of microarray data.** *BMC bioinformatics* 2010, **11**:553.
181. Etienne W, Meyer MH, Peppers J, Meyer RA, Jr.: **Comparison of mRNA gene expression by RT-PCR and DNA microarray.** *BioTechniques* 2004, **36**(4):618-620, 622, 624-616.
182. Rajeevan MS, Vernon SD, Taysavang N, Unger ER: **Validation of array-based gene expression profiles by real-time (kinetic) RT-PCR.** *The Journal of molecular diagnostics : JMD* 2001, **3**(1):26-31.
183. Rajeevan MS, Ranamukhaarachchi DG, Vernon SD, Unger ER: **Use of real-time quantitative PCR to validate the results of cDNA array and differential display PCR technologies.** *Methods (San Diego, Calif)* 2001, **25**(4):443-451.
184. Yuen T, Wurmbach E, Pfeffer RL, Ebersole BJ, Sealfon SC: **Accuracy and calibration of commercial oligonucleotide and custom cDNA microarrays.** *Nucleic acids research* 2002, **30**(10):e48.
185. Osada T, Nagashima I, Tsuno NH, Kitayama J, Nagawa H: **Prognostic significance of glutamine synthetase expression in unifocal advanced hepatocellular carcinoma.** *Journal of hepatology* 2000, **33**(2):247-253.
186. Cadoret A, Ovejero C, Terris B, Souil E, Levy L, Lamers WH, Kitajewski J, Kahn A, Perret C: **New targets of beta-catenin signaling in the liver are involved in the glutamine metabolism.** *Oncogene* 2002, **21**(54):8293-8301.
187. Planas-Paz L, Orsini V, Boulter L, Calabrese D, Pikiolek M, Nigsch F, Xie Y, Roma G, Donovan A, Marti P *et al*: **The RSPO-LGR4/5-ZNRF3/RNF43 module controls liver zonation and size.** *Nature cell biology* 2016.
188. Saito K, Negishi M, James Squires E: **Sexual dimorphisms in zonal gene expression in mouse liver.** *Biochemical and biophysical research communications* 2013, **436**(4):730-735.
189. Bastida G, Nos P, Aguas M, Beltran B, Rubin A, Dasi F, Ponce J: **Incidence, risk factors and clinical course of thiopurine-induced liver injury in patients with inflammatory bowel disease.** *Alimentary pharmacology & therapeutics* 2005, **22**(9):775-782.

Gene signatures

Rat bile duct signature

Probe Set ID	Corrected p--value	p--value	FCAbsolute	Gene Symbol	Gene Title
APFX_Rat_Hexokinase_5_at	2.02E--0	9.09E--0	13.693078	Hk1	hexokinase 1
1367571_a_at	4.66E--0	4.10E--0	12.500559	Igf2	insulin--like growth factor 2
1367501_a_at	1.27E--0	2.97E--1	36.448708	Ipp1	secreted phosphoprotein 1
1367504_at	2.63E--0	2.46E--0	13.694988	Anxa2	annexin A2
1367592_at	3.42E--0	9.05E--0	49.07222	Tnni2	troponin T type 2 (cardiac)
1367614_at	3.85E--0	1.70E--0	23.178629	Anxa1	annexin A1
1367655_at	1.45E--0	6.03E--0	14.330635	Tnfrsf10	thymosin beta--10--like//thymosin, beta 10
1367661_at	7.10E--0	4.01E--0	37.7763	S100a6	S100 calcium binding protein A6
1367823_at	1.83E--0	1.57E--0	13.835695	Timp2	TIMP metalloproteinase inhibitor 2
1367851_at	3.09E--0	3.07E--0	27.330727	Ptgsd	prostaglandin D2 synthase (brain)
1367858_at	4.05E--0	3.52E--0	10.284656	Mmp11	matrix metalloproteinase 11
1367880_at	1.43E--0	5.88E--0	12.941892	Lamb2	laminin, beta 2
1368003_at	8.10E--0	1.09E--0	95.26397	Aldh1a2	aldehyde dehydrogenase 1 family, member A2
1368005_at	8.57E--0	5.53E--0	9.883257	Ipp3	inositol 1,4,5--trisphosphate receptor, type 3
1368007_at	1.59E--1	1.95E--1	50.854095	Dmbx1//LOC100131031	deleted in malignant brain tumors 1//deleted in malignant brain tumors 1 protein--like
1368008_at	1.88E--0	1.42E--0	12.854971	Prom1	prominin 1
1368013_at	4.55E--0	1.31E--0	9.427295	Ddit4l//LOC100363484	DNA--damage--inducible transcript 4--like//DNA--damage--inducible transcript 4--
1368052_at	1.76E--0	3.91E--0	86.02309	Tspan8	tetraspanin 8
1368097_a_at	1.05E--0	7.05E--0	10.079666	Rtn1	reticulin 1
1368123_at	3.57E--0	3.04E--0	21.487787	Igf1r	insulin--like growth factor 1 receptor
1368131_at	1.59E--0	3.25E--0	37.547344	Capn6	calpain 6
1368200_at	4.39E--0	1.25E--0	18.500254	Cx3cl1	chemokine (C--X3--C motif) ligand 1
1368250_at	5.78E--0	3.39E--0	13.464029	Tekt1	tektin 1
1368254_a_at	2.01E--0	1.80E--0	21.959936	Sphk1	sphingosine kinase 1
1368278_at	2.15E--0	1.98E--0	54.886753	Lgals2	lectin, galactoside--binding, soluble, 2
1368281_at	3.83E--0	3.30E--0	10.997819	Dpep1	dipeptidase 1 (renal)
1368350_at	1.25E--0	8.67E--0	34.15715	Ptprz1	protein tyrosine phosphatase, receptor--type, Z polypeptide 1
1368363_at	1.24E--0	4.85E--0	32.857944	Klf5	Kruppel--like factor 5
1368374_a_at	1.14E--0	2.29E--1	56.173866	Ggt1	gamma--glutamyltransferase 1
1368391_at	3.10E--0	1.53E--0	11.326229	Slc7a1	solute carrier family 7 (cationic amino acid transporter, y+ system), member 1
1368392_at	0.002102866	0.002051262	9.339462	Slc7a1	solute carrier family 7 (cationic amino acid transporter, y+ system), member 1
1368395_at	1.78E--0	4.06E--0	14.945976	Gpc3	glypican 3
1368398_at	1.70E--0	1.25E--0	11.446347	Cacna1h	calcium channel, voltage--dependent, T type, alpha 1H subunit
1368404_at	8.03E--0	2.81E--0	13.423091	Dbn1	drebrin 1
1368411_a_at	4.04E--0	3.10E--1	62.83263	Map2	microtubule--associated protein 2
1368413_at	2.76E--0	1.32E--0	11.373006	Abp1	amiloride binding protein 1 (amine oxidase, copper--containing)
1368441_at	5.19E--0	6.11E--0	106.69083	Msln	mesothelin
1368469_at	8.73E--0	1.07E--1	157.86432	Aqp5	aquaporin 5
1368515_at	1.45E--0	1.05E--0	10.89343	Epb41l3	erythrocyte membrane protein band 4.1--like 3
1368521_at	3.25E--0	8.43E--0	10.534752	Napsa	napasin A aspartic peptidase
1368527_at	6.51E--0	8.39E--0	48.73094	Ptgs2	prostaglandin--endoperoxide synthase 2
1368555_at	4.72E--0	4.18E--0	9.211765	Cd37	CD37 molecule
1368612_at	8.15E--0	2.89E--0	10.481842	Itgab4	integrin, beta 4
1368887_at	1.46E--0	6.09E--0	40.16622	Cdh22	cadherin 22
1368920_at	7.83E--0	1.02E--0	45.95985	Slit3	slit homolog 3 (Drosophila)
1368921_a_at	5.61E--0	1.71E--0	30.379755	Cd44	CD44 molecule
1368949_at	5.07E--0	2.86E--0	10.462679	Ebf1	early B--cell factor 1
1368983_at	8.12E--0	5.16E--0	9.253278	Hbegf	heparin--binding EGF--like growth factor
1369105_a_at	1.32E--0	9.35E--0	22.487028	Pkib	protein kinase (cAMP--dependent, catalytic) inhibitor beta
1369128_at	1.27E--0	8.82E--0	9.439171	Grik5	glutamate receptor, ionotropic, kainate 5
1369135_at	1.56E--0	1.14E--0	16.748272	Syt11	synaptotagmin XI
1369167_at	2.73E--0	2.22E--0	25.706429	Gfra2	GDNF family receptor alpha 2
1369185_a_at	2.40E--0	1.10E--0	16.476957	Syt7	synaptotagmin VII
1369213_at	8.19E--0	2.91E--0	11.828588	L1cam	L1 cell adhesion molecule
1369263_at	3.99E--0	3.46E--0	10.105852	Wnt5a	wingless--type MMTV integration site family, member 5A
1369301_at	2.00E--0	8.96E--0	25.398272	Aplnr	apelin receptor
1369336_at	1.47E--0	6.13E--0	16.566042	Hr	hair growth associated
1369353_at	1.11E--0	7.52E--0	21.358007	ErbB4	v--erb--a erythroblastic leukemia viral oncogene homolog 4 (avian)
1369358_a_at	1.86E--0	4.31E--0	12.13524	Hap1	huntingtin--associated protein 1
1369373_at	1.76E--0	1.30E--0	10.354804	Fgfr3	fibroblast growth factor receptor 3
1369381_a_at	4.73E--0	1.38E--0	30.748932	Slc15a1	solute carrier family 15 (oligopeptide transporter), member 1
1369385_at	1.74E--0	1.28E--0	10.134165	Afp1	actin filament associated protein 1
1369441_at	4.22E--0	2.27E--0	9.354585	Capn5	calpain 5
1369458_at	2.65E--0	1.26E--0	12.489753	Gab2	GRB2--associated binding protein 2
1369484_at	6.23E--0	7.95E--0	112.22871	Wisp2	WNT1 inducible signaling pathway protein 2
1369500_at	5.61E--0	3.23E--0	12.561653	Kcnk1	potassium channel, subfamily K, member 1
1369513_at	6.28E--0	5.71E--0	10.85835	Ccl28	chemokine (C--C motif) ligand 28
1369516_at	7.22E--0	4.46E--0	22.151363	Pdx1	pancreatic and duodenal homeobox 1
1369640_at	3.85E--0	1.65E--0	19.856825	Gja1	gap junction protein, alpha 1
1369670_at	6.63E--0	2.13E--0	27.442968	Cd200	CD200 molecule
1369686_at	3.35E--0	1.27E--0	22.78919	Dclk1	doublecortin--like kinase 1
1369698_at	2.01E--0	1.53E--0	11.581351	Abcc3	ATP--binding cassette, subfamily C (CFTR/MRP), member 3
1369735_at	5.48E--0	2.89E--0	18.456982	Cas6	growth arrest specific 6
1369759_at	2.15E--0	1.66E--0	16.507908	Slc5a1	solute carrier family 5 (sodium/glucose cotransporter), member 1
1369798_at	3.78E--0	3.24E--0	9.236135	Atfb2	ATPase, Na+/K+ transporting, beta 2 polypeptide
1369949_at	1.27E--0	8.70E--0	24.296352	Bcam	basal cell adhesion molecule (Lutheran blood group)
1369953_a_at	4.05E--1	9.95E--1	27.058285	Cd24	CD24 molecule
1369963_at	3.15E--0	2.64E--0	9.25386	Fafah1b3	platelet--activating factor acetylhydrolase 1b, catalytic subunit 3
1370011_at	1.50E--0	1.09E--0	20.099453	Akl1	adenylate kinase 1
1370026_at	2.43E--0	8.06E--1	22.020063	Cryab	crystallin, alpha B
1370072_at	3.42E--0	1.75E--0	17.481222	Mme	membrane metallo--endopeptidase
1370122_at	5.80E--0	1.80E--0	33.097958	Rab27b	RAB27B, member RAS oncogene family
1370143_at	1.78E--0	4.06E--0	10.144477	Smo	smoothened, frizzled family receptor
1370217_at	1.53E--0	3.10E--0	15.142731		
1370218_at	5.31E--0	1.60E--0	20.30291	Ldhh	lactate dehydrogenase B
1370233_at	4.94E--0	4.40E--0	10.535631	Fgfl2	fibroblast growth factor 12
1370269_at	6.13E--0	3.62E--0	35.851364	Cyp11a1	cytochrome P450, family 1, subfamily a, polypeptide 1
1370367_at	1.21E--0	8.32E--0	10.029843	Slc1a1	solute carrier family 1 (neuronal/epithelial high affinity glutamate transporter, system Xag, member 1)
1370379_at	1.71E--0	3.70E--0	15.166229	Prss8	protease, serine, 8
1370406_a_at	0.002605047	0.002560298	9.537443	Cd55	CD55 molecule
1370410_at	7.35E--0	6.75E--0	14.036026	Igslf1	immunoglobulin superfamily, member 1
1370418_a_at	5.09E--0	2.88E--0	18.103872	Syt17	synaptotagmin XVII
1370448_at	2.52E--0	1.18E--0	13.860155	Cpc2	glypican 2
1370514_a_at	5.25E--0	6.44E--0	33.56122	Syt7	synaptotagmin VII
1370515_x_at	5.55E--0	3.19E--0	11.055471	Syt7	synaptotagmin VII
1370561_at	1.17E--0	4.50E--0	15.606807	A3galt2	alpha 1,3--galactosyltransferase 2
1370594_at	1.24E--0	4.82E--0	41.762447	Igslf1	immunoglobulin superfamily, member 1
1370657_at	5.72E--0	3.32E--0	25.157446	Cthb6	cadherin 6
1370692_at	0.001035933	9.80E--0	9.792784	Il1rl1	interleukin 1 receptor--like 1
1370727_at	2.54E--0	6.38E--0	24.19306	Pdgfrd	platelet derived growth factor D
1370864_at	5.35E--0	6.64E--0	11.312916	Col1a1	collagen, type I, alpha 1
1370894_at	1.37E--0	2.41E--0	56.5471	Cldn7	claudin 7
1370902_at	1.52E--0	3.04E--0	21.273922	Akr1b8	aldo--keto reductase family 1, member B8
1370912_at	1.36E--0	9.65E--0	12.633699	Hspa1a	heat shock 70kD protein 1A
1370956_at	3.72E--0	1.02E--0	14.101621	Dcn	decorin
1370963_at	7.37E--0	4.59E--0	16.265783	Gas7	growth arrest specific 7
1370973_at	3.13E--0	2.62E--0	18.037725	Scn7a	sodium channel, voltage--gated, type VII, alpha

1371130_at	1.62E--0	6.89E--0	9.662579	Slc1a3	solute carrier family 1 (glial high affinity glutamate transporter), member 3
1371133_a_at	1.56E--0	6.62E--0	13.122443	Prkar2b	protein kinase, cAMP dependent regulatory, type II beta
1371164_at	3.70E--0	1.93E--0	15.912628	Mcp1010///RGD1565970	mast cell protease 10///similar to mast cell protease 8
1371256_at	5.91E--0	3.47E--0	12.501319	Ptpn18	protein tyrosine phosphatase, non--receptor type 18
1371260_at	4.45E--0	3.92E--0	15.473067	Mcp12	mast cell protease 2
1371360_at	8.57E--0	5.53E--0	17.334116	Ndrp1	N--myc downstream regulated 1
1371393_at	1.14E--0	2.39E--1	12.367773	Cln1	calsynenin 1
1371472_at	4.07E--0	4.30E--0	12.167263		
1371499_at	2.52E--0	6.23E--0	11.708584	Cd9	CD9 molecule
1371527_at	1.16E--0	1.87E--0	12.16712	Emp1	epithelial membrane protein 1
1371671_at	0.001260288	0.001206166	11.366027		
1371696_at	1.36E--0	2.35E--0	19.252666	Gpr56	G protein--coupled receptor 56
1371700_at	1.38E--0	1.02E--0	14.689907	LOC100911714//Misp4	microfibril--associated glycoprotein 4--like//microfibrillar--associated protein 4
1371861_at	1.44E--0	1.04E--0	10.911258	Sfrp1	secreted frizzled--related protein 1
1371883_at	5.16E--0	1.55E--0	14.574821	Mmd	monocyte to macrophage differentiation--associated
1372002_at	5.41E--1	1.99E--1	10.582753	Gja1	gap junction protein, alpha 1
1372063_at	1.09E--0	4.10E--0	12.944598		
1372064_at	1.64E--0	1.29E--0	14.624378	Cxcl16	chemokine (C--X--C motif) ligand 16
1372111_at	1.52E--0	2.98E--0	12.275206	Cav1	caveolin 1, caveolae protein
1372162_at	5.03E--0	5.78E--0	11.715216	Acas1	acyl--CoA synthetase short--chain family member 1
1372179_at	3.02E--0	2.93E--0	9.3302765	Hpcal1	hippocalcin--like 1
1372208_at	7.24E--0	2.42E--0	26.82274	Ppp1r1b	protein phosphatase 1, regulatory (inhibitor) subunit 1B
1372256_at	1.40E--0	2.57E--0	13.957351	Crip1	cysteine--rich protein 1 (intestinal)
1372481_at	1.24E--0	4.79E--0	18.029274		
1372615_at	2.59E--0	6.59E--0	15.894693	Aoc3	amine oxidase, copper containing 3
1372641_at	1.79E--0	1.33E--0	12.194944	Alpk3	alpha--kinase 3
1372658_at	1.90E--0	4.50E--0	14.413948	Synn	synemin, intermediate filament protein
1372708_at	1.93E--0	8.58E--0	23.943815		
1372725_at	4.22E--0	2.27E--0	23.33735	Pfcer2	phospholipid scramblase 2
1372805_at	9.60E--0	3.51E--0	20.450375	Endod1	endonuclease domain containing 1
1372818_at	7.71E--0	7.11E--0	10.684435	Colec12	collectin sub--family member 12
1372820_at	6.65E--0	2.15E--0	23.599646	LOC691984	similar to Glypican--6 precursor
1372967_at	1.78E--0	1.32E--0	9.255879	Arhgef25	Rho guanine nucleotide exchange factor (GEF) 25
1373000_at	7.39E--0	4.62E--0	18.801155	Srpx2	sushi--repeat--containing protein, X--linked 2
1373006_at	3.76E--0	1.97E--0	12.144326	Tmem171	transmembrane protein 171
1373008_x_at	4.27E--0	3.74E--0	13.407098	Rtn4r	reticulon 4 receptor
1373035_at	6.62E--0	4.01E--0	12.2618		
1373089_at	1.86E--0	4.33E--0	23.76456	Cdh3	cadherin 3
1373148_at	1.02E--0	6.76E--0	10.292156	Cpxm2	carboxypeptidase X (M14 family), member 2
1373210_at	2.86E--0	1.40E--0	12.738761	Lamb1	laminin, beta 1
1373224_at	1.81E--0	4.88E--1	11.811304	St3gal4	ST3 beta--galactoside alpha--2,3--sialyltransferase 4
1373232_at	1.70E--0	3.65E--0	23.180397	LOC302022	similar to nidogen 2 protein
1373330_at	2.80E--0	1.36E--0	14.919093	LOC690323	similar to Myosin--15 (Myosin XV) (Unconventional myosin--15)
1373458_at	4.04E--0	3.07E--1	22.041267	Bex4	brain expressed, X--linked 4
1373485_at	4.38E--0	2.38E--0	20.451302		
1373521_at	4.72E--0	4.18E--0	9.50532	Sh3tc2	SH3 domain and tetratricopeptide repeats 2
1373631_at	5.03E--0	5.77E--0	61.254997	Rap1gap	Rap1 GTPase--activating protein
1373651_at	4.53E--0	2.48E--0	22.103037		
1373696_at	4.75E--0	2.64E--0	12.527222	LOC100910558	uncharacterized LOC100910558
1373725_at	2.40E--0	1.10E--0	22.412664		
1373839_at	8.54E--0	7.96E--0	12.593703		
1373860_at	1.36E--0	2.39E--0	9.241785	Sox4	SRY (sex determining region Y)--box 4
1373900_at	6.38E--0	3.83E--0	61.61385	Krt7	keratin 7
1373902_at	5.97E--0	5.41E--0	11.736959	Rimkb	ribosomal modification protein rimK--like family member B
1373908_at	6.59E--0	2.11E--0	13.293645		
1373914_at	3.37E--0	2.84E--0	18.194729		
1373928_at	1.24E--0	4.83E--0	28.494877	Il17re	interleukin 17 receptor E
1373977_at	3.29E--0	8.61E--0	9.845295		
1373985_at	1.24E--0	4.88E--0	12.060419		
1374022_at	5.03E--0	5.78E--0	36.05377		
1374056_at	1.72E--0	1.27E--0	11.899961	Rbm24	RNA binding motif protein 24
1374070_at	8.25E--0	2.95E--0	74.624214	Gpx2	glutathione peroxidase 2
1374089_at	6.38E--0	3.83E--0	13.56553		
1374106_at	7.43E--0	4.65E--0	26.521767		
1374119_at	1.06E--0	3.93E--0	10.975694	Eif3	E74--like factor 3
1374122_at	2.86E--0	1.40E--0	38.222332	Myo5c	myosin VC
1374151_at	5.35E--0	3.05E--0	11.93909		
1374193_at	5.25E--0	4.70E--0	11.04623		
1374195_at	1.35E--0	9.60E--0	14.124624	Lad1	ladinin 1
1374342_at	5.51E--0	4.96E--0	9.492553	Ly6g6c	lymphocyte antigen 6 complex, locus G6C
1374376_at	3.65E--0	3.67E--0	15.596862	Arhgef28	Rho guanine nucleotide exchange factor (GEF) 28
1374427_at	1.21E--0	8.27E--0	22.748371		
1374434_at	7.41E--0	2.51E--0	23.213726	LOC498222	similar to specifically androgen--regulated protein
1374488_at	1.81E--0	4.17E--0	22.39445	Gramd1b	GRAM domain containing 1B
1374496_at	8.04E--0	7.46E--0	9.200513	Tril	TLR4 interactor with leucine--rich repeats
1374557_at	1.38E--0	9.89E--0	13.465133	Wls	wntless homolog (Drosophila)
1374573_at	4.54E--0	2.49E--0	12.199232	Dync2h1	dynein cytoplasmic 2 light intermediate chain 1
1374594_at	1.39E--0	5.63E--0	61.74779	LOC363060	similar to RIKEN cDNA 1600029D21
1374630_at	3.23E--0	1.19E--0	56.059574	Clic3	chloride intracellular channel 3
1374691_at	1.76E--0	3.96E--0	22.866798	Sult5a1	sulfotransferase family 5A, member 1
1374699_at	3.15E--0	1.57E--0	39.059124	Fam84a	family with sequence similarity 84, member A
1374705_at	3.16E--0	1.59E--0	13.600379	Col4a5	collagen, type IV, alpha 5
1374708_at	2.51E--0	2.02E--0	10.279355	RGD1565043	similar to Rho guanine nucleotide exchange factor (GEF) 10
1374726_at	3.79E--0	2.00E--0	10.783984	Fndc1	fibronectin type III domain containing 1
1374728_at	3.05E--0	2.53E--0	11.212997		
1374768_at	5.40E--0	3.09E--0	15.707371	Ccdc65	coiled--coil domain containing 65
1374774_at	1.76E--0	3.95E--0	15.635612		
1374812_at	3.76E--0	1.57E--0	13.4769745	Ptpn13	protein tyrosine phosphatase, non--receptor type 13
1374817_at	8.29E--0	1.14E--0	37.459064		
1374870_at	3.42E--0	2.89E--0	10.816524		
1374910_at	2.31E--0	5.58E--0	25.026775	Celr2	cadherin, EGF LAG seven--pass G--type receptor 2
1374963_x_at	6.34E--0	3.77E--0	18.970654		
1374976_a_at	3.56E--0	1.85E--0	18.247913	Soat1	sterol O--acyltransferase 1
1375030_at	1.42E--0	2.65E--0	50.26162	B3gal5	UDP--Gal:beta-GlcNAc beta 1,3--galactosyltransferase, polypeptide 5
1375032_at	1.82E--0	1.54E--0	82.186005	Kndc1	kinase non--catalytic C--lobe domain (KIND) containing 1
1375039_x_at	2.45E--0	1.96E--0	9.804144	Fcgbp1	Fc fragment of IgG binding protein--like 1
1375051_at	0.001628648	0.001572695	9.648176		
1375062_at	1.09E--0	4.10E--0	19.397228	Ap1m2	adaptor--related protein complex 1, mu 2 subunit
1375083_at	4.00E--0	2.11E--0	36.525898		
1375084_at	1.78E--0	4.01E--0	26.43655	Serinc2	serine incorporator 2
1375136_at	4.90E--0	1.44E--0	9.371695		
1375170_at	1.14E--0	1.80E--1	32.225735	S100a11	S100 calcium binding protein A11
1375267_at	3.54E--0	1.43E--0	20.533499	Ppic	peptidylprolyl isomerase C
1375320_at	3.57E--0	3.03E--0	15.71609		
1375358_at	1.07E--0	1.69E--0	21.041254		
1375359_at	1.76E--0	1.30E--0	17.94388	Gfra2	GDNF family receptor alpha 2
1375377_at	3.27E--0	1.67E--0	21.766483	Igfb3	immunoglobulin superfamily, member 3
1375485_at	2.76E--0	1.33E--0	10.310503	Prrx1	paired related homeobox 1
1375708_at	3.20E--0	2.68E--0	13.255325	Col27a1	collagen, type XXVII, alpha 1
1375719_s_at	2.38E--0	1.87E--0	10.560182	Cdh13	cadherin 13
1375849_at	1.84E--0	1.39E--0	11.833174	Rgma	RCM domain family, member A
1375908_at	5.76E--0	7.28E--0	13.846147	Mpz12	myelin protein zero--like 2
1375958_at	2.43E--0	1.93E--0	10.672437	Tsc22d4	TSC22 domain family, member 4

1376025_at	2.03E--0	1.56E--0	10.097886	Prmt2	protein arginine methyltransferase 2
1376102_at	1.52E--0	3.06E--0	11.710049	Tmbim1	transmembrane BAX inhibitor motif containing 1
1376104_at	1.24E--0	4.90E--0	10.3597975	Soga2	SOGA family member 2
1376109_at	5.61E--0	3.23E--0	15.3869		
1376198_at	1.09E--0	7.32E--0	13.470737	Clmp	CXADR--like membrane protein
1376292_at	9.17E--0	1.32E--0	94.05401		
1376297_at	1.64E--0	7.00E--0	11.935768	Arrdc1	arrestin domain containing 1
1376362_at	1.29E--0	5.16E--0	13.867951	Nptxr	neuronal pentraxin receptor
1376457_at	7.81E--0	2.68E--0	32.761745	Crispld2	cysteine--rich secretory protein LCCL domain containing 2
1376465_at	1.65E--0	7.07E--0	13.777263		
1376564_at	6.62E--0	4.01E--0	10.780192	Sptbn4	spectrin, beta, non--erythrocytic 4
1376632_at	7.83E--0	1.03E--0	14.634426	Lmcd1	LIM and cysteine--rich domains 1
1376640_at	1.63E--0	3.39E--0	13.753034	Fam171a1	family with sequence similarity 171, member A1
1376661_at	1.60E--0	1.17E--0	9.63517	Kazn	kazrin, periplakin interacting protein
1376770_at	3.02E--0	2.92E--0	15.225313	Efhf1	EF--hand domain family, member D1
1376877_at	1.16E--0	1.90E--0	30.346548	Cdcp1	CUB domain containing protein 1
1376937_at	0.001056015	0.001000299	9.217573	Filp11	filamin A interacting protein 1--like
1376953_at	7.66E--0	7.05E--0	9.947374	Unc5c1	unc--5 homolog C (C. elegans)--like
1377008_at	8.36E--0	7.77E--0	12.75111	RGD1566401	similar to GTL2, imprinted maternally expressed untranslated
1377018_at	2.24E--0	6.87E--1	21.025244		
1377034_at	1.95E--0	5.50E--1	30.448162	Serpnb1a	serine (or cysteine) proteinase inhibitor, clade B, member 1a
1377046_at	1.35E--0	5.48E--0	14.686747	Ankrd6	ankyrin repeat domain 6
1377088_at	1.90E--0	4.53E--0	33.31594	Slc52a3	solute carrier family 52, riboflavin transporter, member 3
1377180_at	3.15E--0	1.58E--0	23.011261		
1377249_at	6.77E--0	6.19E--0	11.117941	Gsp12	G1 to S phase transition 2
1377308_a_at	3.06E--0	2.54E--0	12.293895		
1377336_at	1.16E--0	7.88E--0	17.960976	Sema3b	sema domain, immunoglobulin domain (Ig), short basic domain, secreted, (semaphorin) 3B
1377363_at	5.03E--0	5.80E--0	12.715094	Rab25	RAB25, member RAS oncogene family
1377365_at	3.50E--0	9.32E--0	15.139032	Plekhn1	pleckstrin homology domain containing, family N member 1
1377366_at	5.19E--0	6.10E--0	59.286716		
1377383_at	2.00E--0	8.93E--0	40.24625	Efs	embryonal Fyn--associated substrate
1377428_at	4.16E--0	2.22E--0	12.263563	Lama5	laminin, alpha 5
1377449_at	1.08E--0	1.73E--0	22.9782	Pvr14	poliovirus receptor--related 4
1377450_s_at	9.89E--0	1.44E--0	38.76371	Pvr14	poliovirus receptor--related 4
1377522_a_at	5.25E--0	2.99E--0	19.815933	Zfr2	zinc finger RNA binding protein 2
1377606_at	6.96E--0	2.30E--0	13.590374	Cdk14	cyclin--dependent kinase 14
1377867_at	2.52E--0	6.24E--0	9.537132	RGD1562284	similar to Glutaminyl--peptide cyclotransferase precursor (QC)
1378421_at	2.43E--0	1.93E--0	9.418797	LOC100910996	uncharacterized LOC100910996
1379031_at	1.04E--0	3.84E--0	24.523722	Gca	grancalcin
1379451_at	4.20E--0	3.66E--0	13.12676		
1379936_at	1.25E--0	2.08E--0	49.771782		
1381341_at	5.61E--0	1.72E--0	38.729553	LOC688459	hypothetical protein LOC688459
1382320_at	5.61E--0	1.72E--0	17.960115	RGD1307315	LOC362793
1382375_at	8.63E--0	9.53E--1	94.69858		
1382581_at	1.28E--0	2.17E--0	26.30913	Ehf	ets homologous factor
1382849_at	1.29E--0	5.14E--0	35.12849		
1383058_at	9.02E--0	3.24E--0	26.19916		
1383322_at	5.61E--0	3.24E--0	25.40111	Ras11b	RAS--like family 11 member B
1383460_at	1.37E--0	2.45E--0	33.874184		
1383649_a_at	0.001743348	0.001687732	15.475113	Ddx26b	DEAD/H (Asp--Glu--Ala--Asp/His) box polypeptide 26B
1383855_at	1.14E--0	2.21E--1	47.80753	Degs2	delta(4)--desaturase, sphingolipid 2
1383935_at	6.43E--0	3.47E--0	13.840781		
1384027_a_at	5.68E--0	7.11E--0	85.607506		
1384028_at	2.62E--0	6.70E--0	26.478008		
1384329_at	5.07E--0	2.86E--0	19.057688	Prss22	protease, serine, 22
1384473_at	4.74E--0	2.63E--0	9.581018		
1385088_at	4.91E--0	4.36E--0	11.561647	RGD1310262	hypothetical LOC304650
1385805_at	1.25E--0	2.09E--0	17.987728		
1386466_at	2.30E--0	1.80E--0	16.720318		
1386862_at	1.27E--0	2.88E--1	16.405445	Anxa5	annexin A5
1386903_at	2.72E--0	1.30E--0	20.4798	S100b	S100 calcium binding protein B
1386911_at	8.03E--0	2.81E--0	13.242101	Atp1a2	ATPase, Na+/K+ transporting, alpha 2 polypeptide
1386921_at	2.29E--0	1.79E--0	17.455502	Cpe	carboxypeptidase E
1386943_at	8.47E--0	5.42E--0	29.594782	Pllp	plasmalipin
1386974_at	3.02E--0	2.50E--0	11.743908	Phldb1	pleckstrin homology--like domain, family B, member 1
1387004_at	0.001479186	0.001424738	11.30693	Nhl1	neuroblastoma 1, DAN family BMP antagonist
1387011_at	8.65E--0	1.20E--0	89.603325	Lcn2	lipocalin 2
1387040_at	1.28E--0	9.03E--0	25.030117	Mal	mal, T--cell differentiation protein
1387043_at	0.004582734	0.004560242	9.821113	Lypd3	Ly6/Plaur domain containing 3
1387059_at	0.001210771	0.001157289	10.051012	Stk39	serine threonine kinase 39
1387122_at	2.93E--0	1.44E--0	81.27568	Plagl1	pleiomorphic adenoma gene--like 1
1387153_at	4.75E--0	5.18E--0	24.505636	Ril	reversion induced LIM gene
1387195_at	1.07E--0	1.64E--0	16.865726	St14	suppression of tumorigenicity 14 (colon carcinoma)
1387276_at	1.21E--0	8.01E--0	15.8604145	Dclk1	doublecortin--like kinase 1
1387315_at	1.00E--0	1.48E--0	17.810762	Sftpd	surfactant protein D
1387348_at	1.17E--0	4.46E--0	14.967701	Igfbp5	insulin--like growth factor binding protein 5
1387439_at	1.82E--0	1.52E--0	41.994915	Megf6	multiple EGF--like--domains 6
1387454_at	1.43E--0	5.88E--0	10.222892	Fam129a	family with sequence similarity 129, member A
1387459_at	4.15E--0	2.21E--0	21.004295	Pkib	protein kinase (cAMP--dependent, catalytic) inhibitor beta
1387483_at	1.80E--0	1.36E--0	9.235196	Plcg2	phospholipase C, gamma 2
1387581_at	0.002578954	0.002531489	10.670871	Rassf9	Ras association (RalGDS/AF--6) domain family N--terminal member 9
1387600_at	5.21E--0	6.27E--0	41.38266	Gabbr2	gamma--aminobutyric acid (GABA--A) receptor, pi
1387611_at	2.69E--0	2.17E--0	20.667196	Bcl2	B--cell CLL/lymphoma 2
1387671_at	1.75E--0	3.86E--0	28.843006	Sctr	secretin receptor
1387713_a_at	5.85E--0	5.30E--0	9.704559	Fcer1a	Fc fragment of IgE, high affinity 1, receptor for; alpha polypeptide
1387791_at	7.83E--0	1.04E--0	15.13041	Ace	angiotensin I converting enzyme (peptidyl--dipeptidase A) 1
1387813_at	1.21E--0	7.87E--0	54.650253	ErbB2	v--erb--b2 erythroblastic leukemia viral oncogene homolog 2, neuro/glioblastoma derived oncogene homolog (avian)
1387922_at	4.82E--0	1.41E--0	23.322363	Crispld2	cysteine--rich secretory protein LCCL domain containing 2
1387932_at	1.21E--0	8.34E--0	15.162415	Slc1a1	solute carrier family 1 (neuronal/epithelial high affinity glutamate transporter, system Xag), member 1
1387952_a_at	1.57E--0	3.20E--0	11.562165	Cd44	CD44 molecule
1388011_a_at	7.44E--0	4.68E--0	14.010181	Tgfb2	transforming growth factor, beta 2
1388015_at	1.53E--0	1.12E--0	10.227247	Ptprz1	protein tyrosine phosphatase, receptor--type, Z polypeptide 1
1388074_at	1.49E--0	1.14E--0	108.330734	Krt20	keratin 20
1388111_at	3.66E--0	3.13E--0	9.707632	Eln	elastin
1388152_at	2.32E--0	1.06E--0	27.87469	Map2	microtubule--associated protein 2
1388176_at	1.05E--0	7.01E--0	21.007301	Cml5	camello--like 5
1388199_at	1.14E--0	1.73E--1	14.865608	Epcam	epithelial cell adhesion molecule
1388227_at	2.86E--0	2.34E--0	9.290555	Mri1	major histocompatibility complex, class I--related
1388274_at	3.61E--0	1.88E--0	10.518496	Bmyc	brain expressed myelocytomatosis oncogene
1388335_at	2.38E--0	7.60E--1	12.113955	Tagln2	transgelin 2
1388433_at	1.81E--0	4.77E--1	46.840206	Krt19	keratin 19
1388439_at	1.00E--0	6.62E--0	10.94992	Fkbp10	FK506 binding protein 10
1388547_at	4.72E--0	2.29E--0	88.98381	Cldn4	claudin 4
1388557_at	1.44E--0	1.08E--0	16.91733	C7//Tubb4b	complement component 7//tubulin, beta 4B class IVb
1388618_at	2.37E--0	5.77E--0	9.747248	Nid2	nidogen 2 (osteonidogen)
1388670_at	2.25E--0	1.75E--0	13.572557		
1388802_at	3.12E--0	1.07E--0	114.31808	Bex1//LOC100912195	brain expressed, X--linked 1//protein BEX1--like
1388856_at	8.57E--0	5.52E--0	11.81065	Krtlg	KIT ligand
1388902_at	2.19E--0	1.69E--0	9.232997	Loxl1	lysyl oxidase--like 1
1388932_at	1.52E--0	3.02E--0	91.28662	Lama5	laminin, alpha 5
1388939_at	5.98E--0	1.88E--0	25.853521	Col15a1//LOC100909752	collagen, type XV, alpha 1//collagen alpha--1(XV) chain--like

1388955_at	1.07E--0	1.70E--0	9.573545		
1388963_at	1.91E--0	8.47E--0	16.460987	Astn1	astrotactin 1
1388972_at	3.10E--0	2.58E--0	10.575199	Rtn4r	reticulon 4 receptor
1388991_at	2.89E--0	2.37E--0	11.765579	Sestd1	SEC14 and spectrin domains 1
1389067_at	8.61E--0	5.57E--0	16.197939	Sloca41	solute carrier organic anion transporter family, member 4a1
1389085_at	1.17E--0	7.48E--0	39.918575		
1389095_at	5.57E--0	1.69E--0	24.668417	Boc	BOC cell adhesion associated, oncogene regulated
1389186_at	1.66E--0	3.53E--0	29.645475		
1389193_at	3.72E--0	1.02E--0	10.920559	Sorcs2	soritin--related VPS10 domain containing receptor 2
1389282_at	9.32E--0	1.35E--0	80.933334	Itga3	integrin, alpha 3
1389349_s_at	1.64E--0	1.28E--0	46.179253	Il17re	interleukin 17 receptor E
1389360_at	5.03E--0	5.66E--0	31.939844	Fxyd3	PXYD domain--containing ion transport regulator 3
1389367_at	2.02E--0	4.82E--0	9.508542	Schip1	schwannomin interacting protein 1
1389409_at	7.84E--0	2.70E--0	13.454418	Tes	testis derived transcript
1389424_at	7.59E--0	4.80E--0	21.686674	LOC688452	hypothetical protein LOC688452
1389502_at	4.61E--0	2.54E--0	14.437923		
1389532_at	2.14E--0	1.65E--0	14.472314		
1389584_at	1.12E--0	7.55E--0	11.608463		
1389697_at	1.09E--0	4.05E--0	13.927736		
1389706_at	2.91E--0	1.43E--0	106.52444	Dclk1	doublecortin--like kinase 1
1389745_at	1.36E--0	2.37E--0	35.10711		
1389755_at	3.99E--0	3.46E--0	9.220638	Cdca7l	cell division cycle associated 7 like
1389759_at	4.62E--0	2.55E--0	24.639694		
1389762_at	4.36E--0	3.83E--0	9.670752	Fcgbp	Fc fragment of IgG binding protein
1389763_at	2.98E--0	2.45E--0	16.61675		
1389783_s_at	9.59E--0	3.49E--0	14.673447	Fcgbp///Fcgbp1	Fc fragment of IgG binding protein///Fc fragment of IgG binding protein--like 1
1389787_at	1.00E--0	6.58E--0	16.722956	Ptk7	protein tyrosine kinase 7
1389788_at	4.20E--0	3.67E--0	12.701558	Morn4	MORN repeat containing 4
1389795_at	8.92E--0	5.47E--0	58.41622		
1389800_at	2.57E--0	1.21E--0	14.25204	Pwmp2b	PWWP domain containing 2B
1389803_at	5.72E--0	3.33E--0	12.763009		
1389921_at	5.88E--0	1.84E--0	32.802216	Evl	Enah/Vasp--like
1390070_at	1.45E--0	6.03E--0	25.619055	LOC100911253	uncharacterized LOC100911253
1390121_at	1.63E--0	3.39E--0	12.06244	Glis2	GLIS family zinc finger 2
1390123_at	4.72E--0	2.61E--0	18.948364	Tmem45b	transmembrane protein 45b
1390191_at	6.38E--0	3.82E--0	22.399778	Hunk	hormonally upregulated Neu--associated kinase
1390192_at	4.74E--0	2.63E--0	17.250414	Slc27a3	solute carrier family 27 (fatty acid transporter), member 3
1390312_at	3.11E--0	2.59E--0	9.210211	LOC500013///LOC684193///Samd9l	similar to sterile alpha motif domain containing 9--like///similar to sterile alpha motif domain containing 9--like///sterile alpha motif domain containing 9--like
1390379_at	7.31E--0	4.54E--0	12.390947	Lmo4	LIM domain only 4
1390437_at	1.52E--0	3.06E--0	13.947505	Sema5a	sema domain, seven thrombospondin repeats (type 1 and type 1--like), transmembrane domain (TM) and short cytoplasmic domain, (semaphorin) 5A
1390459_at	1.28E--0	9.01E--0	9.414595		
1390471_at	3.93E--0	4.05E--0	12.389903		
1390495_at	7.43E--0	4.67E--0	11.388913		
1390547_at	2.46E--0	1.97E--0	21.699644		
1390557_at	5.20E--0	6.19E--0	16.90128	Gca	granulecalcin
1390566_a_at	3.15E--0	1.58E--0	52.090405	Kcnt1b	creatine kinase, mitochondrial 1B
1390656_at	3.52E--0	9.47E--0	21.913763		
1390659_at	1.01E--0	1.50E--0	59.544975		
1390724_at	1.51E--0	1.10E--0	19.69446		
1390741_at	1.45E--0	2.76E--0	15.502336	Zfr2	zinc finger RNA binding protein 2
1391012_at	2.25E--0	1.74E--0	18.681198	Fam83f	family with sequence similarity 83, member F
1391228_at	2.36E--0	1.08E--0	36.517487	RspH1	radial spoke head 1 homolog (Chlamydomonas)
1391509_at	1.80E--0	7.87E--0	26.101778	Tacstd2	tumor--associated calcium signal transducer 2
1391611_at	3.39E--0	1.33E--0	26.07404	Kif12	kinesin family member 12
1392053_at	1.08E--0	7.28E--0	13.31703	Mmrn1	multimerin 1
1392209_at	1.50E--0	2.88E--0	57.176632	Gcnt3	glucosaminyl (N--acetyl) transferase 3, mucin type
1392778_at	4.38E--0	2.38E--0	13.038555	LOC100910594	uncharacterized LOC100910594
1393018_at	5.30E--0	4.74E--0	14.234815	LOC100912649	uncharacterized LOC100912649
1393031_at	1.16E--0	7.93E--0	14.9234085	Abo	ABO blood group (transferase A, alpha 1--3--N--acetylgalactosaminyltransferase; transferase B, alpha 1--3--galactosyltransferase)
1398245_at	4.74E--0	4.65E--1	64.41337	Snccg	synuclein, gamma (breast cancer--specific protein 1)
1398287_at	8.45E--0	7.87E--0	20.763414	Plau	plasminogen activator, urokinase
1398305_at	9.12E--0	5.95E--0	12.640652	Syt17	synaptotagmin XVII
1398318_at	5.63E--0	1.73E--0	28.047886	Muc1	mucin 1, cell surface associated
1398365_at	1.14E--0	1.84E--0	16.268112	Tppp3	tubulin polymerization--promoting protein family member 3
1398373_at	1.40E--0	2.57E--0	53.34996	B3galnt1	beta--1,3--N--acetylgalactosaminyltransferase 1 (globoside blood group)
1398445_at	6.77E--0	2.22E--0	11.381075		
1398458_at	1.40E--0	5.71E--0	14.8164625	Wnk2	WNK lysine deficient protein kinase 2
1377546_at	7.54E--0	4.76E--0	25.361177		
1377631_at	5.69E--0	1.76E--0	34.336933	Col9a3	collagen, type IX, alpha 3
1377635_at	1.30E--0	5.22E--0	12.111018	Fmo2	flavin containing monooxygenase 2
1377636_at	2.29E--0	1.04E--0	17.117167		
1377646_at	0.001415647	0.001358326	10.158515		
1377655_at	0.002031373	0.00197903	10.747581	Fgf12	fibroblast growth factor 12
1377778_at	2.04E--0	1.57E--0	10.138667	Vofl6	ischemia related factor vof--16
1377877_at	6.77E--0	2.21E--0	10.907633		
1377928_at	4.92E--0	4.37E--0	15.835536	Tm4sf20	transmembrane 4 L six family member 20
1377940_at	3.86E--0	1.07E--0	33.672817	Fam101b	family with sequence similarity 101, member B
1377954_at	1.39E--0	2.52E--0	29.20925		
1377974_at	1.89E--0	4.44E--0	99.063255		
1377993_at	4.04E--0	2.67E--1	248.86186	Gng13	guanine nucleotide binding protein (G protein), gamma 13
1378015_at	7.22E--0	4.46E--0	21.18032	Ccl21	chemokine (C--C motif) ligand 21
1378063_at	8.98E--0	8.42E--0	10.80965		
1378107_at	1.21E--0	1.98E--0	63.552532		
1378156_at	1.89E--0	8.32E--0	19.586706	Cys1	cystin 1
1378168_at	7.24E--0	2.43E--0	35.013176	Fam101b	family with sequence similarity 101, member B
1378241_at	1.48E--0	6.21E--0	24.329958		
1378262_at	3.72E--0	1.02E--0	20.842182		
1378302_at	2.52E--0	1.18E--0	11.067706		
1378305_at	1.81E--0	7.91E--0	24.204073	Tm4sf1	transmembrane 4 L six family member 1
1378348_at	2.66E--0	1.26E--0	25.817154	Tmem200c	transmembrane protein 200C
1378420_at	4.73E--0	1.37E--0	10.117996		
1378424_at	1.85E--0	1.40E--0	14.051369	Trim46	tripartite motif--containing 46
1378470_at	1.37E--0	2.45E--0	9.292493	Paqr5	progesterin and adipoQ receptor family member V
1378480_at	3.65E--0	3.11E--0	10.355568		
1378484_at	2.26E--0	1.02E--0	16.442146	RasH12	RAS--like, family 12
1378523_at	1.24E--0	4.85E--0	10.30297	Ttc12	tetratricopeptide repeat domain 12
1378645_at	0.001072231	0.001018291	20.197554		
1378665_at	2.50E--0	2.00E--0	14.548567		
1378667_at	0.001959899	0.001904589	10.632616		
1378801_at	3.06E--0	7.89E--0	23.907564		
1378857_at	0.002828256	0.002786613	10.563026	Tceal5	transcription elongation factor A (SII)--like 5
1378867_at	7.15E--0	4.41E--0	19.091784	LOC100912465	uncharacterized LOC100912465
1378915_x_at	2.54E--0	6.39E--0	9.386923	LOC308990	hypothetical protein LOC308990
1378930_a_at	1.16E--0	7.85E--0	13.783088	LOC100912518	uncharacterized LOC100912518
1378947_at	4.89E--0	2.74E--0	11.009889	Tns4	tensin 4
1379008_at	7.10E--0	2.36E--0	15.744608		
1379081_at	7.24E--0	2.43E--0	14.721452	Noxo1	NADPH oxidase organizer 1
1379106_at	4.33E--0	3.79E--0	11.804127		
1379142_at	0.00262327	0.002581426	9.275517		
1379143_at	1.17E--0	4.52E--0	12.527533		
1379324_at	1.64E--0	1.31E--0	40.9145		
1379340_at	2.01E--0	1.82E--0	49.34641	Lamc2	laminin, gamma 2

1379345_at	7.95E--0	2.76E--0	32.291435	Col15a1///LOC100909752	collagen, type XV, alpha 1///collagen alpha--1(XV) chain--like
1379390_at	3.90E--0	1.82E--0	11.250758	St6galaac2	ST6 (alpha--N--acetyl--neuraminyl--2,3--beta--galactosyl--1,3)--N--acetylgalactosaminide alpha--2,6--sialyltransferase 2
1379393_at	3.18E--0	1.60E--0	16.51206	Vil1	villin 1
1379416_at	7.92E--0	2.74E--0	19.688921		
1379440_at	1.09E--0	4.04E--0	31.337374	Fstl3	folistatin--like 3 (secreted glycoprotein)
1379474_at	1.42E--0	5.81E--0	31.00735		
1379614_at	3.16E--0	1.12E--0	95.25962		
1379681_at	7.01E--0	2.68E--0	14.549558	Ttc22	tetratricopeptide repeat domain 22
1379705_at	5.14E--0	2.91E--0	10.950823		
1379741_at	5.70E--0	5.14E--0	15.271897	Atp6v0a4	ATPase, H+ transporting, lysosomal V0 subunit A4
1379761_at	1.48E--0	1.07E--0	25.399488	LOC100911253	uncharacterized LOC100911253
1379772_at	2.90E--0	7.45E--0	13.162013	Aplnr	apelin receptor
1379791_at	3.43E--0	1.77E--0	9.822134	Gd3e	CD3 molecule, epsilon
1379889_at	2.53E--0	1.19E--0	15.327981	Lamc2	laminin, gamma 2
1379903_at	0.007573801	0.007573801	10.516568		
1379906_at	1.52E--0	2.96E--0	11.270258	Atp1b2	ATPase, Na+/K+ transporting, beta 2 polypeptide
1380052_at	2.76E--0	1.33E--0	9.668791		
1380084_at	1.17E--0	4.45E--0	9.200554		
1380086_at	2.01E--0	1.54E--0	10.422925		
1380105_at	1.07E--0	1.70E--0	52.491142		
1380172_at	5.80E--0	1.81E--0	15.780717	Kif5c	kinesin family member 5C
1380222_at	3.15E--0	1.57E--0	26.722694		
1380249_at	9.47E--0	8.89E--0	11.8609085		
1380261_at	1.79E--0	1.34E--0	18.656294	Erich2	glutamate--rich 2
1380346_at	1.17E--0	4.46E--0	21.334492	Serpinb1a	serine (or cysteine) proteinase inhibitor, clade B, member 1a
1380424_at	2.42E--0	1.91E--0	9.457797	Ubxn11	UBX domain protein 11
1380460_at	1.94E--0	1.47E--0	10.418154	RGD1311267	similar to RIKEN cDNA 4931426K16 gene
1380477_at	6.77E--0	2.22E--0	12.485085		
1380574_at	6.77E--0	2.22E--0	32.03558		
1380642_at	0.001066378	0.001011423	9.213547		
1380684_at	1.45E--0	6.01E--0	20.023506		
1380725_at	8.67E--0	5.64E--0	11.219623	Tspan5	tetraspanin 5
1380766_a_at	9.61E--0	9.04E--0	9.597875	RGD1563510	similar to RIKEN cDNA 8430427H17 gene
1380804_at	1.30E--0	9.13E--0	17.943388		
1380806_at	2.32E--0	1.82E--0	10.125011		
1380851_at	1.16E--0	7.83E--0	11.250254	Sema3f	sema domain, immunoglobulin domain (Ig), short basic domain, secreted, (semaphorin) 3 F
1380908_at	4.96E--0	1.48E--0	19.787077		
1380909_at	2.27E--0	5.45E--0	10.905282	Slc25a24	solute carrier family 25 (mitochondrial carrier, phosphate carrier), member 24
1380934_at	3.77E--0	3.23E--0	10.443719		
1380971_at	4.21E--0	1.20E--0	24.60701		
1381003_at	1.41E--0	1.01E--0	10.853533	Ikarf2	IKAROS family zinc finger 2
1381125_at	1.98E--0	1.51E--0	16.06805		
1381135_at	6.77E--0	2.20E--0	15.361736		
1381160_at	3.23E--0	1.63E--0	18.422583	Tmem200c	transmembrane protein 200C
1381218_at	5.25E--0	6.42E--0	26.854576		
1381388_at	1.42E--0	1.02E--0	13.101712	Ccdc19	coiled--coil domain containing 19
1381418_at	0.001084984	0.001031733	9.614085		
1381434_s_at	5.69E--0	3.29E--0	28.040277	LOC100912349///LOC302022	nidogen--2--like///similar to nidogen 2 protein
1381517_at	7.85E--0	7.27E--0	10.490591		
1381537_at	9.61E--0	3.53E--0	12.13241	Klc3	kinesin light chain 3
1381591_at	5.77E--0	3.38E--0	11.650048		
1381643_at	0.001283033	0.001229507	14.59521		
1381668_at	6.92E--0	4.24E--0	23.602009		
1381696_at	0.001030117	9.73E--0	9.756935		
1381747_at	3.09E--0	1.53E--0	9.807296		
1381775_at	1.07E--0	7.17E--0	13.237714	RGD1566102	RGD1566102
1381795_at	1.79E--0	1.33E--0	22.178213		
1381848_at	4.88E--0	2.73E--0	12.823439		
1381956_at	3.23E--0	2.71E--0	9.997453		
1381960_at	2.98E--0	2.46E--0	16.100039	Ropn1l	rhophilin associated tail protein 1--like
1381963_at	2.40E--0	1.11E--0	12.348793	Thsd4	thrombospondin, type I, domain containing 4
1382021_at	8.15E--0	2.89E--0	45.828182	Pkd2	polycystic kidney disease 2 (autosomal dominant)
1382050_at	1.63E--0	1.19E--0	12.237961		
1382072_at	4.14E--0	1.17E--0	43.883057	Olfrml2a	olfactomedin--like 2A
1382089_at	1.75E--0	3.80E--0	19.382765		
1382185_at	0.001628353	0.001570412	11.275856	C1qtnf2	C1q and tumor necrosis factor related protein 2
1382211_at	4.18E--0	3.63E--0	18.626793		
1382217_at	2.55E--0	6.45E--0	36.176918		
1382258_at	1.90E--0	4.50E--0	19.497894	Arhgef28	Rho guanine nucleotide exchange factor (GEF) 28
1382291_at	8.66E--0	5.20E--0	38.22118		
1382356_at	8.12E--0	7.54E--0	10.947568	Efhc2	EF--hand domain (C--terminal) containing 2
1382387_at	1.63E--0	3.44E--0	28.228888	Ano1	anoctamin 1, calcium activated chloride channel
1382403_at	1.27E--0	8.84E--0	13.611981	LOC498662	similar to RIKEN cDNA 2610019F03
1382439_at	3.29E--0	8.55E--0	78.806404	Itgb6	integrin, beta 6
1382444_at	7.89E--0	1.06E--0	135.32335	Pitpnm3	PITPNM family member 3
1382591_at	2.41E--0	1.91E--0	10.728073		
1382638_at	1.56E--0	6.59E--0	28.890053		
1382647_at	8.90E--0	8.33E--0	10.391697		
1382686_at	4.20E--0	3.66E--0	10.386313		
1382710_at	7.01E--0	2.32E--0	9.8385725	Enc1	ectodermal--neural cortex 1
1382745_at	1.58E--0	6.73E--0	9.429281		
1382776_at	1.52E--0	6.40E--0	14.513216	Mboat1	membrane bound O--acyltransferase domain containing 1
1382781_at	1.66E--0	1.36E--0	40.278545		
1382814_at	1.35E--0	9.60E--0	31.124146	Tenm3	teneurin transmembrane protein 3
1382835_at	1.50E--0	1.09E--0	12.133341		
1382878_at	2.03E--0	1.55E--0	16.248476	Sfrp1	secreted frizzled--related protein 1
1382882_x_at	3.68E--0	3.15E--0	17.847145		
1382913_at	3.50E--0	9.36E--0	12.027652	Cttnbp2	cortactin binding protein 2
1382937_at	1.68E--0	3.60E--0	19.786959	Spdef	SAM pointed domain containing ets transcription factor
1382964_at	5.26E--0	3.00E--0	37.7751		
1382983_at	2.37E--0	1.86E--0	10.201146		
1383129_at	9.11E--0	3.29E--0	22.485722	Wls	wntless homolog (Drosophila)
1383137_at	9.46E--0	3.44E--0	16.480057	Sox4	SRY (sex determining region Y)--box 4
1383143_at	1.36E--0	2.33E--0	18.049498		
1383173_at	1.75E--0	3.82E--0	13.478271	Mapre3	microtubule--associated protein, RP/EB family, member 3
1383266_at	3.77E--0	1.04E--0	32.500725	Sfrp1	secreted frizzled--related protein 1
1383290_at	1.07E--0	1.64E--0	20.492765	Spint1	serine peptidase inhibitor, Kunitz type 1
1383291_at	6.21E--0	1.96E--0	20.244171	C7///Tubb4b	complement component 7///tubulin, beta 4B class IVb
1383311_at	1.78E--0	1.33E--0	9.873728	Mtmr11	myotubularin related protein 11
1383353_at	3.23E--0	1.63E--0	10.53137		
1383401_at	1.39E--0	2.53E--0	13.854533	Tes	testis derived transcript
1383419_at	2.65E--0	2.14E--0	14.738533	Ldnlpl3	lipoma HMGIC fusion partner--like 3
1383422_at	3.12E--0	2.61E--0	16.964212	Ben5d	BEN domain containing 5
1383433_at	8.67E--0	5.64E--0	10.448679	Klhl23	kelch--like family member 23
1383496_at	1.32E--0	5.32E--0	29.213024	Esrp1	epithelial splicing regulatory protein 1
1383571_at	0.003919413	0.003895367	9.929289	Rapgef1	Rap guanine nucleotide exchange factor (GEF)--like 1
1383645_at	1.07E--0	1.67E--0	92.38302		
1383668_at	4.13E--0	1.16E--0	9.270344	Mmp15	matrix metalloproteinase 15
1383673_at	0.003245082	0.00321721	9.817131	Nap1i2	nucleosome assembly protein 1--like 2
1383694_at	2.54E--0	6.39E--0	22.098726	Rnf208	ring finger protein 208
1383750_at	4.43E--0	2.41E--0	19.041412		
1383766_at	0.001862203	0.001807365	10.586014	Sgcb	sarcoglycan, beta (dystrophin--associated glycoprotein)

1383879_at	3.62E--0	9.78E--0	43.24303	LOC688163	hypothetical protein LOC688163
1383900_at	1.79E--0	7.79E--0	19.862154	Qrich2	glutamine rich 2
1383989_at	6.66E--0	4.04E--0	12.946113	Sox4	SRY (sex determining region Y)---box 4
1383991_at	2.76E--0	1.33E--0	13.519815	Lrrc8e	leucine rich repeat containing 8 family, member E
1384000_at	3.77E--0	3.84E--0	17.173275	Sox4	SRY (sex determining region Y)---box 4
1384036_s_at	0.005385248	0.005372032	11.021998		
1384079_at	4.75E--0	5.18E--0	38.321655	Eps8l1	EPS8---like 1
1384206_at	6.32E--0	5.76E--0	10.994225	Sdr16c5	short chain dehydrogenase/reductase family 16c, member 5
1384208_at	0.001693521	0.001637416	12.672404	Igi	immunoglobulin joining chain
1384264_at	4.07E--0	4.29E--0	10.861856	Myh14	myosin, heavy chain 14, non---muscle
1384276_at	0.002336342	0.002284742	9.522519	LOC363458	similar to procollagen, type IV, alpha 6
1384322_at	3.27E--0	1.66E--0	16.498205		
1384438_at	1.28E--0	8.95E--0	19.626469		
1384442_at	1.52E--0	3.73E--1	39.02556	Cldn6	claudin 6
1384468_at	1.41E--0	2.62E--0	56.083447		
1384479_at	1.13E--0	5.37E--0	9.249574	Galnt3	UDP---N---acetyl---alpha---D---galactosamine:polypeptide N---acetylgalactosaminyltransferase 3 (GalNAc---T3)
1384485_at	9.02E--0	3.24E--0	9.605184	Ptprr	protein tyrosine phosphatase, receptor type, U
1384500_at	9.97E--0	9.40E--0	12.656652	Ccdc30	coiled---coil domain containing 30
1384509_s_at	1.77E--0	7.68E--0	10.327072	Pcdh17	protocadherin 17
1384536_at	6.91E--0	6.33E--0	10.522925		
1384554_at	1.65E--0	7.05E--0	10.295791		
1384701_at	1.77E--0	1.31E--0	10.398885		
1384707_at	3.30E--0	8.70E--0	18.677006	Scara5	scavenger receptor class A, member 5 (putative)
1384925_at	5.37E--0	4.82E--0	16.145845	LOC100912219	uncharacterized LOC100912219
1384927_at	7.54E--0	2.56E--0	22.836277	Tubb4a	tubulin, beta 4A class IVa
1384939_at	1.43E--0	1.03E--0	9.523808		
1384944_at	1.21E--0	8.28E--0	13.680715	Bcl11b	B---cell CLL/lymphoma 11B (zinc finger protein)
1384960_at	1.05E--0	3.86E--0	36.319767	Ctfr	cystic fibrosis transmembrane conductance regulator
1384993_at	1.77E--0	7.67E--0	17.365559	RGD1309847	similar to peptidylglycine alpha---amidating monooxygenase COOH---terminal interactor; peptidylglycine alpha---amidating monooxygenase (COOH---terminal interactor protein---1
1385014_at	0.006355397	0.006347599	12.621086	Nudt10	nudix (nucleoside diphosphate linked moiety X)---type motif 10
1385033_at	4.10E--0	2.18E--0	15.07728		
1385058_at	6.68E--0	4.06E--0	15.346487	Cldn8	claudin 8
1385120_at	7.62E--0	2.60E--0	26.392225	Pof1b	premature ovarian failure 1B
1385166_at	5.00E--0	2.81E--0	15.989807		
1385190_at	4.58E--0	4.89E--0	107.99972	Gabrp	gamma---aminobutyric acid (GABA---A) receptor, pi
1385274_at	0.002134164	0.00208441	10.1672535	Pcdhb19	protocadherin beta 19
1385357_at	3.97E--0	3.44E--0	11.726316		
1385369_at	8.39E--0	4.84E--0	28.409658	Dnig11	DAZ interacting zinc finger protein 1---like
1385436_at	1.37E--0	9.90E--0	25.186365	LOC100909619///Tmc4	transmembrane channel---like protein 4---like///transmembrane channel---like 4
1385464_at	2.26E--0	1.02E--0	24.762989	Foxq1	forkhead box Q1
1385472_at	2.43E--0	1.13E--0	9.898441	Zbtb8a	zinc finger and BTR domain containing 8a
1385534_at	6.46E--0	3.88E--0	10.483006	Ngrap1	nerve growth factor receptor (TNFRSF16) associated protein 1
1385591_at	1.00E--0	6.60E--0	14.531951		
1385614_at	1.23E--0	2.03E--0	28.44431	Mlph	melanophilin
1385701_at	7.38E--0	2.49E--0	10.461933		
1385706_at	1.07E--0	1.61E--0	12.168478		
1385714_at	6.76E--0	6.17E--0	15.618451	LOC100909619///Tmc4	transmembrane channel---like protein 4---like///transmembrane channel---like 4
1385716_at	8.53E--0	5.03E--0	50.09981		
1385778_at	1.94E--0	1.47E--0	13.708647	Siat7E	sialyltransferase 7E
1385830_at	8.71E--0	8.13E--0	9.619808	RGD1561507	similar to hypothetical protein FLJ31606
1385875_at	1.76E--0	7.60E--0	11.691571		
1385876_at	0.003422362	0.003397167	15.576265	LOC691984	similar to Glypican---6 precursor
1385899_at	2.50E--0	2.01E--0	10.790482	Trim16	tripartite motif---containing 16
1385961_at	7.10E--0	4.00E--0	121.492676		
1385969_at	3.12E--0	1.55E--0	18.991758		
1385978_at	2.08E--0	6.11E--1	56.918144		
1386628_at	3.89E--0	3.36E--0	11.787127		
1386695_at	5.06E--0	4.51E--0	22.925386		
1386724_at	4.89E--0	1.43E--0	18.214127		
1390931_at	8.11E--0	2.85E--0	37.49837	Adams15	ADAM metalloproteinase with thrombospondin type 1 motif, 15
1390936_at	3.90E--0	1.79E--0	423.01794		
1391022_at	1.29E--0	5.12E--0	27.028555	Lamb3	laminin, beta 3
1391026_at	8.47E--0	5.44E--0	14.031144		
1391051_at	2.73E--0	1.30E--0	16.925434		
1391060_at	4.22E--0	2.28E--0	10.908334		
1391063_at	1.25E--0	8.65E--0	14.135125	Kif23	kinesin family member 23
1391067_at	4.19E--0	2.25E--0	22.093008		
1391162_at	8.99E--0	1.27E--0	41.68468	Dcdc2	doublecortin domain containing 2
1391187_at	4.39E--0	1.26E--0	11.846029	Ppl	periplakin
1391209_at	8.13E--0	5.20E--0	23.890455		
1391251_at	1.09E--0	4.07E--0	16.626629		
1391331_at	3.05E--0	2.99E--0	28.908821		
1391337_at	1.27E--0	8.86E--0	10.707527		
1391341_at	2.76E--0	2.24E--0	9.696374	Plxdc1	plexin domain containing 1
1391375_at	9.20E--0	6.01E--0	38.64931		
1391459_at	6.91E--0	6.34E--0	13.236974	Nudt11	nudix (nucleoside diphosphate linked moiety X)---type motif 11
1391520_at	4.96E--0	1.48E--0	34.60108		
1391542_at	6.88E--0	4.21E--0	14.079774		
1391582_at	1.19E--0	8.10E--0	13.178047		
1391673_at	4.35E--0	3.82E--0	9.3122	Arhgap20	Rho GTPase activating protein 20
1391684_at	1.04E--0	6.92E--0	13.806882	Tmem14a	transmembrane protein 14A
1391810_at	2.99E--0	2.47E--0	9.800334	Rbm20	RNA binding motif protein 20
1391856_at	1.05E--0	7.01E--0	17.232664	Sema3g	sema domain, immunoglobulin domain (Ig), short basic domain, secreted, (semaphorin) 3G
1391887_at	3.30E--0	1.69E--0	10.699146	Igsf9	immunoglobulin superfamily, member 9
1392003_at	0.003160681	0.003125778	9.29454		
1392068_at	1.97E--0	8.80E--0	10.408668		
1392117_at	1.45E--0	2.73E--0	25.85493		
1392155_at	5.82E--0	5.27E--0	9.520539		
1392364_at	9.76E--0	9.19E--0	9.315585		
1392409_at	5.48E--0	2.89E--0	115.09578		
1392489_at	2.09E--0	1.61E--0	21.208672		
1392556_at	1.27E--0	8.61E--0	9.900584	Shroom3	shroom family member 3
1392557_at	8.27E--0	1.13E--0	29.435995		
1392619_at	2.19E--0	1.70E--0	12.045918	Ebf1	early B---cell factor 1
1392754_at	3.70E--0	1.00E--0	19.764801	Adam8	ADAM metalloproteinase domain 8
1392782_at	0.003125279	0.003086932	9.574871		
1392813_at	4.04E--0	3.47E--1	43.626003		
1392863_at	1.71E--0	7.34E--0	26.725548		
1392865_at	1.19E--0	8.12E--0	16.520456	Fgf9	fibroblast growth factor 9
1392901_at	4.90E--0	1.45E--0	15.06059	Lrrc1	leucine rich repeat containing 1
1392971_at	4.69E--0	4.14E--0	12.917377		
1393003_at	3.50E--0	2.97E--0	9.618179		
1393167_at	2.80E--0	1.36E--0	12.436018		
1393206_at	3.91E--0	1.09E--0	44.442936		
1393210_at	2.33E--0	1.83E--0	11.69808	LOC100361383	extracellular matrix protein 2---like
1393234_at	2.80E--0	2.29E--0	16.806387	LOC687105	hypothetical protein LOC687105
1393240_at	2.45E--0	1.14E--0	10.977029	Efemp2	EGF---containing fibulin---like extracellular matrix protein 2
1393252_at	2.82E--0	2.66E--0	25.24019		
1393263_at	2.29E--0	1.04E--0	24.213043	Snhg11	small nucleolar RNA host gene 11 (non---protein coding)
1393281_at	4.72E--0	2.32E--0	13.156326	Cav1	caveolin 1, caveolae protein

1393282_at	1.21E--0	8.30E--0	9.359753	Spns2	spinster homolog 2
1393297_at	0.001125008	0.001071173	9.930364	Pou2zf1	POU class 2 associating factor 1
1393337_at	4.72E--0	2.37E--0	16.095142	Tlcp2l1	transcription factor CP2--like 1
1393338_at	9.36E--0	3.39E--0	26.963902	Scx	scleraxis
1393368_at	1.08E--0	6.79E--0	11.883907	Oshpl5	oxysterol binding protein--like 5
1393401_at	0.002448426	0.002400359	11.284812		
1393452_at	1.14E--0	1.85E--1	62.1806	Car9	carbonic anhydrase 9
1393454_at	5.37E--0	4.81E--0	16.05036	Pcdh17	protocadherin 17
1393469_at	3.78E--0	3.26E--0	18.686608		
1393510_at	5.97E--0	5.42E--0	21.60685	Sybu	syntabulin (syntaxin--interacting)
1393559_at	0.001030117	9.73E--0	14.926427		
1393570_at	1.04E--0	1.55E--0	51.18359		
1393571_at	6.40E--0	2.03E--0	38.40082	Sov4	SRY (sex determining region Y)--box 4
1393584_at	3.91E--0	3.38E--0	10.094089	Tnfrsf21	tumor necrosis factor receptor superfamily, member 21
1393613_at	6.05E--0	3.57E--0	14.495151	Zfp462	zinc finger protein 462
1393617_at	4.96E--0	1.49E--0	28.052345		
1393633_at	3.91E--0	1.09E--0	20.307856	Ano9	anoctamin 9
1393635_x_at	2.74E--0	1.31E--0	26.936386	Tubb4a	tubulin, beta 4A class IVa
1393638_at	1.63E--0	3.42E--0	20.29371		
1393641_at	3.45E--0	2.93E--0	9.567698	Blnk	B--cell linker
1393719_at	7.84E--0	7.25E--0	22.392132		
1393732_at	7.23E--0	4.48E--0	17.726828		
1393740_at	2.42E--0	1.91E--0	14.751152	Cnksr1	connector enhancer of kinase suppressor of Ras 1
1393806_at	1.14E--0	1.99E--1	12.273276		
1393845_a_at	1.86E--0	1.64E--0	67.98524	LOC100909619//Tmc4	transmembrane channel--like protein 4--like//transmembrane channel--like 4
1393850_at	2.83E--0	1.38E--0	10.056748	Cfcl1	cripto, FRL--1, cryptic family 1
1393896_at	1.00E--0	6.57E--0	19.596245	Lamc3	laminin gamma 3
1393911_at	6.80E--0	4.15E--0	11.494704	Sh3bp4	SH3--domain binding protein 4
1393935_at	2.52E--0	1.18E--0	19.589827	Tmem139	transmembrane protein 139
1393953_at	7.37E--0	4.60E--0	23.837893	Eps8l3//LOC100912384	EPS8--like 3//epidermal growth factor receptor kinase substrate 8--like protein 3--
1394039_at	1.75E--0	3.84E--0	146.67313	Klf5	Kruppel--like factor 5
1394047_at	7.71E--0	7.11E--0	9.937352		
1394156_at	3.72E--0	1.94E--0	11.434554	Igsf3	immunoglobulin superfamily, member 3
1394408_at	8.03E--0	2.82E--0	16.391623	RGD1563692	similar to hypothetical protein FLJ22671
1394451_at	1.89E--0	8.33E--0	12.705467	Anxa1	annexin A1
1394571_at	6.62E--0	4.01E--0	26.889793	Fam227a	family with sequence similarity 227, member A
1394594_at	2.45E--0	1.95E--0	13.778246		
1394709_at	1.27E--0	5.04E--0	54.665806		
1394754_at	4.52E--0	2.47E--0	13.783065	LOC100911253	uncharacterized LOC100911253
1394786_at	3.54E--0	1.83E--0	14.265297	Sortl	sortilin--related receptor, LDLR class A repeats--containing
1394802_at	5.77E--0	3.38E--0	12.996676		
1394831_at	1.66E--0	1.36E--0	10.494431		
1394847_at	2.52E--0	2.03E--0	11.581087	Syde1	synapse defective 1, Rho GTPase, homolog 1 (C. elegans)
1394896_at	1.33E--0	9.42E--0	18.243921		
1395176_at	1.78E--0	1.32E--0	10.286077		
1395249_at	0.001159925	0.001105842	14.614697	Snhg11	small nucleolar RNA host gene 11 (non--protein coding)
1395357_at	8.73E--0	5.69E--0	17.422134	Map1b	microtubule--associated protein 1B
1395365_at	2.43E--0	1.94E--0	9.629207		
1395372_at	3.51E--0	1.81E--0	10.761291		
1395390_at	3.30E--0	8.68E--0	44.01907		
1395437_at	6.40E--0	2.03E--0	13.206172		
1395663_at	3.09E--0	2.57E--0	14.873993	Mall	mal, T--cell differentiation protein--like
1395673_at	4.43E--0	2.41E--0	20.342983		
1395754_at	8.13E--0	5.18E--0	18.488964	Frem2	Fras1 related extracellular matrix protein 2
1395761_at	1.52E--0	2.96E--0	13.3368025		
1395887_at	1.45E--0	2.72E--0	21.867783	LOC363060	similar to RIKEN cDNA 1600029D21
1395966_at	2.43E--0	1.93E--0	10.776749	Kctd14	potassium channel tetramerisation domain containing 14
1395968_at	6.34E--0	3.77E--0	15.791612	LOC690323	similar to Myosin--15 (Myosin XV) (Unconventional myosin--15)
1395986_at	4.03E--0	2.14E--0	18.938015	Slit2	slit homolog 2 (Drosophila)
1396009_at	6.57E--0	2.09E--0	35.93999		
1396073_at	3.93E--0	2.07E--0	9.316064		
1396087_at	3.39E--0	2.87E--0	9.554482	Arhgef28	Rho guanine nucleotide exchange factor (GEF) 28
1396180_at	8.76E--0	8.19E--0	10.354705	Lrrc16a	leucine rich repeat containing 16A
1396214_at	4.62E--0	2.55E--0	12.421315	Kitlg	KIT ligand
1396289_at	6.97E--0	4.28E--0	14.53337	Mdga1	MAM domain containing glycosylphosphatidylinositol anchor 1
1396295_at	1.35E--0	9.61E--0	18.684168		
1396450_at	1.61E--0	3.32E--0	13.833416	Enah	enabled homolog (Drosophila)
1396451_at	1.61E--0	1.18E--0	19.985548		
1396472_at	1.14E--0	4.33E--0	10.173385		
1396473_at	1.47E--0	1.06E--0	16.081354		
1396533_at	2.09E--0	1.61E--0	10.343154		
1396877_at	3.66E--0	3.12E--0	17.113886		
1396894_at	0.001998209	0.00194427	11.504197		
1397045_at	2.02E--0	1.55E--0	10.265491		
1397165_at	8.99E--0	1.27E--0	9.351287		
1397166_at	2.89E--0	2.38E--0	13.546398		
1397217_at	0.00283257	0.002794339	12.0261545		
1397247_at	1.84E--0	8.08E--0	22.898329	Cdcp1	CUB domain containing protein 1
1397301_at	1.36E--0	2.39E--0	67.580696		
1397340_at	4.83E--0	2.70E--0	22.609924		
1397343_at	2.53E--0	1.19E--0	13.363558		
1397397_at	5.52E--0	3.16E--0	17.601234	Pof1b	premature ovarian failure 1B
1397429_at	1.86E--0	1.64E--0	53.784847	Creb5	cAMP responsive element binding protein 5
1397437_at	5.73E--0	5.17E--0	15.621894	Arid5a	AT rich interactive domain 5A (Mrf1 like)
1397449_at	7.83E--0	7.23E--0	11.14315		
1397496_at	6.34E--0	3.78E--0	21.460426		
1397505_at	2.32E--0	1.06E--0	13.507577	Kif1a	kinesin family member 1A
1397581_at	1.52E--0	2.95E--0	15.820169	Rhov	ras homolog family member V
1397622_at	4.14E--0	1.17E--0	9.560967		
1397729_x_at	8.99E--0	1.28E--0	14.286232	LOC363060	similar to RIKEN cDNA 1600029D21
1397769_at	0.001196739	0.001142408	10.821973		
1397853_s_at	2.77E--0	2.26E--0	9.898485	Arhgef9//LOC100912165	Cdc42 guanine nucleotide exchange factor (GEF) 9//rho guanine nucleotide exchange factor 9--like
1397929_at	2.43E--0	5.96E--0	20.89912		
1398071_at	6.31E--0	3.74E--0	21.912308		
1398116_at	3.30E--0	1.69E--0	21.120111		
1398149_at	1.27E--0	8.90E--0	14.068488	Sema5a	sema domain, seven thrombospondin repeats (type 1 and type 1--like), transmembrane domain (TM) and short cytoplasmic domain, (semaphorin) 5A
1398491_at	8.12E--0	5.16E--0	10.2140465	Ildl1	immunoglobulin--like domain containing receptor 1
1398624_x_at	1.79E--0	1.35E--0	16.012417	Tubb4a	tubulin, beta 4A class IVa
1398645_at	2.40E--0	1.11E--0	21.713133	Wnt7a	wingless--type MMTV integration site family, member 7A
1398660_at	3.39E--0	2.86E--0	11.173163	Slc35f2	solute carrier family 35, member F2
1398661_at	3.09E--0	2.57E--0	11.0808041	Egflam	EGF--like, fibronectin type III and laminin G domains
1398716_at	1.48E--0	6.19E--0	21.686409		

Rat liver zone I signature

Probe Set ID	Corrected p--value	p--value	FCAbsolute	Gene Symbol	Gene Title
1367648_at	1.66173E--0	6.63638E--0	3.6937318	Igfbp2	insulin--like growth factor binding protein 2
1367794_at	7.74949E--0	2.83698E--0	4.4454145	A2m//LOC100911545	alpha--2--macroglobulin//alpha--2--macroglobulin--like
1367838_at	8.74562E--1	3.74218E--1	2.0272317	Cth	cystathionase (cystathionine gamma--lyase)
1367847_at	0.0012359	0.001152303	2.2924562	Nupr1	nuclear protein, transcriptional regulator, 1
1367937_at	0.000820913	0.000694719	2.981706	Miox	myo--inositol oxygenase

1368102_at	0.000150731	8.98176E--0	4.1293287	Hsd11b2	hydroxysteroid 11--beta dehydrogenase 2
1368266_at	4.59332E--1	1.67427E--1	2.094581	Arg1	arginase, liver
1368416_at	0.000597629	0.00047261	3.279828	Ibsp	integrin--binding sialoprotein
1368426_at	2.17058E--0	9.11574E--0	2.4443064	Crot	carnitine O--octanoyltransferase
1368453_at	5.78058E--0	1.43827E--0	3.2385973	Fads2	fatty acid desaturase 2
1368520_at	7.22804E--0	2.58881E--0	2.0486774	Apoa4	apolipoprotein A--IV
1368720_at	7.21106E--1	4.57119E--1	2.387428	Tdo2	tryptophan 2,3--dioxygenase
1368729_a_at	0.000574704	0.000450838	2.8171394	Adcyap1r1	adenylate cyclase activating polypeptide 1 receptor 1
1368778_at	7.91622E--0	9.66005E--1	5.8277526	Slc6a6	solute carrier family 6 (neurotransmitter transporter, taurine), member 6
1369074_at	2.50963E--1	6.36356E--1	3.1168466	Slc38a4	solute carrier family 38, member 4
1369126_at	0.000226138	0.000148011	3.2452126	Ptgfr	prostaglandin F receptor
1369195_at	0.00073948	0.000619944	2.036656	Fabp2	fatty acid binding protein 2, intestinal
1369455_at	0.001096129	0.000990165	3.844251	Abcg5	ATP--binding cassette, subfamily G (WHITE), member 5
1369460_at	1.72483E--0	3.6902E--0	2.955335	Slc7a2	solute carrier family 7 (cationic amino acid transporter, y+ system), member 2
1369864_a_at	1.10558E--0	2.26022E--0	8.347958	Sds	serine dehydratase
1370053_at	0.001354706	0.001286005	2.873849	Dlgap1	discs, large (Drosophila) homolog--associated protein 1
1370080_at	0.000710423	0.000585071	2.1743906	Hmox1	heme oxygenase (decycling) 1
1370089_at	0.001393068	0.001333625	2.4282	Ppargc1a	peroxisome proliferator--activated receptor gamma, coactivator 1 alpha
1370241_at	0.000397491	0.000291661	2.0246	Cyp2c7///LOC100911552	cytochrome P450, family 2, subfamily c, polypeptide 7 ///cytochrome P450 2C7--like
1370374_at	2.05418E--0	4.59163E--0	3.4965487	Steap3	STEAP family member 3, metalloredutase
1370375_at	2.12564E--1	5.05302E--1	6.3545413	Gls2	glutaminase 2 (liver, mitochondrial)
1370964_at	6.03146E--1	4.6837E--1	2.3260958	Ass1	argininosuccinate synthase 1
1371904_at	6.086E--0	7.04085E--1	3.5865204	Smyd2	SET and MYND domain containing 2
1371922_at	9.10919E--0	5.03821E--0	5.8845096		
1372715_at	1.89667E--1	3.90756E--1	2.991027	Sfxn1	sideroflexin 1
1372966_at	0.000154644	9.23944E--0	2.5092628	Msd2a	major facilitator superfamily domain containing 2A
1373146_at	0.001057496	0.000950238	2.4072814	Sxx2ip	synovial sarcoma, X breakpoint 2 interacting protein
1373386_at	1.09026E--0	2.92003E--0	7.3849897	Gjb2	gap junction protein, beta 2
1373710_at	1.92218E--1	4.26474E--1	3.2702208		
1374140_at	0.001511965	0.001480815	2.10401		
1374176_at	9.82265E--0	5.49508E--0	2.2728093	Lurap1l	leucine rich adaptor protein 1--like
1374204_at	3.70403E--0	6.1636E--0	2.499544	Wsb1	WD repeat and SOCS box--containing 1
1374249_at	0.001119731	0.001015033	3.0191834	LOC100911963///Syn4	nesprin--4--like ///spectrin repeat containing, nuclear envelope family member 4
1374307_at	0.000139287	8.1453E--0	2.5931883		
1374531_at	4.90556E--0	1.20501E--0	3.9573247		
1374635_at	1.95688E--0	4.34173E--0	2.1834464		
1374863_at	0.000179461	0.000111488	4.4275994	Rbp7	retinol binding protein 7, cellular
1374883_at	7.25906E--0	2.63199E--0	2.6764364	Mtmr7	myotubularin related protein 7
1375615_at	0.000329045	0.000229967	3.2495608	Ntrk1	neurotrophic tyrosine kinase, receptor, type 1
1375781_at	5.52611E--0	2.6711E--0	2.761816		
1375845_at	0.000168782	0.000102981	2.237519	Aig1	androgen--induced 1
1375854_at	9.96514E--0	1.31079E--0	2.5078256	Ctnnbip1	catenin, beta--interacting protein 1
1376051_at	9.81411E--0	1.8975E--0	7.632752	Cryl1	crystallin, lambda 1
1376082_at	0.00089463	0.000769864	2.1529212	Mecom	MD51 and EVI1 complex locus
1376279_at	0.000506009	0.000387325	3.6832664	Pop1	processing of precursor 1, ribonuclease P/MRP subunit (S. cerevisiae)
1376295_at	0.001404824	0.001352624	3.0598922		
1376427_a_at	1.86094E--0	4.09937E--0	10.539987	Gldc	glycine dehydrogenase (decarboxylating)
1376977_at	1.73489E--0	2.47909E--0	4.811215	Ptger3	prostaglandin E receptor 3 (subtype EP3)
1377733_at	2.55576E--0	3.96933E--0	2.4493504	Ctnnbip1	catenin, beta--interacting protein 1
1377758_at	9.23918E--1	1.75705E--1	6.0091925	Hsd17b13	hydroxysteroid (17--beta) dehydrogenase 13
1383165_at	1.50574E--0	1.52721E--1	9.436019	RGD1310209	similar to KIAA1324 protein
1387052_at	1.40303E--0	2.91278E--0	4.690243	Gpt	glutamic--pyruvate transaminase (alanine aminotransferase)
1387111_at	0.000271484	0.000183869	3.134345	Ddah1	dimethylarginine dimethylaminohydrolase 1
1387196_at	0.001161264	0.001063725	2.1306484	Khdrbs3	KH domain containing, RNA binding, signal transduction associated 3
1387215_at	7.59049E--0	1.41946E--0	2.2417426	Agxt	alanine--glyoxylate aminotransferase
1387302_at	0.000315352	0.000217898	2.636403	Adcyap1r1	adenylate cyclase activating polypeptide 1 receptor 1
1387307_at	3.64818E--1	1.15632E--1	5.841219	Hal	histidine ammonia lyase
1387396_at	7.25906E--0	2.63443E--0	2.393595	Hamp	hepcidin antimicrobial peptide
1387470_at	0.000111311	6.30506E--0	3.4535	Cldn1	claudin 1
1387877_at	1.45177E--0	1.44947E--1	2.0452023	Ptcd	formiminotransferase cyclodeaminase
1387901_at	2.73387E--0	6.36892E--0	2.1149042	Ptprs	protein tyrosine phosphatase, receptor type, S
1387933_s_at	0.001587569	0.001587569	2.1596723	Podxl	podocalyxin--like
1387959_at	1.1598E--0	1.08444E--1	5.032056	Aspg	asparaginase homolog (S. cerevisiae)
1388271_at	0.001017392	0.000910977	2.1525948	Mt2A	metallothionein 2A
1388753_at	0.000316567	0.000219239	2.5514033	Sulf2	sulfatase 2
1389066_at	1.74545E--0	6.99839E--0	3.9805324	Rcan2	regulator of calcineurin 2
1389486_at	1.64391E--0	4.63998E--0	2.548056		
1389876_at	5.84277E--0	2.85194E--0	2.3595757	Camk2n1	calcium/calmodulin--dependent protein kinase II inhibitor 1
1390507_at	0.000667778	0.000540784	2.817059	Isq20	interferon stimulated exonuclease gene 20
1391981_at	0.000227411	0.000149335	2.237152		
1398348_at	3.6198E--0	1.62257E--0	3.1626263		
1398433_at	0.000441785	0.000330463	4.2805495		
137968_at	1.63146E--0	3.43873E--0	3.2775307		
1378798_at	0.000193149	0.00012239	3.2295156	Stox2	storkhead box 2
1378927_at	9.88365E--1	4.6516E--1	2.6971712		
1379076_at	8.79281E--1	7.6641E--1	12.220338		
1379334_at	9.88365E--1	4.72771E--1	6.828374	Gldc	glycine dehydrogenase (decarboxylating)
1379493_at	0.0006172	0.000492	3.0510228		
1379716_at	2.01278E--0	8.2531E--0	2.3512921		
1379812_at	6.83998E--0	1.75606E--0	2.305712	Nnmt	nicotinamide N--methyltransferase
1379888_at	8.7967E--1	5.85518E--1	8.185714	LOC100912602	uncharacterized LOC100912602
1380306_at	0.000716983	0.000594266	4.746584		
1380389_at	4.03586E--0	6.84369E--0	7.093584		
1380738_at	0.000179461	0.000111252	2.0285673		
1381238_at	0.001120099	0.001018917	2.4229047		
1381474_at	0.001017392	0.000909685	3.6478584	Mbnl3	muscleblind--like splicing regulator 3
1382410_at	0.001172507	0.001080163	2.7802474	Cd209b	CD209b antigen
1382631_at	0.001393166	0.001337969	4.38149		
138353_at	2.46554E--0	7.42398E--0	2.9383965		
1383472_at	8.07149E--0	2.09782E--0	15.884483	Aldh1b1	aldehyde dehydrogenase 1 family, member B1
1383600_at	0.000144762	8.55727E--0	4.7522774	Slc13a5	solute carrier family 13 (sodium--dependent citrate transporter), member 5
1383605_at	8.74562E--1	3.70956E--1	2.1274457	LOC360919	similar to alpha--fetoprotein
1383946_at	7.16742E--0	8.63271E--1	3.5352538	Cldn1	claudin 1
1384035_at	0.000179194	0.000110754	8.594747		
1384036_s_at	0.000896455	0.00072855	3.8624878		
1384086_at	6.06165E--0	2.9972E--0	3.9952228		
1384225_at	0.000167329	0.000101829	3.2368116		
1384226_at	0.000719902	0.000599832	3.207952		
1384510_at	2.39828E--1	1.36827E--1	2.9424775		
1385670_at	1.22925E--0	4.64022E--0	4.530677	Sds1	serine dehydratase--like
1385798_at	0.000967704	0.000851236	2.9534197		
1386379_at	0.001151437	0.001052899	3.0645876		
1386656_at	1.24585E--0	1.67824E--0	5.2525334		
1390765_at	5.16104E--0	9.01986E--0	4.3436403	Wfd2	WAP four--disulfide core domain 2
1391206_at	9.61923E--0	5.35079E--0	4.8279605	RGD1311892	similar to hypothetical protein FLJ10901
1391345_at	0.001576065	0.001566167	3.1383886	Bmper	BMP--binding endothelial regulator
1393241_at	0.000644899	0.000518168	4.0441394	Prss32	protease, serine, 32
1393266_at	0.001331721	0.001257854	3.1408734		
1393831_at	0.001578267	0.001573264	5.0113277		
1393875_at	6.83417E--0	1.74374E--0	2.6981573		
1393917_at	1.24257E--0	3.36734E--0	2.1066668	Cd163	CD163 molecule
1394503_at	0.000179539	0.000111821	5.45474		
1395287_at	0.000504905	0.00038568	3.4769726		

1395518_at	0.001404824	0.001355845	3.4780712		
1395519_at	0.00067553	0.000548132	2.1330464	MGC95152	similar to B230212L03Rik protein
1395536_at	1.04164E--0	2.06347E--0	4.959511		
1396028_at	0.000121595	6.99509E--0	3.0576525		
1396051_at	0.00069082	0.000564918	2.0172832		
1396136_at	0.00025567	0.000170581	3.3224285		
1396150_at	1.29657E--0	3.55477E--0	3.0579352	Cldn1	claudin 1
1396155_at	0.000822243	0.000697148	3.6707249		
1396467_at	0.000338254	0.000239083	2.7516313		
1396729_at	0.001225822	0.001140345	2.658079	Fer115	fer--1--like 5 (C. elegans)
1397225_at	2.29058E--0	9.65602E--0	3.5713804		
1397740_at	1.30614E--0	1.26267E--1	5.936366	Sfrn1	sideroflexin 1

Rat liver zone III signature

Probe Set ID	Corrected p--value	p--value	FCAbsolute	Gene Symbol	Gene Title
1367568_a_at	9.23918E--1	1.46884E--1	30.590137	Mgp	matrix Gla protein
1367570_at	2.33361E--0	9.94835E--0	5.567781	Tagln	transgelin
1367574_at	1.94916E--0	5.65286E--0	2.3459675	Vim	vimentin
1367584_at	6.59193E--0	3.39521E--0	2.8423278	Anxa2	annexin A2
1367614_at	1.70066E--0	4.85134E--0	3.0449252	Anxa1	annexin A1
1367628_at	0.000362706	0.000260964	2.4219353	Lgals1	lectin, galactoside--binding, soluble, 1
1367631_at	5.07698E--0	8.77006E--0	3.80143	Ctgf	connective tissue growth factor
1367632_at	3.28169E--2	1.56024E--2	7.031913	GluI	glutamate--ammonia ligase
1367633_at	6.79745E--2	1.07725E--2	14.239751	GluI	glutamate--ammonia ligase
1367652_at	9.42176E--0	1.20945E--0	2.559163	Igfbp3	insulin--like growth factor binding protein 3
1367655_at	1.2596E--0	4.81084E--0	3.4847858	LOC100359493//LOC100359496//LOC100361392//LOC100361596//LOC100361620//LOC100364435//LOC100908211//LOC100911590//Tmsb10	thymosin, beta 10--like//thymosin, beta 10--like//thymosin, beta 10--like//hypothetical protein LOC100361596//thymosin, beta 10--like//thymosin, beta 10--like//thymosin beta--10--like//thymosin beta--10--like//thymosin, beta 10
1367661_at	0.000126516	7.33831E--0	3.4628007	S100a6	S100 calcium binding protein A6
1367668_a_at	0.001104796	0.000999744	2.0738163	LOC100912469//Scd	acyl--CoA desaturase 2--like//stearoyl--CoA desaturase (delta--9--desaturase)
1367679_at	1.11585E--1	1.06103E--1	3.2851596	Cd74	Cd74 molecule, major histocompatibility complex, class II invariant chain
1367722_at	6.68056E--0	3.46203E--0	2.0210023	Dpp7	dipeptidylpeptidase 7
1367729_at	5.20956E--0	5.77922E--1	3.5751574	Oat	ornithine aminotransferase
1367733_at	1.80867E--0	2.66571E--0	7.8691754	Ca2	carbonic anhydrase 2
1367749_at	1.76667E--0	7.11149E--0	8.093615	Lum	lumican
1367765_at	8.52364E--1	7.15932E--1	2.97117	Tcn2	transcubalin 2
1367806_at	0.000196241	0.000125022	2.373126	Gls	glutaminase
1367823_at	6.08546E--0	1.52378E--0	4.3489704	Timp2	TIMP metalloproteinase inhibitor 2
1367846_at	0.000909124	0.000790981	3.7208025	S100a4	S100 calcium--binding protein A4
1367866_at	0.000932478	0.000815733	2.1600084	Fbln5	fibulin 5
1367880_at	2.01278E--0	8.20105E--0	2.3676596	Lamb2	laminin, beta 2
1367912_at	2.01512E--1	1.43709E--1	2.7338285	Ltbp1	latent transforming growth factor beta binding protein 1
1367940_at	7.25906E--0	2.62705E--0	2.5055134	Cxcr7	chemokine (C--X--C motif) receptor 7
1367964_at	2.38324E--0	1.02355E--0	2.187739	Tnni2	troponin I type 2 (skeletal, fast)
1367998_at	1.30508E--0	2.68875E--0	7.9457197	Sijp1	secretory leukocyte peptidase inhibitor
1368007_at	4.97582E--0	8.51646E--0	5.686052	Dmbt1//LOC100913031	deleted in malignant brain tumors 1//deleted in malignant brain tumors 1 protein--like
1368047_at	9.04539E--1	6.16405E--1	9.068183	Slc13a3	solute carrier family 13 (sodium--dependent dicarboxylate transporter), member 3
1368105_at	0.001493471	0.001457968	2.9996443	Tspan2	tetraspanin 2
1368128_at	0.001552682	0.001532997	2.276957	Pla2g2a	phospholipase A2, group IIA (platelets, synovial fluid)
1368144_at	0.000227411	0.000149565	3.8337867	Rgs2	regulator of G--protein signaling 2
1368167_at	7.49475E--0	1.38968E--0	10.275245	Ctse	cathepsin E
1368171_at	5.2349E--0	2.52204E--0	13.622135	Lox	lysyl oxidase
1368172_a_at	0.000355849	0.000254339	8.14488	Lox	lysyl oxidase
1368191_a_at	2.24155E--0	5.07991E--0	2.382594	Slc22a1	solute carrier family 22 (organic cation transporter), member 1
1368192_at	0.000568558	0.000445115	2.2764735	Cxcr3	chemokine (C--X--C motif) receptor 3
1368207_at	5.0228E--0	1.69549E--0	2.5181236	Fxyd5	FXVD domain--containing ion transport regulator 5
1368281_at	4.22341E--0	1.96111E--0	3.963022	Dpep1	dipeptidase 1 (renal)
1368282_at	4.04462E--0	1.83963E--0	3.5054543	Dpep1	dipeptidase 1 (renal)
1368284_at	2.3939E--0	1.03192E--0	3.3803117	Pilvap	plasmalemma vesicle associated protein
1368290_at	2.01278E--0	8.26167E--0	3.2573795	Cyr61	cysteine--rich, angiogenic inducer, 61
1368293_at	3.65151E--0	8.79602E--0	5.657552	Cpr	carboxypeptidase Z
1368320_at	6.32103E--0	3.17554E--0	3.915199	Ncam1	neural cell adhesion molecule 1
1368358_a_at	5.13918E--0	1.27054E--0	5.36159	Ptprrr	protein tyrosine phosphatase, receptor type, R
1368369_at	5.44668E--0	9.66764E--0	7.118615	Pnoc	prepronociceptin
1368370_at	4.40509E--0	2.06546E--0	2.9944942	Adcy4	adenylate cyclase 4
1368448_at	5.69409E--0	6.49722E--1	13.023233	Ltbp2	latent transforming growth factor beta binding protein 2
1368458_at	2.45139E--0	5.67199E--0	0.099698	Cyp7a1	cytochrome P450, family 7, subfamily a, polypeptide 1
1368474_at	2.24419E--0	6.72191E--0	2.506247	LOC100912479//Vcam1	vascular cell adhesion protein 1--like//vascular cell adhesion molecule 1
1368482_at	4.40509E--0	2.06641E--0	3.561673	Bcl2a1	BCL2--related protein A1
1368490_at	7.91148E--0	4.25038E--0	2.0579531	Cd14	CD14 molecule
1368533_at	1.76596E--0	3.86215E--0	4.4054756	Heph	hephestin
1368604_at	0.000193612	0.00012304	4.0279293	Mefv	Mediterranean fever
1368637_at	7.34765E--0	3.88925E--0	2.4678326	Card9	caspase recruitment domain family, member 9
1368671_at	0.000440803	0.00032903	2.4177887	Srpx	sushi--repeat--containing protein, X--linked
1368754_at	1.44134E--0	3.99736E--0	6.5009184	P2ry6	pyrimidinergic receptor P2Y, G--protein coupled, 6
1368797_at	9.08315E--0	5.00153E--0	5.207363	Nr1i3	nuclear receptor subfamily 1, group 1, member 3
1368829_at	1.81603E--0	5.21143E--0	2.1618636	Fbn1	fibrillin 1
1368884_at	0.0006954	0.000569765	3.62847	Entpd1	ectonucleoside triphosphate diphosphohydrolase 1
1368885_at	4.16707E--0	1.90771E--0	4.7927313		
1368901_at	2.38324E--0	1.02168E--0	3.1886022	Thbd	thrombomodulin
1368921_a_at	0.000374101	0.000271534	2.3644216	Cd44	CD44 molecule
1368926_at	6.11053E--0	2.11371E--0	3.282264	Sema4f	sema domain, immunoglobulin domain (Ig), transmembrane domain (TM) and short cytoplasmic domain, (semaphorin) 4f
1368991_at	4.99317E--0	1.66967E--0	2.1962628	Smpd3	sphingomyelin phosphodiesterase 3, neutral membrane
1369105_a_at	8.92814E--0	4.87623E--0	5.16415	Plkb	protein kinase (cAMP--dependent, catalytic) inhibitor beta
1369146_a_at	2.05418E--0	4.62272E--0	2.7706332	Ahr	aryl hydrocarbon receptor
1369214_a_at	0.000279071	0.000189733	3.4900792	Ctla	class II, major histocompatibility complex, transactivator
1369264_at	0.000420854	0.000310805	3.405944	Cyp21a1	cytochrome P450, family 21, subfamily a, polypeptide 1
1369518_at	0.001199546	0.00111286	2.9583325	Plk3r3	phosphoinositide--3--kinase, regulatory subunit 3 (gamma)
1369527_at	0.000107282	6.05266E--0	4.3797193	Cxcr1	chemokine (C--X3--C motif) receptor 1
1369547_at	0.000582596	0.000458875	3.2385366	Serpinp7	serpin peptidase inhibitor, clade B (ovalbumin), member 7
1369625_at	3.63063E--0	1.13925E--0	3.5069585	Aqp1	aquaporin 1
1369693_a_at	1.08375E--1	8.58754E--1	72.1144	Slc1a2	solute carrier family 1 (glial high affinity glutamate transporter), member 2
1369694_at	3.9195E--1	1.30443E--1	14.504282	Slc1a2	solute carrier family 1 (glial high affinity glutamate transporter), member 2
1369732_a_at	0.000156451	9.37217E--0	2.6942098	Stga2	ST3 beta--galactoside alpha--2,3--sialyltransferase 2
1369736_at	7.65559E--0	4.08864E--0	3.722521	Emp1	epithelial membrane protein 1
1369837_at	4.59332E--1	1.60623E--1	2.9848118	Gulo	gulonolactone (L--)-oxidase
1369921_at	8.81628E--0	4.7784E--0	4.600448	Gstm3	glutathione S--transferase mu 3
1369926_at	7.04586E--1	5.58309E--1	2.9906623	Gpx3	glutathione peroxidase 3
1369931_at	0.000200904	0.00012863	2.0650628	LOC100364062//Pkm	M2 pyruvate kinase--like//pyruvate kinase, muscle
1369964_at	0.000176268	0.000108387	3.0173218	Coro1a	coronin, actin binding protein 1A
1369968_at	2.23679E--0	3.40944E--0	3.0142543	Ptn	pleiotrophin
1370018_at	0.0012359	0.001153637	2.380999	Hspb2	heat shock protein beta 2
1370026_at	3.07579E--0	4.96992E--0	5.802904	Cryab	crystallin, alpha B

1370056_at	7.61206E--0	2.7746E--0	5.2907915	LOC100911104//LOC100912078//Ly6c	lymphocyte antigen 6B--like//lymphocyte antigen 6B--like//Ly6--C antigen
1370154_at	5.56683E--1	4.23467E--1	2.6449745	Ly22	lysozyme 2
1370155_at	1.73489E--0	2.45028E--0	6.565148	Col1a2//LOC100912118	collagen, type I, alpha 2//collagen alpha--2(I) chain--like
1370156_at	2.10561E--0	6.24009E--0	3.1348898	Prnp	prion protein
1370236_at	3.11932E--0	5.09176E--0	2.0483217	Ppt1	palmitoyl--protein thioesterase 1
1370247_a_at	6.34757E--0	3.20899E--0	2.4112895	Pmp22	peripheral myelin protein 22
1370269_at	0.000190061	0.00011988	6.705091	Cyp11a1	cytochrome P450, family 1, subfamily a, polypeptide 1
1370282_at	3.95984E--0	1.2802E--0	3.1376367	Csrp2	cysteine and glycine--rich protein 2
1370291_at	0.000710536	0.000586671	2.0945866	Pdlim3	PDZ and LIM domain 3
1370301_at	0.000689134	0.000560263	2.7007055	Mmp2	matrix metalloproteinase 2
1370312_at	1.50188E--0	5.879E--0	3.2338943	Spon1	spondin 1, extracellular matrix protein
1370328_at	1.06603E--0	2.12868E--0	3.4779558	Dkk3	Dickkopf WNT signaling pathway inhibitor 3
1370382_at	2.06701E--0	6.06016E--0	6.919508	RT1--Db1	RT1 class II, locus Db1
1370383_s_at	3.22697E--1	8.69389E--1	6.4288993	RT1--Db1	RT1 class II, locus Db1
1370389_at	8.81628E--0	4.77459E--0	4.1359377	Gpm6b	glycoprotein m6b
1370423_at	0.001136775	0.00103769	2.9050167	Gna15	guanine nucleotide binding protein, alpha 15
1370433_at	0.000126089	7.29361E--0	2.1174026	Hsd3b7	hydroxy--delta--5--steroid dehydrogenase, 3 beta-- and steroid delta--isomerase 7
1370436_at	0.001393068	0.001332405	3.7552779	AcsM2a	acyl--CoA synthetase medium--chain family member 2A
1370454_at	6.61226E--0	3.41616E--0	2.411264	Homer1	homer homolog 1 (Drosophila)
1370476_at	0.001350926	0.001280276	2.149745	Stambp	Stam binding protein
1370538_at	6.22077E--0	2.17875E--0	4.3305287	Lama3	laminin, alpha 3
1370603_a_at	0.000105991	5.96303E--0	2.0525808	Ptpcr	protein tyrosine phosphatase, receptor type, C
1370740_at	6.09329E--0	3.0225E--0	4.257574	Klra5	killer cell lectin--like receptor, subfamily A, member 5
1370822_at	0.000467894	0.000353701	3.918141	RT1--Ba	RT1 class II, locus Ba
1370834_at	0.000184392	0.00011572	5.4341273	Hs3st1	heparan sulfate (glucosamine) 3--O--sulfotransferase 1
1370855_at	1.43486E--0	1.40985E--1	2.8090081	Cx3c1	cystatin C
1370857_at	2.01849E--0	8.31706E--0	3.7574267	Acta2	smooth muscle alpha--actin
1370864_at	9.23918E--1	1.62935E--1	47.731823	Col1a1	collagen, type I, alpha 1
1370883_at	9.23918E--1	1.67924E--1	5.1444645	RT1--Da	RT1 class II, locus Da
1370887_at	1.15486E--0	4.33757E--0	3.1824033	Tgfb1l1	transforming growth factor beta 1 induced transcript 1
1370895_at	0.000955865	0.000837707	2.1287818	Col5a2	collagen, type V, alpha 2
1370896_a_at	1.27236E--0	4.87971E--0	3.7565975	Myh11	myosin, heavy chain 11, smooth muscle
1370904_at	0.00034099	0.000242098	2.7643263	LOC100909593//RT1--DMA	class II histocompatibility antigen, M alpha chain--like//RT1 class II, locus DMA
1370956_at	0.000117163	6.66584E--0	4.812715	Dcn	decorin
1370959_at	9.94529E--1	5.08309E--1	2.647053	Col3a1	collagen, type III, alpha 1
1370962_at	0.000409884	0.000301405	2.7735686	Parm1	prostate androgen--regulated mucin--like protein 1
1371076_at	1.56173E--0	6.16277E--0	5.36581	Cyp2b1//Cyp2b2//LOC100909962	cytochrome P450, family 2, subfamily b, polypeptide 1//cytochrome P450, family 2, subfamily b, polypeptide 2//cytochrome P450 2B1--like
1371247_at	4.87213E--0	1.61375E--0	4.9732723	Tnni3	troponin T type 3 (skeletal, fast)
1371349_at	8.4315E--0	1.04225E--0	2.9132755	Col6a1	collagen, type VI, alpha 1
1371360_at	7.60714E--0	4.05071E--0	3.0052998	Ndrp1	N--myc downstream regulated 1
1371369_at	4.70518E--0	2.237E--0	4.2548704	Col6a2	collagen, type VI, alpha 2
1371382_at	0.000718012	0.000596257	2.242717	Flna	filamin A, alpha
1371406_at	4.01046E--0	1.81774E--0	2.5902507		
1371414_at	2.53188E--1	1.48462E--1	4.883963	Gsn	gelsolin
1371441_at	3.40418E--0	1.06279E--0	2.0579555	Pea15	phosphoprotein enriched in astrocytes 15
1371447_at	2.85291E--0	1.25239E--0	2.1467342	Plac8	placenta--specific 8
1371527_at	6.12918E--0	2.13696E--0	3.286014	Emp1	epithelial membrane protein 1
1371575_at	5.06475E--0	2.4274E--0	2.0098178	Msn	moesin
1371700_at	3.23472E--1	1.94801E--1	36.09538	LOC100911714//Mfap4	microfibril--associated glycoprotein 4--like//microfibrillar--associated protein 4
1371703_at	8.79281E--1	7.54291E--1	4.1900077	Ahnak	AHNAK nucleoprotein
1371937_at	6.70572E--0	3.49633E--0	2.5508134	RGD1562618	similar to RIKEN cDNA 6030419C18 gene
1371951_at	5.92163E--0	2.8092E--0	3.922168	Fhl2	four and a half LIM domains 2
1372006_at	9.72034E--0	5.42244E--0	2.249812		
1372015_at	0.000320817	0.000223199	2.4218733	Tacc1	transforming, acidic coiled--coil containing protein 1
1372016_at	0.001298241	0.001218001	3.3958252	Ga8d45b	growth arrest and DNA--damage--inducible, beta
1372055_at	2.07047E--0	8.59689E--0	2.3032584		
1372064_at	5.39285E--0	6.06803E--1	3.41978	Cxcl16	chemokine (C--X--C motif) ligand 16
1372097_at	2.94548E--0	7.00194E--0	4.3218775		
1372107_at	3.3612E--0	1.4915E--0	3.3110003	Fhl1	four and a half LIM domains 1
1372110_at	0.000842045	0.000719275	3.380638		
1372111_at	6.34757E--0	3.2035E--0	5.7374754	Cav1	caveolin 1, caveolae protein
1372168_s_at	4.16707E--0	1.90853E--0	3.0117838	Igfbp6	insulin--like growth factor binding protein 6
1372219_at	1.1153E--1	6.00956E--1	14.144561	Tpm2	tropomyosin 2, beta
1372256_at	0.000108093	6.11556E--0	2.5870664	Crip1	cysteine--rich protein 1 (intestinal)
1372280_at	0.000519752	0.000400316	3.2911317	Asb2//LOC100909439	ankyrin repeat and SOCS box--containing 2//ankyrin repeat and SOCS box protein 2--like
1372301_at	6.86902E--0	1.25188E--0	7.721273	Aebp1	AE binding protein 1
1372440_at	2.33773E--0	5.3349E--0	2.2202873	Serpine2	serpin peptidase inhibitor, clade E (nexin, plasminogen activator inhibitor type 1), member 2
1372449_at	0.000214917	0.000139645	2.9540925	Slc8a1	solute carrier family 8 (sodium/calcium exchanger), member 1
1372481_at	1.86301E--1	1.03337E--1	15.638624		
1372516_at	0.00074393	0.000624854	2.4959576	Kif22	kinesin family member 22
1372518_at	0.001366399	0.00129927	2.5174825	Fbln1	fibulin 1
1372521_at	7.19362E--0	2.56508E--0	2.1323028	Rnd2	Rho family GTPase 2
1372539_at	2.23679E--0	3.43848E--0	10.870731		
1372615_at	1.22542E--0	1.16521E--1	17.58193	Aoc3	amine oxidase, copper containing 3
1372729_at	7.68429E--0	1.46135E--0	6.118515	Procr	protein C receptor, endothelial
1372750_at	1.98688E--0	8.03733E--0	5.862038		
1372897_at	0.000200236	0.000127884	3.0137339	Plod2	procollagen lysine, 2--oxoglutarate 5--dioxygenase 2
1372926_at	0.000566504	0.000442609	3.2089514		
1372935_at	0.000367721	0.000265738	3.3936296	Tmem119	transmembrane protein 119
1372980_at	2.83883E--0	8.77294E--0	2.748683	Tspan33	tetraspanin 33
1373000_at	2.7749E--0	6.50848E--0	11.171035	Srrp2	sushi--repeat--containing protein, X--linked 2
1373257_at	0.000538036	0.000416957	2.1065607	Sh3yl1	SH3 domain containing, Ysc84--like 1 (S. cerevisiae)
1373286_at	0.00146993	0.001430328	2.9702616	Fblim1	filamin binding LIM protein 1
1373401_at	7.87593E--0	2.89575E--0	7.614543	Tnc	tenascin C
1373463_at	5.0228E--0	1.69013E--0	2.9158478	Col5a2	collagen, type V, alpha 2
1373504_at	0.000559733	0.000435545	2.1544402	Glipr1	GLI pathogenesis--related 1
1373544_at	0.00063082	0.000564047	2.4786491	Cxcl9	chemokine (C--X--C motif) ligand 9
1373615_at	2.14091E--0	1.04307E--0	3.156928	Frzb	frizzled--related protein
1373651_at	7.84099E--0	4.20008E--0	5.9315524		
1373734_at	0.000187997	0.00011828	3.361332		
1373839_at	8.76099E--0	3.23504E--0	7.8314867		
1373882_at	1.5092E--0	2.84414E--0	10.278648		
1373908_at	6.42547E--0	1.62928E--0	11.04327		
1373938_at	0.000283179	0.000192975	5.3121576	Il17re	interleukin 17 receptor E
1373935_at	0.000493867	0.000375684	2.1099338	Pold2	polymerase (DNA directed), delta 2, accessory subunit
1374142_at	1.2901E--0	1.75829E--0	15.159431	Prr15	proline rich 15
1374172_at	0.001172507	0.001081457	3.6418538	Col8a2	collagen, type VIII, alpha 2
1374237_at	9.74577E--0	2.57931E--0	6.182794	Lmod1	leiomodin 1 (smooth muscle)
1374265_at	9.65631E--0	1.25486E--0	4.750055		
1374298_at	8.92814E--0	4.88147E--0	5.813765		
1374774_at	0.000450689	0.000338553	3.4809675		
1374818_at	0.001576065	0.001567231	2.3610883	Nxph3	neurexophilin 3
1374830_at	0.000532796	0.000412051	2.6066055	Ccdc3	coiled--coil domain containing 3
1374969_at	3.88938E--0	1.2451E--0	2.8820775		
1375014_at	0.000362655	0.000260353	3.7106023	Ar14c	ADP--ribosylation factor--like 4C
1375026_at	2.31259E--0	9.8221E--0	3.1402228	Calml4	calmodulin--like 4
1375043_at	0.000844281	0.000722523	3.9040523		
1375138_at	0.000465836	0.000350669	2.5476942	Timp3	TIMP metalloproteinase inhibitor 3

1375144_at	6.11053E--0	2.12077E--0	2.6039722	
1375170_at	3.41823E--1	1.02926E--1	7.8860073	S100a11
1375267_at	9.08315E--0	5.00941E--0	4.8477945	Ppic
1375633_at	0.001413522	0.00136648	2.00457	Clc1
1375726_at	0.000971262	0.000861975	2.1619089	Lmo7
1375739_at	0.000300149	0.000206441	2.0188825	Ehd4
1375857_at	0.000931598	0.000813487	2.7843993	Myof
1375862_at	0.000210971	0.000136078	2.587309	Pxdn
1375945_at	0.001120099	0.001018496	2.8157635	Pldc2
1375959_at	1.55435E--0	6.10903E--0	3.2381563	Nkd1
1375961_at	5.16104E--0	9.07886E--0	4.1456947	Frzb
1376110_at	2.71987E--0	8.3622E--0	3.7979505	Rpp25
1376218_a_at	0.001393068	0.001335667	2.1709888	LOC685152
1376287_at	0.000166161	0.000100065	5.235001	Capn13
1376394_at	1.29284E--1	9.01504E--1	15.328652	Clec9a
1376398_at	0.000531034	0.000409847	3.4356234	Synpo2
1376457_at	0.000484099	0.000367486	3.2282748	Crispld2
1376481_at	0.000969097	0.00085645	2.8673854	Adams9
1376617_at	2.22959E--0	2.43806E--1	5.5237285	
1376632_at	5.94498E--0	2.93009E--0	2.1659467	Lmcd1
1376749_at	0.001375146	0.001309767	2.1276767	LOC100910855//Ogn
1376750_at	0.000340752	0.000241388	2.7029169	
1376816_at	9.5179E--0	5.27934E--0	5.1691785	
1376818_at	0.000231435	0.000152578	2.9976008	Wtip
1376895_at	0.000285696	0.000195548	3.1649199	Il16
1376897_at	4.3964E--0	1.44224E--0	6.6599474	Kif26b
1376905_at	2.77161E--0	1.2123E--0	4.555384	
1376937_at	0.000258157	0.00017265	2.1764693	Filip1l
1376943_at	0.000362404	0.000259598	2.778507	LOC100910940
1377001_at	0.000967704	0.000852684	3.980909	Nrcam
1377034_at	9.92795E--0	2.64326E--0	6.885087	Serpinb1a
1377091_at	0.000239224	0.000158995	2.9769216	Prrt1
1377161_at	5.90297E--0	2.89068E--0	6.0779376	
1377177_at	0.000285696	0.000195595	3.3277717	Irx1
1377182_at	0.00082633	0.000701922	2.948495	Itgb3bp
1377267_at	0.001170068	0.001073644	2.0916424	Magel1
1377334_at	0.000214673	0.000139146	4.922169	RT1--Ba
1377369_at	0.000193149	0.00012244	2.1617262	Cybrd1
1377423_at	0.000971262	0.000860987	2.13079	
1379492_at	5.06475E--0	2.43204E--0	3.2367957	
1379936_at	3.6198E--0	1.62346E--0	4.833004	
1381464_at	0.000909124	0.000789159	4.101349	Tbx3
1381504_at	1.48505E--0	5.78956E--0	5.3469934	Aspn
1383017_at	7.27076E--0	3.81398E--0	2.012063	Ptpm
1383058_at	0.000235283	0.000155861	3.7698	
1383263_at	1.22925E--0	4.65596E--0	2.9274406	LOC100910855//Ogn
1383322_at	0.001322317	0.00124478	2.8262334	Rasf11b
1384420_at	1.61945E--0	1.69388E--1	9.703562	
1384778_at	0.001240321	0.001159729	2.1145556	Ctrc
1385047_x_at	0.00033866	0.000236863	2.3374574	LOC685048//RGD1559588//RGD1562525
1385248_a_at	0.000335232	0.000235353	3.2476156	LOC100910855//Ogn
1385354_at	0.000184344	0.000115398	2.6651628	Itga8
1386857_at	9.52663E--0	3.54795E--0	2.4564466	RGD1565395//Stmnl
1386865_at	3.03758E--0	7.26901E--0	4.9240646	Sparcl1
1386870_at	7.14238E--2	2.26383E--2	9.579763	Glul
1386881_at	9.88365E--1	4.85568E--1	2.2923703	Igfbp3
1386911_at	0.001537545	0.001513178	2.9552596	Atp1a2
1386921_at	8.07228E--1	6.65225E--1	21.6365	Cpe
1386922_at	2.42886E--0	5.58137E--0	5.4277296	Ca2
1386940_at	0.000610862	0.000485011	2.0748522	Timp2
1386965_at	6.1217E--0	1.54255E--0	5.4441376	Lpl
1387053_at	8.05679E--1	6.51183E--1	6.8947177	Fmo1
1387074_at	7.33096E--0	3.8688E--0	2.4041564	Rgs2
1387135_at	0.000132987	7.7558E--0	2.6292737	Adam15
1387146_a_at	1.04796E--0	1.39507E--0	3.2032824	Ednrb
1387184_at	6.44803E--0	7.56187E--1	4.711103	Axin2
1387232_at	2.7647E--0	4.33764E--0	8.973679	Bmp4
1387348_at	0.001346999	0.001274419	2.9215627	Igfbp5
1387351_at	4.21532E--0	1.944E--0	2.52121	Fbn1
1387581_at	3.94419E--0	6.62574E--0	9.810616	Rassf9
1387616_at	0.000704222	0.00057811	3.4130201	Pdgfr
1387651_at	0.000371942	0.000269378	2.4839175	Aqp1
1387725_at	9.88365E--1	4.57845E--1	2.7208862	Gulo
1387819_at	2.78724E--0	6.5816E--0	7.7816772	Cela1
1387854_at	9.71238E--1	8.77347E--1	6.1171376	Col1a2//LOC10091218
1387922_at	0.000440803	0.000328475	3.643623	Crispld2
1387925_at	0.000506366	0.000388401	3.5533633	Asns
1387952_a_at	6.70572E--0	3.49393E--0	2.554428	Cd44
1388014_at	1.03848E--0	2.04074E--0	16.181425	Odp1f
1388111_at	5.08557E--1	6.44763E--1	23.46591	Eln
1388112_at	0.000783254	0.000660366	2.2467024	Slc25a4
1388116_at	1.83823E--1	2.03924E--1	13.399812	Col1a1
1388131_at	3.07579E--0	4.97196E--0	13.104549	Tubb2b
1388142_at	0.000925674	0.000806848	4.29704	Vcan
1388145_at	6.85645E--0	3.58578E--0	2.9667175	Tnxb
1388146_at	1.08375E--1	7.99359E--1	45.8538	LOC100912222
1388312_at	0.001393068	0.001330802	2.1300669	
1388427_at	0.000167329	0.000101703	3.6383202	Mara8
1388557_at	9.26937E--1	8.22639E--1	27.796534	C7//Tubb4b
1388673_at	7.68429E--0	1.46031E--0	4.866844	Lsp1
1388763_at	2.11691E--0	8.82333E--0	2.0544763	
1388796_at	0.000728351	0.000606493	2.2497241	
1388879_at	9.25868E--0	1.17384E--0	2.8467658	Abi3bp
1388936_at	0.000969097	0.000856983	3.0707588	Cdh11
1388955_at	2.50849E--0	7.60606E--0	3.2211163	
1389020_at	0.001571732	0.001554296	2.1612043	LOC686539
1389092_at	0.001172507	0.001078411	2.293468	Il2rg
1389112_at	7.174E--0	1.31883E--0	2.886483	Nkd1
1389185_at	9.08315E--0	5.00399E--0	3.0755537	Ak1
1389210_at	1.73631E--0	3.74228E--0	3.79275	Lcp4
1389234_at	8.20406E--1	5.33069E--1	51.40059	Vwf
1389250_at	0.000467894	0.000353251	2.5476272	
1389253_at	7.5239E--0	3.99446E--0	7.4233227	Vnn1
1389413_at	0.000345252	0.00024567	4.6462426	Evi2a
1389512_at	2.03509E--0	8.41773E--0	3.008208	
1389533_at	6.70754E--0	7.97252E--1	9.41373	Fbln2
1389568_at	1.56903E--0	6.21644E--0	3.34711	Calhm2
1389586_at	2.07244E--0	6.10893E--0	2.422569	

1389611_at	8.92768E--0	4.85292E--0	5.3722205	Vldlr	very low density lipoprotein receptor
1389698_at	0.000908751	0.000786336	2.712509		
1389836_a_at	0.000144288	8.50639E--0	2.394913	Timpt3	TIMP metalloproteinase inhibitor 3
1389873_at	4.96222E--0	1.65145E--0	2.1449242	Pycard	PYD and CARD domain containing
1389966_at	0.001067442	0.000960867	4.1509485	Col6a3	collagen, type VI, alpha 3
1390027_at	1.39587E--0	5.37552E--0	13.328595	Pcp4l1	Purkinje cell protein 4--like 1
1390250_x_at	0.000167329	0.000101518	2.5900575	LOC685152	ATPase, class I, type 8B, member 2
1390306_at	0.00011858	6.76528E--0	2.4352193	LOC100912470	uncharacterized LOC100912470
1390312_at	0.000560792	0.000437258	2.2658095	LOC500013///LOC684193///Samd9l	similar to sterile alpha motif domain containing 9--like//similar to sterile alpha motif domain containing 9--like//sterile alpha motif domain containing 9--like
1390429_at	3.79316E--0	1.20828E--0	2.5057359		
1390450_a_at	0.000865805	0.000742315	2.942699	LOC100910855///Ogn	nmecan--like//osteoglycin
1390472_at	0.000301373	0.000207761	4.1313148	Naaa	N--acylethanolamine acid amidase
1390506_at	0.00069082	0.000563582	2.0670316	Med1	mediator complex subunit 1
1390532_at	4.71264E--0	1.15015E--0	3.104424	Slc13a4	solute carrier family 13 (sodium/sulfate symporters), member 4
1390533_at	4.21532E--0	1.95067E--0	2.6234598	LOC691920	similar to kinesin--like motor protein C20orf23
1390547_at	0.00144634	0.00140279	4.531088		
1390632_at	2.93854E--0	4.65696E--0	2.8503778		
1390687_at	0.000376569	0.000274519	2.0481522	Plek	pleckstrin
1390707_at	1.09196E--0	2.21507E--0	3.7147343	Rgs10	regulator of G--protein signaling 10
1392407_at	0.000353912	0.000252394	4.275584	Arhgap30	Rho GTPase activating protein 30
1393528_at	0.000956899	0.00084013	3.8725975	Synpo2	synaptopodin 2
1393688_at	0.000710423	0.000585451	2.4814289	LOC685048///RGD1559588///RGD1562525	similar to paired immunoglobulin--like type 2 receptor beta//similar to cell surface receptor FDFACT//similar to cell surface receptor FDFACT
1398286_at	1.84241E--0	1.95628E--1	5.0844216	Csad	cysteine sulfonic acid decarboxylase
1398347_at	0.000719902	0.000600108	2.1893353	Axl	Axl receptor tyrosine kinase
1398350_at	2.50849E--0	7.63281E--0	3.2989917	Basp1	brain abundant, membrane attached signal protein 1
1398373_at	1.48373E--0	5.73741E--0	5.828922	B3galnt1	beta--1,3--N--acetylglactosaminyltransferase 1 (globoside blood group)
1398390_at	1.58051E--0	1.63274E--1	26.053364	Cxcl13	chemokine (C--X--C motif) ligand 13
1377546_at	0.000262835	0.000176612	5.388679		
1377761_at	0.000164379	9.87316E--0	2.8196638	Gltpt2	glutamine--fructose--6--phosphate transaminase 2
1377795_at	0.001576065	0.001568572	3.8781815		
1377882_at	2.14273E--0	8.96485E--0	4.0582356	Ftk3	fms--related tyrosine kinase 3
1377994_at	0.000132943	7.7322E--0	3.7058427		
1378213_at	1.19816E--0	3.22801E--0	4.415251		
1378258_at	6.21111E--0	3.09079E--0	3.926266		
1378396_at	0.001034686	0.000928102	2.0818934		
1378418_at	5.6177E--0	2.72427E--0	2.3754206	Tifab	TRAF--interacting protein with forkhead--associated domain, family member 8
1378443_at	0.000166675	0.000100639	3.6071338	Slamf9	SLAM family member 9
1378645_at	0.000450251	0.00033751	5.1012154		
1378699_at	9.94529E--1	5.20118E--1	11.548689	Pkhd1l1	polycystic kidney and hepatic disease 1--like 1
1378780_at	0.001583329	0.00158082	2.451916		
1378916_at	5.85478E--0	2.00417E--0	2.1797583		
1379008_at	0.001526866	0.001500248	2.8380694		
1379022_at	0.001176903	0.001087376	3.669268	Adamts8	ADAM metalloproteinase with thrombospondin type 1 motif, 8
1379381_at	1.64391E--0	4.66339E--0	4.5342946	Ctla	class II, major histocompatibility complex, transactivator
1379541_at	0.000269256	0.000181353	2.9466634		
1379625_at	0.000665379	0.000537786	2.5378683	Zc2hc1a	zinc finger, C2HC--type containing 1A
1379633_a_at	7.46411E--0	1.92813E--0	2.0026662	Uba7	ubiquitin--like modifier activating enzyme 7
1379639_at	0.000728351	0.00060946	2.6838512		
1379656_a_at	0.001199546	0.001114	2.9362245	Coro2a	coronin, actin binding protein 2A
1379742_at	6.8391E--0	2.41699E--0	2.1034894	Sp100	SP100 nuclear antigen
1379785_at	0.000119324	6.84555E--0	2.7587144	Slc1a4	solute carrier family 1 (glutamate/neutral amino acid transporter), member 4
1380017_at	0.001007488	0.000898916	2.034759		
1380063_at	0.000836384	0.000713113	3.401918	Ch25h	cholesterol 25--hydroxylase
1380077_at	8.68975E--0	2.27228E--0	7.460445		
1380079_at	2.87358E--0	1.26601E--0	2.8126707	Samd9l	sterile alpha motif domain containing 9--like
1380244_at	1.64391E--0	4.66055E--0	3.4277337	Jam2	junctional adhesion molecule 2
1380351_at	3.38872E--1	9.6667E--1	4.150351		
1380363_at	0.000654483	0.000526906	3.1657624	Klf7	Kruppel--like factor 7 (ubiquitous)
1380410_at	6.27258E--0	3.14126E--0	3.8753777		
1380455_at	6.45963E--0	3.28612E--0	3.4581037	Col6a5	collagen, type VI, alpha 5
1380545_at	0.000211192	0.000136555	2.2745008	Asap1	ARFAP with SH3 domain, ankyrin repeat and PH domain 1
1380682_at	0.000582596	0.000458687	2.696835	Mex3b	mex3 homolog B (C. elegans)
1380726_at	1.09196E--0	2.20494E--0	5.78175		
1380784_at	0.000144122	8.46515E--0	2.0823224	Klhl5	kelch--like family member 5
1380930_at	2.30413E--0	9.74963E--0	2.5968668	RGD1564142	similar to chromosome 10 open reading frame 64
1380967_at	0.00023282	0.000153861	4.22098	Nts	neurotensin
1381088_at	0.000385274	0.000282086	2.683475		
1381221_at	0.000590165	0.000465772	5.534136	RGD1311300	similar to T cell receptor V delta 6
1381357_at	0.000900534	0.000777799	3.9428735	Ptpn22	protein tyrosine phosphatase, non--receptor type 22 (lymphoid)
1381387_at	0.000378213	0.000276317	2.8366952		
1381450_at	0.000644899	0.000517313	2.9568226		
1381487_at	0.0013296	0.001253743	2.4990027	Angpt1	angiopoietin 1
1381591_at	0.00042843	0.000317279	3.7640345		
1381715_at	0.000125489	7.239E--0	3.0313687		
1381986_at	0.000605733	0.000479979	3.0387967		
1382031_at	0.000715826	0.000592173	3.782801		
1382072_at	1.2877E--0	3.51004E--0	8.211142	Olfml2a	olfactomedin--like 2A
1382083_at	3.20753E--0	1.41823E--0	2.5138676	Coch	cochlin
1382351_at	0.000514082	0.000395134	4.500563	Gem	GTP binding protein overexpressed in skeletal muscle
1382372_at	1.08443E--0	9.96783E--1	3.4179208		
1382442_at	1.11247E--0	4.16076E--0	5.375487		37495 septin 6
1382454_at	0.000271484	0.000184144	2.9294903	Cxcl9	chemokine (C--X--C motif) ligand 9
1382566_at	0.000239224	0.00015923	3.1046593	Il7r//LOC100911254	interleukin 7 receptor//interleukin--7 receptor subunit alpha--like
1382692_at	1.98688E--0	8.06089E--0	3.6539237	Clec7a	C--type lectin domain family 7, member A
1382700_at	0.000208377	0.000133745	3.9614873		
1382726_at	0.000662769	0.000534627	3.856265	Nkd1	naked cuticle homolog 1 (Drosophila)
1382873_at	0.000420553	0.000309916	2.079076	Cttnbp2nl	CTTNBP2 N--terminal like
1382905_at	5.5704E--0	1.898E--0	3.9724796		
1382926_s_at	0.000215111	0.000140199	3.7336886		
1382953_at	1.80867E--0	2.63883E--0	4.276895		
1383197_at	2.84722E--0	8.84399E--0	6.1478	Jam2	junctional adhesion molecule 2
1383284_at	5.65158E--0	2.74966E--0	4.7206135		
1383291_at	8.60079E--0	1.64928E--0	8.324201	C7//Tubb4b	complement component 7//tubulin, beta 4B class IVb
1383330_at	6.58621E--0	3.38182E--0	2.4705935		
1383398_at	0.001404824	0.001354421	2.7090008	Itga8	integrin, alpha 8
1383404_at	6.58089E--0	3.36867E--0	4.564208		
1383453_at	0.000119324	6.83448E--0	2.2679532	Olfml1	olfactomedin--like 1
1383469_at	1.51626E--0	2.11459E--0	6.253115	Aldh1a3	aldehyde dehydrogenase 1 family, member A3
1383546_at	3.55034E--0	5.8516E--0	8.411332	Gdpd2	glycerophosphodiester phosphodiesterase domain containing 2
1383708_at	5.23444E--1	2.07387E--1	6.1856084	Itgb1	integrin, beta--like 1
1383914_at	1.75417E--0	3.80859E--0	2.9510264	Mrv1	murine retrovirus integration site 1 homolog
1384161_at	0.00036602	0.000263929	3.0665708	Csnk1e	casein kinase 1, epsilon
1384187_at	4.16888E--0	1.361E--0	3.4986734	Ap1s2	adaptor--related protein complex 1, sigma 2 subunit
1384312_at	3.67184E--0	1.16326E--0	5.9537754	Irx1	irx1 homeobox 1
1384406_at	1.60179E--0	3.3508E--0	2.380763	Ccr1	chemokine (C--C motif) receptor--like 1
1384460_at	0.000998222	0.00087484	3.3615768		
1384509_s_at	2.75364E--0	1.20008E--0	6.14418	Pcdh17	protocadherin 17
1384558_at	6.72654E--0	1.21525E--0	5.481333	Plac9	placenta--specific 9
1384707_at	7.27853E--0	3.82959E--0	5.0429606	Scara5	scavenger receptor class A, member 5 (putative)
1384812_at	0.00157467	0.001559696	5.185218		

1385143_at	0.000335729	0.000236234	2.3905818	RGD1561963	similar to Dedicator of cytokinesis protein 10 (Protein zizimin 3)
1385608_at	0.000271484	0.000183592	3.8665802	Rab7b	Rab7b, member RAS oncogene family
1385637_at	1.30017E--0	3.58525E--0	8.294608		
1385659_at	8.65358E--0	1.08341E--0	13.83722	Apcdd1	adenomatosis polyposis coli down--regulated 1
1385701_at	4.01046E--0	1.81674E--0	5.35733		
1385702_at	4.69716E--0	2.22575E--0	3.3473763	Ifi204	interferon activated gene 204
1385707_at	1.81603E--0	5.238E--0	2.0418074	Lect2	leukocyte cell--derived chemotaxin 2
1385925_at	2.54358E--0	0.000011045	6.9560733		
1386043_at	0.000831481	0.000707615	2.3222082		
1386061_at	0.00042843	0.000317758	2.660119		
1386125_at	5.88574E--0	2.0241E--0	2.6817493	Hoxb4	homeo box B4
1386242_at	0.000215111	0.000140453	4.763677		
1386795_at	0.000376569	0.000274365	3.1833355	Hepacam2	HEPACAM family member 2
1390843_at	0.000559733	0.000434979	2.6082654	Ccdc102a	coiled--coil domain containing 102A
1390901_at	0.001136775	0.001036315	2.620268	Igslf10	immunoglobulin superfamily, member 10
1390912_at	1.70167E--0	3.61369E--0	15.125416	Pcp4l1	Purkinje cell protein 4--like 1
1390931_at	0.00050098	0.000381888	3.759329	Adams15	ADAM metalloproteinase with thrombospondin type 1 motif, 15
1390946_at	4.06133E--0	1.31945E--0	3.9268203	Runx3	runt--related transcription factor 3
1391039_at	6.27258E--0	3.13456E--0	5.919039		
1391083_at	1.00367E--0	1.95643E--0	7.6426916	Arhgap22	Rho GTPase activating protein 22
1391450_at	4.75823E--0	2.26977E--0	5.37836	Loxl2	lysyl oxidase--like 2
1391468_at	1.64852E--0	6.55751E--0	4.700059	Myc11	myc target 1
1391557_at	0.000632235	0.000504987	3.3011181	Sox15	SRX (sex determining region Y)--box 15
1391562_at	0.001485415	0.00144775	3.2878757		
1391721_at	5.58733E--0	1.00058E--0	11.781904		
1391925_at	0.000878525	0.000754613	2.2548354	Ccl19	chemokine (C--C motif) ligand 19
1392274_at	0.000182573	0.000114	3.074976		
1392296_at	1.73489E--0	2.50198E--0	5.365514		
1392309_at	4.13386E--0	1.00235E--0	4.262889	Jam2	junctional adhesion molecule 2
1392352_at	6.45963E--0	3.27837E--0	3.1624131		
1392510_at	4.31894E--0	2.01231E--0	4.847744	Fam180a	family with sequence similarity 180, member A
1392515_at	6.35378E--0	2.2354E--0	2.9912188	Klra17///Klra7///LOC100910264///LOC100910679///LOC497796///LOC502907///LOC690097///Ly49s1i///Ly49s2i///Ly49s3i///RGD1561306	killer cell lectin--like receptor, subfamily A, member 17///killer cell lectin--like receptor, subfamily A, member 7///T--cell surface glycoprotein YE1/48--like///killer cell lectin--like receptor 5--like///hypothetical protein LOC497796///similar to immunoreceptor Ly49s1i///similar to immunoreceptor Ly49s3i///immunoreceptor Ly49s1i///immunoreceptor Ly49s2i///immunoreceptor Ly49s3i///similar to immunoreceptor Ly49s3
1392521_at	0.000172188	0.000105605	4.020242		
1392578_at	8.8977E--0	2.34076E--0	8.093776		
1392645_at	2.15193E--0	6.41146E--0	3.2168238		
1392754_at	0.001305113	0.001226517	2.8363743	Adam8	ADAM metalloproteinase domain 8
1392886_a_at	5.20914E--0	1.76665E--0	4.722019	Fcrla	Fc receptor--like A
1392899_at	0.001297551	0.001215298	3.0418608	Prc1	protein regulator of cytokinesis 1
1392965_a_at	5.03291E--1	1.91426E--1	5.1339905	LOC100909873///LOC100910861///Smoc2	SPARC--related modular calcium--binding protein 2--like///SPARC--related modular calcium--binding protein 2--like
1393060_at	1.32816E--0	1.83121E--0	4.8255806	Adams12	ADAMTS--like 2
1393067_at	4.40195E--0	1.48071E--0	2.3442204	Tek	TEK tyrosine kinase, endothelial
1393109_at	9.21423E--0	3.41701E--0	3.1697443		
1393160_at	2.03634E--0	2.19448E--1	3.7208838		
1393174_at	3.95984E--0	1.27766E--0	3.340138	Fam171b	family with sequence similarity 171, member B
1393210_at	2.56353E--0	7.8409E--0	6.3344035	LOC1009361383	extracellular matrix protein 2--like
1393225_at	6.4629E--0	3.29803E--0	2.0690155	Adams10	ADAM metalloproteinase with thrombospondin type 1 motif, 10
1393227_at	4.66631E--0	2.20374E--0	5.5482545		
1393240_at	0.001468247	0.001426364	2.982464	Efemp2	EGF--containing fibulin--like extracellular matrix protein 2
1393250_at	1.24912E--0	4.75103E--0	4.0126305		
1393252_at	4.73286E--1	2.92523E--1	18.770403		
1393281_at	3.67184E--0	1.16382E--0	9.119468	Cav1	caveolin 1, caveolae protein
1393324_at	1.62007E--0	4.51874E--0	3.8163154	Jam2	junctional adhesion molecule 2
1393330_at	0.000104851	5.88229E--0	3.9773836	LOC100909539	uncharacterized LOC100909539
1393401_at	0.000643674	0.000515143	6.1602025		
1393449_at	2.15597E--1	1.57171E--1	3.908153	Jam2	junctional adhesion molecule 2
1393454_at	0.000259889	0.00017422	4.6113076	Pcdh17	protocadherin 17
1393559_at	0.000437204	0.000324958	7.9346104		
1393571_at	4.20448E--0	1.93233E--0	4.130112	Sox4	SRX (sex determining region Y)--box 4
1393708_at	0.000332246	0.00023273	4.680258	Bhlhe22	basic helix--loop--helix family, member e22
1393927_at	2.01614E--0	3.0354E--0	12.253391		
1394200_at	0.001085454	0.000978801	3.2939148	Hspa2	heat shock protein 2
1394415_at	4.42498E--0	2.08275E--0	3.9674797	LOC687813	similar to Tnf receptor--associated factor 1
1394451_at	0.000909124	0.000790797	3.529826	Anxa1	annexin A1
1394475_at	0.000758611	0.000638387	2.704211		
1394517_at	3.94825E--0	1.77702E--0	4.759022		
1394678_at	8.46645E--0	4.56196E--0	2.0297542	Fgd2	PYVE, RhoGEF and PH domain containing 2
1394681_at	0.000144122	8.47372E--0	2.111798	Akr1c1	aldo--keto reductase family 1, member C--like
1395166_at	0.000616155	0.00049019	2.3888547	Ehd2	EH--domain containing 2
1395184_at	6.86854E--0	2.43828E--0	4.8504725	Clec12a	C--type lectin domain family 12, member A
1395301_x_at	1.95147E--0	5.69049E--0	6.981174	LOC100910801///RGD1561143	paired immunoglobulin--like type 2 receptor alpha--like///similar to cell surface receptor FDFACT
1395472_at	0.000148794	8.81915E--0	2.9568658	Lrrc17	leucine rich repeat containing 17
1395501_at	0.000520817	0.000223044	3.7562106		
1395644_at	0.000474109	0.000359151	2.1377718	Abca8	ATP--binding cassette, subfamily A (ABC1), member 8
1395753_at	1.48483E--0	5.7652E--0	7.404484	Elm	elastin
1395983_at	0.001519816	0.001490913	2.2411356	Rmdn2	regulator of microtubule dynamics 2
1396055_at	0.000328845	0.000229306	2.151869	Col6a3	collagen, type VI, alpha 3
1396132_at	0.000171489	0.000104905	2.4429908	Fcrla	Fc receptor--like A
1396613_at	0.001540156	0.001518189	2.7671452		
1396694_at	0.001414344	0.001369515	2.4392087		
1396974_at	0.001199546	0.001110874	2.4224997		
1397022_at	0.001511965	0.001479757	2.770665		
1397050_at	0.001002586	0.000892953	2.4066973	Cpne8	copine VIII
1397249_at	0.000295577	0.000202828	4.254638		
1397427_at	0.000149125	8.86241E--0	4.3747163	Ces1c	carboxylesterase 1C
1397429_at	0.000210283	0.000135301	5.8441133	Creb5	cAMP responsive element binding protein 5
1397668_at	0.000800096	0.000675833	3.808793		
1398231_at	0.000176472	0.000108792	3.8051686		
1398616_at	3.47456E--0	1.54731E--0	2.4632313	Ap1s2	adaptor--related protein complex 1, sigma 2 subunit
1398703_at	3.02858E--1	2.25583E--1	7.2161446		

Male rat liver zone I signature

Probe Set ID	Corrected p--value	p--value	FCAbsolute	Gene Symbol	Gene Title
1367794_at	0.034083895	0.009176433	2.0320027	A2m///LOC100911545	alpha--2--macroglobulin///alpha--2--macroglobulin--like
1374307_at	1.66E--0	1.53E--0	2.6543653		
1376082_at	0.009171167	0.001693139	2.5005655	Mecom	MD51 and EVI1 complex locus
1387111_at	2.57E--0	5.94E--0	3.5038505	Ddah1	dimethylarginine dimethylaminohydrolase 1
1389876_at	0.007545118	0.00160787	2.113492	Camk2n1	calcium/calmodulin--dependent protein kinase II inhibitor 1
1398348_at	4.17E--0	1.93E--0	2.6440198		
1378798_at	0.037235864	0.010624247	2.204123	Stox2	storkhead box 2
1379076_at	0.018219834	0.004064424	2.6486177		
1380389_at	0.030691367	0.007790885	2.0545697		
1382631_at	3.88E--0	4.48E--0	4.664542		
1384035_at	5.24E--0	2.82E--0	13.242892		
1384036_s_at	1.52E--0	5.83E--0	7.124467		

1385670_at	0.021947639	0.00506484	2.0117233	Sds1	serine dehydratase--like
1390765_at	4.74E--0	1.46E--0	3.075217	Wfdc2	WAP four--disulfide core domain 2

Female rat liver zone I signature

Probe Set ID	Corrected p--value	p--value	FCAbsolute	Gene Symbol	Gene Title
1367847_at	3.38E--0	3.38E--0	2.274325	Nupr1	nuclear protein, transcriptional regulator, 1
1369126_at	0.027340967	0.006730084	2.0997062	Ptgr	prostaglandin F receptor
1369195_at	1.39E--0	1.18E--0	2.0734417	Fabp2	fatty acid binding protein 2, intestinal
1370080_at	6.74E--0	4.67E--0	2.3850334	Hmox1	heme oxygenase (decycling) 1
1370241_at	3.24E--0	1.99E--0	2.1842568	Cyp2c7///LOC100911552	cytochrome P450, family 2, subfamily c, polypeptide 7///cytochrome P450 2C7--like
1371922_at	0.003324047	4.60E--0	3.4437294		
1373386_at	0.001667833	2.18E--0	3.287276	Gjb2	gap junction protein, beta 2
1376279_at	0.010885246	0.002093317	2.5299816	Pop1	processing of precursor 1, ribonuclease P/MRP subunit (S. cerevisiae)
1383472_at	0.004852043	7.09E--0	3.9102445	Aldh1b1	aldehyde dehydrogenase 1 family, member B1
1384225_at	3.88E--0	4.24E--0	3.515745		
1384226_at	0.013258733	0.002753737	2.174665		
1393241_at	1.61E--0	2.48E--0	4.933111	Prss32	protease, serine, 32
1396155_at	1.01E--0	7.80E--1	6.4710135		

Male rat liver zone III signature

Probe Set ID	Corrected p--value	p--value	FCAbsolute	Gene Symbol	Gene Title
1367568_p_at	1.97E--0	7.20E--0	3.4364784	Mgp	matrix Gla protein
1367570_at	0.002994248	0.000363	5.066586	Tagln	transgelin
1367574_at	0.003296671	0.000447	2.3799796	Vim	vimentin
1367584_at	1.99E--0	7.34E--0	2.2204938	Anxa2	annexin A2
1367614_at	0.019996617	0.007543634	2.3689913	Anxa1	annexin A1
1367628_at	0.000163	0.00000422	3.041819	Lgals1	lectin, galectoside--binding, soluble, 1
1367655_at	6.74E--0	1.56E--0	2.438251	LOC100359493//LOC100359496//LOC100361392//LOC100361596//LOC100361620//LOC100364435//LOC100909821//LOC100911590//Tmsb10	thymosin, beta 10--like//thymosin, beta 10--like//thymosin, beta 10--like//hypothetical protein LOC100361596//thymosin, beta 10--like//thymosin, beta 10--like//thymosin beta--10--like//thymosin beta--10--like//thymosin, beta 10
1367661_at	6.55E--0	4.45E--0	4.9478893	S100a6	S100 calcium binding protein A6
1367749_at	0.00049	0.0000274	5.5054755	Lum	lumican
1367823_at	3.75E--0	1.81E--0	2.332806	Timp2	TIMP metalloproteinase inhibitor 2
1367846_at	1.40E--0	4.14E--0	3.3632684	S100a4	S100 calcium--binding protein A4
1367866_at	0.003555084	0.000504	2.2241719	Fbln5	fibulin 5
1367880_at	0.00225122	0.000225	2.9701128	Lamb2	laminin, beta 2
1367940_at	0.006249851	0.001372223	2.31592	Cxcr7	chemokine (C--X--C motif) receptor 7
1367998_at	1.08E--0	2.88E--0	2.4994542	Slpi	secretory leukocyte peptidase inhibitor
1368007_at	0.03755658	1.82E--0	3.1357284	Dmbt1///LOC100913031	deleted in malignant brain tumors 1//deleted in malignant brain tumors 1 protein--like
1368128_at	0.000604391	0.001186496	2.6273537	Pla2g2a	phospholipase A2, group IIA (platelets, synovial fluid)
1368167_at	0.019541342	0.007059846	2.705863	Ctse	cathepsin E
1368171_at	2.81E--1	1.68E--1	22.392555	Lox	lysyl oxidase
1368172_a_at	1.21E--1	4.84E--1	15.957376	Lox	lysyl oxidase
1368207_at	5.12E--0	9.40E--0	2.230316	Fxyd5	FXyD domain--containing ion transport regulator 5
1368281_at	0.003233416	4.20E--0	4.841948	Dpep1	dipeptidase 1 (renal)
1368282_at	3.62E--0	5.20E--0	3.6044595	Dpep1	dipeptidase 1 (renal)
1368284_at	2.65E--0	1.14E--0	2.0511272	Plivap	plasmalemma vesicle associated protein
1368320_at	0.015223616	0.004732144	2.5161479	Ncam1	neural cell adhesion molecule 1
1368448_at	1.32E--0	3.77E--0	3.3078399	Ltbp2	latent transforming growth factor beta binding protein 2
1368797_at	0.004900231	0.000861	3.0210655	Nr1i3	nuclear receptor subfamily 1, group I, member 3
1368829_at	0.001606949	0.000144	2.1843097	Fbn1	fibrillin 1
1368921_a_at	7.20E--0	1.74E--0	2.9003222	Cd44	Cd44 molecule
1368926_at	0.006249851	0.001357982	2.2086632	Sema4f	sema domain, immunoglobulin domain (Ig), transmembrane domain (TM) and short cytoplasmic domain, (semaphorin) 4f
1369527_at	0.015542509	0.00491718	2.653278	Cx3cr1	chemokine (C--X3--C motif) receptor 1
1369921_at	5.03E--0	9.14E--0	2.5903316	Gstm3	glutathione S--transferase mu 3
1369926_at	2.00E--0	5.99E--0	3.031266	Gpx3	glutathione peroxidase 3
1369931_at	0.005215114	0.001006712	2.2140355	LOC100364062//Pkm	M2 pyruvate kinase--like//pyruvate kinase, muscle
1369964_at	6.15E--0	1.28E--0	2.273728	Coro1a	coronin, actin binding protein 1A
1369968_at	2.83E--0	1.12E--0	2.1539533	Ptin	pleiotrophin
1370018_at	0.003620693	0.000528	2.6014082	Hspb2	heat shock protein beta 2
1370026_at	0.025581494	0.010875965	2.3872756	Cryab	crystallin, alpha B
1370155_at	0.001262971	0.000103	3.1400864	Col1a2///LOC100911218	collagen, type I, alpha 2//collagen alpha--2(I) chain--like
1370156_at	2.41E--0	2.60E--0	2.537972	Prnp	prion protein
1370247_a_at	0.00382353	5.88E--0	2.4264011	Pmp22	peripheral myelin protein 22
1370291_at	0.002746988	0.000316	2.8277662	Pdlim3	PDZ and LIM domain 3
1370301_at	0.000263	0.0000084	3.214848	Mmp2	matrix metalloproteinase 2
1370312_at	0.006145863	1.31E--0	2.6855993	Spon1	spondin 1, extracellular matrix protein
1370328_at	3.66E--0	5.41E--0	2.2414434	Dkk3	Dickkopf WNT signaling pathway inhibitor 3
1370423_at	5.22E--0	9.95E--0	2.4440804	Gna15	guanine nucleotide binding protein, alpha 15
1370538_at	0.007523394	1.83E--0	2.106403	Lama3	laminin, alpha 3
1370857_at	6.15E--0	1.29E--0	3.6731007	Acta2	smooth muscle alpha--actin
1370864_at	3.56E--0	1.68E--0	3.4342391	Col1a1	collagen, type I, alpha 1
1370887_at	0.003194604	0.000408	2.6827934	Tgfb1l1	transforming growth factor beta 1 induced transcript 1
1370895_at	2.41E--0	2.57E--0	2.0990355	Col5a2	collagen, type V, alpha 2
1370896_a_at	0.01739069	0.005803644	3.2328322	Myh11	myosin, heavy chain 11, smooth muscle
1370956_at	0.006145863	0.001307725	3.499347	Dcn	decorin
1370962_at	2.42E--0	9.99E--0	2.0388489	Parm1	prostate androgen--regulated mucin--like protein 1
1371247_at	0.03293959	0.015187716	2.1964839	Tnni3	troponin T type 3 (skeletal, fast)
1371349_at	0.00116446	0.000093	2.2794113	Col6a1	collagen, type VI, alpha 1
1371360_at	6.08E--0	1.24E--0	2.9441957	Ndrp1	N--myc downstream regulated 1
1371369_at	2.76E--0	9.60E--0	4.4959407	Col6a2	collagen, type VI, alpha 2
1371382_at	0.000429	0.0000216	3.7944925	Flna	filamin A, alpha
1371406_at	4.88E--0	8.47E--0	2.584559		
1371414_at	3.48E--0	4.86E--0	2.909865	Gsn	gelsolin
1371447_at	0.010109841	0.002643491	2.0089037	Plac8	placenta--specific 8
1371527_at	0.005215114	0.000981	3.0236259	Emp1	epithelial membrane protein 1
1371700_at	0.021330351	0.008302232	3.8000288	LOC100911714//Mfap4	microfibril--associated glycoprotein 4--like//microfibrillar--associated protein 4
1371951_at	9.86E--0	2.56E--0	2.407298	Fhl2	four and a half LIM domains 2
1372107_at	0.02197756	8.79E--0	2.360852	Fhl1	four and a half LIM domains 1
1372111_at	0.017063163	0.005585547	3.4560928	Cav1	caveolin 1, caveolae protein
1372168_s_at	0.000901	0.0000647	3.411398	Igfbp6	insulin--like growth factor binding protein 6
1372256_at	0.00306171	3.85E--0	2.8317332	Crip1	cysteine--rich protein 1 (intestinal)
1372280_at	1.76E--0	5.97E--0	2.6545665	Asb2///LOC100909439	ankyrin repeat and SOCS box--containing 2//ankyrin repeat and SOCS box protein 2--like
1372301_at	6.02E--0	1.20E--0	3.3762465	Aebp1	AE binding protein 1
1372481_at	0.008606446	2.15E--0	3.9705498		
1372518_at	3.35E--0	4.62E--0	3.1681821	Fbln1	fibulin 1
1372539_at	4.50E--0	2.27E--0	2.5117233		
1372615_at	0.003945599	0.000614	5.5381174	Aoc3	amine oxidase, copper containing 3
1372897_at	2.75E--0	3.18E--0	2.839459	Plo2	procollagen lysine, 2--oxoglutarate 5--dioxygenase 2
1372935_at	8.35E--0	8.33E--1	5.645368	Tmem119	transmembrane protein 119
1373000_at	0.009662118	0.002487851	3.8154464	Srpx2	sushi--repeat--containing protein, X--linked 2

1373401_at	1.52E-0	4.69E-0	2.970261	Tnc	tenascin C
1373463_at	0.00092	0.0000716	2.9104047	Col5a2	collagen, type V, alpha 2
1373651_at	0.000613	0.0000355	6.495147		
1373839_at	5.22E-0	9.74E-0	4.155223		
1373882_at	3.98E-0	1.97E-0	2.473075		
1373908_at	0.006081592	0.001235174	4.2663445		
1373928_at	4.78E-0	8.20E-0	4.6853886	Il17re	interleukin 17 receptor E
1374172_at	4.05E-0	6.38E-0	3.5346124	Col8a2	collagen, type VIII, alpha 2
1374237_at	0.0216732	0.008565457	2.9913423	Lmod1	leiomodlin 1 (smooth muscle)
1375043_at	0.04799066	0.024809543	2.2700224		
1375144_at	0.006888195	0.001608664	2.374481		
1375170_at	4.24E-0	6.85E-0	3.698078	S100a11	S100 calcium binding protein A11
1375267_at	0.038247757	1.88E-0	2.4829235	Ppic	peptidylglycol isomerase C
1375739_at	0.00092	0.000069	2.4270043	Ehd4	EH--domain containing 4
1375857_at	0.03293959	0.0151767	2.095752	Myof	myoferlin
1376457_at	0.042823758	2.14E-0	2.8666012	Crispld2	cysteine--rich secretory protein LCCL domain containing 2
1376632_at	1.35E-0	3.96E-0	2.168106	Lmcd1	LIM and cysteine--rich domains 1
1376750_at	1.32E-0	3.78E-0	2.0378191		
1376818_at	0.024395643	1.01E-0	2.1558822	Whip	Wilms tumor 1 interacting protein
1376905_at	2.68E-0	1.16E-0	2.1944203		
1376937_at	1.45E-0	3.46E-0	3.8603601	Filip1l	filamin A interacting protein 1--like
1379936_at	0.004138464	0.000661	4.7772703		
1381504_at	2.45E-0	1.02E-0	2.603942	Aspn	asporin
1383058_at	0.004782096	0.000821	3.9789212		
1383322_at	0.006145863	0.001308714	3.5566857	Ras11b	RAS--like family 11 member 8
1385354_at	1.77E-0	6.07E-0	2.2685876	Itga8	integrin, alpha 8
1386911_at	0.0405929	0.020174915	2.378294	Atp1a2	ATPase, Na+/K+ transporting, alpha 2 polypeptide
1386921_at	0.01312728	0.003694504	6.138241	Cpe	carboxypeptidase E
1386940_at	3.27E-0	4.31E-0	2.397868	Timp2	TIMP metalloproteinase inhibitor 2
1386965_at	2.01E-0	7.63E-0	2.4958344	Lpl	lipoprotein lipase
1387232_at	0.00145111	0.000125	4.398603	Bmp4	bone morphogenetic protein 4
1387348_at	7.07E-0	1.68E-0	3.4784317	Igfbp5	insulin--like growth factor binding protein 5
1387351_at	6.33E-0	4.14E-0	3.1855562	Fbn1	fibrillin 1
1387581_at	0.011933667	0.003287118	3.499845	Rass9	Ras association (RalGDS/AF--6) domain family (N--terminal) member 9
1387616_at	0.011782614	0.00322196	2.4712117	Pdgfr	platelet derived growth factor C
1387854_at	0.000633	0.0000399	3.303193	Col1a2-LOC10091218	collagen, type I, alpha 2[[collagen alpha--2(I)] chain--like
1387922_at	2.20E-0	8.80E-0	3.1326766	Crispld2	cysteine--rich secretory protein LCCL domain containing 2
1387925_at	0.02888819	1.29E-0	2.0813034	Asns	asparagine synthetase (glutamine--hydrolyzing)
1387952_a_at	0.020473994	0.007887187	2.2983193	Cd44	Cd44 molecule
1388014_at	0.002994248	0.000358	4.152831	Obp1f	odorant binding protein 1 f
1388116_at	0.014139078	4.21E-0	3.0266993	Col1a1	collagen, type I, alpha 1
1388142_at	4.91E-0	8.82E-0	3.2232754	Vcan	versican
1388312_at	1.55E-0	4.93E-0	2.023181		
1388427_at	0.002043257	1.88E-0	3.2201211	Mara8	matrix--remodelling associated 8
1388557_at	2.00E-0	7.50E-0	4.9911227	C7/Tub4b	complement component 7[[tubulin, beta 48 class IVb
1388673_at	1.59E-0	5.16E-0	2.0289483	Lsp1	lymphocyte--specific protein 1
1388955_at	0.006249851	0.001363676	2.7368715		
1389092_at	2.21E-0	8.91E-0	2.0110495	Il2rg	interleukin 2 receptor, gamma
1389185_at	0.009171339	0.00232487	2.1861207	Ak1	adenylate kinase 1
1389234_at	0.031225063	0.014272533	3.757972	Vwf	von Willebrand factor
1389253_at	7.16E-0	1.72E-0	3.091454	Vnn1	vanin 1
1389533_at	0.028530663	0.012555627	2.5693622	Fbln2	fibulin 2
1389611_at	0.028530663	0.01264233	2.773913	Vldlr	very low density lipoprotein receptor
1389698_at	5.22E-0	1.01E-0	2.4832437		
1389966_at	2.83E-0	1.18E-0	4.744158	Col6a3	collagen, type VI, alpha 3
1390027_at	0.000181	0.00000506	6.7924924	Pcp4l1	Purkinje cell protein 4--like 1
1390250_x_at	1.08E-0	2.86E-0	2.2128115	LOC685152	ATPase, class I, type 8B, member 2
1390306_at	6.61E-0	1.50E-0	2.0875475	LOC100912470	uncharacterized LOC100912470
1390450_a_at	0.002994248	0.000365	2.89168	LOC100910855/Ogn	mimcan--like[[osteoglycin
1390472_at	0.02007464	0.007653206	2.431504	Naa	N--acylethanolamine acid amidase
1390547_at	0.025651934	0.010957114	3.3583617		
1393528_at	3.60E-0	1.71E-0	2.7502158	Synpo2	synaptopodin 2
1377761_at	0.003296671	4.44E-0	2.1618855	Gfpt2	glutamine--fructose--6--phosphate transaminase 2
1378258_at	0.015436175	0.004837284	2.2217898		
1378645_at	0.000633	0.0000417	6.4879146		
1378699_at	0.038017657	1.85E-0	2.4988987	Pkhd11	polycystic kidney and hepatic disease 1--like 1
1379022_at	1.52E-0	4.74E-0	2.7357194	Adams18	ADAM metalloproteinase with thrombospondin type 1 motif, 8
1380017_at	6.61E-0	1.50E-0	2.0447373		
1380063_at	0.039815117	1.96E-0	2.2410743	Ch25h	cholesterol 25--hydroxylase
1380077_at	3.82E-0	1.88E-0	2.2269967		
1380410_at	4.70E-0	2.40E-0	2.0704854		
1380682_at	0.00306171	0.000384	2.084744	Mex3b	mex3 homolog B (C. elegans)
1380726_at	1.32E-0	3.80E-0	2.7375722		
1380930_at	0.001606949	0.000144	2.021375	RGD1564142	similar to chromosome 10 open reading frame 64
1381088_at	0.019882035	0.007381354	2.0599062		
1381357_at	4.86E-0	2.53E-0	2.2652588	Ptpn22	protein tyrosine phosphatase, non--receptor type 22 (lymphoid)
1381450_at	0.020456001	0.007839426	2.3194776		
1382072_at	0.021586416	0.008444985	3.3730297	Olfml2a	olfactomedin--like 2A
1382905_at	1.35E-0	3.96E-0	2.459424		
1383284_at	1.57E-0	5.02E-0	2.43935		
1383291_at	0.019217895	0.006843543	3.8926442	C7/Tub4b	complement component 7[[tubulin, beta 48 class IVb
1383398_at	6.59E-0	1.46E-0	2.8107495	Itga8	integrin, alpha 8
1383469_at	1.18E-0	3.17E-0	2.4359684	Aldh1a3	aldehyde dehydrogenase 1 family, member A3
1383708_at	0.004782096	0.000812	2.9687467	Itgbl1	integrin, beta--like 1
1384707_at	0.019217895	0.006866886	2.9341333	Scara5	scavenger receptor class A, member 5 (putative)
1384812_at	0.012606613	0.003520929	3.7688484		
1385608_at	2.31E-0	9.46E-0	2.189908	Rab7b	Rab7b, member RAS oncogene family
1385637_at	0.026473254	1.14E-0	2.7373888		
1385701_at	0.002746988	0.000309	4.1846795		
1386242_at	0.018725293	0.006503395	2.463274		
1390843_at	0.000122	2.44E-0	3.1479461	Cdc102a	coiled--coil domain containing 102A
1390912_at	1.87E-0	2.62E-0	6.5733566	Pcp4l1	Purkinje cell protein 4--like 1
1391039_at	1.27E-0	1.06E-0	3.8312535		
1391562_at	0.018939046	6.69E-0	2.4742591		
1391925_at	1.26E-0	3.52E-0	2.2955365	Ccl19	chemokine (C--C motif) ligand 19
1392274_at	2.84E-0	1.25E-0	3.1828156		
1392521_at	0.015912475	0.00511359	2.4317882		
1392645_at	2.06E-0	1.98E-0	2.5804687		
1392754_at	0.015020075	0.004586969	2.653747	Adam8	ADAM metalloproteinase domain 8
1392886_a_at	0.006736134	0.001549219	2.5240977	Fcrla	Fc receptor--like A
1393109_at	1.44E-0	4.34E-0	2.466343		
1393210_at	0.036970377	0.017784154	2.5019417	LOC100961383	extracellular matrix protein 2--like
1393225_at	0.000296	0.0000136	2.3276951	Adams10	ADAM metalloproteinase with thrombospondin type 1 motif, 10
1393240_at	2.26E-0	9.17E-0	2.4385018	Efemp2	EGF--containing fibulin--like extracellular matrix protein 2
1393250_at	2.26E-0	9.20E-0	2.0880785		
1393281_at	0.018798737	0.006603947	3.5936713	Cav1	caveolin 1, caveolae protein
1393330_at	2.37E-0	2.46E-0	3.36193	LOC100909539	uncharacterized LOC100909539
1393401_at	1.76E-0	6.00E-0	3.6327126		
1393559_at	0.00092	0.0000717	6.3740506		
1393708_at	0.03561064	0.016845752	2.3613	Bhlhe22	basic helix--loop--helix family, member e22
1394200_at	0.023150388	0.009518922	3.0160742	Hspa2	heat shock protein 2
1394451_at	3.12E-0	1.41E-0	2.5684376	Anxa1	annexin A1
1395166_at	0.004590933	7.61E-0	2.6662836	Ehd2	EH--domain containing 2

1395184_at	0.014385296	0.004317068	2.300228	Clec12a	C---type lectin domain family 12, member A
1395753_at	0.02160576	0.008495678	3.3889565	Eln	elastin
1396055_at	0.000633	3.84E--0	2.5738285	Col6a3	collagen, type VI, alpha 3

Female rat liver zone III signature

Probe Set ID	Corrected p--value	p--value	FCAbsolute	Gene Symbol	Gene Title
1367729_at	7.40E--0	8.87E--0	3.3560843	Oat	ornithine aminotransferase
1367733_at	0.009332594	0.002384375	2.2751527	Ca2	carbonic anhydrase 2
1368047_at	0.008036036	0.001988959	3.41109	Slc13a3	solute carrier family 13 (sodium--dependent dicarboxylate transporter), member 3
1368458_at	8.50E--0	5.94E--0	5.9561276	Cyp7a1	cytochrome P450, family 7, subfamily a, polypeptide 1
1369693_a_at	0.031172356	0.014183976	3.360717	Slc1a2	solute carrier family 1 (glial high affinity glutamate transporter), member 2
1369694_at	0.04495169	0.022670021	2.1028576	Slc1a2	solute carrier family 1 (glial high affinity glutamate transporter), member 2
1370282_at	8.47E--0	1.35E--0	2.6022782	Csrp2	cysteine and glycine--rich protein 2
1370436_at	6.78E--1	1.35E--1	10.747984	Acsm2a	acyl--CoA synthetase medium--chain family member 2A
1376897_at	0.011782614	0.003221992	2.517401	Kif26b	kinesin family member 26B
1377161_at	4.29E--0	2.23E--0	3.9994276		
1377177_at	4.12E--0	1.97E--0	4.073607	Irx1	irquois homeobox 1
1377423_at	0.005939242	0.001161768	2.251542		
1381464_at	0.019707581	0.007159241	2.4482985	Tbx3	T--box 3
1388146_at	0.017932095	0.006192121	3.8361456	LOC100912222	uncharacterized LOC100912222
1379541_at	4.42E--1	3.53E--1	4.181176		
1379656_a_at	0.002539977	2.79E--0	2.589711	Coro2a	coronin, actin binding protein 2A
1380351_at	0.045627158	0.023223404	2.1178446		
1381221_at	0.019988563	0.007491838	2.570647	RGD1311300	similar to T cell receptor V delta 6
1382953_at	0.004914751	8.83E--0	2.3394399		
1384312_at	9.25E--0	1.66E--0	6.597049	Irx1	irquois homeobox 1
1385707_at	1.39E--0	3.05E--0	2.9118605	Lect2	leukocyte cell--derived chemotaxin 2
1393160_at	0.003672809	5.57E--0	2.3327503		
1394681_at	2.83E--0	1.19E--0	2.2198792	Akr1c1	aldo--keto reductase family 1, member C--like
1395983_at	2.76E--0	9.92E--0	3.5884063	Rmdn2	regulator of microtubule dynamics 2

Dog bile duct signature

Probe Set ID	Corrected p--value	p--value	FCAbsolute	Gene Symbol	Gene Title
AFFX--PheX--5_at	0.003869136	0.003559725	10.043593		
AFFX--r2--Bs--thr--M_s_at	0.003742879	0.003421874	9.843218		
AFFX--Cfa--r2--Bs--thr--	0.004291911	0.00399201	11.424598		
Cfa.3796.1.A1_s_at	2.37638E--0	1.54981E--0	15.539841	ANXA13	annexin A13
Cfa.5.1.S1_s_at	0.007331138	0.007240068	12.706672	GNB3	guanine nucleotide binding protein (G protein), beta polypeptide 3
Cfa.305.1.A2_at	0.000972938	0.000667007	26.147636	HSPB8	heat shock 22kDa protein 8
CfaAffx.14256.1.S1_s_at	0.001234545	0.000901947	14.36072	PFKM	phosphofructokinase, muscle
Cfa.3524.1.S1_s_at	1.39486E--0	2.3392E--0	19.016079	EGF	epidermal growth factor
Cfa.3524.1.S2_at	4.17443E--0	9.82027E--0	16.59218	EGF	epidermal growth factor
Cfa.3514.1.S1_s_at	7.64362E--0	2.25511E--0	8.998031	CLDN2	claudin 2
Cfa.3850.1.S2_at	3.83694E--0	8.81084E--0	12.501918	CAV1	caveolin 1, caveolae protein, 22kDa
CfaAffx.21188.1.S1_s_at	0.005655398	0.005435856	8.941732	DUOX1	dual oxidase 1
Cfa.16181.1.S1_s_at	0.000471733	0.000256023	24.304327	CFTR	cystic fibrosis transmembrane conductance regulator (ATP--binding cassette sub--family
CfaAffx.7499.1.S1_s_at	0.000975191	0.000669308	16.594934	SOX9	SRY (sex determining region Y)--box 9
Cfa.3484.1.S1_at	3.64074E--0	3.42026E--0	11.330937	PGR	progesterone receptor
CfaAffx.20792.1.S1_s_at	2.15434E--0	3.93067E--0	93.27175	SLCSA1	solute carrier family 5 (sodium/glucose cotransporter), member 1
Cfa.16330.1.S1_s_at	8.44046E--0	2.52296E--0	52.612694	SLCO2A1	solute carrier organic anion transporter family, member 2A1
Cfa.15829.1.S1_at	5.07165E--0	5.59142E--0	14.0841465	CAV2	caveolin 2
Cfa.15812.1.S1_at	0.000187115	7.56887E--0	9.176506	CCL20	chemokine (C--C motif) ligand 20
Cfa.15798.1.S1_s_at	5.25678E--0	1.26522E--0	16.751566	FUT8	fucosyltransferase 8 (alpha (1,6) fucosyltransferase)
Cfa.3473.1.S1_at	9.75793E--0	1.44702E--0	11.389474	CAV2	caveolin 2
CfaAffx.10800.1.S1_s_at	0.000593791	0.000351218	22.233406	EOGT	glycosyltransferase AER61
Cfa.3780.1.S1_at	5.24963E--0	1.19898E--0	98.86601	WFDC2	WAP four--disulfide core domain 2
Cfa.138.1.A1_at	3.14967E--0	6.1135E--0	8.20898	ANXA2	annexin A2
Cfa.6416.1.A1_at	5.81695E--0	6.95505E--0	40.79555	SGCG	sarcoglycan, gamma (35kDa dystrophin--associated glycoprotein)
Cfa.200.1.A1_at	2.43162E--0	1.74963E--0	53.49894	TFF3	trefoil factor 3 (intestinal)
Cfa.3872.1.S1_at	0.000645192	0.000395089	11.260409	GP2	glycoprotein 2 (zymogen granule membrane)
Cfa.16246.1.S1_at	0.002043447	0.001661094	17.606924	GIF	gastric intrinsic factor (vitamin B synthesis)
Cfa.81.1.S1_at	2.22494E--0	1.37478E--0	8.526816	ANXA4	annexin A4
Cfa.135.1.S1_at	0.00017338	6.78139E--0	45.842575	LAMC2	laminin, gamma 2
Cfa.15807.1.S1_at	0.000906825	0.000611121	21.823992	CCL28	chemokine (C--C motif) ligand 28
Cfa.3800.1.S1_s_at	1.42943E--0	7.10276E--0	46.887123	CD44//LOC100688143	CD44 molecule (Indian blood group)//CD44 antigen--like
Cfa.7074.1.A1_at	2.55595E--0	1.94474E--0	220.8137	MUC1	mucin 1, cell surface associated
Cfa.797.1.S1_at	3.40139E--0	7.44715E--0	29.41107	LGALS3	lectin, galactoside--binding, soluble, 3
CfaAffx.22164.1.S1_s_at	0.000104302	3.37517E--0	13.130114	LGALS3	lectin, galactoside--binding, soluble, 3
CfaAffx.9899.1.S1_s_at	2.43162E--0	1.71508E--0	8.841413	SPINT2	serine peptidase inhibitor, Kunitz type, 2
Cfa.3586.1.S1_at	5.59529E--0	1.45964E--0	171.23973	DUOX2	dual oxidase 2
Cfa.3854.1.S1_at	1.76859E--0	9.6119E--0	23.907526	CD9	CD9 molecule
Cfa.20172.1.S1_s_at	0.001840153	0.001457372	14.153175	SLIT2	slit homolog 2 (Drosophila)
Cfa.3915.1.S1_s_at	1.29669E--0	2.09694E--0	89.85594	LAMB3	laminin, beta 3
Cfa.3911.1.S1_s_at	0.006643785	0.00649355	8.525797	IGF1R//LOC100687483	insulin--like growth factor 1 receptor//uncharacterized LOC100687483
Cfa.299.1.A1_at	0.000426081	0.000227265	18.573118	FABP3	fatty acid binding protein 3, muscle and heart (mammary--derived growth inhibitor)
Cfa.299.1.A1_s_at	0.002594559	0.002203764	22.271511	FABP3	fatty acid binding protein 3, muscle and heart (mammary--derived growth inhibitor)
Cfa.1238.1.A1_at	3.83706E--0	3.75364E--0	8.268237	GSN	gelsolin
Cfa.5295.1.A1_at	0.000112549	3.79415E--0	8.750082	PLP2	proteolipid protein 2 (colonic epithelium--enriched)
Cfa.410.1.A1_at	2.81129E--0	5.544E--0	28.783533	PLLP	plasmalipin
Cfa.12226.1.A1_at	0.001562756	0.00119148	17.580036	LOC478056	double--headed protease inhibitor, submandibular gland--like
Cfa.7131.1.A1_at	4.54676E--0	1.08315E--0	12.81181		
Cfa.12202.1.A1_at	1.73037E--0	8.96368E--0	103.865326	GPX2	glutathione peroxidase 2 (gastrointestinal)
Cfa.11754.1.A1_at	3.80055E--0	2.72657E--0	13.1838	ZNFS32	zinc finger protein 532
CfaAffx.1121.1.S1_s_at	2.42024E--0	4.58492E--0	16.640472	ZNFS32	zinc finger protein 532
Cfa.2400.1.A1_at	8.72809E--0	2.87519E--0	13.771323	FRZB	frizzled--related protein
Cfa.6341.1.A1_at	1.4277E--0	6.87248E--0	9.095833	PDZK1IP1	PDZK1 interacting protein 1
Cfa.12206.1.A1_at	1.25855E--0	2.9314E--1	17.045073	LOC100685470	placenta--specific gene 8 protein--like
Cfa.12411.1.A1_at	4.31498E--0	4.99734E--1	18.171152	GALNT12	UDP--N--acetyl--alpha--D--galactosamine-polypeptide N--acetylglucosaminyltransferase
Cfa.6355.1.A1_at	4.56855E--0	9.57693E--0	42.157864	SLC13A2	solute carrier family 13 (sodium--dependent dicarboxylate transporter), member 2
Cfa.11867.1.A1_at	0.000529917	0.000301233	9.485682	FAM129A	family with sequence similarity 129, member A
Cfa.12228.1.A1_at	1.53355E--0	2.60752E--0	26.757048	SCGB1A1	secretoglobin, family 1A, member 1 (uterogloblin)
Cfa.12228.1.A1_s_at	3.66864E--0	8.23164E--0	14.342029	SCGB1A1	secretoglobin, family 1A, member 1 (uterogloblin)
Cfa.9465.1.A1_at	1.36184E--0	2.26369E--0	9.303793	SYT13	synaptotagmin XIII
Cfa.15610.1.A1_at	8.47325E--0	2.55508E--0	11.443425	GPR116	G protein--coupled receptor 116
Cfa.11992.1.A1_at	8.93141E--0	2.75293E--0	18.947681	TCEA2	transcription elongation factor A (SII), 2
Cfa.12149.1.S1_at	2.43162E--0	1.70948E--0	8.549634	ANXA5	annexin A5
Cfa.15654.1.A1_at	1.49387E--0	7.53896E--0	190.44144		
Cfa.10919.1.A1_at	0.000240513	0.000105131	31.484049	LOC100684429	protein BEK2--like
Cfa.2364.1.A1_at	0.000383856	0.000198186	13.561629		
Cfa.4902.1.A1_at	4.61022E--0	4.86794E--0	21.765694	PDGFD	platelet derived growth factor D
Cfa.12054.1.A1_s_at	2.43162E--0	1.82007E--0	17.810598	AHCYL2	adenosylhomocysteine--like 2
Cfa.7473.1.A1_at	1.83149E--0	1.76373E--0	19.267792	LOC100856512	epithelial discoidin domain--containing receptor 1--like
Cfa.13560.1.A1_at	0.00013376	4.73561E--0	22.416117	ARHGEF28	Rho guanine nucleotide exchange factor (GEF) 28
Cfa.11815.1.A1_at	2.35816E--0	1.50131E--0	40.20934	C3OH15orf48	chromosome 30 open reading frame, human C15orf48
Cfa.15678.1.A1_at	0.000125588	4.41443E--0	9.237352		
Cfa.11829.1.A1_s_at	0.000329412	0.000159776	16.668087	LOC100685413	uncharacterized LOC100685413
Cfa.6730.1.A1_at	0.001785864	0.001401793	12.475679	YPEL1	yippee--like 1 (Drosophila)
Cfa.13779.1.A1_at	2.43162E--0	1.81907E--0	18.245874	HNF1B	HNF1 homeobox B
Cfa.9812.1.A1_at	0.000122212	4.20174E--0	10.201421		

Cfa.4784.1.A1_at	0.000473699	0.000257813	8.9	LOC100856418	RIMS---binding protein 2---like
Cfa.12558.1.A1_s_at	6.34435E--Q	1.71439E--Q	10.627808	PRKD1	protein kinase D1
Cfa.9356.1.A1_at	2.38014E--Q	1.62618E--Q	18.04852	GOLM1	golgi membrane protein 1
Cfa.12344.1.A1_at	0.000529917	0.000301576	8.48218		
Cfa.6869.1.A1_at	0.000220324	9.32153E--Q	16.324532	C10H22orf23	chromosome 10 open reading frame, human C22orf23
Cfa.8427.1.A1_s_at	0.002564652	0.002159241	8.807109	AGBL5	ATP/GTP binding protein---like 5
Cfa.15675.1.A1_at	0.000182503	7.32562E--Q	29.112425		
Cfa.15783.1.A1_at	0.000232359	0.000100845	39.556606	FBP2	fructose---1,6---biphosphatase 2
Cfa.6345.1.A1_at	0.00025583	0.000115203	40.068394		
Cfa.11499.1.A1_at	0.006333116	0.006151601	9.5127125	FAM188B	family with sequence similarity 188, member B
Cfa.11200.1.A1_at	2.43162E--Q	1.76221E--Q	32.61186	MAP2	microtubule---associated protein 2
Cfa.11405.1.A1_at	0.002667964	0.002286827	8.56738	ALDH1L2	aldehyde dehydrogenase 1 family, member L2
Cfa.9852.1.A1_at	0.000916762	0.000620665	14.606047		
Cfa.7017.1.A1_s_at	6.34435E--Q	1.71908E--Q	16.092505	PDGFD	platelet derived growth factor D
Cfa.9405.1.A1_at	2.38014E--Q	1.60145E--Q	15.862546		
Cfa.12168.1.A1_s_at	6.35497E--Q	1.72689E--Q	64.0456	FAM38	family with sequence similarity 38, member B
Cfa.4763.1.A1_at	0.00500597	0.004745566	10.747296	FAM83F	family with sequence similarity 83, member F
Cfa.15635.1.A1_s_at	0.001557834	0.001184099	9.019208	NBEA	neurobeschin
Cfa.11944.1.A1_at	0.000928926	0.000631943	12.515857	LOC607638	uncharacterized LOC607638
Cfa.6733.1.A1_s_at	0.00023617	0.000102682	16.534458	AS89	ankyrin repeat and SOCS box containing 9
Cfa.9931.1.A1_at	8.48933E--Q	1.15344E--Q	15.2504425		
Cfa.2644.1.A1_at	9.01468E--Q	1.2667E--Q	10.687785	CA2	carbonic anhydrase II
Cfa.11162.1.A1_s_at	2.63116E--Q	2.05639E--Q	9.6108465	PPP2R2B	protein phosphatase 2, regulatory subunit B, beta
Cfa.9134.1.A1_at	9.56813E--Q	3.02749E--Q	19.740377		
Cfa.5536.1.A1_at	0.003228046	0.002877171	31.240194		
Cfa.9626.1.A1_at	0.005136023	0.004880817	15.981504	CCDC181	coiled---coil domain containing 181
Cfa.11192.1.A1_at	2.89827E--Q	2.47523E--Q	8.850655	ZNFS32	zinc finger protein 532
Cfa.10957.1.A1_at	1.07512E--Q	1.6611E--Q	27.859629	PLCB4	phospholipase C, beta 4
Cfa.11304.1.A1_at	0.000506688	0.000283241	24.45029	TPBG	trophoblast glycoprotein
Cfa.9613.1.A1_at	0.001198288	0.000869876	20.311426		
Cfa.8914.1.A1_at	0.002564652	0.002157676	15.412039	KCNIP1	kv channel interacting protein 1
Cfa.13606.1.A1_at	0.000248735	0.000111236	8.864612		
Cfa.6303.1.A1_at	1.18299E--Q	5.1746E--Q	17.025253	LENG1	leukocyte receptor cluster (LRC) member 1
Cfa.6303.1.A1_s_at	1.83149E--Q	1.71641E--Q	11.837524	TMC4	transmembrane channel---like 4
Cfa.10075.1.A1_at	3.29525E--Q	7.01008E--Q	11.215967	TTC39A	tetratricopeptide repeat domain 39A
Cfa.6250.2.A1_a_at	2.82493E--Q	5.59284E--Q	45.2246	LOC100685189	uncharacterized LOC100685189
Cfa.13946.1.A1_a_at	2.02653E--Q	1.16431E--Q	72.41698	FXVD	FXVD domain containing ion transport regulator 2
Cfa.13946.1.S1_s_at	1.79199E--Q	8.27163E--1	43.401356	FXVD2	FXVD domain containing ion transport regulator 2
Cfa.4050.1.A1_a_at	6.90787E--Q	1.97904E--Q	49.175045	TAC1	tachykinin, precursor 1
Cfa.6237.1.S1_at	5.78307E--Q	1.57149E--Q	40.79857	TPSAN8	tetraspanin 8
Cfa.9763.1.A1_at	0.00136314	0.001009756	10.531444		
Cfa.13845.1.A1_at	6.29106E--Q	1.75837E--Q	9.718362	CLDN2	claudin 2
Cfa.12050.1.A1_a_at	0.000166264	6.33816E--Q	34.11384	TPSAN5	tetraspanin 5
Cfa.13673.1.A1_at	9.21042E--Q	1.32293E--Q	100.64316	EHF	ets homologous factor
Cfa.8942.1.A1_at	0.002781115	0.002405405	13.618081		
Cfa.12462.1.A1_at	0.001647695	0.001279266	9.463901		
Cfa.12089.1.A1_at	0.003815219	0.003498272	42.163746	GRIP1	glutamate receptor interacting protein 1
Cfa.15294.1.A1_at	9.04904E--Q	3.21367E--Q	35.625492		
Cfa.9040.1.A1_at	0.000632845	0.000383245	21.525782		
Cfa.3167.1.A1_at	0.000105613	3.47337E--Q	52.66287	HGSF11	immunoglobulin superfamily, member 11
Cfa.9199.1.A1_at	3.726E--Q	3.54161E--Q	33.00564	FA2H	fatty acid 2---hydroxylase
Cfa.9240.1.S1_at	2.63116E--Q	2.07774E--Q	26.734303	SPP1	secreted phosphoprotein 1
Cfa.568.1.A1_at	0.002512046	0.002106374	9.927288		
Cfa.2576.1.S1_at	4.98594E--Q	1.22713E--Q	9.844979		
Cfa.7626.1.S1_s_at	0.001309742	0.00096502	18.615887	SPATA6	spermatogenesis associated 6
Cfa.448.1.S1_at	0.000434688	0.000232194	20.422358	TTC8	tetratricopeptide repeat domain 8
Cfa.9013.1.A1_at	0.002653102	0.002265848	8.560938		
Cfa.6848.1.A1_a_at	0.002593707	0.002201026	9.365253		
Cfa.6219.1.A1_at	6.99376E--Q	2.01984E--Q	79.31575	TMEM54	transmembrane protein 54
Cfa.6219.1.A1_s_at	0.000144151	5.15943E--Q	8.951576	TMEM54	transmembrane protein 54
Cfa.9487.1.A1_at	2.86766E--Q	5.83328E--Q	10.271737	MATN2	matrilin 2
Cfa.1629.1.A1_at	4.00496E--Q	4.01118E--Q	17.071047	DMXL2	Dmx---like 2
Cfa.10505.1.A1_at	2.27978E--Q	3.54003E--Q	47.12045	GPDI1	glycerol---3---phosphate dehydrogenase 1---like
Cfa.12666.1.A1_at	8.4289E--Q	2.51296E--Q	11.700338	FRAS1	Fraser syndrome 1
Cfa.15394.1.A1_at	2.18785E--Q	4.02578E--Q	18.510633	PDGFD	platelet derived growth factor D
Cfa.8787.1.A1_at	0.000149046	5.35779E--Q	17.388319		
Cfa.10048.1.A1_at	0.000672633	0.00041674	8.342149		
Cfa.18202.2.S1_a_at	0.000237232	0.000103513	25.82871	FEZ1	fasciculation and elongation protein zeta 1 (zyglin I)
Cfa.16308.1.S1_a_at	0.000295128	0.000137369	8.456769	PMP22	peripheral myelin protein 22
Cfa.16308.1.S1_s_at	0.005042257	0.004877796	9.202114	PMP22	peripheral myelin protein 22
Cfa.1637.1.S1_s_at	6.36162E--Q	7.85325E--Q	25.229582	SSBP2	single---stranded DNA binding protein 2
Cfa.1851.1.S1_at	1.3856E--Q	2.31292E--Q	23.51836	B3GALNT1	beta---1,3---N---acetylglactosaminyltransferase 1 (globoside blood group)
Cfa.9951.1.A1_at	5.76855E--Q	1.47797E--Q	11.192989		
Cfa.19449.1.S1_at	0.001498262	0.00112835	9.14352	GULP1	GULP, engulfment adaptor PTB domain containing 1
Cfa.16392.1.A1_at	3.89732E--Q	3.84286E--Q	16.956415		
Cfa.20396.1.S1_at	1.42943E--Q	7.0875E--Q	15.376722	BACE2	beta---site APP---cleaving enzyme 2
Cfa.2557.1.S1_at	0.004474087	0.004175351	11.688553	PLA2G4A	phospholipase A2, group IVA (cytosolic, calcium---dependent)
Cfa.2112.1.A1_at	1.14955E--Q	4.46255E--Q	14.489094		
Cfa.6261.1.S1_at	6.41178E--Q	7.96495E--Q	14.153604	KRTCAP3	keratinocyte associated protein 3
CfaAffx.13535.1.S1_s_at	0.000179098	7.14723E--Q	11.550629	MEIS2	Meis homeobox 2
Cfa.2730.1.S1_at	5.30574E--Q	5.89668E--Q	27.163088	RASEF	RAS and EF---hand domain containing
Cfa.19564.1.S1_at	0.000369317	0.000188966	25.519695	WNT5A	wingless---type MMTV integration site family, member 5A
Cfa.19670.1.S1_s_at	0.000171176	6.56529E--Q	15.045179	SORBS1	sorbin and SH3 domain containing 1
Cfa.16945.1.S1_at	0.001845267	0.001464179	15.017514	CCDC164	coiled---coil domain containing 164
CfaAffx.7441.1.S1_at	0.00514452	0.00489688	15.478372	CCDC164	coiled---coil domain containing 164
CfaAffx.7441.1.S1_s_at	0.000405237	0.000212057	16.535223	CCDC164	coiled---coil domain containing 164
Cfa.19675.1.S1_at	4.44219E--Q	4.62153E--Q	16.051968		
Cfa.6795.1.S1_at	0.000191069	7.75848E--Q	39.011192	LOC100683874	putative uncharacterized protein C17orf110---like
Cfa.14311.1.A1_at	1.45728E--Q	2.4552E--Q	126.81184	LOC100856604	riboflavin transporter 2---like
Cfa.9712.1.A1_at	7.71168E--Q	2.28117E--Q	10.10267		
Cfa.2624.1.A1_at	0.000370242	0.000190295	8.976321	ADAMTS6	ADAM metalloproteinase with thrombospondin type 1 motif, 6
Cfa.5528.1.S1_at	0.003491935	0.003153044	9.217439	PPP2R2B	protein phosphatase 2, regulatory subunit B, beta
Cfa.8772.1.A1_a_at	0.000092672	2.8996E--Q	60.3723	ADTRP	androgen---dependent TRP---regulating protein
Cfa.8772.1.A1_s_at	0.000234345	0.000156129	15.761602	ADTRP	androgen---dependent TRP---regulating protein
Cfa.7424.1.S1_s_at	0.001954213	0.001576418	9.576307	AMPO3	adenosine monophosphate deaminase 3
Cfa.13580.1.S1_at	0.000172218	6.68463E--Q	11.094712	LOC100856418	RIMS---binding protein 2---like
Cfa.11894.1.A1_s_at	2.84543E--Q	5.72936E--Q	44.619247		
Cfa.10538.1.A1_at	8.06558E--Q	1.06456E--Q	9.818013	PIDN	pigeon homolog (Drosophila)
Cfa.18211.1.A1_s_at	0.000999753	0.000691599	18.922766	EFCA11	EF---hand calcium binding domain 11
Cfa.7090.1.S1_s_at	9.44042E--Q	2.96846E--Q	8.721469	ABI2	abi---interactor 2
Cfa.14245.1.A1_s_at	1.1018E--Q	1.71942E--Q	35.557804	GPR110	G protein---coupled receptor 110
Cfa.14251.1.A1_at	0.000175667	6.94165E--Q	50.415653	ITIC12	tetratricopeptide repeat domain 12
Cfa.14251.1.A1_s_at	0.000582842	0.00033984	10.492943	ITIC12	tetratricopeptide repeat domain 12
Cfa.1387.1.A1_at	5.97131E--Q	7.27869E--Q	12.418851	AGRN	agrin
Cfa.2927.1.S1_at	1.79199E--Q	1.27915E--Q	40.349648	LOC100683693	signal transducer CD24---like
Cfa.17958.1.S1_s_at	1.79199E--Q	9.03941E--1	16.685595	MARCKSL1	MARCKS---like 1
Cfa.10891.1.A1_at	0.00179293	0.00140895	15.239695	TMEM218	transmembrane protein 218
Cfa.1193.1.S1_at	8.96837E--Q	1.24638E--Q	12.186453		
Cfa.15083.1.S1_at	0.000638686	0.000389757	11.237442	EFEMP1	EGF containing fibulin---like extracellular matrix protein 1
CfaAffx.5306.1.S1_s_at	0.001051459	0.000741246	16.361128	EFEMP1	EGF containing fibulin---like extracellular matrix protein 1
Cfa.11001.1.A1_at	0.000545716	0.000312261	23.016708		
Cfa.4306.1.S1_a_at	5.78307E--Q	1.54603E--Q	16.107666	S100A6	S100 calcium binding protein A6
Cfa.4306.1.S1_s_at	2.27978E--Q	3.441E--Q	10.680236	S100A6	S100 calcium binding protein A6
Cfa.1851.2.S1_s_at	0.000574439	0.000333603	51.33899	B3GALNT1	beta---1,3---N---acetylglactosaminyltransferase 1 (globoside blood group)
Cfa.4322.1.A1_at	2.83092E--Q	2.3298E--Q	17.23415		

Cfa.233.1.A1_at	0.000312638	0.000147823	35.695683	KIAA1324	KIAA1324 ortholog
Cfa.13795.1.A1_at	9.14188E-0	1.29179E-0	11.809833	CYBRD1	cytochrome b reductase 1
Cfa.17853.1.S1_at	4.54676E-0	1.08374E-0	8.419062	LOC100856291	neuronal protein 3.1--like
Cfa.19443.1.S1_at	0.000206488	8.59266E-0	14.231235	CDC160	coiled--coil domain--containing protein 160--like
Cfa.15316.1.A1_at	0.000376621	0.000193866	15.592182	ECSCR	endothelial cell surface expressed chemotaxis and apoptosis regulator
Cfa.432.1.A1_at	1.79199E-0	1.20008E-0	12.247755	PRSS23	protease, serine, 23
Cfa.10902.1.S1_at	8.46977E-0	2.54488E-0	49.476177	UGT8	UDP glycosyltransferase 8
Cfa.16364.1.A1_at	7.03631E-0	8.90464E-0	10.878502		
Cfa.9769.1.A1_at	0.00252043	0.002115361	9.432722		
Cfa.12664.2.A1_s_at	7.47728E-0	9.62025E-0	8.367712	ANK3	ankyrin 3, node of Ranvier (ankyrin G)
Cfa.8772.2.A1_at	6.86343E-0	8.61819E-0	264.53848	ADTRP	androgen--dependent TFPI--regulating protein
Cfa.13994.1.S1_at	0.000437261	0.000233907	71.30538	TFPI2	tissue factor pathway inhibitor 2
Cfa.4115.1.A1_at	0.006868676	0.006740688	13.140668	DSCAML1	Down syndrome cell adhesion molecule like 1
Cfa.10484.1.S1_at	1.06179E-0	1.59927E-0	8.721476	SLC38A1	solute carrier family 38, member 1
Cfa.10484.1.S1_s_at	0.002756828	0.002380119	9.269938	SLC38A1	solute carrier family 38, member 1
Cfa.1339.1.A1_at	6.71065E-0	1.90691E-0	8.186108	CHGA	chromogranin A (parathyroid secretory protein 1)
Cfa.15992.1.S1_at	1.79199E-0	1.04071E-0	16.636522	ROGDI	rogdi homolog (Drosophila)
Cfa.16704.1.S1_at	4.63676E-0	4.93196E-0	54.43405	ST6GALNAC2	ST6 (alpha--N--acetyl--neuraminy--2,3--beta--galactosyl--1,3)--N--acetylgalactosaminide alpha--2,6--sialyltransferase 2
Cfa.4077.1.S1_at	2.27978E-0	3.47749E-0	107.21464	CA4	carbonic anhydrase IV
Cfa.4077.1.S1_s_at	7.24987E-0	9.2312E-0	99.15406	CA4	carbonic anhydrase IV
Cfa.16994.1.S1_at	1.55125E-0	2.66169E-0	8.877538	ITGA3	integrin, alpha 3 (antigen CD49C, alpha 3 subunit of VLA--3 receptor)
Cfa.4359.1.S1_at	0.000366501	0.000187234	17.194208	LOC484210	serine/threonine--protein kinase WNK2--like
Cfa.16786.1.S1_at	1.79199E-0	1.39129E-0	13.79786	RRAGD	Ras--related GTP binding D
Cfa.18710.1.S1_at	0.007119413	0.00701439	12.993197	GATM	glycine amidinotransferase (L--arginine:glycine amidinotransferase)
Cfa.4306.2.S1_a_at	8.10883E-0	2.39236E-0	16.26344	S100A6	S100 calcium binding protein A6
Cfa.21327.1.S1_at	0.000242746	0.000106673	14.941704	LCN	allergen Fel d 4--like
Cfa.21053.1.S1_s_at	0.000687201	0.000430034	8.488392	OXCT1	3--oxoacid CoA transferase 1
Cfa.20636.1.S1_at	7.10232E-0	2.05681E-0	10.106704	PPP1R1B	protein phosphatase 1, regulatory (inhibitor) subunit 1B
CfaAffx.7185.1.S1_s_at	0.001874397	0.001496025	13.840655	SPAG6	sperm associated antigen 6
Cfa.18546.1.S1_at	3.93658E-0	9.13799E-0	48.862844	SPAM1	sperm adhesion molecule 1 (PH--20 hyaluronidase, zona pellucida binding)
Cfa.16067.1.S1_at	0.002464639	0.002055142	10.80802	DNAJA4	DnaI (Hsp40) homolog, subfamily A, member 4
Cfa.18258.1.S1_a_at	0.000276742	0.000126553	11.285985	LOC100856746	protein FAM107A--like
Cfa.20479.1.S1_s_at	0.007937967	0.007870174	9.452199	KIF5C	kinesin family member 5C
Cfa.20847.1.S1_s_at	3.64699E-0	8.09812E-0	66.21445	TCN1	transcobalamin I (vitamin B12 binding protein, R binder family)
Cfa.20309.1.S1_s_at	0.003609962	0.003273219	10.050318	PDE1C	phosphodiesterase 1C, calmodulin--dependent 70kDa
CfaAffx.22343.1.S1_at	0.003866478	0.003554278	9.335956	SAV1	salvador homolog 1 (Drosophila)
Cfa.20005.1.S1_s_at	6.38256E-0	1.73935E-0	12.749285	ATL1	atlantin GTPase 1
Cfa.21572.1.S1_at	2.74062E-0	2.21292E-0	11.265955	AGRN	agrin
Cfa.19066.1.S1_at	0.00393876	0.00362684	10.475471	NXN	nucleoredoxin
Cfa.19027.1.S1_s_at	6.52426E-0	1.87421E-0	10.889626	ME2	malic enzyme 2, NAD(+)--dependent, mitochondrial
Cfa.19237.1.S1_at	0.001421088	0.001055886	8.466962	GMD5	GDP--mannose 4,6--dehydratase
Cfa.17122.1.S1_at	2.27978E-0	3.01574E-0	52.886612	RIPPLY1	ripplly1 homolog (zebrafish)
Cfa.16962.1.S1_s_at	0.000324345	0.000156015	13.148721	LTBP2	latent transforming growth factor beta binding protein 2
Cfa.5528.2.S1_s_at	0.000418388	0.000221862	15.769544	PPP2R2B	protein phosphatase 2, regulatory subunit B, beta
Cfa.18961.1.S1_s_at	5.73496E-0	6.76837E-0	11.699898	SLC25A24	solute carrier family 25 (mitochondrial carrier; phosphate carrier), member 24
Cfa.20994.1.S1_s_at	0.005325746	0.005085922	8.650565	SBSPO1	somatomedin B and thrombospondin, type 1 domain containing
Cfa.17930.1.S1_s_at	0.000849041	0.000564929	14.38387	KCNK1	potassium channel, subfamily K, member 1
Cfa.17644.1.S1_s_at	0.000113158	3.8393E-0	11.530364	RRAGD	Ras--related GTP binding D
CfaAffx.4331.1.S1_at	0.00293813	0.002577707	25.150396	LRRIC1	leucine rich repeat containing 1
CfaAffx.7184.1.S1_s_at	0.000617721	0.000370729	9.024984	SPAG6	sperm associated antigen 6
Cfa.20373.1.S1_at	6.30708E-0	1.69919E-0	8.69777	ABR	active BCR--related
Cfa.17440.1.S1_s_at	0.001648207	0.001280943	16.945232	GPDI1	glycerol--3--phosphate dehydrogenase 1--like
Cfa.18519.1.S1_s_at	0.00041756	0.0002211	9.162884	CDC30	coiled--coil domain containing 30
Cfa.17191.1.S1_a_at	4.03343E-0	9.39463E-0	106.09082	KIAA1324	KIAA1324 ortholog
Cfa.20876.1.S1_s_at	0.001033539	0.000722194	14.438117	LOC100856197//LOC403737//LOC608055	d--3--phosphoglycerate dehydrogenase--like//d--3--phosphoglycerate dehydrogenase--like//d--3--phosphoglycerate dehydrogenase--like//d--3--phosphoglycerate dehydrogenase--like
CfaAffx.23343.1.S1_s_at	0.000860261	0.000574462	12.771817	CD9	CD9 molecule
Cfa.1186.1.A1_a_at	5.24963E-0	1.14669E-0	13.117786	CDC30	coiled--coil domain containing 30
Cfa.1186.1.A1_s_at	0.000105613	3.47668E-0	21.997078	CDC30	coiled--coil domain containing 30
Cfa.17318.1.S1_at	1.15825E-0	4.65623E-0	25.228182	KRT7//KRT86	keratin 7//keratin 86
CfaAffx.7229.1.S1_s_at	0.000172218	6.68548E-0	11.69753	ARMC3	armadillo repeat containing 3
Cfa.21268.1.S1_at	0.001203322	0.000874464	9.769259	LOC10085509//P	serine/threonine--protein phosphatase 2A regulatory subunit B" subunit beta--like//protein phosphatase 2, regulatory subunit B", beta
Cfa.20087.1.S1_s_at	8.69476E-0	1.19485E-0	18.12254	GALNT3	UDP--N--acetyl--alpha--D--galactosamine:polypeptide N--acetylglucosaminyltransferase
Cfa.20111.1.S1_s_at	1.69929E-0	2.99486E-0	17.963196	NSUN7	NOP2/Sun domain family, member 7
Cfa.14170.1.S1_s_at	3.0806E-0	6.40995E-0	36.635574	USH1C	Usher syndrome 1C (autosomal recessive, severe)
Cfa.17229.1.S1_s_at	8.48091E-0	2.56798E-0	13.963705	CHD3	chromodomain helicase DNA binding protein 3
Cfa.19166.1.S1_at	8.10614E-0	1.0762E-0	11.440071	KDM4B	lysine (K)--specific demethylase 4B
CfaAffx.14914.1.S1_s_at	0.000567662	0.000328703	8.328977	INPP1	inositol polyphosphate--1--phosphatase
Cfa.17207.1.S1_at	2.37638E-0	1.53907E-0	17.904182	LOC490390	uncharacterized LOC490390
Cfa.20055.1.A1_at	0.000474754	0.000259124	16.038736		
Cfa.21549.1.S1_at	3.37741E-0	7.35622E-0	23.89694	AQP3	aquaporin 3 (Gill blood group)
Cfa.9685.2.S1_a_at	8.48933E-0	1.13423E-0	8.386961	TSC2D1	TSC22 domain family, member 1
Cfa.15592.1.A1_at	0.000351687	0.000177482	12.443376		
Cfa.7054.1.A1_at	0.001444866	0.001078041	8.938738		
Cfa.7273.2.A1_a_at	0.001035165	0.000724133	11.468615		
Cfa.13829.1.A1_at	1.18299E-0	5.40078E-0	76.33072	MUC20	mucin 20, cell surface associated
Cfa.13946.2.A1_at	2.31118E-0	4.30256E-0	176.84499	FXVD2	FXVD domain containing ion transport regulator 2
Cfa.9383.1.A1_at	0.000835725	0.000554101	8.759654		
Cfa.5013.1.A1_at	0.000736	0.000468	22.861055		
Cfa.8021.1.A1_at	0.002359462	0.001954616	8.305117		
Cfa.15774.1.A1_at	0.002377298	0.00197493	8.487178		
Cfa.11662.1.A1_s_at	0.001091216	0.000775204	11.581353	LRRIC48	leucine rich repeat containing 48
Cfa.11503.1.A1_at	0.000111873	3.73488E-0	38.67133	MUC5B	mucin 5B, oligomeric mucus/gel--forming
Cfa.13470.2.A1_a_at	0.000242746	0.000106612	19.365654	DPEP1	dipeptidase 1 (renal)
Cfa.14260.1.A1_at	0.000227212	9.7529E-0	12.337224		
Cfa.2595.1.A1_at	0.005016063	0.004759029	17.13894	BAMBI	BMP and activin membrane--bound inhibitor homolog (Xenopus laevis)
Cfa.12531.1.A1_at	1.29721E-0	2.11502E-0	29.914022		
Cfa.6572.1.A1_a_at	0.001105755	0.000790683	16.627436		
Cfa.5104.1.A1_at	0.000563297	0.00032534	25.635275		
Cfa.12309.1.A1_s_at	5.36362E-0	1.35756E-0	28.35283	NSUN7	NOP2/Sun domain family, member 7
Cfa.10032.1.A1_at	0.000294983	0.000136764	21.372498		
Cfa.12467.2.A1_a_at	3.33042E-0	7.16247E-0	14.517796		
Cfa.9064.1.A1_at	0.00655419	0.006406619	10.495075	PLXNA2	plexin A2
Cfa.10739.1.S1_s_at	4.10135E-0	4.1714E-0	10.933695	CADMI1	cell adhesion molecule 1
Cfa.4720.1.A1_at	8.04512E-0	1.05561E-0	406.2316	DMBT1	deleted in malignant brain tumors 1
Cfa.15612.1.A1_at	0.000823612	0.000542893	36.006004		
Cfa.6228.1.A1_at	6.02377E-0	1.60883E-0	24.088121	SLC28A3	solute carrier family 28 (sodium--coupled nucleoside transporter), member 3
Cfa.432.2.A1_at	0.000124015	4.32319E-0	9.523299	PRSS23	protease, serine, 23
Cfa.12399.1.A1_at	0.005306216	0.005059032	8.325382		
Cfa.7057.1.A1_at	0.001473659	0.001104279	8.589191		
Cfa.7842.1.A1_s_at	1.22564E-0	1.96977E-0	8.735041	ENPP3	ectonucleotide pyrophosphatase/phosphodiesterase 3
Cfa.5672.1.A1_s_at	0.00491648	0.004637829	9.145544	LOC481027	kita--kyushu lung cancer antigen 1 homolog
Cfa.7163.1.A1_at	9.01468E-0	1.26681E-0	15.067506	TMEM51	transmembrane protein 51
Cfa.14357.1.A1_at	1.1823E-0	1.87258E-0	38.062428	DMBT1	deleted in malignant brain tumors 1
Cfa.14085.1.A1_at	2.18517E-0	4.00389E-0	29.697372		
Cfa.3164.1.A1_at	0.002769334	0.002393066	8.927593		
Cfa.8233.1.A1_s_at	0.000575018	0.00034385	12.923119	FHAD1	forkhead--associated (FHA) phosphopeptide binding domain 1
Cfa.7798.1.A1_at	0.000354401	0.000179127	46.60583	IGSF11	immunoglobulin superfamily, member 11
Cfa.9800.1.A1_at	0.000244302	0.000108305	58.60764	CTNND2	catenin (cadherin--associated protein), delta 2
Cfa.15600.1.A1_at	0.0018717	0.001492419	36.040375		
Cfa.11643.1.A1_at	0.001967299	0.001590029	13.703433		

Cfa.443.1.A1_at	2.06888E--0	1.22201E--0	18.593288		
Cfa.1553.1.A1_at	3.2053E--0	2.96142E--0	11.715248		
Cfa.2633.1.A1_at	0.001116881	0.000802474	29.366852	AVIL	advillin
Cfa.2428.1.A1_at	0.000563297	0.000325383	13.068334		
Cfa.2871.1.A1_at	0.003743216	0.003426437	14.25448	CLHC1	clathrin heavy chain linker domain containing 1
Cfa.13542.1.A1_at	5.82823E--0	7.01379E--0	42.930687	PKHD1	polycystic kidney and hepatic disease 1 (autosomal recessive)
Cfa.5582.1.A1_at	0.001234545	0.00090101	14.923911		
Cfa.2608.1.A1_at	0.000193509	7.90261E--0	50.38765	CDC42BPG	CDC42 binding protein kinase gamma (DMPK--like)
Cfa.9561.1.A1_at	0.004009479	0.003707523	9.048995		
Cfa.9165.1.A1_s_at	0.003473769	0.003133944	13.204778	EVA1C	eva--1 homolog C (C. elegans)
Cfa.6275.1.A1_at	0.007452053	0.007365266	9.88584		
Cfa.14200.1.A1_s_at	1.20991E--0	5.63624E--0	39.93073	ATP2C2	ATPase, Ca++ transporting, type 2C, member 2
Cfa.13645.1.A1_at	5.6036E--0	6.43892E--0	85.479256		
Cfa.14035.1.A1_at	8.03534E--0	1.04809E--0	17.227924		
Cfa.13720.1.A1_at	0.000747474	0.000478198	20.80519		
Cfa.7663.1.A1_at	0.003673806	0.003341876	8.311094		
Cfa.9166.1.A1_at	0.001847657	0.001468945	8.341711		
Cfa.13653.1.A1_at	3.83256E--0	8.71848E--0	21.15787	WFDC2	WAP four--disulfide core domain 2
Cfa.6288.1.A1_at	2.68868E--0	2.15011E--0	52.92139		
Cfa.13819.1.A1_at	0.000687201	0.00042842	18.518661	AHCYL2	adenosylhomocysteinase--like 2
Cfa.7146.1.A1_at	3.32894E--0	7.13345E--0	37.10383	LOC100685154	uncharacterized LOC100685154
Cfa.5138.1.A1_at	0.000699151	0.000663658	27.316141		
Cfa.6650.1.A1_at	0.003418094	0.0030731	9.507441		
Cfa.4896.1.A1_at	0.004583865	0.004281359	10.630574		
Cfa.6163.1.A1_at	0.001225255	0.000892305	16.857897		
Cfa.14884.1.A1_at	0.000681433	0.000423779	8.424942		
Cfa.13523.1.A1_at	0.000206543	8.62736E--0	24.255383		
Cfa.9770.1.A1_at	0.000370242	0.000190266	17.392803		
Cfa.1636.1.A1_s_at	4.50119E--0	4.71787E--0	9.899923	SSBP2	single--stranded DNA binding protein 2
Cfa.8974.1.A1_s_at	0.000764569	0.000496851	25.178776	PCSK1	proprotein convertase subtilisin/kexin type 1
Cfa.7863.1.A1_at	1.08817E--0	1.6897E--0	12.640788		
Cfa.14663.1.A1_at	0.001054697	0.000744347	32.580128		
Cfa.13135.1.A1_s_at	6.49341E--0	1.80485E--0	4.904747	CHD3	chromodomain helicase DNA binding protein 3
Cfa.9117.1.A1_at	5.74851E--0	1.50407E--0	13.558179	ELOVL7	ELOVL fatty acid elongase 7
CfaAffx.12643.1.S1_s_at	0.000459694	0.000248406	24.29481	O3FAR1	omega--3 fatty acid receptor 1
Cfa.5354.1.A1_at	3.92832E--0	3.90392E--0	8.186849	PIGR	polymeric immunoglobulin receptor
Cfa.9413.1.A1_at	0.001050327	0.000739057	20.306393	SVT13	synaptotagmin XIII
Cfa.6405.1.A1_at	0.005388094	0.005153829	9.564256		
Cfa.5182.1.A1_at	0.002108516	0.001720536	12.487829		
Cfa.10063.1.A1_at	0.001515429	0.001143631	9.324904	PTK2B	PTK2B protein tyrosine kinase 2 beta
Cfa.13369.1.A1_at	0.000152023	5.58077E--0	13.295719	PTX3	pentraxin 3, long
Cfa.7866.1.A1_at	6.99376E--0	2.01944E--0	17.879051		
Cfa.5150.1.A1_at	0.000657863	0.000405546	9.132712		
Cfa.4847.1.A1_at	2.8545E--0	2.41569E--0	19.487076		
Cfa.4686.1.A1_at	0.002158544	0.00176471	10.819988	MCAM	melanoma cell adhesion molecule
Cfa.4621.1.A1_at	0.00483238	0.004550992	8.743851		
Cfa.12645.1.A1_at	0.000105613	3.46454E--0	9.152567	C17H1orf56	chromosome 17 open reading frame, human C1orf56
Cfa.5913.1.A1_at	0.000293629	0.000135872	12.45811	GULP1	GULP, engulfment adaptor PTB domain containing 1
Cfa.5913.1.A1_s_at	3.06789E--0	2.69155E--0	15.204512	GULP1	GULP, engulfment adaptor PTB domain containing 1
Cfa.19508.1.A1_at	0.000125588	4.41704E--0	17.740232		
Cfa.9053.1.A1_at	0.001256946	0.000919288	14.37992		
Cfa.14003.1.A1_at	0.001961296	0.001583655	9.455918		
Cfa.13744.1.A1_at	3.82933E--0	3.71635E--0	119.84223		
Cfa.12837.1.A1_at	0.002832006	0.002456506	12.036987	LRRIC148	leucine rich repeat containing 148
Cfa.5475.1.A1_at	0.00136314	0.001011772	21.14226		
Cfa.3073.1.A1_at	1.16814E--0	4.80681E--0	11.233287		
Cfa.6574.1.A1_at	0.004086056	0.003786244	8.337941	DZIP1L	DAZ interacting protein 1--like
Cfa.8323.1.A1_at	0.000149963	5.43731E--0	17.878927		
Cfa.14061.1.A1_at	0.004439037	0.004139195	8.369896		
Cfa.6646.1.A1_at	8.70874E--0	2.66401E--0	10.048485	CEP104	centrosomal protein 104kDa
Cfa.2704.1.A1_at	9.18071E--0	1.3044E--0	15.417641		
Cfa.12976.1.A1_at	0.001455456	0.001088432	13.988864		
Cfa.6436.1.A1_at	2.3688E--0	4.4323E--0	39.493702	BAIAP2L2	BAI1--associated protein 2--like 2
Cfa.5711.1.A1_at	0.005655398	0.005432665	13.802143		
Cfa.3409.1.A1_at	5.73496E--0	6.76367E--0	27.067104	EHF	ets homologous factor
Cfa.16572.1.A1_at	1.05349E--0	1.57859E--0	15.730888		
Cfa.16636.1.S1_at	4.56855E--0	9.34294E--0	46.151787		
Cfa.3401.1.A1_at	0.002590283	0.002192172	8.556105		
CfaAffx.13709.1.S1_s_at	0.006333116	0.006156103	8.21997	CA13	carbonic anhydrase XIII
CfaAffx.230.1.S1_at	0.000333561	0.000163414	25.099607	LOC608794	uncharacterized LOC608794
CfaAffx.268.1.S1_at	0.001100522	0.000786087	18.499342	LOC481027	kita--kyushu lung cancer antigen 1 homolog
CfaAffx.297.1.S1_at	0.000758929	0.000488472	20.099873		
CfaAffx.324.1.S1_at	0.002239322	0.00184292	16.18011	LOC100856280	uncharacterized LOC100856280
CfaAffx.426.1.S1_at	0.000859025	0.000572239	14.487288	COR2AV2	COR2AV2 olfactory receptor family 2 subfamily AV--like
CfaAffx.491.1.S1_at	0.000622841	0.000375591	10.201038		
CfaAffx.808.1.S1_s_at	3.35579E--0	7.25061E--0	33.33017	CLC28	chemokine (C--C motif) ligand 28
CfaAffx.851.1.S1_s_at	5.33885E--0	1.343E--0	27.723545	C20H15orf48	chromosome 30 open reading frame, human C15orf48
CfaAffx.1041.1.S1_at	0.00022232	0.00010061	14.499216	SEPPINB8	serpin peptidase inhibitor, clade B (ovalbumin), member 8
CfaAffx.1224.1.S1_s_at	2.23679E--0	4.1332E--0	10.316443	ME2	malic enzyme 2, NAD(+)-dependent, mitochondrial
CfaAffx.1271.1.S1_at	0.000575323	0.000335009	10.90161	STAC3	SH3 and cysteine rich domain 3
CfaAffx.1400.1.S1_at	0.000724003	0.000459247	31.027843	AVIL	advillin
CfaAffx.1435.1.S1_at	0.001005349	0.000696563	9.146038	ZNF354C	zinc finger protein 354C
CfaAffx.1463.1.S1_s_at	0.000301525	0.00014093	19.872036	LOC100856646	calpain--7--like protein--like
CfaAffx.1465.1.S1_s_at	0.000404793	0.000211126	22.973515	LOC100856646	calpain--7--like protein--like
CfaAffx.1466.1.S1_at	1.07512E--0	1.64328E--0	55.601704	LOC100856646	calpain--7--like protein--like
CfaAffx.1646.1.S1_s_at	8.40561E--0	2.5938E--0	25.467722	TSPAN8	tetraspanin 8
CfaAffx.1679.1.S1_at	0.001311066	0.000967013	9.302989	NIPAL2	NIPA--like domain containing 2
CfaAffx.1750.1.S1_s_at	3.7253E--0	8.42317E--0	13.651545	SPAG1	sperm associated antigen 1
CfaAffx.1885.1.S1_s_at	1.14258E--0	4.34677E--0	13.382188	SLC12A2	solute carrier family 12 (sodium/potassium/chloride transporters), member 2
CfaAffx.1888.1.S1_at	5.73496E--0	6.81249E--0	20.577137	SLC12A2	solute carrier family 12 (sodium/potassium/chloride transporters), member 2
CfaAffx.1888.1.S1_s_at	3.1349E--0	2.85623E--0	19.66593	SLC12A2	solute carrier family 12 (sodium/potassium/chloride transporters), member 2
CfaAffx.1922.1.S1_s_at	8.40561E--0	2.6757E--0	51.051975	SLC44A4	solute carrier family 44, member 4
CfaAffx.2078.1.S1_s_at	0.00162223	0.001251198	8.699302	PACRG	PARK2 co--regulated
CfaAffx.2119.1.S1_s_at	0.007120309	0.007020801	8.568912	LOC481728	butyrophilin--like protein 1--like
CfaAffx.2121.1.S1_at	2.42899E--0	4.62036E--0	30.862347	LOC100856021	butyrophilin subfamily 1 member A1--like
CfaAffx.2174.1.S1_at	3.726E--0	3.55822E--0	35.4295	SAMD12	sterile alpha motif domain containing 12
CfaAffx.2292.1.S1_at	6.59819E--0	1.85998E--0	11.755526	ROS1	c--ros oncogene 1, receptor tyrosine kinase
CfaAffx.2294.1.S1_at	5.35824E--0	1.35204E--0	14.945389	ROS1	c--ros oncogene 1, receptor tyrosine kinase
CfaAffx.2591.1.S1_s_at	0.002048797	0.001667034	9.697935	NDRG1	N--myc downstream regulated 1
CfaAffx.2916.1.S1_at	2.90576E--0	5.41446E--0	20.030636	GOLM1	golgi membrane protein 1
CfaAffx.2951.1.S1_at	0.000780736	0.000509782	14.960096	MAPK13	mitogen--activated protein kinase 13
CfaAffx.2963.1.S1_at	6.73307E--0	1.91851E--0	58.973026	SLC28A3	solute carrier family 28 (sodium--coupled nucleoside transporter), member 3
CfaAffx.3038.1.S1_at	0.007059157	0.006938581	8.333131	BAIAP2L2	BAI1--associated protein 2--like 2
CfaAffx.3050.1.S1_at	0.000122212	4.20341E--0	11.514186	C10H2Zorf23	chromosome 10 open reading frame, human C22orf23
CfaAffx.3084.1.S1_at	0.000179469	7.17598E--0	23.122366	RASEF	RAS and EF--hand domain containing
CfaAffx.3139.1.S1_at	0.000253241	0.000113841	15.183069	CDC42EP1	CDC42 effector protein (Rho GTPase binding) 1
CfaAffx.3228.1.S1_s_at	1.17469E--0	4.92493E--0	28.60948	KCNK16	potassium channel, subfamily K, member 16
CfaAffx.3229.1.S1_at	0.002471367	0.002062671	8.895413	KCNK17	potassium channel, subfamily K, member 17
CfaAffx.3263.1.S1_at	0.005858573	0.005644789	22.412739	UNC5CL	unc--5 homolog C (C. elegans)--like
CfaAffx.3294.1.S1_at	4.05096E--0	9.46692E--0	38.19013	NCR2	natural cytotoxicity triggering receptor 2
CfaAffx.3408.1.S1_at	0.000176888	7.01784E--0	40.895737	IFNE	interferon, epsilon
CfaAffx.3545.1.S1_at	1.07059E--0	3.98977E--0	179.16513	SPAM1	sperm adhesion molecule 1 (PH--20 hyaluronidase, zona pellucida binding)
CfaAffx.3574.1.S1_at	0.000315591	0.000150578	8.350628	ASB15	ankyrin repeat and SOCS box containing 15
CfaAffx.3737.1.S1_s_at	0.003684927	0.003355916	15.022637	C14H7orf63	chromosome 14 open reading frame, human C7orf63
CfaAffx.3948.1.S1_at	9.37478E--0	1.35381E--0	9.805205	ENPP5	ectonucleotide pyrophosphatase/phosphodiesterase 5 (putative)

ClaAffx.3983.1.S1_at	0.000337491	0.000165863	28.241486	TFPI2	tissue factor pathway inhibitor 2
ClaAffx.4020.1.S1_s_at	2.22494E-0	1.37724E-0	19.893684	GLI53	GLI5 family zinc finger 3
ClaAffx.4028.1.S1_s_at	0.000175667	6.93406E-0	12.0417185	GPR110	G protein--coupled receptor 110
ClaAffx.4066.1.S1_at	5.43032E-0	1.39552E-0	22.542818	NCK2	NCK adaptor protein 2
ClaAffx.4072.1.S1_at	3.05974E-0	6.29526E-0	15.5929785	PPP1R9A	protein phosphatase 1, regulatory subunit 9A
ClaAffx.4106.1.S1_s_at	3.1349E-0	2.82467E-0	8.316679	ANXA2	annexin A2
ClaAffx.4150.1.S1_s_at	3.11645E-0	6.53294E-0	21.15254	PKHD1	polycystic kidney and hepatic disease 1 (autosomal recessive)
ClaAffx.4200.1.S1_s_at	0.008022028	0.007959745	9.97598	EFHC1	EF--hand domain (C--terminal) containing 1
ClaAffx.4293.1.S1_at	2.06888E-0	1.23683E-0	22.554296	THSD7A	thrombospondin, type I, domain containing 7A
ClaAffx.4318.1.S1_at	0.000590211	0.000346378	12.481081	LOC100856559	clathrin light chain A--like
ClaAffx.4351.1.S1_at	8.60092E-0	2.61767E-0	49.85847	FAM83B	family with sequence similarity 83, member 8
ClaAffx.4532.1.S1_at	4.76435E-0	1.1504E-0	280.35873	AGR2	anterior gradient 2 homolog (Xenopus laevis)
ClaAffx.4532.1.S1_s_at	5.8699E-0	1.54344E-0	127.03371	AGR2	anterior gradient 2 homolog (Xenopus laevis)
ClaAffx.4549.1.S1_at	2.52459E-0	4.82181E-0	16.906698	BEND6	BEN domain--containing protein 6--like
ClaAffx.4615.1.S1_at	0.000109659	3.62694E-0	16.49695	GALNT12	UDP--N--acetyl--alpha--D--galactosamine:polypeptide N--acetylglucosaminyltransferase
ClaAffx.4623.1.S1_s_at	0.00060261	0.000576402	8.853461	DYNC2L1	dynein, cytoplasmic 2, light intermediate chain 1
ClaAffx.4646.1.S1_at	6.46002E-0	1.7755E-0	9.623337	MACC1	metastasis associated in colon cancer 1
ClaAffx.4655.1.S1_at	0.000154336	5.70373E-0	16.588612	ITGB8	integrin, beta 8
ClaAffx.4986.1.S1_s_at	0.001892844	0.001516626	16.454208	DNAH11	dynein, axonemal, heavy chain 11
ClaAffx.4988.1.S1_s_at	0.000822924	0.000541801	30.106031	DNAH11	dynein, axonemal, heavy chain 11
ClaAffx.5064.1.S1_s_at	0.004105404	0.003808974	14.966041	EML6	echinoderm microtubule associated protein like 6
ClaAffx.5079.1.S1_at	0.000223004	9.53832E-0	19.215984	ZNF462	zinc finger protein 462
ClaAffx.5084.1.S1_at	6.59819E-0	1.86471E-0	12.785454	ZNF462	zinc finger protein 462
ClaAffx.5146.1.S1_at	0.000835725	0.000552236	15.337511	LOC611704	uncharacterized LOC611704
ClaAffx.5550.1.S1_s_at	0.004993203	0.004729587	10.307933	LCN	allergen Fel d 4--like
ClaAffx.5565.1.S1_at	2.84543E-0	5.74388E-0	15.530967	SPACA1	sperm acrosome associated 1
ClaAffx.5584.1.S1_at	0.001115984	0.000800597	12.73976	LOC100856633	peptidase M20 domain--containing protein 2--like
ClaAffx.5585.1.S1_s_at	0.000404592	0.000210463	9.566137	GABRR11//GABRR2	gamma--aminobutyric acid (GABA) A receptor, rho 11//gamma--aminobutyric acid (GABA) A receptor, rho 2
ClaAffx.5597.1.S1_s_at	0.000359197	0.000182108	18.123672	ANKRD6	ankyrin repeat domain 6
ClaAffx.5712.1.S1_s_at	0.000805193	0.000526376	10.998292	NPSR1	neuropeptide S receptor 1
ClaAffx.5761.1.S1_at	0.002590383	0.002190581	16.262945	LOC482707	solute carrier family 23 member 2--like
ClaAffx.5787.1.S1_s_at	0.000174527	6.84286E-0	18.807266	BSPRY	B--box and SPRY domain containing
ClaAffx.5886.1.S1_s_at	2.43931E-0	4.16653E-0	10.975632	ANXA4	annexin A4
ClaAffx.6001.1.S1_at	0.002614392	0.002224669	8.695706	OSCP1	organic solute carrier partner 1
ClaAffx.6032.1.S1_s_at	0.000763916	0.00049524	10.664287	GRHL1	grainyhead--like 1 (Drosophila)
ClaAffx.6036.1.S1_s_at	1.20611E-0	1.91967E-0	23.64786	CAV2	caveolin 2
ClaAffx.6117.1.S1_s_at	0.000591446	0.000348071	11.806558	KLHL32	kelch--like 32 (Drosophila)
ClaAffx.6223.1.S1_s_at	1.99576E-0	3.56386E-0	15.133091	LOC482730	protein FAM115A--like
ClaAffx.6291.1.S1_at	0.000479983	0.000263096	17.041191	POU6F2	POU class 6 homeobox 2
ClaAffx.6292.1.S1_at	0.000344227	0.000170777	61.92335	POU6F2	POU class 6 homeobox 2
ClaAffx.6296.1.S1_at	0.000155112	5.75055E-0	63.453423	SLC13A1	solute carrier family 13 (sodium/sulfate symporters), member 1
ClaAffx.6296.1.S1_s_at	0.000744586	0.000475194	51.401405	SLC13A1	solute carrier family 13 (sodium/sulfate symporters), member 1
ClaAffx.6489.1.S1_at	0.000209917	8.78457E-0	154.2489	SCOC	short coiled--coil protein
ClaAffx.6555.1.S1_at	5.43345E-0	1.40055E-0	21.140106	SCML4	sex comb on midleg--like 4 (Drosophila)
ClaAffx.6581.1.S1_s_at	0.003243874	0.002893797	8.315182	TRPM4	transient receptor potential cation channel, subfamily M, member 4
ClaAffx.6687.1.S1_at	0.000518171	0.000291672	9.338868	AKD1	adenylyate kinase domain containing 1
ClaAffx.6688.1.S1_at	5.28326E-0	1.31261E-0	17.425278	AKD1	adenylyate kinase domain containing 1
ClaAffx.6699.1.S1_at	0.001840153	0.001458693	15.043034	AKD1	adenylyate kinase domain containing 1
ClaAffx.6747.1.S1_s_at	5.89748E-0	7.14291E-0	107.91786	SLC26A3	solute carrier family 26, member 3
ClaAffx.6743.1.S1_s_at	5.544E-0	1.44196E-0	46.823425	SLC26A3	solute carrier family 26, member 3
ClaAffx.6771.1.S1_s_at	9.95878E-0	3.1933E-0	27.7467	TTC39A	tetratricopeptide repeat domain 39A
ClaAffx.6866.1.S1_at	8.62054E-0	2.63034E-0	14.327895	RAB19	RAB19, member RAS oncogene family
ClaAffx.6875.1.S1_at	0.004816898	0.004532671	9.888635	TP53I3	tumor protein p53 inducible protein 3
ClaAffx.6885.1.S1_s_at	0.000212997	8.96308E-0	28.937567	PGR	progesterone receptor
ClaAffx.6975.1.S1_at	6.47396E-0	1.78939E-0	11.80613	C19orf68	chromosome 19 open reading frame 68
ClaAffx.7045.1.S1_s_at	0.001523158	0.001151829	19.802452	LOC100856352	tetratricopeptide repeat protein 26--like
ClaAffx.7149.1.S1_at	0.003534831	0.003197266	12.284031	ANXA5	annexin A5
ClaAffx.7149.1.S1_x_at	0.000975692	0.000671167	11.332041	ANXA5	annexin A5
ClaAffx.7221.1.S1_s_at	4.95888E-0	1.20891E-0	25.914322	SLC1A5	solute carrier family 1 (neutral amino acid transporter), member 5
ClaAffx.7346.1.S1_s_at	0.000610733	0.00036558	24.199978	ATP6V0A4	ATPase, H+ transporting, lysosomal V0 subunit a4
ClaAffx.7310.1.S1_s_at	0.00805424	0.00801672	8.802979	PRKD2	protein kinase D2
ClaAffx.7338.1.S1_s_at	0.001348446	0.00099563	39.187878	ATP6V0A4	ATPase, H+ transporting, lysosomal V0 subunit a4
ClaAffx.7375.1.S1_at	2.57291E-0	4.94144E-0	6.608115	PION	pigeon homolog (Drosophila)
ClaAffx.7390.1.S1_s_at	4.76435E-0	1.15031E-0	18.240587	PION	pigeon homolog (Drosophila)
ClaAffx.7608.1.S1_s_at	7.86483E-0	2.33258E-0	34.028984	MYO7B	myosin VIIb
ClaAffx.7845.1.S1_s_at	2.90576E-0	5.39491E-0	8.734603	TSC22D1	TSC22 domain family, member 1
ClaAffx.7972.1.S1_s_at	0.000191618	7.79562E-0	27.01191	HID1	HID1 domain containing
ClaAffx.8025.1.S1_s_at	0.00060261	0.000576303	10.258968	FRMD4A	FERM domain containing 4A
ClaAffx.8210.1.S1_at	2.38014E-0	1.62359E-0	86.568344	OLFM4	olfactomedin 4
ClaAffx.8262.1.S1_at	2.83666E-0	2.3689E-0	40.819233	PCDP1	primary ciliary dyskinesia protein 1
ClaAffx.8272.1.S1_at	2.38014E-0	1.58977E-0	23.90965	SCTR	secretin receptor
ClaAffx.8275.1.S1_at	0.003119594	0.002761131	9.155202	TMEM37	transmembrane protein 37
ClaAffx.8298.1.S1_s_at	0.000509964	0.000285469	10.386502	ITGB4	integrin, beta 4
ClaAffx.8384.1.S1_s_at	0.000104302	3.37687E-0	10.955408	DACH1	dachshund homolog 1 (Drosophila)
ClaAffx.8473.1.S1_s_at	2.40353E-0	3.91881E-0	36.17533	KLP5	Kruppel--like factor 5 (intestinal)
ClaAffx.8612.1.S1_s_at	3.41368E-0	7.50055E-0	48.608734	ST6GALNAC2	ST6 (alpha--N--acetyl--neuraminyl--2,3--beta--galactosyl--1,3)--N--acetylglucosaminide alpha--2,6--sialyltransferase 2
ClaAffx.9032.1.S1_at	0.000590267	0.000346919	32.814957	GPDL1	glycerol--3--phosphate dehydrogenase 1--like
ClaAffx.9033.1.S1_s_at	1.40546E-0	6.65632E-0	184.49016	FCGBP	Fc fragment of IgG binding protein
ClaAffx.9034.1.S1_s_at	4.36958E-0	4.51207E-0	360.41922	FCGBP	Fc fragment of IgG binding protein
ClaAffx.9035.1.S1_at	3.06789E-0	2.67819E-0	105.744	FCGBP	Fc fragment of IgG binding protein
ClaAffx.9199.1.S1_at	0.002507798	0.002100865	9.147075	DNAH17	dynein, axonemal, heavy chain 17
ClaAffx.9443.1.S1_at	0.000247567	0.000110137	33.347427	NEK10	NIMA (never in mitosis gene a)--related kinase 10
ClaAffx.9443.1.S1_s_at	0.001132642	0.000816944	11.057043	NEK10	NIMA (never in mitosis gene a)--related kinase 10
ClaAffx.9447.1.S1_s_at	0.000916762	0.000620618	8.649264	NEK10	NIMA (never in mitosis gene a)--related kinase 10
ClaAffx.9457.1.S1_s_at	0.000105613	3.44734E-0	8.847667	LGALS4	lectin, galactoside--binding, soluble, 4
ClaAffx.9559.1.S1_at	0.001984501	0.001605474	25.555239	ZMAT4	zinc finger, matrix--type 4
ClaAffx.9677.1.S1_s_at	4.67098E-0	5.04088E-0	29.371775	PLCB4	phospholipase C, beta 4
ClaAffx.9700.1.S1_at	2.13519E-0	3.87914E-0	21.480347	PLCB4	phospholipase C, beta 4
ClaAffx.9723.1.S1_at	0.000471714	0.000255525	16.612885	PLCB4	phospholipase C, beta 4
ClaAffx.9727.1.S1_at	0.008050141	0.007994059	10.242696	ADAM32	ADAM metalloproteinase domain 32
ClaAffx.9873.1.S1_at	0.006817245	0.006684923	12.779023	LOC607806	carbonyl reductase [NADPH] 2--like
ClaAffx.9928.1.S1_s_at	0.002564652	0.002156576	12.908589	LRRIQ1	leucine--rich repeats and IQ motif containing 1
ClaAffx.9930.1.S1_at	0.001577641	0.001207728	28.44302	LRRIQ1	leucine--rich repeats and IQ motif containing 1
ClaAffx.9992.1.S1_at	7.4676E-0	2.17998E-0	8.96077	FREM2	FRAS1 related extracellular matrix protein 2
ClaAffx.10165.1.S1_at	0.000140328	5.00081E-0	23.99654		
ClaAffx.10285.1.S1_at	0.003493907	0.003157537	8.748336	ATP11A	ATPase, class VI, type 11A
ClaAffx.10947.1.S1_s_at	0.001591508	0.00122051	12.734059	LOC478056	double--headed protease inhibitor, submandibular gland--like
ClaAffx.11002.1.S1_at	4.97776E-0	1.21739E-0	13.823738	LOC100856418	RIMS--binding protein 2--like
ClaAffx.11032.1.S1_s_at	0.00129207	0.000950995	9.699824	LOC475605	low--density lipoprotein receptor--related protein 2--like
ClaAffx.11235.1.S1_s_at	1.15825E-0	4.67615E-0	12.087567	CD44//LOC100688143	CD44 molecule (Indian blood group)///CD44 antigen--like
ClaAffx.11273.1.S1_at	9.18852E-0	1.31265E-0	57.24826	EHF	ets homologous factor
ClaAffx.11273.1.S1_s_at	8.40561E-0	2.6538E-0	33.874596	EHF	ets homologous factor
ClaAffx.11304.1.S1_at	8.70319E-0	1.20277E-0	85.689995	SLCSA8	solute carrier family 5 (iodide transporter), member 8
ClaAffx.11553.1.S1_at	0.002348833	0.001943988	14.275229	FXYD3	FXYD domain containing ion transport regulator 3
ClaAffx.11587.1.S1_at	7.5327E-0	9.76678E-0	11.448601	ELOVL7	ELOVL fatty acid elongase 7
ClaAffx.11609.1.S1_s_at	0.003332214	0.002977778	8.72305	SGCG	sarcoglycan, gamma (35kDa dystrophin--associated glycoprotein)
ClaAffx.11702.1.S1_at	0.000758929	0.000488389	25.114868	LOC100856692	protein FAM3D--like
ClaAffx.11721.1.S1_s_at	2.43162E-0	1.77885E-0	73.382706	LOC100683693//LOC100687322	signal transducer CD24--like//signal transducer CD24--like
ClaAffx.11840.1.S1_at	2.22494E-0	1.38195E-0	36.10939	KRT7//KRT86	keratin 7//keratin 86
ClaAffx.11969.1.S1_s_at	0.000755149	0.00048428	9.102153	TMEM232	transmembrane protein 232
ClaAffx.11972.1.S1_at	9.56163E-0	1.40307E-0	36.99334	TMEM232	transmembrane protein 232

ClaAffx.12064.1.S1_s_at	0.000250027	0.000112008	10.651009	GLTRD2	glycosyltransferase 8 domain containing 2
ClaAffx.12107.1.S1_s_at	0.000487164	0.000269215	19.524998	DZIP1L	DAZ interacting protein 1--like
ClaAffx.12169.1.S1_s_at	3.7253E-0	8.44555E-0	46.387142		
ClaAffx.12172.1.S1_s_at	0.000444135	0.000238964	8.813687	LOC100686326//LOC607646	ankyrin repeat domain--containing protein 26--like//ankyrin repeat domain--containing protein 26--like
ClaAffx.12187.1.S1_s_at	9.52585E-0	1.38838E-0	10.077421		
ClaAffx.12232.1.S1_s_at	3.82933E-0	3.71506E-0	16.010983	MAST4	microtubule associated serine/threonine kinase family member 4
ClaAffx.12239.1.S1_s_at	0.003271056	0.002920586	16.88818	MAST4	microtubule associated serine/threonine kinase family member 4
ClaAffx.12305.1.S1_s_at	0.00017569	6.95668E-0	11.893179	LOC100685840//LOC100685932	olfactory receptor SAN1--like//olfactory receptor SAN1--like
ClaAffx.12378.1.S1_s_at	0.000425228	0.00022648	21.960958	ABC89//VPS37B	ATP--binding cassette, sub--family B (MDR/TAP), member 9//vacuolar protein sorting 37 homolog B (S. cerevisiae)
ClaAffx.12438.1.S1_s_at	0.000153146	5.64784E-0	16.822815	SLC4A8	solute carrier family 4, sodium bicarbonate cotransporter, member 8
ClaAffx.12475.1.S1_s_at	0.002593707	0.002197335	12.150907	GALNT6	UDP--N--acetyl--alpha--D--galactosamine:polypeptide N--acetylglucosaminyltransferase
ClaAffx.12515.1.S1_s_at	0.008050141	0.008000915	9.95546	HIP1R	huntingtin interacting protein 1 related
ClaAffx.12524.1.S1_s_at	0.000652544	0.000401254	13.02908	HIP1R	huntingtin interacting protein 1 related
ClaAffx.12642.1.S1_s_at	0.006116667	0.005926709	10.601462	PCSK1	proprotein convertase subtilisin/kexin type 1
ClaAffx.12726.1.S1_s_at	0.000719325	0.000455721	10.501227	ASB14	ankyrin repeat and SOCS box containing 14
ClaAffx.12806.1.S1_s_at	0.005340368	0.005104031	10.077652	SRSF10	somatostatin B and thrombospondin, type 1 domain containing
ClaAffx.13041.1.S1_s_at	3.1349E-0	2.87203E-0	29.469414	FMN1	formin 1
ClaAffx.13140.1.S1_s_at	0.000172218	6.67317E-0	12.174981	ARHGEF28	Rho guanine nucleotide exchange factor (GEF) 28
ClaAffx.13169.1.S1_s_at	0.000601362	0.000357364	9.451588	SORBS1	sorbin and SH3 domain containing 1
ClaAffx.13191.1.S1_s_at	0.001684757	0.001314582	9.401873	SORBS1	sorbin and SH3 domain containing 1
ClaAffx.13633.1.S1_s_at	0.000476237	0.000260615	13.60731	E2F5	E2F transcription factor 5, p130--binding
ClaAffx.13680.1.S1_s_at	2.34933E-0	1.47745E-0	13.569626	SHROOM3	shroom family member 3
ClaAffx.13723.1.S1_s_at	4.24713E-0	4.35265E-0	12.6563015	CA2	carbonic anhydrase II
ClaAffx.13758.1.S1_s_at	0.003673806	0.003342935	9.189729	PRKCD	protein kinase C, delta 1
ClaAffx.13847.1.S1_s_at	0.000838813	0.000556821	16.712887	PLCH1	phospholipase C, eta 1
ClaAffx.13856.1.S1_s_at	0.000498974	0.000277418	9.769147	CX3CL1	chemokine (C--CX--C motif) ligand 1
ClaAffx.13886.1.S1_s_at	0.000987074	0.000680724	20.43905	FRAS1	Fraser syndrome 1
ClaAffx.13910.1.S1_s_at	0.000117016	3.99744E-0	8.436265	FRAS1	Fraser syndrome 1
ClaAffx.13926.1.S1_s_at	0.0001614	6.07756E-0	10.676167	LOC100680046//LOC10068579//LOC100855701//LOC478864//LOC607788//LOC609391//RPL21	60S ribosomal protein L21--like//60S ribosomal protein L21--like//60S ribosomal protein L21--like//60S ribosomal protein L21--like//60S ribosomal protein L21--like//60S ribosomal protein L21--like
ClaAffx.14036.1.S1_s_at	0.000471733	0.000256377	11.10872	KIAA1755	KIAA1755 ortholog
ClaAffx.14042.1.S1_s_at	6.17584E-0	1.65424E-0	20.344181	VEPH1	ventricular zone expressed PH domain homolog 1 (zebrafish)
ClaAffx.14202.1.S1_s_at	9.04904E-0	3.14582E-0	34.716095	DOCK5	dedicator of cytokinesis 5
ClaAffx.14222.1.S1_s_at	3.83694E-0	8.81781E-0	12.792562	DOCK5	dedicator of cytokinesis 5
ClaAffx.14227.1.S1_s_at	0.000264576	0.000120579	12.894	USH1C	Usher syndrome 1C (autosomal recessive, severe)
ClaAffx.14328.1.S1_s_at	1.18299E-0	5.40624E-0	38.942463	ADAM28	ADAM metalloproteinase domain 28
ClaAffx.14362.1.S1_s_at	1.00274E-0	1.49477E-0	9.281099	ADAM28	ADAM metalloproteinase domain 28
ClaAffx.14440.1.S1_s_at	9.48651E-0	2.99031E-0	21.798832	CDH17	cadherin 17, Li cadherin (liver--intestine)
ClaAffx.14527.1.S1_s_at	2.84517E-0	5.6616E-0	10.602098	GMD5	GDP--mannose 4,6--dehydratase
ClaAffx.14583.1.S1_s_at	0.000123828	4.30706E-0	80.58489	SFRP5	secreted frizzled--related protein 5
ClaAffx.14587.1.S1_s_at	0.000305705	0.000143596	37.05416	BCI2L15	BCI2--like 15
ClaAffx.14615.1.S1_s_at	0.000303975	0.000142311	9.479598	F2RL1	coagulation factor II (thrombin) receptor--like 1
ClaAffx.14676.1.S1_s_at	0.003158068	0.002800088	12.075594	ESRP1	epithelial splicing regulatory protein 1
ClaAffx.14683.1.S1_s_at	0.000247567	0.000110019	43.04233	ESRP1	epithelial splicing regulatory protein 1
ClaAffx.14702.1.S1_s_at	0.000114605	3.90389E-0	41.273003	CDC148	coiled--coil domain containing 148
ClaAffx.14756.1.S1_s_at	0.005912953	0.005701776	9.128182	LOC100855577	protein phosphatase 1 regulatory subunit 14D--like
ClaAffx.14775.1.S1_s_at	0.001126315	0.000810632	16.810213	SPINT1	serine peptidase inhibitor, Kunitz type 1
ClaAffx.15042.1.S1_s_at	5.24963E-0	1.22274E-0	25.425577	SPP1	secreted phosphoprotein 1
ClaAffx.15043.1.S1_s_at	1.06745E-0	1.6161E-0	35.5832	CLIC6	chloride intracellular channel 6
ClaAffx.15085.1.S1_s_at	6.49101E-0	1.79914E-0	15.453947	RUNX1	runx--related transcription factor 1
ClaAffx.15143.1.S1_s_at	9.52585E-0	1.39042E-0	8.219752	CBR3	carbonyl reductase 3
ClaAffx.15227.1.S1_s_at	1.55125E-0	2.65968E-0	45.651367	WFDX2	WAP four--disulfide core domain 2
ClaAffx.15538.1.S1_s_at	5.9161E-0	1.57054E-0	119.44347	ITGB6	integrin, beta 6
ClaAffx.15557.1.S1_s_at	0.000230413	9.91061E-0	69.44786	ITGB6	integrin, beta 6
ClaAffx.15557.1.S1_s_at	8.48718E-0	2.57647E-0	39.46737	ITGB6	integrin, beta 6
ClaAffx.15563.1.S1_s_at	0.000260978	0.000118129	80.769684		
ClaAffx.15565.1.S1_s_at	0.001176596	0.000851387	18.882612		
ClaAffx.15591.1.S1_s_at	0.000187467	7.59763E-0	17.282396	MUC5B	mucin 5B, oligomeric mucus/gel--forming
ClaAffx.15602.1.S1_s_at	4.89115E-0	1.18481E-0	163.58846	MUC5B	mucin 5B, oligomeric mucus/gel--forming
ClaAffx.15659.1.S1_s_at	0.003011295	0.002657768	9.276832	CTNND2	catenin (cadherin--associated protein), delta 2
ClaAffx.15668.1.S1_s_at	0.002890804	0.002520476	11.821953	CTNND2	catenin (cadherin--associated protein), delta 2
ClaAffx.15892.1.S1_s_at	0.002920206	0.002557448	27.857567	DSG1	Down syndrome cell adhesion molecule
ClaAffx.15899.1.S1_s_at	2.97655E-0	6.0779E-0	9.753296	BACE2	beta--site APP--cleaving enzyme 2
ClaAffx.15940.1.S1_s_at	0.000529877	0.000300318	11.08372	TMPS52	transmembrane protease, serine 2
ClaAffx.15971.1.S1_s_at	5.37562E-0	6.11536E-0	23.40372	MBOAT1	membrane bound O--acyltransferase domain containing 1
ClaAffx.15999.1.S1_s_at	0.001086294	0.00077002	14.146239	KCNQ1	potassium voltage--gated channel, KQT--like subfamily, member 1
ClaAffx.16002.1.S1_s_at	0.000351562	0.000177146	28.037931	KCNQ1	potassium voltage--gated channel, KQT--like subfamily, member 1
ClaAffx.16042.1.S1_s_at	2.4011E-0	4.51814E-0	16.160902	DCDC2	doublecortin domain containing 2
ClaAffx.16101.1.S1_s_at	0.000177705	7.06404E-0	9.903347	TPSAB5	tetraspanin 5
ClaAffx.16182.1.S1_s_at	5.73496E-0	6.79448E-0	38.51755	TCN1	transcobalamin 1 (vitamin B12 binding protein, R binder family)
ClaAffx.16190.1.S1_s_at	2.43162E-0	8.8127E-0	124.19287	TFPI3	trefoil factor 3 (intestinal)
ClaAffx.16335.1.S1_s_at	0.000232322	0.000100531	15.388324	TMA5F20	transmembrane 4 L six family member 20
ClaAffx.16375.1.S1_s_at	0.001883547	0.00150479	10.620576	SLC37A1	solute carrier family 37 (glycerol--3--phosphate transporter), member 1
ClaAffx.16571.1.S1_s_at	0.000232478	0.000155209	12.106237	ROC	Roc homolog (mouse)
ClaAffx.16576.1.S1_s_at	0.000997357	0.000689168	20.83024	LRRK1	leucine--rich repeat kinase 1
ClaAffx.16581.1.S1_s_at	0.000420584	0.000223354	23.015741	ELF3	ETV4--like factor 3 (ets domain transcription factor, epithelial--specific)
ClaAffx.16691.1.S1_s_at	0.000476237	0.000260673	13.443485	SOD1	SOD1 transmembrane family, member 1
ClaAffx.16714.1.S1_s_at	0.00293813	0.002575573	8.490257	CERS3	ceramide synthase 3
ClaAffx.16869.1.S1_s_at	0.001473659	0.001105244	8.741915	SPATA17	spermatogenesis associated 17
ClaAffx.16936.1.S1_s_at	0.000135784	4.81779E-0	9.786066	LOC100856197//LOC475815//LOC607327//LOC607890//LOC608055//LOC610301	d--3--phosphoglycerate dehydrogenase--like//d--3--phosphoglycerate dehydrogenase--like//d--3--phosphoglycerate dehydrogenase--like//d--3--phosphoglycerate dehydrogenase--like//d--3--phosphoglycerate dehydrogenase--like
ClaAffx.16982.1.S1_s_at	0.000291298	0.000134115	10.651318	IGSF11	immunoglobulin superfamily, member 11
ClaAffx.16998.1.S1_s_at	1.56461E-0	2.69854E-0	11.405106	ARHGEF38	Rho guanine nucleotide exchange factor (GEF) 38
ClaAffx.17007.1.S1_s_at	0.000187115	7.56104E-0	31.928825	ARHGEF38	Rho guanine nucleotide exchange factor (GEF) 38
ClaAffx.17027.1.S1_s_at	0.000618009	0.000371381	14.903154	SLC9A3	solute carrier family 9 (sodium/hydrogen exchanger), member 3
ClaAffx.17211.1.S1_s_at	0.001903122	0.001527817	12.446191	GIMAP1	GIMAP family P--loop NTPase domain containing 1
ClaAffx.17260.1.S1_s_at	0.000716013	0.000452511	10.4512005	PLEKHG4B	pleckstrin homology domain containing, family G (with RhoGEF domain) member 4B
ClaAffx.17264.1.S1_s_at	0.000151621	5.54453E-0	8.246776	ROBO4	roundabout, axon guidance receptor, homolog 4 (Drosophila)
ClaAffx.17273.1.S1_s_at	0.005323429	0.005079576	10.253711	PLEKHG4B	pleckstrin homology domain containing, family G (with RhoGEF domain) member 4B
ClaAffx.17421.1.S1_s_at	0.003992272	0.003682313	14.695663	PLEKH51	pleckstrin homology domain containing, family 5 member 1
ClaAffx.17424.1.S1_s_at	0.000206488	8.56439E-0	23.525618	PLEKH51	pleckstrin homology domain containing, family 5 member 1
ClaAffx.17517.1.S1_s_at	0.002854371	0.002482061	14.9277	SLC03A1	solute carrier organic anion transporter family, member 3A1
ClaAffx.17792.1.S1_s_at	0.000634457	0.000385699	17.808702	CASC1	cancer susceptibility candidate 1
ClaAffx.17875.1.S1_s_at	0.00048241	0.000265176	15.498193	BCAT1	branched chain amino--acid transaminase 1, cytosolic
ClaAffx.17962.1.S1_s_at	8.48933E-0	1.15115E-0	19.872154	KCNK1	potassium channel, subfamily K, member 1
ClaAffx.18050.1.S1_s_at	3.65522E-0	8.14545E-0	9.441288	GRAMD1B	GRAM domain containing 1B
ClaAffx.18086.1.S1_s_at	0.001713722	0.001339843	10.412281	ZFH2	zinc finger homeobox 2
ClaAffx.18401.1.S1_s_at	0.00198887	0.001612097	12.10773	PLXNA2	plexin A2
ClaAffx.18415.1.S1_s_at	0.000860261	0.000574199	20.14643	ST8SIA1	ST8 alpha--N--acetyl--neuraminidase 1
ClaAffx.18424.1.S1_s_at	0.000341267	0.000168514	12.144808		
ClaAffx.18577.1.S1_s_at	9.14676E-0	1.41831E-0	11.704167	TRPM8	transient receptor potential cation channel, subfamily M, member 8
ClaAffx.18590.1.S1_s_at	0.001785864	0.001401324	9.237141	TRPM8	transient receptor potential cation channel, subfamily M, member 8
ClaAffx.18590.1.S1_s_at	5.89206E-0	1.55336E-0	114.512985	TRPM8	transient receptor potential cation channel, subfamily M, member 8
ClaAffx.18867.1.S1_s_at	5.37212E-0	1.36388E-0	19.512232	AGAP1	ArfGAP with GTPase domain, ankyrin repeat and PH domain 1
ClaAffx.18890.1.S1_s_at	0.000304537	0.000142811	33.91604	ARSL	arylsulfatase family, member 1

CfaAffx.18933.1.S1_at	3.12321E--0	6.59394E--0	58.92371	UGT8	UDP glycosyltransferase 8
CfaAffx.18944.1.S1_s_at	2.69004E--0	5.22135E--0	66.03307	UGT8	UDP glycosyltransferase 8
CfaAffx.19017.1.S1_s_at	0.00017338	6.76716E--0	9.5354805	MLPH	melanophilin
CfaAffx.19098.1.S1_at	0.006381285	0.006207881	11.808089	cOR52A10//cOR52A12//cOR52A16//cOR52A17//cOR52A8//LOC609179//LOC610039	cOR52A10 olfactory receptor family 52 subfamily A--like//cOR52A12 olfactory receptor family 52 subfamily A--like//olfactory receptor family 52 subfamily A member 16//cOR52A17 olfactory receptor family 52 subfamily A--like//cOR52A8 olfactory receptor family 52 subfamily A--like//olfactory receptor 52A5--like//olfactory receptor 52A5--like
CfaAffx.19425.1.S1_s_at	1.76859E--0	9.55591E--0	58.310722	MUC13	mucin 13, cell surface associated
CfaAffx.19474.1.S1_s_at	9.84206E--0	3.14361E--0	139.55843	DMBT1	deleted in malignant brain tumors 1
CfaAffx.19521.1.S1_s_at	2.57698E--0	1.98075E--0	88.76967	DMBT1	deleted in malignant brain tumors 1
CfaAffx.19516.1.S1_s_at	1.76929E--0	3.13197E--0	91.078156	DMBT1	deleted in malignant brain tumors 1
CfaAffx.19517.1.S1_at	0.002911371	0.002546378	10.235342	BBS1	Bardet--Biedl syndrome 1
CfaAffx.19822.1.S1_at	1.87562E--0	1.06304E--0	382.56808	MUC20	mucin 20, cell surface associated
CfaAffx.19822.1.S1_s_at	2.31118E--0	4.30654E--0	31.736591	MUC20	mucin 20, cell surface associated
CfaAffx.20104.1.S1_at	6.46002E--0	1.76618E--0	9.578731	GPR64	G protein--coupled receptor 64
CfaAffx.20266.1.S1_at	0.000711135	0.000448877	8.683356	CXHXorf23	chromosome X open reading frame, human CXorf23
CfaAffx.20331.1.S1_at	6.54654E--0	1.83994E--0	14.949099	CLRN3	clarin 3
CfaAffx.20501.1.S1_s_at	0.000159368	5.97632E--0	8.892198	LOC100856156	lipase member H--like
CfaAffx.20618.1.S1_s_at	0.000122212	4.19978E--0	10.3375	IGF2BP2	insulin--like growth factor 2 mRNA binding protein 2
CfaAffx.20839.1.S1_at	1.73037E--0	9.00117E--0	13.587931	CADM1	cell adhesion molecule 1
CfaAffx.20842.1.S1_at	0.000902031	0.00060719	16.921839	CADM1	cell adhesion molecule 1
CfaAffx.20845.1.S1_s_at	5.8699E--0	1.54495E--0	8.360872	CADM1	cell adhesion molecule 1
CfaAffx.21149.1.S1_s_at	0.00015734	5.88802E--0	34.53605	DUOX2	dual oxidase 2
CfaAffx.21225.1.S1_s_at	2.27978E--0	3.01064E--0	19.77938	MAP2	microtubule--associated protein 2
CfaAffx.21232.1.S1_s_at	2.43162E--0	1.73238E--0	24.723236	MAP2	microtubule--associated protein 2
CfaAffx.21245.1.S1_at	0.000835725	0.000554122	8.460225	CUX1	cut--like homeobox 1
CfaAffx.21464.1.S1_at	2.03383E--0	3.64763E--0	102.57415	APOBEC1	apolipoprotein B mRNA editing enzyme, catalytic polypeptide 1
CfaAffx.21495.1.S1_x_at	1.83149E--0	1.84855E--0	9.070598	HNRNPAL12//LOC100684045//LOC100684375//LOC100685571//LOC100685095//LOC487279//LOC607505//LOC608035	heterogeneous nuclear ribonucleoprotein A1--like//putative heterogeneous nuclear ribonucleoprotein A1--like 3--like//uncharacterized LOC100684375//uncharacterized LOC100685571//putative heterogeneous nuclear ribonucleoprotein A1--like 3--like//heterogeneous nuclear ribonucleoprotein A1--like//heterogeneous nuclear ribonucleoprotein A1--like
CfaAffx.21539.1.S1_at	0.000369317	0.000189246	9.599781	TSKAN15	tetraspanin 15
CfaAffx.21545.1.S1_at	2.4011E--0	4.53002E--0	8.818848	VP551	vascular protein sorting 51 homolog (S. cerevisiae)
CfaAffx.21632.1.S1_s_at	2.74385E--0	2.15568E--0	32.588024	ATP2A3	ATPase, Ca++ transporting, ubiquitous
CfaAffx.21611.1.S1_s_at	0.00587248	0.005353	10.151468	PHI1D2	PIH1 domain containing 2
CfaAffx.21683.1.S1_at	0.000291473	0.000134422	9.675335	CDCP1	CUB domain containing protein 1
CfaAffx.21803.1.S1_at	0.000248299	0.000110848	44.45582	C18H7orf57	chromosome 18 open reading frame, human C7orf57
CfaAffx.21925.1.S1_at	8.4579E--0	2.53474E--0	24.000021	C11orf53	chromosome 11 open reading frame 53
CfaAffx.21934.1.S1_s_at	0.001812814	0.001428576	15.197305	DNAI4	DnaI (Hsp40) homolog, subfamily A, member 4
CfaAffx.22128.1.S1_at	0.000182007	7.2916E--0	17.440243	S100P	S100 calcium binding protein P
CfaAffx.22283.1.S1_s_at	0.000740356	0.000471345	12.858521	SI	sucrase--isomaltase (alpha--glucosidase)
CfaAffx.22699.1.S1_at	0.002658393	0.002276558	13.937722	VIL1	villin 1
CfaAffx.22795.1.S1_at	1.18299E--0	5.41899E--0	16.278305	GULP1	GULP, engulfment adaptor PTB domain containing 1
CfaAffx.23201.1.S1_at	7.58907E--0	2.22134E--0	259.17712	MMMP7	matrix metalloproteinase 7 (matrilysin, uterine)
CfaAffx.23286.1.S1_at	0.000149118	5.38353E--0	27.431824	KIAA1377	KIAA1377 ortholog
CfaAffx.23448.1.S1_at	2.63116E--0	2.08368E--0	33.831665	CBH14orf105	chromosome 8 open reading frame, human C14orf105
CfaAffx.23488.1.S1_s_at	4.98594E--0	1.22576E--0	104.61509	PROM1	prominin 1
CfaAffx.23594.1.S1_s_at	9.84206E--0	3.13719E--0	9.618271	TNXB	tenascin XB
CfaAffx.24036.1.S1_at	0.001010513	0.00070375	10.115947	MW5C	myosin VC
CfaAffx.24148.1.S1_at	1.18115E--0	5.04371E--0	18.28551	SFTPD	surfactant protein D
CfaAffx.24247.1.S1_at	0.005603432	0.005371897	9.89372	PADI2	peptidyl arginine deiminase, type II
CfaAffx.24360.1.S1_s_at	0.000891142	0.000599169	8.752004	F8BP10	PKCdelta binding protein 10, 65 kDa
CfaAffx.24359.1.S1_at	0.002182016	0.001787288	13.489994	NSUN7	NOP2/Sun domain family, member 7
CfaAffx.24358.1.S1_s_at	0.000195166	8.0006E--0	12.289798	NSUN7	NOP2/Sun domain family, member 7
CfaAffx.24412.1.S1_at	0.00155663	0.00110565	8.713625	DYX1C1	dylexia susceptibility 1 candidate 1
CfaAffx.24542.1.S1_at	0.000655126	0.00040335	35.672562	KRT23	keratin 23 (histone deacetylase inducible)
CfaAffx.24612.1.S1_at	0.000338008	0.000166381	11.469828	TEX9	testis expressed 9
CfaAffx.24647.1.S1_s_at	0.001115984	0.000800084	8.424809	C18H11orf9	chromosome 18 open reading frame, human C11orf9
CfaAffx.24730.1.S1_at	6.86343E--0	8.63258E--0	11.998539	CLDN7	claudin 7
CfaAffx.24822.1.S1_s_at	0.001831483	0.001448977	22.759684	ANXA8L1	annexin A8--like 1
CfaAffx.24807.1.S1_at	7.47728E--0	9.63686E--0	436.4179	GPX2	glutathione peroxidase 2 (gastrointestinal)
CfaAffx.24807.1.S1_s_at	9.8491E--0	3.594E--0	128.37411	GPX2	glutathione peroxidase 2 (gastrointestinal)
CfaAffx.24813.1.S1_at	1.61938E--0	2.84145E--0	38.193752	RAB15	RAB15, member RAS oncogene family
CfaAffx.24826.1.S1_s_at	5.37562E--0	6.10367E--0	25.382092	ANXA8L1	annexin A8--like 1
CfaAffx.24850.1.S1_s_at	4.92436E--0	5.3908E--0	10.488416	LOC490390	uncharacterized LOC490390
CfaAffx.25019.1.S1_at	7.96108E--0	2.36731E--0	32.63243	FHAD1	forkhead--associated (FHA) phosphopeptide binding domain 1
CfaAffx.25025.1.S1_s_at	0.000406977	0.000213915	11.36839	FHAD1	forkhead--associated (FHA) phosphopeptide binding domain 1
CfaAffx.25104.1.S1_at	0.006372724	0.006053255	10.038526	LOC100686830	cytochrome c oxidase subunit 6A1, mitochondrial--like
CfaAffx.25134.1.S1_at	0.000705719	0.00044491	8.48998	SEL1L3	sel-1 suppressor of lin--12--like 3 (C. elegans)
CfaAffx.25298.1.S1_s_at	0.000587461	0.00034299	33.510532	ALDH1A2	aldehyde dehydrogenase 1 family, member A2
CfaAffx.25306.1.S1_x_at	9.04904E--0	3.2318E--0	59.830795	C30H15orf48	chromosome 30 open reading frame, human C15orf48
CfaAffx.25463.1.S1_at	0.000747474	0.00047781	30.790516	HEPH	hephaestin
CfaAffx.25479.1.S1_at	0.000232144	0.000100211	11.171734	FAM81A	family with sequence similarity 81, member A
CfaAffx.25482.1.S1_at	0.000123533	4.28719E--0	81.10276	GCNT3	glucosaminyl (N--acetyl) transferase 3, mucin type
CfaAffx.25604.1.S1_at	9.79598E--0	3.11182E--0	48.464787	DNAH2	dynein, axonemal, heavy chain 2
CfaAffx.25667.1.S1_s_at	0.001591499	0.001220808	12.131167	DNAH2	dynein, axonemal, heavy chain 2
CfaAffx.25710.1.S1_at	0.001050327	0.000739633	13.516623	PRR15L	proline rich 15--like
CfaAffx.25784.1.S1_at	0.000315591	0.000150935	19.976757	RAB25	RAB25, member RAS oncogene family
CfaAffx.25799.1.S1_s_at	3.9008E--0	8.99487E--0	27.6081	TTL6	tubulin tyrosine ligase--like family, member 6
CfaAffx.25874.1.S1_at	0.000626105	0.000378191	16.696285	GON4L	gon-4--like (C. elegans)
CfaAffx.25914.1.S1_s_at	0.000485293	0.000267137	35.454086	KCNIP1	Kv channel interacting protein 1
CfaAffx.26061.1.S1_at	8.72809E--0	2.91388E--0	29.727827	MUC1	mucin 1, cell surface associated
CfaAffx.26165.1.S1_s_at	0.00179293	0.001410123	10.473141	LOC100855729	glycerophosphodiester phosphodiesterase domain--containing protein 3--like
CfaAffx.26409.1.S1_at	0.002874053	0.00250364	10.804853	ATP10B	ATPase, class V, type 10B
CfaAffx.26410.1.S1_s_at	3.10629E--0	6.48751E--0	48.73429	ATP10B	ATPase, class V, type 10B
CfaAffx.26620.1.S1_at	0.000164675	6.25608E--0	97.89524	POF1B	premature ovarian failure, 1B
CfaAffx.26635.1.S1_at	5.34857E--0	5.97977E--0	8.418213	RGL3	ral guanine nucleotide dissociation stimulator--like 3
CfaAffx.26924.1.S1_at	0.000291039	0.000133769	14.013778	GDPD1	glycerophosphodiester phosphodiesterase domain containing 1
CfaAffx.26924.1.S1_s_at	6.47396E--0	1.78657E--0	9.126445	GDPD1	glycerophosphodiester phosphodiesterase domain containing 1
CfaAffx.26999.1.S1_at	4.73309E--0	1.13183E--0	8.764973	GALNT10	UDP--N--acetyl--alpha--D--galactosamine-polypeptide N--acetylglucosaminyltransferase
CfaAffx.27004.1.S1_s_at	0.000294983	0.000136956	49.775665	ERN2	endoplasmic reticulum to nucleus signaling 2
CfaAffx.27034.1.S1_at	0.002590253	0.002186029	15.623755	SLC14A1	solute carrier family 14 (urea transporter), member 1 (Kidd blood group)
CfaAffx.27080.1.S1_at	0.000247789	0.000110428	10.328145	SCNN1B	sodium channel, non--voltage--gated 1, beta subunit
CfaAffx.27504.1.S1_at	0.000211095	8.85024E--0	31.173523		
CfaAffx.27538.1.S1_at	0.003224326	0.002868849	13.801069		
CfaAffx.27600.1.S1_at	3.1349E--0	2.80667E--0	13.899856	CENPV	centromere protein V
CfaAffx.27609.1.S1_s_at	0.000633656	0.000384228	27.92573	GP2	glycoprotein 2 (zymogen granule membrane)
CfaAffx.27726.1.S1_s_at	0.00041756	0.000221019	11.420585	TMC5	transmembrane channel--like 5
CfaAffx.27789.1.S1_at	4.31498E--0	6.70027E--1	19.620419	HNF1B	HNF1 homeobox B
CfaAffx.27870.1.S1_s_at	0.004661599	0.004361201	10.1471405	MFAP4	microfibrillar--associated protein 4
CfaAffx.27890.1.S1_s_at	0.000622841	0.000375736	22.567442	ABCC1	ATP--binding cassette, sub--family C (CFTR/MRP), member 1
CfaAffx.27900.1.S1_s_at	0.002964111	0.002605104	10.488089	AMOT	angiostatin
CfaAffx.27957.1.S1_at	2.69833E--0	5.28057E--0	35.391438	SLC6A14	solute carrier family 6 (amino acid transporter), member 14
CfaAffx.28023.1.S1_at	0.00704333	0.006917556	10.896791	LLGL1	lethal giant larvae homolog 1 (Drosophila)
CfaAffx.28173.1.S1_s_at	0.001560005	0.00118696	10.74902	LRRC48	leucine rich repeat containing 48
CfaAffx.28187.1.S1_at	0.000203927	8.42306E--0	73.5849	ITGA2	integrin, alpha 2 (CD49b, alpha 2 subunit of VLA--2 receptor)
CfaAffx.28191.1.S1_s_at	3.0747E--0	6.3738E--0	18.339886	ITGA2	integrin, alpha 2 (CD49b, alpha 2 subunit of VLA--2 receptor)
CfaAffx.28378.1.S1_s_at	0.000329412	0.000159512	10.478395	GRIIA3	glutamate receptor, ionotropic, AMPA 3
CfaAffx.28412.1.S1_at	4.67098E--0	5.02704E--0	15.669679	DXCT1	3--oxoacid CoA transferase 1
CfaAffx.28412.1.S1_s_at	0.000498974	0.000277768	12.7633505	DXCT1	3--oxoacid CoA transferase 1
CfaAffx.28417.1.S1_s_at	0.003981067	0.003668887	11.673332	ARHGAP28	Rho GTPase activating protein 28

ClaAffx.28540.1.S1_at	6.51682E-0	1.81814E-0	17.551582	CCDC165	coiled---coil domain containing 165
ClaAffx.28574.1.S1_s_at	1.07512E-0	1.65907E-0	25.523348	SLC13A2	solute carrier family 13 (sodium---dependent dicarboxylate transporter), member 2
ClaAffx.28935.1.S1_at	0.002731117	0.002347318	8.49313	UHRF1	ubiquitin---like with PHD and ring finger domains 1
ClaAffx.29013.1.S1_at	0.002234845	0.001837501	10.28491	TTC22	tetratricopeptide repeat domain 22
ClaAffx.29105.1.S1_s_at	0.000242753	0.000107037	26.965755	ABR	active BCR---related
ClaAffx.29124.1.S1_s_at	0.000182847	7.36784E-0	17.566816	NXN	nucleoredoxin
ClaAffx.29150.1.S1_at	8.81404E-0	2.70306E-0	21.125515	STAP2	signal transducing adaptor family member 2
ClaAffx.29235.1.S1_s_at	5.958E-0	1.58664E-0	42.145603	LRP8	low density lipoprotein receptor---related protein 8, apolipoprotein e receptor
ClaAffx.29230.1.S1_at	0.003718613	0.003392369	8.225798	LRP8	low density lipoprotein receptor---related protein 8, apolipoprotein e receptor
ClaAffx.29237.1.S1_at	0.000100078	3.2168E-0	65.13065	GABRE	gamma---aminobutyric acid (GABA) A receptor, epsilon
ClaAffx.29519.1.S1_at	2.10812E-0	3.81361E-0	27.56459	TTL10	tubulin tyrosine ligase---like family, member 10
ClaAffx.29521.1.S1_s_at	2.84517E-0	5.68207E-0	12.819419	TTL10	tubulin tyrosine ligase---like family, member 10
ClaAffx.29842.1.S1_at	2.06099E-0	3.71235E-0	16.21091	NPOC1	neural proliferation, differentiation and control, 1
ClaAffx.29979.1.S1_at	2.15099E-0	2.33803E-0	22.785696	NGG13	guanine nucleotide binding protein (G protein), gamma 13
ClaAffx.30305.1.S1_at	0.000510872	0.000286374	18.823105	EP58L3	EP58---like 3
ClaAffx.30305.1.S1_s_at	0.0001614	6.07003E-0	9.637291	EP58L3	EP58---like 3
ClaAffx.30313.1.S1_s_at	0.004155927	0.003862302	8.265865	VAV2	vav 2 guanine nucleotide exchange factor
ClaAffx.30380.1.S1_s_at	0.000492874	0.000272935	10.000504	KIAA1324	KIAA1324 ortholog
ClaAffx.30511.1.S1_s_at	0.000105613	3.47671E-0	9.02191	SLC25A24	solute carrier family 25 (mitochondrial carrier; phosphate carrier), member 24
ClaAffx.30515.1.S1_at	0.000123533	4.28673E-0	28.872879	LOC611915	calcium---binding mitochondrial carrier protein ScaMC---1---like
ClaAffx.30543.1.S1_at	1.79199E-0	1.04298E-0	18.397976	ATP2C2	ATPase, Ca++ transporting, type 2C, member 2
ClaAffx.30543.1.S1_s_at	5.61687E-0	1.3955E-0	38.978043	ATP2C2	ATPase, Ca++ transporting, type 2C, member 2
ClaAffx.30723.1.S1_s_at	0.000347397	0.000173429	15.193184	GOLGA2	golgin A2
ClaAffx.30776.1.S1_s_at	0.006212803	0.006024682	13.926233	FA2H	fatty acid 2---hydroxylase
ClaAffx.31009.1.S1_s_at	2.27978E-0	2.75308E-0	71.22375	CLCA4	chloride channel accessory 4
ClaAffx.31067.1.S1_s_at	0.001529618	0.001157902	8.310162	DAB2IP	DAB2 interacting protein
ClaAffx.31080.1.S1_s_at	0.000309458	0.00014608	16.705046	MCOLN2///MCOLN3	mucoilin 2///mucoilin 3
ClaAffx.31178.1.S1_at	0.000333351	0.000162702	17.105856	ZDHHC1	zinc finger, DHHC---type containing 1
ClaAffx.31251.1.S1_at	0.003220776	0.00286319	13.553174	LRRIQ3	leucine---rich repeats and IQ motif containing 3
ClaAffx.31261.1.S1_at	3.0747E-0	6.37216E-0	10.797248	CMTM4	CKLF---like MARVEL transmembrane domain containing 4

Dog liver zone I signature

Probe Set ID	Corrected p---value	p---value	FCabsolute	Gene Symbol	Gene Title
ClaAffx.51.1.S1_at	4.47E-0	2.36E-0	2.3622184		
ClaAffx.51.1.S1_s_at	4.60E-0	2.63E-0	2.7912495		
RPTR---Cfa---A0002682---	0.001023478	9.43E-0	2.066429		
RPTR---Cfa---U89963---1_s_at	7.20E-0	5.30E-0	5.35554		
RPTR---Cfa---XXU09476---1_at	4.88E-0	2.81E-0	2.5119522		
Cfa.115.1.S1_at	2.19E-0	3.84E-0	9.281441	DNASE1	deoxyribonuclease I
Cfa.19.1.S1_s_at	7.45E-0	9.15E-0	2.0813742	ABCB1	ATP---binding cassette, sub---family B (MDR/TAP), member 1
Cfa.16248.1.S1_at	4.43E-0	2.33E-0	6.082133	CNOD1	cyclin D1
Cfa.88.1.S1_s_at	4.52E-0	2.47E-0	3.9615724	GCG	glucagon
Cfa.3822.1.S1_s_at	0.001137103	0.001130162	2.2908456	CXCR7	chemokine (C---X---C motif) receptor 7
Cfa.3039.1.A1_at	2.14E-0	3.53E-0	3.3773682	ATP1A1	ATPase, Na+/K+ transporting, alpha 1 polypeptide
Cfa.200.1.A1_at	5.62E-0	1.33E-0	7.2378883	TFF3	trefoil factor 3 (intestinal)
Cfa.14486.1.S1_at	1.70E-0	1.39E-0	6.290087	HAMP	hepcidin antimicrobial peptide
Cfa.14486.1.S1_s_at	4.79E-0	2.90E-0	4.991958	HAMP	hepcidin antimicrobial peptide
Cfa.10248.1.S1_at	3.05E-0	9.89E-1	2.6874793	HS01181	hydroxysteroid (11---beta) dehydrogenase 1
Cfa.13172.1.S1_at	2.68E-0	2.49E-0	4.8278613	HS0382	hydroxy---delta---5---steroid dehydrogenase, 3 beta--- and steroid delta---isomerase 2
Cfa.3900.1.S1_s_at	4.71E-0	2.66E-0	5.9206276	IFNG	interferon gamma
Cfa.77.1.S1_s_at	0.001109468	0.001070823	3.5266132	PKC1	phosphoenolpyruvate carboxykinase 1 (soluble)
Cfa.3460.1.S1_s_at	6.89E-0	4.85E-0	4.7177715	KCNIP2	Kv channel interacting protein 2
Cfa.3579.1.S1_s_at	1.19E-0	3.87E-0	4.103144	SRD5A2	steroid---5---alpha---reductase, alpha polypeptide 2 (3---oxo---5 alpha---steroid delta 4---)
Cfa.4540.1.S1_at	2.55E-0	1.04E-0	2.0706987	TARP	TCR gamma alternate reading frame protein
Cfa.3262.1.A1_at	0.001052334	9.86E-0	2.032218	MDH1	malate dehydrogenase 1, NAD (soluble)
Cfa.1293.1.A1_at	0.001135682	0.0011211	2.7871902	LOC100856197///LOC475815///LOC607890///LOC608055///LOC610301	d---3---phosphoglycerate dehydrogenase---like///d---3---phosphoglycerate dehydrogenase---like///d---3---phosphoglycerate dehydrogenase---like///d---3---phosphoglycerate dehydrogenase---like///d---3---phosphoglycerate dehydrogenase---like
Cfa.11243.1.A1_at	1.70E-0	3.83E-1	3.1972885	GOT1	glutamic---oxaloacetic transaminase 1, soluble (aspartate aminotransferase 1)
Cfa.4791.1.A1_at	2.73E-0	1.15E-0	2.1429024	GSTT1	glutathione S---transferase theta 1
Cfa.12186.1.A1_at	1.38E-0	4.71E-0	2.3316627	PKC1	phosphoenolpyruvate carboxykinase 1 (soluble)
Cfa.6341.1.A1_at	1.76E-0	6.26E-0	2.7850494	PDZK1IP1	PDZK1 interacting protein 1
Cfa.12127.1.A1_at	2.19E-0	3.75E-0	2.7573106	INMT	indolethylamine N---methyltransferase
Cfa.10250.1.A1_at	1.49E-0	2.21E-0	2.1126008	CISD1	CDGSH iron sulfur domain 1
Cfa.12031.1.A1_at	0.001137103	0.001132292	2.2310576	FAM46B	family with sequence similarity 46, member 8
Cfa.11563.1.A1_at	1.55E-0	2.36E-0	13.797901	CDKN1A	cyclin---dependent kinase inhibitor 1A (p21, Cip1)
Cfa.12228.1.A1_s_at	1.18E-0	3.81E-0	3.729864	SCGB1A1	secretoglobulin, family 1A, member 1 (uteroglobin)
Cfa.13329.1.A1_at	1.20E-0	1.68E-0	2.2961	A1CF	APOBEC1 complementation factor
Cfa.12533.1.A1_at	6.72E-0	4.46E-0	3.3139002	INSIG1	insulin induced gene 1
Cfa.2065.1.A1_at	1.49E-0	2.19E-0	2.5247438	CTH	cystathionase (cystathionine gamma---lyase)
Cfa.9465.1.A1_at	8.95E-0	2.58E-0	9.477575	SYT13	synaptotagmin XIII
Cfa.7475.1.A1_at	1.17E-0	3.75E-0	3.6872158	SAP30BP	SAP30 binding protein
Cfa.7437.1.A1_at	1.98E-0	2.79E-1	8.119272	GLS2	glutaminase 2 (liver, mitochondrial)
Cfa.261.1.A1_a_at	4.91E-0	5.33E-0	5.100943	CRYM	crystallin, mu
Cfa.10794.1.A1_at	5.32E-0	1.22E-0	18.466257	SCG5	secretogranin V (782 protein)
Cfa.11335.1.A1_at	1.12E-0	4.87E-0	4.1235185	AMDHD1	amidohydrolase domain containing 1
ClaAffx.10568.1.S1_at	3.30E-0	1.50E-0	2.9100509	AMDHD1	amidohydrolase domain containing 1
ClaAffx.10568.1.S1_s_at	8.86E-0	1.15E-0	3.2318864	AMDHD1	amidohydrolase domain containing 1
Cfa.11358.1.A1_at	4.15E-0	2.15E-0	2.1719885		
Cfa.6369.1.A1_at	3.11E-0	6.19E-0	2.0269942	FBP1	fructose---1,6---biphosphatase 1
Cfa.6224.1.A1_at	1.49E-0	2.23E-0	6.3605933		
Cfa.2657.1.A1_at	2.36E-0	2.09E-0	2.490895		
Cfa.5193.1.A1_at	8.89E-0	7.46E-0	2.0879204		
Cfa.6763.1.A1_at	1.49E-0	2.24E-0	3.675365	CRHR2	corticotropin releasing hormone receptor 2
Cfa.10873.1.A1_at	1.54E-0	1.21E-0	2.6299667	PTPN3	protein tyrosine phosphatase, non---receptor type 3
Cfa.15708.1.A1_at	2.94E-0	2.82E-0	2.6508162	CPB2	carboxypeptidase B2 (plasma)
Cfa.9216.1.A1_at	6.40E-0	4.33E-0	2.15436	IER2	immediate early response 2
Cfa.5100.1.A1_at	6.20E-0	4.09E-0	2.1360412		
Cfa.5095.1.A1_s_at	1.17E-0	3.77E-0	3.4504335	KCNN2	potassium intermediate/small conductance calcium---activated channel, subfamily N, member 2
Cfa.12353.1.A1_a_at	7.93E-0	2.14E-0	2.140886	SIK3	SIK family kinase 3
Cfa.11714.1.A1_x_at	5.90E-0	3.83E-0	3.709542	LOC476453	cytochrome P450 2F2---like
Cfa.604.1.A1_at	1.05E-0	8.91E-1	5.867393	LOC100856598	nicotinamide phosphoribosyltransferase---like
Cfa.13946.1.S1_s_at	8.91E-0	7.51E-0	6.1073008	FXYD2	FXYD domain containing ion transport regulator 2
Cfa.11607.1.S1_at	1.83E-0	6.62E-0	6.1609282	AQP8	aquaporin 8
Cfa.13211.1.A1_at	2.71E-0	2.56E-0	2.2727952	TD02	tryptophan 2,3---dioxygenase
ClaAffx.13588.1.S1_at	3.06E-0	1.35E-0	2.415012	TD02	tryptophan 2,3---dioxygenase
ClaAffx.13588.1.S1_s_at	2.72E-0	5.18E-0	2.1222477	TD02	tryptophan 2,3---dioxygenase
ClaAffx.7926.1.S1_s_at	4.64E-0	2.57E-0	4.958221	ABP1	amiloride binding protein 1 (amine oxidase (copper---containing))
Cfa.11241.1.A1_at	3.99E-0	2.01E-0	3.24493		
Cfa.14517.1.A1_at	2.75E-0	5.32E-0	2.26174	FGA	fibrinogen alpha chain
Cfa.12500.1.A1_at	7.73E-0	2.04E-0	2.0471642		
Cfa.6020.1.A1_at	1.66E-0	5.88E-0	4.6586995		
Cfa.15431.1.A1_at	8.16E-0	6.45E-0	2.9712937		
Cfa.12266.1.A1_at	6.17E-0	4.05E-0	6.6837234		
Cfa.10820.1.S1_at	4.91E-0	5.26E-0	3.0222366	TPR	translocated promoter region, nuclear basket protein
Cfa.13146.1.A1_at	8.61E-0	7.03E-0	3.768973	FBXO2	F---box protein 2
Cfa.14986.1.A1_at	6.18E-0	1.51E-0	3.40883		
Cfa.16469.1.S1_x_at	8.86E-0	1.14E-0	2.095468	SERPINA1	serpin peptidase inhibitor, clade A (alpha---1 antiproteinase, antitrypsin), member 1
Cfa.506.1.S1_at	5.36E-0	3.24E-0	2.794601	LOC100686903	uncharacterized LOC100686903
Cfa.2326.1.S1_at	1.04E-0	1.40E-0	2.3006694	LOC100856436	gamma---glutamyl hydrolase---like

Cfa.1760.1.A1_at	8.95E--0	2.56E--0	2.0890467	MAN2A1	mannosidase, alpha, class 2A, member 1
Cfa.2170.1.S1_at	8.86E--0	1.15E--0	4.7451415	ALDH1B1	aldehyde dehydrogenase 1 family, member B1
Cfa.6037.1.S1_at	2.28E--0	6.76E--1	4.986616	A2M	alpha--2--macroglobulin
Cfa.6037.1.S1_s_at	1.09E--0	3.39E--0	4.3954763	A2M	alpha--2--macroglobulin
Cfa.2730.1.S1_at	0.001007302	9.08E--0	6.9273295	RASEF	RAS and EF--hand domain containing
Cfa.15049.1.S1_a_at	7.41E--0	1.93E--0	2.0167336	NMI	N--myc (and STAT) interactor
Cfa.14027.1.A1_at	2.12E--0	8.04E--0	12.260447	AGXT2L1	alanine--glyoxylate aminotransferase 2--like 1
Cfa.14925.1.A1_s_at	2.78E--0	1.53E--0	3.5611627	AMDHD1	amidohydrolase domain containing 1
Cfa.15025.1.S1_at	1.20E--0	3.96E--0	4.8702397	IVNS1ABP	influenza virus NS1A binding protein
Cfa.1818.1.S1_at	9.93E--0	2.95E--0	20.003351		
CfaAffx.11365.1.S1_at	3.06E--0	1.36E--0	2.6706333	PLK2	polo--like kinase 2
Cfa.716.1.S1_at	1.15E--0	5.17E--0	2.3502603	GNMT	glycine N--methyltransferase
CfaAffx.3512.1.S1_s_at	6.61E--0	1.68E--0	2.0003722	GNMT	glycine N--methyltransferase
Cfa.9537.1.S1_at	5.45E--0	6.15E--0	2.0389786		
Cfa.18689.1.S1_at	1.23E--0	4.15E--0	4.5825443	A2M	alpha--2--macroglobulin
Cfa.18689.1.S1_s_at	9.65E--0	8.51E--0	7.4107733	A2M	alpha--2--macroglobulin
Cfa.21446.1.S1_at	9.11E--0	2.63E--0	2.4368663	SDC4	syndecan 4
Cfa.19344.1.S1_at	9.79E--0	8.72E--0	2.478196	TMEM184C	transmembrane protein 184C
Cfa.19549.1.S1_at	7.05E--0	5.09E--0	18.537493	AGXT2L1	alanine--glyoxylate aminotransferase 2--like 1
Cfa.19549.1.S1_s_at	1.83E--0	6.60E--0	10.5841875	AGXT2L1	alanine--glyoxylate aminotransferase 2--like 1
Cfa.4354.1.S1_a_at	3.05E--0	2.97E--0	9.582985	CRYL1	crystallin, lambda 1
Cfa.21147.1.S1_at	1.20E--0	3.95E--0	2.4453192	PRG4	proteoglycan 4
Cfa.20197.1.S1_s_at	6.17E--0	4.05E--0	5.3378077	KLHL10	kelch--like 10 (Drosophila)
Cfa.17338.1.S1_at	8.67E--0	7.14E--0	2.06938	PRKAB1	protein kinase, AMP--activated, beta 1 non--catalytic subunit
Cfa.17754.1.S1_s_at	9.23E--0	7.93E--0	3.7816126	MYPN	myopalladin
Cfa.18110.1.S1_s_at	3.31E--0	1.53E--0	4.5418205	GAS6	growth arrest--specific 6
Cfa.17292.1.S1_at	8.95E--0	2.57E--0	2.3273602	CLK1	CDC--like kinase 1
Cfa.19914.1.S1_at	8.17E--0	6.48E--0	4.515733	C2H16orf78	chromosome 2 open reading frame, human C16orf78
Cfa.18345.1.S1_at	1.04E--0	7.50E--0	7.479455	LOC100856598	nicotinamide phosphoribosyltransferase--like
Cfa.18345.1.S1_s_at	6.37E--0	4.27E--0	5.9291267	LOC100856598	nicotinamide phosphoribosyltransferase--like
Cfa.20905.1.S1_at	5.12E--0	3.03E--0	2.0515904	AGKT//LOC100855679	alanine--glyoxylate aminotransferase//serine--pyruvate aminotransferase, mitochondrial--like
Cfa.16871.1.S1_at	1.56E--0	2.42E--0	2.677464	SLC27A6	solute carrier family 27 (fatty acid transporter), member 6
Cfa.10462.3.S1_a_at	2.55E--0	1.05E--0	2.1855497	TOB1	transducer of ERBB2, 1
Cfa.18520.1.S1_s_at	4.01E--0	2.03E--0	4.342034	ZPBP	zona pellucida binding protein
Cfa.20245.1.S1_s_at	9.23E--0	7.93E--0	2.124119	NNAT	neuronatin
Cfa.18172.1.S1_at	0.00101319	9.29E--0	2.880345	TMEM130	transmembrane protein 130
Cfa.6583.1.A1_at	3.80E--0	1.87E--0	3.0895784	RSPH6A	radial spoke head 6 homolog A (Chlamydomonas)
Cfa.13417.1.A1_at	3.06E--0	1.37E--0	2.002376	LOC480511//LOC90956	membrane primary amine oxidase--like//membrane primary amine oxidase--like
Cfa.14390.1.A1_at	3.50E--0	1.66E--0	2.5185163	HS017B13	hydroxysteroid (17--beta) dehydrogenase 13
Cfa.5149.1.A1_at	9.54E--0	8.33E--0	11.50878	CLDN18	claudin 18
Cfa.14347.1.A1_a_at	8.43E--0	6.76E--0	6.2065945	PABPC1	poly(A) binding protein, cytoplasmic 1
Cfa.6787.1.A1_at	8.03E--0	6.26E--0	5.3045893	FAM211B	family with sequence similarity 211, member B
Cfa.13841.1.A1_at	5.37E--0	3.27E--0	2.3758984		
Cfa.13333.1.A1_at	5.10E--0	5.61E--0	2.867027		
Cfa.6572.1.A1_at	6.69E--0	4.62E--0	4.857863		
Cfa.6500.1.A1_at	3.31E--0	1.53E--0	4.550751		
Cfa.5975.1.A1_at	0.001109468	0.001072649	3.5205276		
Cfa.2817.1.A1_at	4.47E--0	2.40E--0	5.615039		
Cfa.7610.1.A1_at	5.36E--0	3.24E--0	3.790045		
Cfa.14409.1.A1_at	1.07E--0	3.31E--0	2.8406126	LOC100687790	uncharacterized LOC100687790
Cfa.14519.1.A1_at	6.32E--0	1.57E--0	3.4406133	CDA	cytidine deaminase
Cfa.14357.1.A1_at	2.19E--0	3.76E--0	10.819984	DMBT1	deleted in malignant brain tumors 1
Cfa.1331.1.A1_s_at	0.001137103	0.001131316	2.242029	DNPEP	aspartyl aminopeptidase
Cfa.4794.1.A1_x_at	2.55E--0	1.05E--0	2.8934968	RG510	regulator of G--protein signaling 10
Cfa.2593.1.S1_at	6.92E--0	4.96E--0	2.9763377	PLAUR	plasminogen activator, urokinase receptor
Cfa.2391.1.S1_at	5.52E--0	1.29E--0	2.2369497	AASS	aminoadipate--semialdehyde synthase
Cfa.422.1.A1_at	5.55E--0	3.44E--0	16.590569		
Cfa.3095.1.A1_at	7.40E--0	5.51E--0	6.4090285		
Cfa.8795.1.A1_at	8.03E--0	6.26E--0	2.4415514	PKNOX2	PBX/knotted 1 homeobox 2
Cfa.9729.1.A1_at	2.12E--0	8.02E--0	4.8876214		
Cfa.7030.1.A1_at	4.47E--0	2.38E--0	2.3493683		
Cfa.7551.1.A1_at	6.92E--0	4.97E--0	3.4050791	LOC100687680	uncharacterized LOC100687680
Cfa.5383.1.A1_s_at	2.88E--0	1.22E--0	6.457627	SLC22A3	solute carrier family 22 (extraneuronal monoamine transporter), member 3
Cfa.8011.2.S1_at	5.61E--0	3.53E--0	4.9271407	CTU2	cytosolic thiouridylase subunit 2 homolog (S. pombe)
Cfa.14836.1.A1_at	1.67E--0	8.26E--0	4.7328577		
Cfa.9388.1.A1_at	3.73E--0	1.79E--0	2.4713075	STPG1	sperm--tail PG--rich repeat containing 1
Cfa.14510.1.A1_at	2.47E--0	4.59E--0	2.6009297	C8B	complement component B, beta polypeptide
Cfa.5354.1.A1_at	5.35E--0	3.21E--0	3.1786656	PIGR	polymeric immunoglobulin receptor
Cfa.9819.1.A1_at	9.98E--0	2.98E--0	2.2327995	BHMT	betaine--homocysteine S--methyltransferase
Cfa.13273.1.A1_x_at	2.46E--0	9.78E--0	2.3439674	FGG	fibrinogen gamma chain
Cfa.13351.1.A1_at	8.43E--0	6.83E--0	8.0946665	LOC609690	phosphatidylcholine transfer protein--like
Cfa.13959.1.A1_at	9.03E--0	7.67E--0	2.1979938	PKC1	phosphoenolpyruvate carboxykinase 1 (soluble)
Cfa.4874.1.A1_at	6.92E--0	4.96E--0	2.674564		
Cfa.14509.1.A1_at	6.77E--0	4.68E--0	3.6801898	ACE2	angiotensin I converting enzyme (peptidyl--dipeptidase A) 2
Cfa.14509.1.A1_s_at	8.69E--0	3.07E--0	9.317055	ACE2	angiotensin I converting enzyme (peptidyl--dipeptidase A) 2
Cfa.14559.1.A1_at	4.88E--0	2.80E--0	5.2467756		
Cfa.12799.1.A1_at	4.69E--0	2.63E--0	2.9446578		
Cfa.14451.1.A1_at	1.56E--0	5.38E--0	3.1871827	UROCL	urocanate hydratase 1
Cfa.12626.1.A1_at	9.22E--0	7.88E--0	3.084733		
Cfa.6319.1.A1_at	3.05E--0	1.33E--0	3.6481128		
Cfa.14468.1.A1_s_at	9.65E--0	8.54E--0	5.200644	NNMT	nicotinamide N--methyltransferase
Cfa.12914.1.A1_at	5.40E--0	3.30E--0	2.0093505		
Cfa.13427.1.A1_at	4.34E--0	2.28E--0	2.9480019		
Cfa.4873.1.A1_at	3.38E--0	1.59E--0	2.0670514		
Cfa.12871.1.A1_x_at	3.31E--0	1.52E--0	2.8619752	CARKD	carbohydrate kinase domain containing
Cfa.5993.1.A1_at	4.05E--0	2.06E--0	2.264425	FGB	fibrinogen beta chain
Cfa.8857.2.A1_at	8.35E--0	6.66E--0	3.2224762	WFDC3	WAP four--disulfide core domain 3
Cfa.5991.1.A1_x_at	6.74E--0	7.90E--0	2.2316887	ALB	albumin
Cfa.331.1.S1_at	5.89E--0	3.81E--0	4.5389204		
Cfa.15859.1.A1_x_at	8.64E--0	7.08E--0	3.7841198	ACTA1	actin, alpha 1, skeletal muscle
CfaAffx.219.1.S1_at	5.80E--0	3.71E--0	2.5350776		
CfaAffx.222.1.S1_at	5.87E--0	3.79E--0	6.0655875		
CfaAffx.245.1.S1_at	3.06E--0	1.37E--0	2.250774		
CfaAffx.595.1.S1_at	0.00108212	0.001018456	3.0491474	LOC100686490	olfactory receptor 851--like
CfaAffx.945.1.S1_s_at	1.24E--0	4.19E--0	2.0350106	LOC100684574//LOC100855507//LOC100856216//LOC100856236//LOC83167//LOC48317//LOC488275//LOC488277//LOC488298//LOC488306//LOC488307//LOC608586//LOC611519	histone H3.1--like//histone H3.1--like//histone H3.1--like//histone H3.1--like//histone H3.2--like//histone H3.2--like//histone H3.1--like//histone H3.1--like//histone H3.1--like//histone H3.1--like//histone H3.1--like//histone H3.1--like//histone H3.1--like
CfaAffx.1087.1.S1_s_at	7.41E--0	1.92E--0	2.0482466	ORMDL2	ORM1--like 2 (S. cerevisiae)
CfaAffx.1173.1.S1_s_at	9.84E--0	1.30E--0	7.154202	GLS2	glutaminase 2 (liver, mitochondrial)
CfaAffx.1174.1.S1_s_at	7.50E--0	5.60E--0	3.7941115	RBM52	RNA binding motif, single stranded interacting protein 2
CfaAffx.1454.1.S1_at	1.11E--0	3.46E--0	10.854353	AVPR1A	arginine vasopressin receptor 1A
CfaAffx.1463.1.S1_at	6.67E--0	4.58E--0	4.8920646	LOC100856646	calpain--7--like protein--like
CfaAffx.1600.1.S1_at	1.95E--0	2.30E--1	9.849651	CCDC170	coiled--coil domain containing 170
CfaAffx.2031.1.S1_at	1.93E--0	7.11E--0	6.0346947		
CfaAffx.2034.1.S1_s_at	4.74E--0	1.07E--0	9.819643	SLC22A3	solute carrier family 22 (extraneuronal monoamine transporter), member 3

ClaAffx.2039.1.S1_s_at	3.06E-0	1.37E-0	7.1145825	SLC22A1	solute carrier family 22 (organic cation transporter), member 1
ClaAffx.2043.1.S1_at	3.64E-0	7.55E-0	27.338125	SLC22A3	solute carrier family 22 (extraneuronal monoamine transporter), member 3
ClaAffx.2496.1.S1_at	3.38E-0	1.59E-0	2.2496524	NEUROG1	neurogenin 1
ClaAffx.2979.1.S1_x_at	9.72E-0	8.63E-0	2.02278	LOC100856128//LOC610188//PPSMA1	proteasome subunit alpha type--1--like//proteasome subunit alpha type--1--like//proteasome (prosome, macropain) subunit, alpha type, 1
ClaAffx.3022.1.S1_s_at	6.74E-0	7.86E-0	3.291371	GLDC	glycine dehydrogenase (decarboxylating)
ClaAffx.3129.1.S1_at	0.001142826	0.001142826	2.232532	SSMEM1	serine--rich single--pass membrane protein 1
ClaAffx.3747.1.S1_at	8.29E-0	6.59E-0	4.013817	COX7B2	cytochrome c oxidase subunit VIIb2
ClaAffx.4178.1.S1_at	6.83E-0	4.76E-0	2.9879646	RNF149	ring finger protein 149
ClaAffx.4463.1.S1_at	3.92E-0	8.45E-0	7.7291245	ALDH1B1	aldehyde dehydrogenase 1 family, member B1
ClaAffx.4562.1.S1_at	6.40E-0	4.34E-0	4.2133856	FOXK1	forkhead box E1 (thyroid transcription factor 2)
ClaAffx.4714.1.S1_s_at	0.00100411	9.02E-0	2.0869815	COL19A1	collagen, type XIX, alpha 1
ClaAffx.4809.1.S1_at	7.17E-0	5.25E-0	4.5047193	GP6	glycoprotein VI (platelet)
ClaAffx.5174.1.S1_at	6.40E-0	4.33E-0	2.0150173	VSIG10L	V--set and immunoglobulin domain containing 10 like
ClaAffx.5960.1.S1_s_at	0.001109468	0.00107349	3.5105672	C11H9orf91	chromosome 11 open reading frame, human C9orf91
ClaAffx.6209.1.S1_at	7.92E-0	6.10E-0	6.2101383	PTPRZ1	protein tyrosine phosphatase, receptor--type, Z polypeptide 1
ClaAffx.6438.1.S1_at	0.001083552	0.001026711	2.0580971	HMG84	high mobility group box 4
ClaAffx.6722.1.S1_s_at	4.63E-0	1.04E-0	7.8102875	CCDC7	coiled--coil domain containing 7
ClaAffx.6906.1.S1_at	2.17E-0	5.82E-0	5.451332	LOC100856598	nicotinamide phosphoribosyltransferase--like
ClaAffx.6985.1.S1_at	9.01E-0	7.64E-0	2.600856	RFPL48	ret finger protein--like 48
ClaAffx.7050.1.S1_at	2.26E-0	8.80E-0	2.735839	GLTSCR1	glioma tumor suppressor candidate region gene 1
ClaAffx.7578.1.S1_at	4.61E-0	2.54E-0	2.3411555	CDADC1	cytidine and dCMP deaminase domain containing 1
ClaAffx.7713.1.S1_s_at	2.47E-0	2.26E-0	2.230488	CPB2	carboxypeptidase B2 (plasma)
ClaAffx.7883.1.S1_at	8.56E-0	6.98E-0	2.4556303	PVRL2	poliovirus receptor--related 2 (herpesvirus entry mediator B)
ClaAffx.8272.1.S1_at	8.95E-0	2.56E-0	6.0447187	SCTR	secretin receptor
ClaAffx.8833.1.S1_at	5.19E-0	3.08E-0	2.9791503	LOC100856134	urocortin--3--like
ClaAffx.9544.1.S1_s_at	0.001136777	0.001126907	2.1030495	SLC38A10	solute carrier family 38, member 10
ClaAffx.9641.1.S1_at	0.001008789	9.21E-0	2.3556573	ART5	ADP--ribosyltransferase 5
ClaAffx.9846.1.S1_at	6.80E-0	4.71E-0	2.8093987	SPRED3	sprouty--related, EVH1 domain containing 3
ClaAffx.10100.1.S1_at	3.38E-0	1.58E-0	4.943786	SULT6B1	sulfotransferase family, cytosolic, 6B, member 1
ClaAffx.10256.1.S1_at	1.64E-0	5.75E-0	2.062443	HDAC3	histone deacetylase 3
ClaAffx.10607.1.S1_at	9.17E-0	2.68E-0	16.09443	HAL	histidine ammonia--lyase
ClaAffx.10791.1.S1_at	8.43E-0	6.78E-0	2.1881874	DEAF1	deformed epidermal autoregulatory factor 1 (Drosophila)
ClaAffx.10932.1.S1_s_at	2.53E-0	1.02E-0	6.4770274	ANKS18//LOC10068664	ankyrin repeat and sterile alpha motif domain containing 18//ankyrin repeat and sterile alpha motif domain--containing protein 18--like
ClaAffx.10948.1.S1_at	4.87E-0	2.78E-0	2.9258432	TMC2	transmembrane channel--like 2
ClaAffx.11313.1.S1_at	2.41E-0	4.39E-0	3.582794	SLC7A2	solute carrier family 7 (cationic amino acid transporter, y+ system), member 2
ClaAffx.11451.1.S1_at	8.39E-0	6.71E-0	3.6733086	MOS	v--mos Moloney murine sarcoma viral oncogene homolog
ClaAffx.11552.1.S1_s_at	8.81E-0	7.28E-0	4.5987954	C20H3orf14	chromosome 20 open reading frame, human C3orf14
ClaAffx.11741.1.S1_s_at	3.30E-0	1.50E-0	4.125406	IL18	interleukin 1, beta
ClaAffx.11760.1.S1_at	4.91E-0	2.84E-0	3.008066	IL1F8	interleukin 1 family, member 8 (eta)
ClaAffx.11798.1.S1_s_at	3.92E-0	8.47E-0	7.36029	CRYL1	crystallin, lambda 1
ClaAffx.11895.1.S1_at	7.50E-0	5.64E-0	3.379391	KCTD15	potassium channel tetramerisation domain containing 15
ClaAffx.12001.1.S1_s_at	6.31E-0	4.20E-0	2.2082994	MAN2A1	mannosidase, alpha, class 2A, member 1
ClaAffx.12092.1.S1_s_at	5.72E-0	1.38E-0	11.159875	CLDN18	claudin 18
ClaAffx.12380.1.S1_at	3.72E-0	2.20E-0	2.8957467	AADAT	aminoadipate aminotransferase
ClaAffx.12658.1.S1_s_at	4.47E-0	2.40E-0	2.0004745	ELL2	elongation factor, RNA polymerase II, 2
ClaAffx.12764.1.S1_s_at	7.36E-0	5.47E-0	5.4150953	EMC4	ER membrane protein complex subunit 4
ClaAffx.12970.1.S1_at	3.06E-0	1.36E-0	5.390561	LOC100687650	olfactory receptor 4P4--like
ClaAffx.13043.1.S1_at	7.97E-0	6.16E-0	2.8684509		
ClaAffx.13264.1.S1_s_at	8.03E-0	6.24E-0	3.2924228	TMPSR515	transmembrane protease, serine 15
ClaAffx.13328.1.S1_at	6.55E-0	4.48E-0	4.670266	C1QTNF4	C1q and tumor necrosis factor related protein 4
ClaAffx.14193.1.S1_s_at	0.001052243	9.84E-0	2.6901436	LOC100856038	serine/threonine--protein kinase PAK 6--like
ClaAffx.14346.1.S1_s_at	3.71E-0	7.80E-0	9.408821	SDS	serine dehydratase
ClaAffx.14452.1.S1_at	7.24E-0	5.34E-0	5.381346	LOC100856070	olfactory receptor 5K1--like
ClaAffx.14574.1.S1_at	1.30E-0	1.87E-0	6.022402	SLC38A4	solute carrier family 38, member 4
ClaAffx.14612.1.S1_at	9.58E-0	8.42E-0	5.0486627	CRHBP	corticotropin releasing hormone binding protein
ClaAffx.14901.1.S1_s_at	1.04E-0	1.40E-0	2.4154148	GOT1	glutamic--oxaloacetic transaminase 1, soluble (aspartate aminotransferase 1)
ClaAffx.15308.1.S1_at	3.03E-0	1.32E-0	2.7915127	SYCP2L	synaptonemal complex protein 2--like
ClaAffx.15326.1.S1_x_at	8.89E-0	7.44E-0	2.0417626	GAPDH//LOC100682541//LOC100683724//LOC100684096//LOC100686435//LOC10068664//LOC100687814//LOC100689699//LOC100855503//LOC477441//LOC479206//LOC485733//LOC6081153//LOC609929//LOC610683	glyceraldehyde--3--phosphate dehydrogenase//glyceraldehyde--3--phosphate dehydrogenase--like//glyceraldehyde--3--phosphate dehydrogenase--like//glyceraldehyde--3--phosphate dehydrogenase--like//glyceraldehyde--3--phosphate dehydrogenase--like//glyceraldehyde--3--phosphate dehydrogenase--like//glyceraldehyde--3--phosphate dehydrogenase--like//glyceraldehyde--3--phosphate dehydrogenase--like//glyceraldehyde--3--phosphate dehydrogenase--like//glyceraldehyde--3--phosphate dehydrogenase--like//glyceraldehyde--3--phosphate dehydrogenase--like
ClaAffx.15479.1.S1_at	5.71E-0	3.64E-0	2.0457256	SLC6A5	solute carrier family 6 (neurotransmitter transporter, glycine), member 5
ClaAffx.16591.1.S1_at	0.001126333	0.001105681	5.059919	CCDC147	coiled--coil domain containing 147
ClaAffx.16731.1.S1_s_at	3.99E-0	2.00E-0	2.8347592	SLC6A3	solute carrier family 6 (neurotransmitter transporter, dopamine), member 3
ClaAffx.16895.1.S1_at	4.15E-0	2.13E-0	2.4084287	PDCD4	programmed cell death 4 (neoplastic transformation inhibitor)
ClaAffx.17140.1.S1_at	4.89E-0	2.82E-0	4.576503	LOC610995	uncharacterized LOC610995
ClaAffx.17155.1.S1_s_at	0.001093915	0.001039914	2.6258764		
ClaAffx.17541.1.S1_s_at	0.001118269	0.001091456	3.783531	ALDH3B2	aldehyde dehydrogenase 3 family, member B2
ClaAffx.17644.1.S1_at	1.93E-0	7.04E-0	19.054476	AGXT2L1	alanine--glyoxylate aminotransferase 2--like 1
ClaAffx.17740.1.S1_at	6.27E-0	4.15E-0	3.9115338	WSCD2	WSC domain containing 2
ClaAffx.17752.1.S1_at	5.59E-0	3.49E-0	4.4084883	LOC489338	putative olfactory receptor 10D3--like
ClaAffx.17833.1.S1_at	0.001000575	8.95E-0	3.1105645		
ClaAffx.17869.1.S1_at	7.78E-0	5.92E-0	3.332694	LOC488312	olfactory receptor 2G6--like
ClaAffx.17884.1.S1_s_at	3.31E-0	1.52E-0	2.9325092	PIGR	polymeric immunoglobulin receptor
ClaAffx.17915.1.S1_at	2.99E-0	1.29E-0	4.160895	C7H1orf116	chromosome 7 open reading frame, human C1orf116
ClaAffx.18662.1.S1_at	3.32E-0	1.54E-0	2.6680589	BMP7	bone morphogenetic protein 7
ClaAffx.18846.1.S1_at	1.22E-0	4.05E-0	6.4208555	ACE2	angiotensin I converting enzyme (peptidyl--dipeptidase A) 2
ClaAffx.19048.1.S1_s_at	8.06E-0	6.33E-0	5.546906		
ClaAffx.19098.1.S1_s_at	5.63E-0	1.35E-0	7.0807405	cOR52A10	cOR52A10 olfactory receptor family 52 subfamily A--like
ClaAffx.19377.1.S1_at	6.85E-0	4.79E-0	2.8293104	COR52S3	cOR52S3 olfactory receptor family 52 subfamily S--like
ClaAffx.19397.1.S1_at	1.48E-0	2.71E-0	2.9584477	ICAIL	islet cell autoantigen 1.69kDa--like
ClaAffx.19509.1.S1_s_at	2.47E-0	9.88E-0	4.4929786	PIK3C2G	phosphatidylinositol--4--phosphate 3--kinase, catalytic subunit type 2 gamma
ClaAffx.19565.1.S1_at	6.30E-0	4.18E-0	2.0244954	LOC477425	olfactory receptor family 9 subfamily S
ClaAffx.19565.1.S1_x_at	8.82E-0	7.31E-0	2.8546588	LOC477425	olfactory receptor family 9 subfamily S
ClaAffx.19771.1.S1_s_at	4.79E-0	2.72E-0	2.549119	AGXT//LOC100855679	alanine--glyoxylate aminotransferase//serine--pyruvate aminotransferase, mitochondrial--like
ClaAffx.20253.1.S1_at	4.91E-0	2.85E-0	3.380909	NOS1AP	nitric oxide synthase 1 (neuronal) adaptor protein
ClaAffx.20901.1.S1_at	6.92E-0	4.90E-0	6.2004437	NNMT	nicotinamide N--methyltransferase
ClaAffx.20905.1.S1_at	8.29E-0	6.59E-0	3.2357028	NNMT	indolethylamine N--methyltransferase
ClaAffx.20987.1.S1_s_at	1.97E-0	1.70E-0	4.8975644	IVNS1ABP	influenza virus NS1A binding protein
ClaAffx.21142.1.S1_s_at	1.97E-0	1.68E-0	9.750079	PRG4	proteoglycan 4
ClaAffx.21253.1.S1_s_at	2.99E-0	1.69E-0	2.012042	LOC611458	alpha--2--macroglobulin--like
ClaAffx.21435.1.S1_at	0.001098713	0.001050673	5.3653603	RIMKL8	ribosomal modification protein rimK--like family member 8
ClaAffx.21460.1.S1_at	4.34E-0	9.61E-0	17.05622	GGT1	gamma--glutamyltransferase 1
ClaAffx.21462.1.S1_s_at	0.001130208	0.001111079	3.9970117	GGT1	gamma--glutamyltransferase 1
ClaAffx.21670.1.S1_s_at	0.001031781	9.55E-0	2.6099608		
ClaAffx.21967.1.S1_s_at	7.17E-0	1.84E-0	5.237938	YJEFN3	Yjef N--terminal domain containing 3
ClaAffx.22767.1.S1_at	3.41E-0	1.61E-0	2.4412951	LOC100856319	low--density lipoprotein receptor class A domain--containing protein 2--like
ClaAffx.22787.1.S1_at	3.99E-0	2.01E-0	2.6936347	SHC4	SHC (src homology 2 domain containing) family, member 4
ClaAffx.23060.1.S1_at	0.001009791	9.24E-0	4.6272225	C7H1orf129	chromosome 7 open reading frame, human C1orf129
ClaAffx.23448.1.S1_at	9.23E-0	7.91E-0	5.2805195	C8H14orf105	chromosome 8 open reading frame, human C14orf105
ClaAffx.23785.1.S1_x_at	3.81E-0	1.88E-0	2.8482275	LOC607715	
ClaAffx.24373.1.S1_at	7.66E-0	5.80E-0	5.3245897	CACNA1F	calcium channel, voltage--dependent, L type, alpha 1F subunit
ClaAffx.24432.1.S1_at	7.09E-0	5.14E-0	3.5549517	KRT14	keratin 14

CfaAffx.24621.1.S1_s_at	0.001095686	0.001043143	3.4331741	LDB3	LIM domain binding 3
CfaAffx.25033.1.S1_at	7.50E-0	5.63E-0	2.0124445	GNA12	guanine nucleotide binding protein (G protein) alpha 12
CfaAffx.25117.1.S1_at	0.001121901	0.001096817	3.434048	TMEM2298	transmembrane protein 2298
CfaAffx.25347.1.S1_at	4.61E-0	2.54E-0	2.1658816		
CfaAffx.25568.1.S1_s_at	8.89E-0	7.47E-0	2.6252992	STARD8	Star--related lipid transfer (START) domain containing 8
CfaAffx.25710.1.S1_at	0.00100411	9.03E-0	3.384554	PRR15L	proline rich 15--like
CfaAffx.25716.1.S1_at	5.01E-0	2.95E-0	2.1446939	LSMD1	LSM domain containing 1
CfaAffx.25748.1.S1_at	0.001008789	9.19E-0	2.331887	HOXB2	homeobox B2
CfaAffx.25763.1.S1_at	0.00103103	9.51E-0	2.351187	PRSS36	protease, serine, 36
CfaAffx.26532.1.S1_at	7.88E-0	6.06E-0	2.3910594	ZNPF53	zinc finger protein 653
CfaAffx.26577.1.S1_at	4.47E-0	2.41E-0	5.729099	RP56KA6	ribosomal protein S6 kinase, 90kDa, polypeptide 6
CfaAffx.26814.1.S1_at	5.70E-0	3.61E-0	3.0324247	SPC24	SPC24, NDC80 kinetochore complex component, homolog (S. cerevisiae)
CfaAffx.27276.1.S1_at	6.20E-0	4.10E-0	3.6256466	TBC1D21	TBC1 domain family, member 21
CfaAffx.27291.1.S1_at	1.00E-0	3.03E-0	3.6334188	CCDC33	coiled--coil domain containing 33
CfaAffx.27489.1.S1_s_at	0.001008789	9.20E-0	4.0318727	LMAN1L	lectin, mannose--binding, 1 like
CfaAffx.27554.1.S1_at	9.75E-0	8.67E-0	4.8467274	C30H15orf39	chromosome 30 open reading frame, human C15orf39
CfaAffx.27957.1.S1_at	2.67E-0	5.05E-0	19.74556	SLC6A14	solute carrier family 6 (amino acid transporter), member 14
CfaAffx.28037.1.S1_at	1.17E-0	3.75E-0	5.838383	ASPG	asparaginase homolog (S. cerevisiae)
CfaAffx.28043.1.S1_at	7.50E-0	5.61E-0	2.1878998		
CfaAffx.28148.1.S1_s_at	9.43E-0	8.19E-0	3.6768114	AHNAK2	AHNAK nucleoprotein 2
CfaAffx.28389.1.S1_s_at	3.86E-0	1.93E-0	4.4312162	LOC100856415	SH3--containing GRB2--like protein 3--interacting protein 1--like
CfaAffx.28583.1.S1_at	5.43E-0	3.35E-0	3.18739	FOXN1	forkhead box N1
CfaAffx.28608.1.S1_at	5.36E-0	3.25E-0	3.439379	TXNDC2	thioredoxin domain containing 2 (spermatzoa)
CfaAffx.29305.1.S1_at	6.92E-0	4.96E-0	2.1967502	PIP5K1C	phosphatidylinositol--4--phosphate 5--kinase, type I, gamma
CfaAffx.30380.1.S1_s_at	0.001007584	9.15E-0	2.4656074	KIAA1324	KIAA1324 ortholog
CfaAffx.30553.1.S1_at	2.90E-0	1.23E-0	2.2216477	KCNGA4	potassium voltage--gated channel, subfamily G, member 4
CfaAffx.32029.1.S1_at	7.88E-0	6.05E-0	2.4735296		

Dog liver zone III signature

Probe Set ID	Corrected p--value	p--value	FCAbsolute	Gene Symbol	Gene Title
AFX--CP450--2E1.S_s_at	3.74622E-0	7.92571E-0	3.3132603		
AFX--CP450--	5.88112E-0	3.73273E-0	2.9717898		
Cfa.3895.1.A1_s_at	0.000646713	0.000440569	2.163789	SEC61B	Sec61 beta subunit
Cfa.1111.A1_s_at	0.000226226	8.78325E-0	3.6086776	VWVF	von Willebrand factor
Cfa.35.1.A1_s_at	8.9545E-0	3.41003E-0	21.71001	RHBG	Rb family, B glycoprotein
CfaAffx.20286.1.S1_s_at	1.05304E-0	5.83423E-1	15.537946	GLUL	glutamate--ammonia ligase
Cfa.1407.1.S2_at	1.33523E-0	6.40308E-0	13.302963	GLUL//LOC100682914	glutamate--ammonia ligase//glutamine synthetase--like
Cfa.10529.1.S2_at	0.001135682	0.001119046	2.110271	MTPN	myotrophin
Cfa.3709.1.S1_s_at	6.73788E-0	7.98282E-0	4.771196	PLA2G7	phospholipase A2, group VII (platelet--activating factor acetylhydrolase, plasma)
Cfa.184.1.S1_at	1.63119E-0	3.22096E-1	10.397098	KIT	v--kit Hardy--Zuckerman 4 feline sarcoma viral oncogene homolog
Cfa.3590.1.S1_s_at	0.000255424	0.000104623	3.7217104	EDNRB	endothelin receptor type B
Cfa.3662.1.S1_at	0.000862893	0.000705892	3.6257021	MS4A2	membrane--spanning 4--domains, subfamily A, member 2
Cfa.3770.1.S1_at	0.000932148	0.000803304	3.6484907	ADRB2	adrenoreceptor beta 2, surface
Cfa.16336.1.S1_at	7.72542E-0	2.04849E-0	8.208239	CMA1	chymase 1, mast cell
Cfa.11341.1.A1_at	4.96557E-0	1.12758E-0	3.2248018	COMT	catechol--O--methyltransferase
Cfa.2682.1.S1_s_at	0.001008789	0.000921996	2.5253048	MITF	microphthalmia--associated transcription factor
Cfa.3648.1.S1_s_at	1.31653E-0	1.00272E-0	3.7671416	DHSD17	dihydrodiol dehydrogenase (dimeric)
CfaAffx.11223.1.S1_s_at	2.31584E-0	1.24121E-0	18.29748	SLC1A2	solute carrier family 1 (glial high affinity glutamate transporter), member 2
Cfa.3565.1.S1_s_at	0.000559414	0.000349535	4.395624	UACA	uveal autoantigen with coiled--coil domains and ankyrin repeats
CfaAffx.10131.1.S1_s_at	0.000215514	8.23756E-0	12.932066	KITLG	KIT ligand
Cfa.3663.1.A1_s_at	2.80974E-0	5.50851E-0	10.472548	FCER1A	Fc fragment of IgE, high affinity I, receptor for; alpha polypeptide
Cfa.12195.1.S1_at	2.98268E-0	5.88964E-0	18.221287		
Cfa.3478.1.S1_at	4.28852E-0	4.41554E-0	22.281797		
Cfa.3741.1.A2_s_at	1.59152E-0	1.2795E-0	2.2347062	CYP2C18	cytochrome P450 2C21
Cfa.3731.1.S1_s_at	0.000749794	0.00056211	2.9175982	RAB12	RAB12, member RAS oncogene family
Cfa.3502.1.S1_at	0.000249916	0.00010046	4.0674777	SULT1D1	sulfotransferase family, cytosolic, 1D, member 1
CfaAffx.5229.1.S1_s_at	0.000138032	4.71138E-0	7.6424556	SULT1D1	sulfotransferase family, cytosolic, 1D, member 1
Cfa.3705.1.S1_at	2.18422E-0	3.63814E-0	5.155496	COL4A3	collagen, type IV, alpha 3 (Goodpasture antigen)
Cfa.99.1.S1_s_at	0.000255032	0.000103789	4.880408	COL6A3	collagen, type VI, alpha 3
Cfa.3515.1.S1_s_at	8.25804E-0	2.24796E-0	7.1844215	SCNN1A	sodium channel, non--voltage--gated 1 alpha subunit
Cfa.16.1.S1_s_at	8.8661E-0	3.25132E-0	3.018781	SLC01B3	solute carrier organic anion transporter family, member 1B3
Cfa.878.1.A1_at	6.32485E-0	1.58068E-0	2.2646947	GSTM3	glutathione S--transferase mu 3 (brain)
Cfa.878.1.A1_s_at	2.28328E-0	6.70762E-1	6.9192905	GSTM3	glutathione S--transferase mu 3 (brain)
CfaAffx.24225.1.S1_s_at	0.00108212	0.001019543	2.2179728	ENOS3	enolase 3 (beta, muscle)
CfaAffx.5916.1.S1_at	0.000708994	0.000514309	2.3673047	LOC100685620	alpha--1--acid glycoprotein--like
CfaAffx.22816.1.S1_s_at	0.000580389	0.000373282	2.2917888	COP56	COP9 constitutive photomorphogenic homolog subunit 6 (Arabidopsis)
Cfa.1145.1.A2_at	2.3385E-0	4.15586E-0	4.474193	DSTN	desmin (actin depolymerizing factor)
Cfa.5408.1.A1_s_at	0.000447449	0.000243318	2.2873194	RARRES2	retinoic acid receptor responder (tazarotene induced) 2
Cfa.13201.A1_at	0.001048153	0.000974235	3.9071565	FXRD	FXRD domain containing ion transport regulator 6
Cfa.4454.1.S1_at	4.02757E-0	8.86179E-0	16.339565	DKK3	Dickkopf 3 homolog (Xenopus laevis)
Cfa.15484.1.A1_at	0.000799016	0.000617928	3.5560951	MYO5B	myosin VB
CfaAffx.29003.1.S1_s_at	1.96308E-0	1.63359E-0	9.979354	MYO5B	myosin VB
CfaAffx.20685.1.S1_s_at	0.000245336	9.72345E-0	3.7215776	APOD	apolipoprotein D
Cfa.1715.1.S1_at	1.11941E-0	4.89444E-0	2.4505908	ALDH1A1	aldehyde dehydrogenase 1 family, member A1
Cfa.4426.1.S1_at	0.000464414	0.000258744	2.8490698	YWHAH	tyrosine 3--monooxygenase/tryptophan 5--monooxygenase activation protein, eta polypeptide
Cfa.4465.2.S1_at	0.000376595	0.000184314	8.410434	LOC100683822//LOC608238	immunoglobulin lambda--like polypeptide 5--like//immunoglobulin lambda--like polypeptide 5--like
Cfa.4465.2.S1_s_at	0.000158265	5.46895E-0	17.275257	LOC100683822//LOC100687054//LOC100856278//LOC486474//LOC607364//LOC607582//LOC608238//LOC608248	immunoglobulin lambda--like polypeptide 5--like//immunoglobulin lambda--like polypeptide 5--like//immunoglobulin lambda--like polypeptide 5--like//immunoglobulin lambda like polypeptide 5--like//immunoglobulin lambda--like polypeptide 5--like//immunoglobulin lambda--like polypeptide 5--like
Cfa.4578.1.A1_s_at	0.000630896	0.000420894	2.1680102	VAMP8	vesicle--associated membrane protein 8
Cfa.4710.1.A1_at	0.001007584	0.000910508	4.2544	GYG1	glycogenin 1
Cfa.11417.1.A1_at	0.00010727	3.30609E-0	3.7455792	AARS	alanyl--tRNA synthetase
Cfa.12076.1.A1_at	2.31584E-0	1.22532E-0	13.682153	SLC13A3	solute carrier family 13 (sodium--dependent dicarboxylate transporter), member 3
Cfa.12192.1.A1_s_at	7.67562E-0	2.01363E-0	2.9230626	PTGR1	prostaglandin reductase 1
Cfa.12195.8.A1_at	3.67438E-0	7.67008E-0	47.341812		
Cfa.1704.1.A1_at	0.000372714	0.000178272	2.5019126	LOC100683892	uncharacterized LOC100683892
Cfa.303.1.A1_at	0.000388689	0.000194618	5.5752703	XG	Xg blood group
Cfa.12290.1.A1_at	0.000705405	0.000508718	3.7441661	SFRP1	secreted frizzled--related protein 1
Cfa.12457.1.A1_at	0.000117222	3.73863E-0	2.3623722		
Cfa.5260.1.A1_at	0.000964912	0.000854675	2.04495	CBR14orf1	chromosome 8 open reading frame, human C14orf1
Cfa.6245.1.A1_at	0.000958026	0.000840182	4.664761	RBP2	retinol binding protein 2, cellular
CfaAffx.23994.1.S1_s_at	3.91866E-0	8.51161E-0	2.7927663	SLC2A9	solute carrier family 2 (facilitated glucose transporter), member 9
Cfa.307.9.A1_s_at	9.16789E-0	2.66872E-0	2.3184936	MRPL14	mitochondrial ribosomal protein L14
Cfa.12045.1.A1_at	0.000808263	0.000637192	2.442836		
Cfa.12118.1.A1_at	5.6345E-0	1.35101E-0	4.9605503	SGPL1	sphingosine--1--phosphate lyase 1
Cfa.5544.1.A1_at	7.79804E-0	2.07874E-0	2.4624555		
Cfa.10986.1.A1_s_at	0.000842522	0.00067938	2.1503632	ZNPF207	zinc finger protein 207
Cfa.400.1.A1_at	0.000415374	0.000213974	3.336148	TACC1	transforming, acidic coiled--coil containing protein 1
Cfa.12307.1.A1_at	0.000613164	0.000399551	6.305845	CHST15	carbohydrate (N--acetyl)galactosamine 4--sulfate 6--O) sulfotransferase 15
Cfa.4127.1.A1_at	0.000162829	5.68245E-0	5.2848372	SYBU	syntabulin (syntaxin--interacting)
Cfa.6387.1.A1_at	0.000203002	7.59475E-0	3.9649045	PPP4	dipeptidyl--peptidase 4
Cfa.12136.1.A1_at	0.000523698	0.000312446	3.9189298	ADA	adenosine deaminase
Cfa.10817.1.A1_at	0.000771661	0.000585548	3.241774		
Cfa.4784.1.A1_at	0.000866656	0.000712638	2.5297263	LOC100856418	RIMS--binding protein 2--like
Cfa.12195.14.S1_s_at	0.000343698	0.000162881	8.812621	IGKC	
Cfa.2571.1.A1_at	0.000550193	0.000340669	3.5736191	OBFC1	oligonucleotide/oligosaccharide--binding fold containing 1
Cfa.11599.1.A1_at	0.000333152	0.000155064	2.2552266	SORT1	soritin 1

Cfa.4712.1.A1_at	0.001071813	0.001066809	4.8869042	ZBTB38	zinc finger and BTB domain containing 38
Cfa.12371.1.A1_s_at	0.000100575	3.04988E--0	8.058077	FMO2	flavin containing monooxygenase 2 (non--functional)
Cfa.537.1.S1_at	7.45187E--0	9.24915E--0	2.1957808	GSTA4	glutathione S--transferase alpha 4
Cfa.1364.1.A1_s_at	0.000459822	0.000252286	2.4105124	RPN2	ribophorin II
Cfa.5627.1.A1_at	0.000684929	0.000479051	6.082355	SFRP4	secreted frizzled---related protein 4
Cfa.1133.1.A1_s_at	6.32485E--0	1.56406E--0	5.9039884	SLC25A33	solute carrier family 25 (pyrimidine nucleotide carrier), member 33
Cfa.15210.1.A1_at	3.67809E--0	2.12696E--0	9.81365		
Cfa.11787.1.A1_at	0.000491787	0.000285777	6.3062377	CYFIP2	cytoplasmic FMR1 interacting protein 2
Cfa.6898.1.A1_at	0.000885302	0.000736392	7.212905		
Cfa.11206.1.A1_at	8.95124E--0	2.52804E--0	4.0430956	GABRB3	gamma--aminobutyric acid (GABA) A receptor, beta 3
Cfa.5258.1.A1_s_at	0.000265028	0.000109957	2.92875	SDC2	syndecan 2
Cfa.1176.1.S1_at	0.000447109	0.000239611	2.499946	GRSF1	G--rich RNA sequence binding factor 1
Cfa.10395.1.A1_at	0.000330652	0.000151294	2.8875067	IRGQ	immunity--related GTPase family, Q
Cfa.349.1.A1_s_at	7.69533E--0	5.31835E--0	2.5315976	DST	dystonin
Cfa.12553.1.A1_s_at	0.000372714	0.000178051	4.260033	GFPT2	glutamine--fructose--6--phosphate transaminase 2
Cfa.11159.1.S1_at	0.000964788	0.000849122	2.627128	ATP6V0D1	ATPase, H+ transporting, lysosomal 38kDa, V0 subunit d1
Cfa.15225.1.S1_s_at	0.000736475	0.000547422	2.0888155	CPT2	carnitine palmitoyltransferase 2
Cfa.6941.1.S1_s_at	0.00083129	0.000662452	7.0080214	ZNF474	zinc finger protein 474--like
Cfa.13710.1.S1_at	0.000561696	0.00035413	2.646721	TGFB3	transforming growth factor, beta receptor III
Cfa.6237.1.S1_at	0.0002354	9.29648E--0	11.46203	TSAN8	tetraspanin 8
Cfa.10879.1.S1_at	0.000972321	0.000863981	2.110705	FSD1L	fibronectin type III and SPRY domain containing 1--like
Cfa.15549.1.A1_s_at	0.00069238	0.000497068	3.5878794	MSN	moesin
Cfa.4948.1.A1_s_at	0.001097984	0.001048428	2.0224166	ECM2	extracellular matrix protein 2, female organ and adipocyte specific
CfaAffx.19812.1.S1_s_at	0.001109468	0.001076607	2.9654722	ANK3	ankyrin 3, node of Ranvier (ankyrin G)
Cfa.1004.1.A1_at	0.000843029	0.000681774	7.594965	ADCY10	adenylate cyclase 10 (soluble)
Cfa.14230.1.A1_at	0.000907407	0.000774303	3.621418	PMPEA1	prostate transmembrane protein, androgen induced 1
Cfa.13057.1.A1_s_at	0.000718476	0.00052695	3.2985606	PDE6D	phosphodiesterase 6D, cGMP---specific, rod, delta
Cfa.7574.1.A1_s_at	0.001052243	0.000983446	2.820961		
Cfa.2048.1.S1_at	1.98035E--0	3.17561E--0	2.0343955	HIBADH	3--hydroxyisobutyrate dehydrogenase
Cfa.1645.1.S1_at	0.000372714	0.00017926	15.523831	MYH11	myosin, heavy chain 11, smooth muscle
Cfa.2294.1.S1_at	0.000615427	0.000401894	2.0155952		
Cfa.1243.1.A1_at	0.000464414	0.000258251	3.9472747	TUSC3	tumor suppressor candidate 3
Cfa.1970.1.S1_at	0.000842522	0.000679722	2.0129232		
Cfa.2111.1.S1_at	0.000535067	0.000321493	5.3657737	SLA	Src--like--adaptor
Cfa.9797.1.A1_at	0.000719982	0.00052907	2.3941298	P2RX4	purinergic receptor P2X, ligand--gated ion channel, 4
Cfa.15691.1.A1_at	1.17904E--0	8.81368E--0	6.274625		
Cfa.14174.1.A1_at	0.000447109	0.000241527	2.3447382		
Cfa.15412.1.A1_s_at	0.000178355	6.38957E--0	2.357841	ABCD4	ATP--binding cassette, sub--family D (ALD), member 4
Cfa.5543.1.A1_at	0.000949939	0.000828004	4.283221		
Cfa.8129.1.A1_s_at	0.000727566	0.000537722	2.4103203	R3HCC1	R3H domain and coiled--coil containing 1
Cfa.9500.1.S1_at	0.000617584	0.000405915	4.7807	TCEAL1	transcription elongation factor A (SII)--like 1
Cfa.21641.1.S1_at	0.000415374	0.00021501	2.046423	RCN2	reticulocalbin 2, EF--hand calcium binding domain
Cfa.10210.1.S1_at	0.000635775	0.000425045	5.966225	ALOX5AP	arachidonate 5--lipoxygenase--activating protein
Cfa.10687.1.S1_at	0.000129211	4.37385E--0	12.138619	STK39	serine threonine kinase 39
Cfa.17716.1.S1_s_at	0.000842522	0.000676815	2.2854202	TMED5	transmembrane emp24 protein transport domain containing 5
Cfa.16351.1.S1_at	2.74704E--0	5.34684E--0	14.262284	FRY	furry homolog (Drosophila)
Cfa.19737.1.S1_at	0.000666841	0.000457364	2.280433	AHR	aryl hydrocarbon receptor
Cfa.19610.1.S1_s_at	0.000447109	0.00023973	2.4912512	SLC30A6	solute carrier family 30 (zinc transporter), member 6
Cfa.6381.1.A1_at	0.000375619	0.000182776	3.0846417	LPHN2	latrophilin 2
Cfa.19866.1.S1_at	0.000302104	0.000130812	2.6602774	SLC1A4	solute carrier family 1 (glutamate/neutral amino acid transporter), member 4
Cfa.9955.1.A1_at	0.000203413	7.66028E--0	2.511433	LOC100685792	interferon--activable protein 203--like
Cfa.15309.1.A1_at	0.000470841	0.000266235	2.8773222	ADPRM	ADP--ribose/CDP--alcohol diphosphatase, manganese--dependent
Cfa.8856.1.A1_s_at	0.000667705	0.000459577	2.7355921	TTL1	tubulin tyrosine ligase--like family, member 7
Cfa.1340.1.S1_at	0.000888601	0.000746353	5.576259	CLTCL1	clathrin, heavy chain--like 1
Cfa.1230.1.S1_at	8.30692E--0	2.27298E--0	4.046356	GPM6A	glycoprotein M6A
Cfa.247.1.S1_at	1.95479E--0	2.38186E--1	2.9497216	GLUD1///LOC100856077	glutamate dehydrogenase 1///interferon gamma receptor 1--like
Cfa.9940.2.S1_at	0.000464414	0.000258025	2.5428064		
Cfa.9007.1.A1_at	0.001007584	0.000911316	6.2394586	ANKRD37	ankyrin repeat domain 37
CfaAffx.16848.1.S1_s_at	0.001019401	0.000937446	3.3601415	LOC100855477	CDGSH iron--sulfur domain--containing protein 2--like
Cfa.18191.1.S1_s_at	0.001136777	0.001127157	3.1705344	CAP2	CAP, adenylate cyclase--associated protein, 2 (yeast)
Cfa.11172.1.A1_at	0.000407252	0.000207934	2.0523455		
Cfa.1373.1.S1_at	2.38444E--0	2.15239E--0	15.373627		
Cfa.2356.1.S1_at	0.000636647	0.000426897	2.2827692	CGGBP1	CGG triplet repeat binding protein 1
Cfa.4399.1.S1_at	0.000464414	0.000259391	2.4086745		
Cfa.10416.1.S1_at	4.25619E--0	4.32223E--0	6.694993	FAM177A1	family with sequence similarity 177, member A1
Cfa.10960.2.A1_s_at	0.000200245	7.42797E--0	2.1633456	CDK2AP1	cyclin--dependent kinase 2 associated protein 1
Cfa.1007.1.S1_at	2.18422E--0	3.69554E--0	2.2912052	PKD1	pyruvate dehydrogenase kinase, isozyme 1
Cfa.9369.1.S1_at	1.56269E--0	2.40316E--0	20.815073		
Cfa.1650.1.S1_at	0.00105121	0.000980042	2.5132136	PPP2R3C	protein phosphatase 2, regulatory subunit B", gamma
Cfa.6009.2.A1_at	0.000802554	0.000626101	2.0153184	FBLN1	fibulin 1
Cfa.13388.1.S1_at	1.21483E--0	1.73057E--0	2.9907348	SLC44A1	solute carrier family 44, member 1
Cfa.1655.2.A1_a_at	2.1186E--0	5.37868E--1	30.454763	KCNJ5	potassium inwardly--rectifying channel, subfamily I, member 5
Cfa.18215.1.S1_at	0.00101319	0.000930306	6.4261928		
Cfa.10541.1.S1_at	6.76839E--0	4.58226E--0	23.238184	NADKD1///RANB P3L	NAD kinase domain containing 1///RAN binding protein 3--like
Cfa.19510.1.S1_at	0.000728266	0.000539266	4.191199	NEO1	neogenin 1
Cfa.14613.1.A1_s_at	2.07069E--0	3.38787E--0	8.389631	RSPO3	R--spondin 3
Cfa.19444.1.S1_at	0.000425615	0.000222112	5.6322074		
CfaAffx.13734.1.S1_s_at	0.000447449	0.000242406	5.2590218	CNCG2	cyclin G2
Cfa.9415.1.S1_s_at	0.000609542	0.000487957	2.0805297	HERC1	HECT and RLD domain containing E3 ubiquitin protein ligase family member 1
Cfa.20099.1.S1_s_at	0.000203002	7.61615E--0	7.294184	LOC100856496	E3 ubiquitin--protein ligase SIAH1--like
Cfa.18229.1.S1_s_at	0.000104711	3.19008E--0	5.7194967	TACC1	transforming, acidic coiled--coil containing protein 1
Cfa.4155.1.A1_at	1.95479E--0	2.4814E--1	22.72636		
Cfa.10658.1.A1_at	1.09643E--0	4.33006E--0	4.3983965	LRAT	lecithin retinol acyltransferase (phosphatidylcholine-----retinol O--
Cfa.17154.1.S1_at	1.15223E--0	1.5764E--0	2.4392455	SORD	sorbitol dehydrogenase
Cfa.16886.1.A1_at	0.00064036	0.000432504	5.552202	LOC100686908	zinc finger protein 652--like
Cfa.4077.1.S1_at	0.00069238	0.000492743	2.7095726	CA4	carbonic anhydrase IV
Cfa.16407.1.A1_at	1.88349E--0	4.51613E--1	13.849963	CDK	deoxycytidine kinase
Cfa.966.1.S1_s_at	7.82572E--0	2.09716E--0	2.0592682	BZW1	basic leucine zipper and W2 domains 1
Cfa.4315.1.S1_at	0.000100349	3.02792E--0	2.2582934	PHB	prohibitin
Cfa.17867.1.S1_s_at	3.16223E--0	6.33338E--0	3.6392202	NUCB1	nucleobindin 1
Cfa.21306.1.S1_at	5.48944E--0	1.26977E--0	6.3926473	TSPAN13	tetraspanin 13
Cfa.4482.1.S1_at	2.40555E--0	4.30895E--0	8.92449	PEG3	paternally expressed 3
Cfa.13282.2.A1_a_at	4.02123E--0	8.79112E--0	2.060062	BRP44	brain protein 44
Cfa.13282.1.S1_s_at	6.72416E--0	4.39369E--0	2.9895825	BRP44	brain protein 44
Cfa.3177.1.S1_at	7.28557E--0	8.83722E--0	6.9751554	GNAI1	guanine nucleotide binding protein (G protein), alpha inhibiting activity polypeptide 1
Cfa.21159.1.S1_at	0.000587177	0.000379305	4.412333	RG55	regulator of G--protein signaling 5
Cfa.17583.1.S1_at	0.000541885	0.000333233	4.619514	RRAD	Ras--related associated with diabetes
Cfa.16552.1.S1_at	0.000384341	0.000190992	2.6200385	TM2D1	TM2 domain containing 1
Cfa.17831.1.S1_s_at	9.55249E--0	2.8159E--0	5.469524	FMOD	fibromodulin
Cfa.17308.1.S1_s_at	0.000809233	0.000639168	3.6815317	AARS	alanyl--tRNA synthetase
Cfa.17338.1.S1_s_at	0.000785079	0.000601186	3.097648	PRKAB1	protein kinase, AMP--activated, beta 1 non--catalytic subunit
Cfa.4276.1.S1_at	0.001083552	0.001025718	2.6564686	C3H4orf48	chromosome 3 open reading frame, human C4orf48
Cfa.21591.1.S1_at	0.000765337	0.00057859	3.3628395	38595	sepin 9
Cfa.21171.1.S1_s_at	0.001109468	0.001076533	2.1432447	PRKAR2A	protein kinase, cAMP--dependent, regulatory, type II, alpha
Cfa.18925.1.S1_s_at	0.000711146	0.000518565	7.0233626	MSN	moesin
CfaAffx.2475.1.S1_s_at	0.00089413	0.000755904	7.3695903	TRMT11	tRNA methyltransferase 11 homolog (S. cerevisiae)
Cfa.20009.1.S1_s_at	0.00025257	0.000102239	3.5902214	PSME4	proteasome (prosome, macropain) activator subunit 4
Cfa.4202.1.S1_at	2.18422E--0	3.69684E--0	2.639591		
Cfa.21480.1.S1_s_at	0.000942658	0.000819009	6.1842012	SIAE	sialic acid acetyltransferase
Cfa.18701.1.S1_s_at	0.000964912	0.000852068	2.0781698	TMEM27	transmembrane protein 27
Cfa.21318.2.S1_at	0.00064036	0.000434433	4.766016	AGPAT9	1--acylglycerol--3--phosphate O--acyltransferase 9
Cfa.18326.1.S1_s_at	3.62662E--0	7.46808E--0	14.165292	SORD	sorbitol dehydrogenase
Cfa.16748.2.S1_s_at	0.000808263	0.000637262	2.834584	CRIPT	cysteine--rich PDZ--binding protein

Cfa.20931.1.S1_s_at	0.00012228	4.07025E--0	2.9557915	PDXK	pyridoxal (pyridoxine, vitamin B6) kinase
Cfa.19950.1.S1_s_at	0.000570153	0.000361874	2.6671698	SESTD1	SEC14 and spectrin domains 1
CfaAffx.1251.1.S1_s_at	0.000936071	0.000810646	2.3345058	LRP1	low density lipoprotein receptor---related protein 1
Cfa.17869.1.S1_s_at	1.21483E--0	1.71617E--0	4.234617	TTC7B	tetratricopeptide repeat domain 7B
Cfa.17312.1.S1_s_at	0.001034634	0.000958751	3.0220814	SSFA2	sperm specific antigen 2
CfaAffx.3839.1.S1_s_at	0.000802554	0.000627102	4.3794575	TXNRD1	thioredoxin reductase 1
Cfa.14623.1.S1_at	0.000291781	0.000124285	3.2112064	TGM2	transglutaminase 2 (C polypeptide, protein---glutamine---gamma---glutamyltransferase)
Cfa.1584.2.S1_s_at	2.07069E--0	3.36605E--0	23.459467	HPGD5	hematopoietic prostaglandin D synthase
Cfa.19943.1.S1_s_at	0.000933946	0.000807488	6.369647	ATP1B3	ATPase, Na+/K+ transporting, beta 3 polypeptide
Cfa.19882.1.S1_s_at	0.000541885	0.000331747	5.2500777	GRINA	glutamate receptor, ionotropic, N---methyl D---aspartate---associated protein 1 (glutamate binding)
Cfa.18719.1.S1_s_at	0.000652019	0.000445102	2.7240605	LOC100856736	heat shock factor---binding protein 1---like
Cfa.17300.1.S1_at	3.72653E--0	5.78164E--1	12.6078825	NADKD1	NAD kinase domain containing 1
Cfa.17300.1.S1_s_at	1.05304E--0	7.00867E--1	21.954231	NADKD1///RANB P3L	NAD kinase domain containing 1///RAN binding protein 3---like
Cfa.19934.1.S1_at	0.000536515	0.000326147	5.123675	NMT2	N---myristoyltransferase 2
Cfa.17299.1.S1_at	8.70168E--1	1.50772E--1	19.232334	NADKD1///RANB P3L	NAD kinase domain containing 1///RAN binding protein 3---like
Cfa.20149.1.S1_at	0.001121901	0.001098166	6.965492	CHD1L	chromodomain helicase DNA binding protein 1---like
Cfa.19578.1.S1_s_at	0.000423563	0.000220444	4.015751	CRYZL1///LOC100856647	crystallin, zeta (quinone reductase)---like 1///quinone oxidoreductase---like protein
Cfa.15967.1.S1_at	9.13862E--0	1.19872E--0	2.2081788	FADS6	fatty acid desaturase domain family, member 6
Cfa.4285.1.A1_at	0.000309434	0.000139706	4.5511416		
Cfa.11597.1.A1_at	0.000493269	0.00028803	5.446816	SAMD11	sterile alpha motif domain containing 11
Cfa.15530.1.A1_at	0.000907051	0.000772721	5.8292747		
Cfa.7780.1.A1_s_at	0.000805603	0.000631756	4.0453043	RANGRF	RAN guanine nucleotide release factor
Cfa.2441.1.A1_at	0.000381539	0.000188886	5.692052		
Cfa.13124.1.A1_at	8.95124E--0	2.54608E--0	2.59982	AKR1D1	3---oxo---5---beta---steroid 4---dehydrogenase---like
Cfa.8532.1.A1_s_at	0.000296038	0.000126933	5.4359665	SEMA3D	sema domain, immunoglobulin domain (Ig), short basic domain, secreted, (semaphorin) 3D
Cfa.13318.1.A1_at	0.00100411	0.000903557	2.6066477		
Cfa.13245.1.A1_at	5.07964E--0	1.16065E--0	2.5273943		
Cfa.5339.1.A1_at	4.39635E--0	4.58857E--0	25.095253		
Cfa.11974.1.A1_at	0.00089413	0.000756668	6.4765005		
Cfa.2388.1.A1_at	0.00012163	4.0143E--0	3.09967	BCO2	beta---carotene oxygenase 2
Cfa.9289.1.A1_at	2.65316E--0	4.97701E--0	17.101181	DAB1	disabled homolog 1 (Drosophila)
Cfa.1817.1.A1_at	0.000579986	0.000372206	3.3853162	PCDH18	protocadherin 18
Cfa.3003.1.A1_s_at	0.000500934	0.000293965	2.0361366	ZAK	sterile alpha motif and leucine zipper containing kinase AZK
Cfa.9744.1.A1_at	2.62432E--0	8.14316E--1	70.02661		
Cfa.10541.2.A1_at	8.70168E--1	2.45464E--1	39.60929		
Cfa.13971.1.A1_at	0.000493269	0.000287547	4.816408		
Cfa.13336.1.A1_at	0.000215481	8.20591E--0	2.840348	AHR	aryl hydrocarbon receptor
Cfa.13181.1.A1_at	0.000272981	0.000114989	3.8197572	SLC6A11	solute carrier family 6 (neurotransmitter transporter, GABA), member 11
Cfa.13297.1.A1_at	0.001007584	0.000912826	4.374981		
Cfa.15285.3.S1_at	0.000888601	0.000741952	6.0946283	CSRP1	cysteine and glycine---rich protein 1
Cfa.13327.1.A1_s_at	0.000118868	3.86369E--0	3.6391299	GALNT13	UDP--N---acetyl--alpha--D---galactosamine:polypeptide N---acetylglucosaminyltransferase 13 (GalNAc---T13)
Cfa.10687.2.S1_s_at	0.000571476	0.000364102	11.637523	STK39	serine threonine kinase 39
Cfa.13607.1.A1_at	0.000510449	0.000300942	2.7555273		
Cfa.9467.1.A1_at	0.000226226	8.80654E--0	2.7485807	RELN	reelin
Cfa.9789.1.A1_at	5.85442E--0	1.42025E--0	5.017309		
Cfa.14588.1.A1_at	0.001116423	0.001088079	6.016479		
Cfa.4752.1.A1_at	1.44458E--0	2.09861E--0	4.5659337		
Cfa.4619.1.A1_at	0.001100508	0.001053942	5.625718		
Cfa.5711.1.A1_at	0.000404964	0.000206195	9.75789		
Cfa.11642.3.A1_s_at	0.000377688	0.000185381	7.782459	ACTG2	actin, gamma 2, smooth muscle, enteric
Cfa.1953.1.A1_at	8.72797E--0	1.09561E--0	3.801019	TMEM168	transmembrane protein 168
Cfa.16452.2.S1_s_at	0.000189774	6.90574E--0	17.11082	MYH11	myosin, heavy chain 11, smooth muscle
CfaAffx.227.1.S1_s_at	0.001136777	0.001125108	2.1219134	BRP44L	brain protein 44---like
CfaAffx.471.1.S1_s_at	0.000541885	0.000333096	6.3948736	LOC478825///TUBB4B	tubulin beta---3 chain---like///tubulin, beta 4b class IVb
CfaAffx.741.1.S1_at	0.000470841	0.000265897	2.991092	FYB	FYB binding protein
CfaAffx.747.1.S1_s_at	2.40826E--0	4.34791E--0	2.184471	DBI///LOC608150	diazepam binding inhibitor (GABA receptor modulator, acyl---CoA binding protein)///acyl---CoA---binding protein---like
CfaAffx.1080.1.S1_at	0.000688951	0.000484202	2.3575935	KDSR	3---ketodihydroxyphenylacetate reductase
CfaAffx.1171.1.S1_at	0.000449158	0.000245168	4.0240787	SPRYD4	SPRY domain containing 4
CfaAffx.1280.1.S1_at	0.000519386	0.000308409	2.0482295	FEM1C	fem---1 homolog C (C. elegans)
CfaAffx.1647.1.S1_at	1.44146E--0	1.1182E--0	10.425791	LGR5	leucine---rich repeat containing G protein---coupled receptor 5
CfaAffx.1657.1.S1_at	0.000958026	0.0008409	2.9815702	TBC1D15	TBC1 domain family, member 15
CfaAffx.1679.1.S1_at	0.000447109	0.00024106	6.4707417	NIPAL2	NIPA---like domain containing 2
CfaAffx.1720.1.S1_s_at	2.19496E--0	3.81129E--0	15.367436	LOC100687624///ZNF474	zinc finger protein 474---like///zinc finger protein 474---like
CfaAffx.1974.1.S1_at	0.000161974	5.61996E--0	3.952404	RSPD2	R---spondin 2
CfaAffx.2129.1.S1_s_at	2.40826E--0	4.41571E--0	5.2711277	FBLN1	fibulin 1
CfaAffx.2197.1.S1_s_at	0.000309434	0.000140096	3.3562727	DLA---DMA	major histocompatibility complex, class II, DM alpha
CfaAffx.2338.1.S1_s_at	0.000179281	6.44803E--0	3.4948668	CYB5K3	cytochrome b5 reductase 3
CfaAffx.2447.1.S1_s_at	0.000888601	0.00074823	4.528036	LOC100683164///LOC609086///NHP2L1	NHP2---like protein 1---like///NHP2---like protein 1---like///NHP2 non---histone chromosome protein 2---like 1 (S. cerevisiae)
CfaAffx.2997.1.S1_x_at	0.00029873	0.000128509	4.1627393		
CfaAffx.3286.1.S1_at	0.00105737	0.000991751	2.933598	GNA14	guanine nucleotide binding protein (G protein), alpha 14
CfaAffx.3464.1.S1_at	0.001140238	0.00113863	3.8542662	TEK	TEK tyrosine kinase, endothelial
CfaAffx.3596.1.S1_s_at	1.69727E--0	3.62372E--1	3.0253198	ALDH1A1	aldehyde dehydrogenase 1 family, member A1
CfaAffx.3791.1.S1_s_at	0.000904094	0.000768926	2.5792792	NUDT2	nudix (nucleoside diphosphate linked moiety X)---type motif 2
CfaAffx.4021.1.S1_s_at	6.44776E--0	7.36627E--0	10.234394	KIT	v---kit Hardy---Zuckerman 4 feline sarcoma viral oncogene homolog
CfaAffx.4145.1.S1_at	0.000888601	0.000742951	2.9290287	SYK	spleen tyrosine kinase
CfaAffx.4252.1.S1_s_at	1.98035E--0	3.18421E--0	2.7453666	GSTA4	glutathione S---transferase alpha 4
CfaAffx.4258.1.S1_s_at	0.000949939	0.000828014	4.0430226	ICK	intestinal cell (MAK---like) kinase
CfaAffx.4323.1.S1_s_at	7.17259E--0	1.84006E--0	2.9262464	ECM2	extracellular matrix protein 2, female organ and adipocyte specific
CfaAffx.4524.1.S1_s_at	0.000981938	0.00087668	4.872234	TSPAN13	tetraspanin 13
CfaAffx.4552.1.S1_at	5.61993E--0	1.3256E--0	3.4679244	AHR	aryl hydrocarbon receptor
CfaAffx.4964.1.S1_s_at	0.001031596	0.000953026	2.5226119	ARF1	ADP---ribosylation factor 1
CfaAffx.5317.1.S1_at	0.000334623	0.000156221	5.295739	CDK	deoxycytidine kinase
CfaAffx.5338.1.S1_at	0.000226627	8.85411E--0	2.1865406	SLC4A4	solute carrier family 4, sodium bicarbonate cotransporter, member 4
CfaAffx.5344.1.S1_at	0.000690088	0.000486663	3.3873628	SLC4A4	solute carrier family 4, sodium bicarbonate cotransporter, member 4
CfaAffx.5402.1.S1_s_at	0.000115309	3.64306E--0	3.4740286	HIBADH	3---hydroxyisobutyrate dehydrogenase
CfaAffx.5887.1.S1_x_at	0.000296038	0.000126607	3.1467137	DOCK4	dedicator of cytokinesis 4
CfaAffx.6119.1.S1_s_at	0.000193352	7.11776E--0	14.682623	TNC	tenascin C
CfaAffx.6597.1.S1_s_at	6.32485E--0	1.57189E--0	2.6400685	FTL	ferritin, light polypeptide
CfaAffx.6815.1.S1_at	9.05611E--0	6.38653E--0	4.677633	SLC16A10	solute carrier family 16, member 10 (aromatic amino acid transporter)
CfaAffx.7216.1.S1_s_at	0.000473418	0.000268426	3.3396316	PIP4K2A	phosphatidylinositol---5---phosphate 4---kinase, type II, alpha
CfaAffx.7249.1.S1_s_at	4.92793E--0	3.05824E--0	2.6368322	GLUD1	glutamate dehydrogenase 1
CfaAffx.8128.1.S1_s_at	0.000272981	0.000115122	6.4206185	GAB2///NARS2	GRB2---associated binding protein 2///asparaginyl---tRNA synthetase 2, mitochondrial (putative)
CfaAffx.8488.1.S1_at	2.40939E--0	4.45177E--0	2.3166409	SLC6A11	solute carrier family 6 (neurotransmitter transporter, GABA), member 11
CfaAffx.9050.1.S1_s_at	0.00023311	9.17315E--0	2.590134	APEX1	APEX nuclease (multifunctional DNA repair enzyme) 1
CfaAffx.9091.1.S1_s_at	0.001096351	0.001045322	2.0753102	SLC02B1	solute carrier organic anion transporter family, member 2B1
CfaAffx.9168.1.S1_at	2.31975E--0	4.08982E--0	6.944003	DSTN	desmin (actin depolymerizing factor)
CfaAffx.9237.1.S1_at	0.00088968	0.000728134	6.3423076	MBNL2	muscleblind---like splicing regulator 2
CfaAffx.9556.1.S1_at	0.001093337	0.001037822	2.6318173	FRP1	secreted frizzled---related protein 1
CfaAffx.10216.1.S1_at	0.001083552	0.001027006	5.6280727	TUBGCP3	tubulin, gamma complex associated protein 3
CfaAffx.10453.1.S1_s_at	0.00024734	9.90755E--0	3.8527875	PKD1	pyruvate dehydrogenase kinase, isozyme 1
CfaAffx.10624.1.S1_at	0.000596747	0.000388012	5.0495954	EIF4E3	eukaryotic translation initiation factor 4E family member 3
CfaAffx.10969.1.S1_at	0.000196849	7.27424E--0	6.94748	FLT1	fms---related tyrosine kinase 1 (vascular endothelial growth factor/vascular permeability factor receptor)
CfaAffx.11014.1.S1_at	0.000304654	0.000133059	5.015389	SYT9	synaptotagmin IX
CfaAffx.11275.1.S1_s_at	0.000226226	8.76752E--0	2.009499	LOC100688649	uncharacterized LOC100688649

ClaAffx.11491.1.S1_at	3.31907E--0	6.69431E--0	11.075902	CSAD	cysteine sulfinic acid decarboxylase
ClaAffx.11514.1.S1_at	1.57479E--0	2.46547E--0	22.331785	CYP7A1	cytochrome P450, family 7, subfamily A, polypeptide 1
ClaAffx.11845.1.S1_at	0.000269147	0.000112366	3.752204	PRRG4	proline rich G4 (G---carboxyglutamic acid) 4 (transmembrane)
ClaAffx.11970.1.S1_at	0.000536041	0.000324346	6.592709	ABHD6	abhydrolase domain containing 6
ClaAffx.12206.1.S1_at	0.000754313	0.000568129	6.080185	LOC100855424	hedgheg--interacting protein--like
ClaAffx.12247.1.S1_at	0.000958026	0.000838239	2.4949484	PAM	peptidylglycine alpha--amidating monooxygenase
ClaAffx.12273.1.S1_s_at	0.001103782	0.001058634	2.6890967	NMNAT3	nicotinamide nucleotide adenyltransferase 3
ClaAffx.12439.1.S1_at	0.000795043	0.000613383	5.5372734	ATP1B3	ATPase, Na+/K+ transporting, beta 3 polypeptide
ClaAffx.12697.1.S1_s_at	7.20569E--0	1.85986E--0	6.069988	ROBO1	roundabout, axon guidance receptor, homolog 1 (Drosophila)
ClaAffx.12712.1.S1_s_at	3.91866E--0	8.41243E--0	3.4833987	ROBO1	roundabout, axon guidance receptor, homolog 1 (Drosophila)
ClaAffx.12761.1.S1_s_at	0.000932331	0.000804777	3.1924503	EMC4	ER membrane protein complex subunit 4
ClaAffx.12853.1.S1_at	0.000535067	0.000320662	2.6022103	LOC611428	UPF0672 protein C3orf58--like
ClaAffx.13018.1.S1_at	0.000444394	0.000234419	3.5755334	FCHO2	FCH domain only 2
ClaAffx.13076.1.S1_at	1.19152E--0	1.64695E--0	17.273584	CPA3	carboxypeptidase A3 (mast cell)
ClaAffx.13342.1.S1_at	0.000557411	0.000346711	2.215817	VEGFC	vascular endothelial growth factor C
ClaAffx.13352.1.S1_at	1.24761E--0	5.80692E--0	29.15885	LOC486100	L--gulonolactone oxidase--like
ClaAffx.13409.1.S1_at	2.1005E--0	1.83683E--0	8.286384	LRAT	lecithin retinol acyltransferase (phosphatidylcholine-----retinol O--
ClaAffx.13623.1.S1_at	0.000304868	0.000133729	3.8605843	STBD1	starch binding domain 1
ClaAffx.13822.1.S1_s_at	0.00054245	0.000334345	2.6787975	THBS1	thrombospondin 1
ClaAffx.14130.1.S1_at	0.000110638	3.46172E--0	5.0477967	SFXN5	sideroflexin 5
ClaAffx.14369.1.S1_at	0.00048708	0.00027892	7.484151	HPSE	heparanase
ClaAffx.14657.1.S1_at	0.000682784	0.000473808	4.048732	FAM82A2	family with sequence similarity 82, member A2
ClaAffx.14671.1.S1_s_at	8.23276E--0	2.22946E--0	2.9472491	FAM82A2	family with sequence similarity 82, member A2
ClaAffx.14892.1.S1_at	4.62343E--0	4.8908E--0	8.701089	FMOD	fibromodulin
ClaAffx.15184.1.S1_s_at	0.000376265	0.000183621	3.1303012	SCD	stearoyl--CoA desaturase (delta--9--desaturase)
ClaAffx.15421.1.S1_s_at	0.000178103	6.35543E--0	8.135605	TBC1D7	TBC1 domain family, member 7
ClaAffx.15444.1.S1_s_at	3.13959E--0	3.09973E--0	13.439858	NKD1	naked cuticle homolog 1 (Drosophila)
ClaAffx.15752.1.S1_at	9.93408E--0	2.9564E--0	16.204338	GABRB3	gamma--aminobutyric acid (GABA) A receptor, beta 3
ClaAffx.15830.1.S1_s_at	4.63365E--0	1.03813E--0	2.0973158	SEMA5A	sema domain, seven thrombospondin repeats (type 1 and type 1--like), transmembrane domain (TM) and short cytoplasmic domain, (semaphorin) 5A
ClaAffx.16017.1.S1_s_at	0.001007584	0.000914103	3.725349	ARHGAP32	Rho GTPase activating protein 32
ClaAffx.16168.1.S1_at	0.00068284	0.000475773	4.8904185	DPFPA2	developmental pluripotency associated 2
ClaAffx.16227.1.S1_at	7.10612E--0	8.51932E--0	8.877456	PHLDB2///PLCXD2	pleckstrin homology--like domain, family B, member 2///phosphatidylinositol--specific phospholipase C, X domain containing 2
ClaAffx.16313.1.S1_s_at	8.85038E--0	2.47162E--0	5.657892	CPNE8	copine VIII
ClaAffx.16356.1.S1_at	0.000375542	0.00018115	2.732608	HSPD1	heat shock 60kDa protein 1 (chaperonin)
ClaAffx.16371.1.S1_at	0.000855977	0.00066613	5.6205015	SYT10	synaptotagmin X
ClaAffx.16401.1.S1_at	0.000885302	0.000736711	7.3724662	SPPL3	signal peptidase like 3
ClaAffx.16457.1.S1_s_at	0.000265028	0.000110273	4.8716867	SLC13A3	solute carrier family 13 (sodium--dependent dicarboxylate transporter), member 3
ClaAffx.16529.1.S1_s_at	0.00069238	0.000493174	2.4281223	VIMP	VCP--interacting membrane protein
ClaAffx.16558.1.S1_at	0.000559542	0.000350405	5.316946	RGS2	regulator of G--protein signaling 2, 24kDa
ClaAffx.16663.1.S1_at	0.000375547	0.000182212	4.985196	SLC16A14	solute carrier family 16, member 14 (monocarboxylic acid transporter 14)
ClaAffx.17171.1.S1_s_at	6.32485E--0	1.5879E--0	2.6268845	CHD1L	chromodomain helicase DNA binding protein 1--like
ClaAffx.17218.1.S1_s_at	0.000122402	4.09159E--0	7.56362	LGMM	legumain
ClaAffx.17446.1.S1_at	0.00105121	0.000979517	5.424298	SIAE	sialic acid acetyltransferase
ClaAffx.17502.1.S1_at	2.31584E--0	1.22192E--0	29.840849	AXIN2	axin 2
ClaAffx.17636.1.S1_at	0.000764269	0.000576705	2.2316697	GET4	golgi to ER traffic protein 4 homolog (S. cerevisiae)
ClaAffx.18273.1.S1_at	0.000423563	0.00022028	5.9526463	FCER1A	Fc fragment of IgE, high affinity 1, receptor for; alpha polypeptide
ClaAffx.18371.1.S1_s_at	0.000688951	0.000483827	2.7532446	CERS6	ceramide synthase 6
ClaAffx.18457.1.S1_at	0.001135682	0.001121265	2.4227931	LOC100688543///LOC100688763	UDP--glucuronosyltransferase 1--B--like//UDP--glucuronosyltransferase 1--A--like
ClaAffx.18602.1.S1_s_at	0.000638096	0.000420281	2.6839082	ZNRF3	zinc and ring finger 3
ClaAffx.18906.1.S1_at	0.00056074	0.000352667	2.208585	LOC100856343	translation initiation factor eIF--2B subunit epsilon--like
ClaAffx.18955.1.S1_s_at	0.000576703	0.000368472	3.0803466	ACTA1	actin, alpha 1, skeletal muscle
ClaAffx.19086.1.S1_at	0.000805603	0.000631271	3.384487	LOC100855619	insulin--like growth factor--binding protein 3--like
ClaAffx.19194.1.S1_at	1.11941E--0	4.80148E--0	2.4686623	SLC01B3	solute carrier organic anion transporter family, member 1B3
ClaAffx.19341.1.S1_at	0.000384341	0.000191357	3.690166	STXBP6	syntaxis binding protein 6 (amisyn)
ClaAffx.19874.1.S1_at	0.000882335	0.000731753	2.4669995		
ClaAffx.19898.1.S1_at	0.000696832	0.000501247	3.8895724	BERG	RAS--like, estrogen--regulated, growth inhibitor
ClaAffx.19964.1.S1_s_at	0.001116423	0.001086259	3.985013	ARHGDIIB	Rho GDP dissociation inhibitor (GDI) beta
ClaAffx.20291.1.S1_at	3.3986E--0	3.40339E--0	14.2934675	RGS1	regulator of G--protein signaling like 1
ClaAffx.20294.1.S1_s_at	0.000785079	0.000601267	3.8037186	RAPGEF4	Rap guanine nucleotide exchange factor (GEF) 4
ClaAffx.20306.1.S1_at	0.000495709	0.000290154	5.6186435	RGS1	regulator of G--protein signaling like 1
ClaAffx.20465.1.S1_s_at	0.000447449	0.000243604	2.7826455	CIR1	corepressor interacting with RBP1, 1
ClaAffx.20572.1.S1_s_at	0.000162829	5.69559E--0	3.1579492	SMS	spermine synthase
ClaAffx.20589.1.S1_at	5.54699E--0	1.87768E--0	21.235073	DNAJC12	DnaJ (Hsp40) homolog, subfamily C, member 12
ClaAffx.20631.1.S1_s_at	0.000229598	9.00256E--0	6.3417835	FAM177A1	family with sequence similarity 177, member A1
ClaAffx.21065.1.S1_s_at	0.000113053	3.55582E--0	24.547401	LOC100683822///LOC100687054///LOC100856278///LOC486474///LOC607364///LOC607582///LOC608238///LOC608248	immunoglobulin lambda--like polypeptide 5--like//immunoglobulin lambda--like polypeptide 5--like//uncharacterized LOC100856278//immunoglobulin lambda like polypeptide 5--like//immunoglobulin lambda--like polypeptide 5--like//immunoglobulin lambda--like polypeptide 5--like//immunoglobulin lambda--like polypeptide 5--like
ClaAffx.21066.1.S1_s_at	0.00016564	5.84063E--0	40.161816	LOC100683822///LOC100687054///LOC100856278///LOC486474///LOC607364///LOC607582///LOC608238///LOC608248	immunoglobulin lambda--like polypeptide 5--like//immunoglobulin lambda--like polypeptide 5--like//uncharacterized LOC100856278//immunoglobulin lambda like polypeptide 5--like//immunoglobulin lambda--like polypeptide 5--like//immunoglobulin lambda--like polypeptide 5--like//immunoglobulin lambda--like polypeptide 5--like
ClaAffx.21119.1.S1_at	2.74704E--0	5.28058E--0	3.7447164	SORD	sorbitol dehydrogenase
ClaAffx.21187.1.S1_at	0.000305893	0.000135453	3.4055922	RTP3	receptor (chemosensory) transporter protein 3
ClaAffx.21778.1.S1_at	0.00015034	5.15269E--0	8.126965	SESTD1	SEC14 and spectrin domains 1
ClaAffx.22010.1.S1_s_at	0.000203002	7.59648E--0	5.095695	COMT	catechol--O--methyltransferase
ClaAffx.22444.1.S1_s_at	1.17904E--0	8.74617E--0	4.9481807	PLCB3///PRDX5	phospholipase C, beta 3 (phosphatidylinositol--specific)///peroxiredoxin 5
ClaAffx.22488.1.S1_at	0.000218698	8.3901E--0	2.1492941	PYGL	phosphorylase, glycogen, liver
ClaAffx.22781.1.S1_s_at	0.000785079	0.000599567	5.4645	PHC3	polyhomeotic homolog 3 (Drosophila)
ClaAffx.22814.1.S1_s_at	1.05304E--0	8.14896E--1	5.7984076	RGN	regucalcin (senescence marker protein--30)
ClaAffx.22992.1.S1_at	0.000410031	0.000209931	2.2796757	CYP27A1	cytochrome P450, family 27, subfamily A, polypeptide 1
ClaAffx.23200.1.S1_at	0.000259643	0.0001073	6.6540155	HDC	histidine decarboxylase
ClaAffx.23264.1.S1_s_at	0.000863661	0.000708957	2.4138463	LOC100682666///REST	RE1--silencing transcription factor--like//RE1--silencing transcription factor
ClaAffx.23615.1.S1_at	0.001126333	0.001105184	2.1587198	CPEB2	cytoplasmic polyadenylation element binding protein 2
ClaAffx.23632.1.S1_s_at	0.001109468	0.00107641	3.6813333	STAT5A	signal transducer and activator of transcription 5A
ClaAffx.23806.1.S1_s_at	3.43896E--0	7.00711E--0	3.3765085	SLC3A2	solute carrier family 3 (activators of dibasic and neutral amino acid transport), member 2
ClaAffx.23960.1.S1_s_at	0.00055239	1.29196E--0	3.6218507	SGMS1	sphingomyelin synthase 1
ClaAffx.23965.1.S1_s_at	0.000712265	0.000520385	2.2152998	TMEM179B	transmembrane protein 179B
ClaAffx.24310.1.S1_at	0.000643182	0.000437255	3.5016887	KIAA1370	KIAA1370 ortholog
ClaAffx.25013.1.S1_s_at	0.00104125	0.000966351	2.6670475	HUWE1	HECT, UBP and WWE domain containing 1, E3 ubiquitin protein ligase
ClaAffx.25070.1.S1_s_at	0.001083552	0.001023739	4.0470896	NVL	nuclear VCP--like
ClaAffx.25078.1.S1_at	0.00046528	0.000686535	3.6596284	PNMT	phenylethanolamine N--methyltransferase
ClaAffx.25131.1.S1_at	0.00070982	0.000516597	11.087355	MAGI2	membrane associated guanylate kinase, WW and PDZ domain containing 2
ClaAffx.25135.1.S1_s_at	6.3398E--0	1.6006E--0	12.534671	GNAI1	guanine nucleotide binding protein (G protein), alpha inhibiting activity polypeptide 1
ClaAffx.25859.1.S1_at	0.001137734	0.001134524	2.2164733	ZNPF52	zinc finger protein 652
ClaAffx.25945.1.S1_at	8.41225E--0	2.31366E--0	2.8218381	AREL1	apoptosis resistant E3 ubiquitin protein ligase 1
ClaAffx.26084.1.S1_s_at	5.45299E--0	6.13393E--0	5.6314144	FLVCR2	feline leukemia virus subgroup C cellular receptor family, member 2
ClaAffx.26084.1.S1_s_at	3.43896E--0	7.03313E--0	3.4451003	CBH14orf1	chromosome 8 open reading frame, human C14orf1
ClaAffx.26270.1.S1_s_at	0.000375547	0.000182085	7.26013	ODZ2	od2, odd Oz/ten--m homolog 2 (Drosophila)
ClaAffx.26434.1.S1_s_at	0.001116423	0.001087729	3.3299744	DIS3L	DIS3 mitotic control homolog (S. cerevisiae)--like
ClaAffx.26916.1.S1_at	0.00085453	0.00069498	3.9066484	LOC100686328	transmembrane protein 220--like
ClaAffx.27017.1.S1_s_at	0.000567833	0.0003588	2.416146	SERPINA11	serpin peptidase inhibitor, clade A (alpha--1 antiprotease, antitrypsin), member 11
ClaAffx.27698.1.S1_s_at	0.000309434	0.000139787	2.9490607	RCN2	reticulocalbin 2, EF--hand calcium binding domain

ClaAffx.27863.1.S1_at	0.000523698	0.000312041	3.5758338	NOM02	NODAL modulator 2
ClaAffx.28227.1.S1_at	0.001105833	0.001063721	3.6831172		
ClaAffx.28431.1.S1_s_at	0.000708904	0.000514931	4.165196	MYH11	myosin, heavy chain 11, smooth muscle
ClaAffx.28586.1.S1_s_at	1.202458E--0	2.03518E--1	117.25511	NADKD1///RANB P3L	NAD kinase domain containing 1///RAN binding protein 3--like
ClaAffx.28593.1.S1_at	1.92738E--0	3.04466E--0	33.489536	NADKD1///RANB P3L	NAD kinase domain containing 1///RAN binding protein 3--like
ClaAffx.28635.1.S1_at	0.000432906	0.000226528	4.765197	MPV17L	MPV17 mitochondrial membrane protein--like
ClaAffx.28987.1.S1_at	0.000932148	0.00080205	8.517217	ZIC3	Zic family member 3
ClaAffx.29054.1.S1_s_at	8.45095E--0	2.33623E--0	2.874679	ATP11C	ATPase, class VI, type 11C
ClaAffx.29256.1.S1_s_at	0.000407088	0.000278682	4.0642586	NSDHL	NAD(P) dependent steroid dehydrogenase--like
ClaAffx.30489.1.S1_s_at	0.001105833	0.001062688	4.018253	COX4NB	COX4 neighbor
ClaAffx.30572.1.S1_at	0.000776732	0.000590493	3.0469193	MLYCD	malonyl--CoA decarboxylase
ClaAffx.30622.1.S1_s_at	0.00010594	3.24245E--0	5.2440095	VCAM1	vascular cell adhesion molecule 1
ClaAffx.30821.1.S1_s_at	9.26314E--0	2.71753E--0	11.883978	AARS	alanyl--tRNA synthetase
ClaAffx.30923.1.S1_s_at	0.00100411	0.000901114	2.849306	PHLPP2	PH domain and leucine rich repeat protein phosphatase 2
ClaAffx.31165.1.S1_s_at	8.78111E--0	2.43989E--0	9.046315	LOC100856678	nexilin--like

Monkey bile duct signature

Probe Set ID	Corrected p---value	p---value	FCAbsolute	Gene Symbol	Gene Title
AFX--LysX--5_at	0.007590598	0.007532947	9.754974		
200632_s_at	8.20E--0	1.89E--0	10.573509	NDRG1	N---myc downstream regulated 1
201136_at	4.25E--0	2.04E--0	13.670461	PLP2	proteolipid protein 2 (colonic epithelium--enriched)
201301_s_at	3.06E--0	5.16E--1	12.829881	ANXA4	annexin A4
201302_at	4.55E--0	1.42E--0	22.364914	ANXA4	annexin A4
201613_s_at	1.42E--0	1.20E--0	29.707111	APIG2	adaptor---related protein complex 1, gamma 2 subunit
201650_at	4.04E--0	6.99E--0	130.87476	KRT19	keratin 19
201839_s_at	1.84E--0	1.77E--0	30.869284	EPCAM	epithelial cell adhesion molecule
201860_s_at	0.003179834	0.002817575	13.198988	PLAT	plasminogen activator, tissue
202018_s_at	9.14E--0	5.89E--0	29.405645	LTF	lactotransferrin
202267_at	1.45E--0	4.33E--0	17.813307	LAMC2	laminin, gamma 2
202286_s_at	7.71E--0	4.73E--0	34.630943	TACSTD2	tumor--associated calcium signal transducer 2
202421_at	8.40E--0	5.26E--0	9.310548	IGSF3	immunoglobulin superfamily, member 3
202488_s_at	0.00336244	0.003002077	10.625242	FXVD3	FXVD domain containing ion transport regulator 3
202790_at	3.88E--0	6.40E--0	13.869911	CLDN7	claudin 7
202826_at	5.44E--0	2.89E--0	16.824333	SPINT1	serine peptidase inhibitor, Kunitz type 1
202831_at	7.86E--0	1.80E--0	191.78606	GPX2	glutathione peroxidase 2 (gastrointestinal)
202921_s_at	1.96E--0	6.76E--0	10.095616	ANK2	ankyrin 2, neuronal
202935_s_at	1.30E--0	6.17E--0	47.543934	SOX9	SRY (sex determining region Y)---box 9
202936_s_at	1.77E--0	2.15E--0	14.076472	SOX9	SRY (sex determining region Y)---box 9
203065_s_at	1.36E--0	1.05E--0	10.533267	CAV1	caveolin 1, caveolae protein, 22kDa
203146_s_at	9.92E--0	6.54E--0	28.41594	GABBR1	gamma--aminobutyric acid (GABA) B receptor, 1
203601_s_at	2.26E--0	8.31E--0	10.912976	ZBTB17	zinc finger and BTB domain containing 17
203631_s_at	2.08E--0	2.42E--0	22.363693	GPRCSB	G protein--coupled receptor, family C, group 5, member B
203726_s_at	4.43E--0	2.18E--0	17.974949	LAMA3	laminin, alpha 3
203783_s_at	9.15E--0	2.23E--0	13.83298	POLRMT	polymerase (RNA) mitochondrial (DNA directed)
203889_at	1.54E--0	4.73E--0	10.748801	SCG5	secretogranin V (782 protein)
203961_at	6.97E--0	3.41E--0	21.029171	NEBL	nebullette
204213_at	1.40E--0	1.17E--0	10.779538	PIGR	polymeric immunoglobulin receptor
204259_at	2.40E--0	3.17E--0	21.396217	MMP7	matrix metalloproteinase 7 (matrilysin, uterine)
204272_at	2.40E--0	3.16E--0	32.379562	LGALS4	lectin, galactoside---binding, soluble, 4
204304_s_at	7.65E--0	4.64E--0	32.711346	PROM1	prominin 1
204358_s_at	7.75E--0	4.77E--0	9.38694	FLRT2///LOC100506718	fibronectin leucine rich transmembrane protein 2///uncharacterized LOC100506718
204519_s_at	1.05E--0	2.79E--0	13.585548	PLLP	plasmolipin
204540_at	1.25E--0	3.53E--0	9.305641	EEF1A2	eukaryotic translation elongation factor 1 alpha 2
204542_at	3.88E--0	6.37E--0	11.425742	STEGALNAC2	ST6 (alpha--N--acetyl--neuraminyl--2,3--beta--galactosyl--1,3)---N--acetyl-galactosaminide alpha--2,6--sialyltransferase 2
204777_s_at	6.01E--0	1.26E--0	25.151676	MAL	mal, T---cell differentiation protein
204875_s_at	0.00147572	0.001077213	23.08333	GMDS	GDP---mannose 4,6--dehydratase
205009_at	2.71E--0	1.10E--0	17.68557	TFPI	trypsin inhibitor 1
205016_at	0.002840828	0.00247164	22.84447	TGFA	transforming growth factor, alpha
205043_at	1.07E--0	2.88E--0	14.782101	CFTF	cystic fibrosis transmembrane conductance regulator (ATP---binding cassette sub-
205044_at	0.00577056	0.005561164	12.389158	GABRP	gamma--aminobutyric acid (GABA) A receptor, pi
205047_s_at	1.07E--0	2.85E--0	32.973373	ASNS	asparagine synthetase (glutamine---hydrolyzing)
205313_at	1.79E--0	2.72E--0	16.084911	HNFB1	HNFB1 homeobox B
205316_at	1.40E--0	1.17E--0	22.952323	SLC15A2	solute carrier family 15 (H+/peptide transporter), member 2
205317_s_at	3.28E--0	4.95E--0	21.514566	SLC15A2	solute carrier family 15 (H+/peptide transporter), member 2
205328_at	1.30E--0	6.60E--0	19.294895	CLDN10	claudin 10
205342_s_at	4.51E--0	2.24E--0	9.643227	SULT1C2	sulfotransferase family, cytosolic, 1C, member 2
205360_at	0.002864503	0.002499491	9.2035055	PFND4	prefoldin subunit 4
205376_at	4.47E--0	2.21E--0	9.142418	INPP4B	inositol polyphosphate---4--phosphatase, type II, 105kDa
205379_at	3.32E--0	5.06E--0	18.467173	CBR3	carbonyl reductase 3
205470_s_at	2.39E--0	9.21E--0	18.128016	KLK11	kallikrein--related peptidase 11
205532_s_at	5.83E--0	3.15E--0	12.5754595	CDH6	cadherin 6, type 2, K--cadherin (fetal kidney)
205533_s_at	0.006122714	0.005957651	9.890403	CDH6	cadherin 6, type 2, K--cadherin (fetal kidney)
205625_s_at	2.01E--0	2.11E--0	15.471472	CALB1	calbindin 1, 28kDa
205626_s_at	1.79E--0	2.60E--0	35.616817	CALB1	calbindin 1, 28kDa
205767_at	0.0011303	7.72E--0	14.258832	EREG	epiregulin
205814_at	4.06E--0	1.94E--0	16.304878	GRM3	glutamate receptor, metabotropic 3
205893_at	2.08E--0	7.42E--0	16.31367	NLG1	neurologin 1
205922_at	2.36E--0	9.10E--0	10.284211	VNN2	vanin 2
205997_at	1.48E--0	4.50E--0	46.06536	ADAM28	ADAM metalloproteinase domain 28
206002_at	1.97E--0	6.81E--0	22.749891	GPR64	G protein--coupled receptor 64
206059_at	6.28E--0	3.50E--0	16.868776	ZNFX1	zinc finger protein 91
206123_at	6.41E--0	3.60E--0	9.43653	LLGL1	lethal giant larvae homolog 1 (Drosophila)
206197_at	4.55E--0	8.41E--0	32.659492	NME5	NME/NM23 family member 5
206208_at	7.45E--0	1.68E--0	19.509794	CA4	carbonic anhydrase IV
206209_s_at	3.37E--0	1.45E--0	9.912885	CA4	carbonic anhydrase IV
206364_at	0.007025329	0.00694233	10.989167	KIF14	kinesin family member 14
206385_s_at	5.24E--0	1.03E--0	20.8784	ANK3	ankyrin 3, node of Ranvier (ankyrin G)
206391_at	0.004282489	0.003975306	10.353978	RARRES1	retinoic acid receptor responder (tazarotene induced) 1
206399_s_at	1.47E--0	1.30E--0	9.806497	CACNA1A	calcium channel, voltage--dependent, P/Q type, alpha 1A subunit
206429_at	0.001162013	8.02E--0	13.585832	F2RL1	coagulation factor II (thrombin) receptor--like 1
206520_s_at	6.73E--0	3.85E--0	11.292526	SIGLEC6	sialic acid binding Ig--like lectin 6
206524_at	0.002701921	0.002317009	11.334983	T	T, brachyury homolog (mouse)
206595_at	6.18E--0	3.41E--0	13.568236	CST6	cystatin E/M
206628_at	3.99E--0	1.88E--0	22.983038	SLC5A1	solute carrier family 5 (sodium/glucose cotransporter), member 1
206661_at	0.007976072	0.007928956	9.451004	DBF4B	DBF4 homolog B (S. cerevisiae)
206804_s_at	9.77E--0	6.41E--0	59.929455	SCEL	scieilin
206940_s_at	3.96E--0	1.84E--0	15.418744	POU4F1	POU class 4 homeobox 1
206946_at	4.28E--0	2.07E--0	10.0242195	HCN4	hyperpolarization activated cyclic nucleotide--gated potassium channel 4
207017_at	3.43E--0	5.30E--0	12.502662	RAB27B	RAB27B, member RAS oncogene family
207169_s_at	4.43E--0	2.17E--0	9.3316145	DDRI1///MIR4640	discoidin domain receptor tyrosine kinase 1///microRNA 4640
207225_at	9.79E--0	6.43E--0	9.495378	AAAT	aralkylamine N--acetyltransferase
207249_s_at	0.001959193	0.001557435	13.312831	SLC28A2	solute carrier family 28 (sodium---coupled nucleoside transporter), member 2
207279_s_at	1.04E--0	6.49E--0	16.267622	NEBL	nebullette
207434_s_at	0.003152431	0.002790633	10.421672	FXVD2///FXVD6---	FXVD domain containing ion transport regulator 2///FXVD6---FXVD2 readthrough
207468_s_at	2.21E--0	8.08E--0	9.385944	SFRP5	secreted frizzled--related protein 5
207615_s_at	0.001911563	0.001514732	11.531261	C16orf3	chromosome 16 open reading frame 3
207847_s_at	0.001157947	7.97E--0	45.562386	MUC1	mucin 1, cell surface associated
207880_at	6.54E--0	1.43E--0	13.157702	ADAM11	ADAM metalloproteinase domain 11
207950_s_at	1.77E--0	2.37E--0	36.158894	ANK3	ankyrin 3, node of Ranvier (ankyrin G)
207989_at	0.006789333	0.006657103	9.329288	OPRM1	opioid receptor, mu 1

208084_at	0.002072633	0.001670969	17.626076	ITGB6	integrin, beta 6
208135_at	2.16E--0	2.64E--0	29.316442	HNF1B	HNF1 homeobox B
208136_s_at	6.23E--0	3.46E--0	13.7232895	ZNF205---AS1	ZNF205 antisense RNA 1
208140_s_at	0.002303465	0.001903031	14.9177265	LRRC48	leucine rich repeat containing 48
208143_s_at	6.48E--0	3.66E--0	10.457069	EDDM3A	epididymal protein 3A
208250_s_at	3.32E--0	5.07E--0	29.432346	DMBT1	deleted in malignant brain tumors 1
208323_s_at	2.68E--0	1.08E--0	41.94592	ANXA13	annexin A13
208358_s_at	0.005798084	0.005592582	18.00785	UGT8	UDP glycosyltransferase 8
208394_x_at	0.002026785	0.001624849	19.778212	ESM1	endothelial cell--specific molecule 1
208430_s_at	0.006567651	0.006418009	9.143717	DTNA	dystrobrevin, alpha
208431_s_at	0.001394233	0.001002699	12.966413	TUB8	tubby homolog (mouse)
208450_at	7.04E--0	4.12E--0	11.336568	LGALS2	lectin, galactoside--binding, soluble, 2
208650_s_at	1.43E--0	1.22E--0	40.748802	CD24	CD24 molecule
209097_s_at	2.53E--0	9.91E--0	11.742224	JAG1	jagged 1
209098_s_at	1.21E--0	8.88E--0	13.330439	JAG1	jagged 1
209173_at	9.34E--0	2.29E--0	206.51149	AGR2	anterior gradient 2 homolog (Xenopus laevis)
209211_at	3.88E--0	6.53E--0	23.698734	KLF5	Kruppel--like factor 5 (intestinal)
209212_s_at	1.63E--0	1.38E--0	24.949917	KLF5	Kruppel--like factor 5 (intestinal)
209369_at	2.71E--0	1.09E--0	15.882639	ANXA3	annexin A3
209442_x_at	1.36E--0	1.05E--0	17.407969	ANK3	ankyrin 3, node of Ranvier (ankyrin G)
209488_s_at	8.35E--0	4.37E--0	9.4250145	RBPMS	RNA binding protein with multiple splicing
209529_at	2.49E--0	9.72E--0	11.067101	PPAP2C	phosphatidic acid phosphatase type 2C
209530_at	0.001003689	6.63E--0	10.679267	CACNB3	calcium channel, voltage--dependent, beta 3 subunit
209615_s_at	5.24E--0	1.04E--0	20.63451	PAK1	p21 protein (Cdc42/Rac)--activated kinase 1
209617_s_at	3.83E--0	6.18E--0	14.187726	CTNND2	catenin (cadherin--associated protein), delta 2
209618_at	2.29E--0	8.49E--0	15.728557	CTNND2	catenin (cadherin--associated protein), delta 2
209728_at	0.007136361	0.007064094	11.252374	HLA--DRB4	major histocompatibility complex, class II, DR beta 4
209772_s_at	3.14E--0	4.59E--0	38.24131	CD24	CD24 molecule
209791_at	0.001146043	7.86E--0	9.781555	PADI2	peptidyl arginine deiminase, type II
209792_s_at	3.88E--0	6.37E--0	51.081463	KLK10	kallikrein--related peptidase 10
209875_s_at	3.75E--0	1.11E--0	59.396572	SPP1	secreted phosphoprotein 1
209908_s_at	5.09E--0	2.63E--0	9.184215	TGFB2	transforming growth factor, beta 2
210119_at	4.32E--0	7.65E--0	107.66456	KCNJ15	potassium inwardly--rectifying channel, subfamily I, member 15
210121_at	3.76E--0	5.93E--0	9.162879	B3GALT2	UDP--Gal:betaGalNAc beta 1,3--galactosyltransferase, polypeptide 2
210505_at	0.006710854	0.006569275	10.83258	ADH7	alcohol dehydrogenase 7 (class IV), mu or sigma polypeptide
210534_s_at	1.45E--0	1.24E--0	30.337643	B9D1	B9 protein domain 1
210641_at	7.32E--0	4.32E--0	12.581538	CAPN9	calpain 9
210736_x_at	0.003527739	0.00317943	21.337812	DTNA	dystrobrevin, alpha
210781_x_at	4.52E--0	2.25E--0	11.905989	GRIN1	glutamate receptor, ionotropic, N--methyl D--aspartate 1
210827_s_at	3.16E--0	1.34E--0	12.3604555	ELF3	ET4--like factor 3 (ets domain transcription factor, epithelial--specific)
210829_s_at	5.16E--0	9.97E--0	10.233593	SSBP2	single--stranded DNA binding protein 2
210869_s_at	1.16E--0	8.04E--0	11.144834	MCAM	melanoma cell adhesion molecule
211002_s_at	9.19E--0	5.95E--0	11.1645975	TRIM29	tripartite motif containing 29
211057_at	3.98E--0	1.86E--0	11.673606	ROR1	receptor tyrosine kinase--like orphan receptor 1
211164_at	0.001051172	7.05E--0	17.599524	EPHA3	EPH receptor A3
211181_x_at	1.97E--0	6.84E--0	12.140086	LOC100506403///	uncharacterized LOC100506403///runt--related transcription factor 1
211258_s_at	3.17E--0	1.34E--0	15.489263	TGFA	transforming growth factor, alpha
211379_x_at	0.002518768	0.002117041	12.293867	B3GALNT1	beta--1,3--N--acetylgalactosaminyltransferase 1 (globoside blood group)
211398_at	4.05E--0	1.93E--0	14.105396	FGFR2	fibroblast growth factor receptor 2
211465_s_at	0.001814013	0.001397632	9.28565	FUT6	fucosyltransferase 6 (alpha 1,3) fucosyltransferase)
211493_x_at	1.99E--0	6.95E--0	15.111289	DTNA	dystrobrevin, alpha
211592_s_at	0.001132926	7.76E--0	11.962104	CACNA1C	calcium channel, voltage--dependent, L type, alpha 1C subunit
211620_x_at	6.97E--0	3.39E--0	10.776594	LOC100506403///	uncharacterized LOC100506403///runt--related transcription factor 1
211695_s_at	1.36E--0	3.95E--0	13.136052	MUC1C	mucin 1, cell surface associated
211806_s_at	8.01E--0	1.84E--0	20.910797	KCNJ15	potassium inwardly--rectifying channel, subfamily I, member 15
211812_s_at	6.15E--0	1.31E--0	29.857916	B3GALNT1	beta--1,3--N--acetylgalactosaminyltransferase 1 (globoside blood group)
211873_s_at	2.30E--0	8.60E--0	10.5178175	PCDHGA9	protocadherin gamma subfamily A, 9
211900_x_at	1.25E--0	3.50E--0	14.129642	CD6	CD6 molecule
212091_s_at	3.92E--0	1.82E--0	11.106757	COL6A1	collagen, type VI, alpha 1
212336_at	1.36E--0	1.06E--0	28.096264	EPBA1L1	erythrocyte membrane protein band 4.1--like 1
212339_at	3.60E--0	5.65E--0	40.527557	EPBA1L1	erythrocyte membrane protein band 4.1--like 1
212533_at	3.58E--0	1.60E--0	9.747216	WEE1	WEE1 homolog (S. pombe)
212611_at	0.001734353	0.001320158	11.672231	DTX4	deltex homolog 4 (Drosophila)
212670_at	6.51E--0	3.70E--0	15.201399	ELN	elastin
212775_at	2.22E--0	8.14E--0	10.265405	OBSL1	obscurin--like 1
212776_s_at	3.21E--0	1.37E--0	24.5508	OBSL1	obscurin--like 1
212906_at	1.37E--0	1.09E--0	56.529102	GRAMD1B	GRAM domain containing 1B
212942_s_at	7.71E--0	4.72E--0	14.312297	KIAA1199	KIAA1199
213280_at	1.20E--0	3.33E--0	47.156425	RAP1GAP2	RAP1 GTPase activating protein 2
213426_s_at	7.88E--0	4.86E--0	10.132942	CAV2	caveolin 2
213429_at	0.002409789	0.002017309	11.708273	BICC1	bicaudal C homolog 1 (Drosophila)
213436_at	0.001683194	0.001274114	11.930345	CNR1	cannabinoid receptor 1 (brain)
213506_at	3.67E--0	1.66E--0	14.172241	F2RL1	coagulation factor II (thrombin) receptor--like 1
213516_at	2.30E--0	8.60E--0	10.135801	AKAP13	A kinase (PRKA) anchor protein 13
213731_s_at	0.001806397	0.001384441	11.781514	TCF3	transcription factor 3
213809_x_at	4.77E--0	2.43E--0	9.722728	TCF3	transcription factor 3
213953_at	0.001351396	9.66E--0	23.160204	KRT20	keratin 20
213989_x_at	2.33E--0	8.86E--0	11.109252	SETD4	SET domain containing 4
213997_at	0.001171411	8.14E--0	9.236968	FAM189A1	family with sequence similarity 189, member A1
214031_s_at	3.94E--0	1.77E--0	36.460464	KRT7	keratin 7
214262_at	2.07E--0	2.37E--0	13.402645	TRIP6	thyroid hormone receptor interactor 6
214341_at	2.68E--0	6.63E--0	25.078867	APIG2	adaptor--related protein complex 1, gamma 2 subunit
214373_at	3.72E--0	1.69E--0	14.956957		
214774_x_at	0.001524796	0.001127683	25.211277	TOX3	TOX high mobility group box family member 3
214803_at	9.63E--0	6.29E--0	9.280332	CDH6	cadherin 6, type 2, K--cadherin (fetal kidney)
214906_at	0.001713679	0.001302694	9.544204	BICD1	bicaudal D homolog 1 (Drosophila)
214966_at	6.35E--0	1.30E--0	16.58	GRIK5	glutamate receptor, ionotropic, kainate 5
215108_x_at	2.31E--0	8.71E--0	26.501263	TOX3	TOX high mobility group box family member 3
215382_s_at	1.49E--0	1.33E--0	16.422377	TPSAB1	tryptase alpha/beta 1
215657_at	3.88E--0	6.55E--0	18.532475	SLC26A3	solute carrier family 26, member 3
215672_s_at	1.25E--0	9.31E--0	9.7296505	AHCYL2	adenosylhomocysteinase--like 2
215702_s_at	1.24E--0	3.13E--0	203.72252	CFTR	cystic fibrosis transmembrane conductance regulator (ATP--binding cassette sub-
215703_at	1.40E--0	1.16E--0	73.2913	CFTR	cystic fibrosis transmembrane conductance regulator (ATP--binding cassette sub-
215711_s_at	4.86E--0	2.48E--0	9.275378	WEE1	WEE1 homolog (S. pombe)
215784_at	0.00471781	0.004403289	12.372058	CD1E	CD1E molecule
215955_x_at	0.001021539	6.78E--0	10.603116	ARHGAP26	Rho GTPase activating protein 26
215971_at	2.87E--0	1.18E--0	9.155803		
216135_at	1.06E--0	2.82E--0	18.836273	IQCK	IQ motif containing K
216142_at	9.15E--0	2.22E--0	10.332584		
216161_at	7.67E--0	4.65E--0	10.667711	SBN01	strawberry notch homolog 1 (Drosophila)
216379_x_at	1.60E--0	5.03E--0	24.011486	CD24	CD24 molecule
216446_at	1.70E--0	5.43E--0	11.72488		
216477_at	7.75E--0	4.77E--0	13.567382	RPL23AP22///RPL	ribosomal protein L23a pseudogene 22///NULL
216623_x_at	3.55E--0	1.58E--0	37.243332	TOX3	TOX high mobility group box family member 3
216782_at	4.90E--0	1.82E--0	71.45796		
216867_s_at	2.07E--0	2.34E--0	15.229227	PDGFA	platelet--derived growth factor alpha polypeptide
216882_s_at	6.55E--0	1.44E--0	16.330215	NEBL	nebulin
216966_at	0.00107372	7.24E--0	18.499031	ITGA2B	integrin, alpha 2b (platelet glycoprotein IIb of IIb/IIIa complex, antigen CD41)
217026_at	9.40E--0	6.11E--0	14.285501	CFTR	cystic fibrosis transmembrane conductance regulator (ATP--binding cassette sub-
217054_at	1.87E--0	6.33E--0	26.531956	OTTHUMG0000015	NULL///NULL
217182_at	8.75E--0	5.53E--0	18.518875		
217187_at	0.001830152	0.001422815	44.77701	MUC5AC	mucin 5AC, oligomeric mucus/gel--forming
217237_at	1.23E--0	3.44E--0	12.013807	ADAM3B///ADAM	NULL///ADAM metallopeptidase domain 3B (pseudogene)

217264_s_at	1.48E--0	4.47E--0	13.601606	SCNN1A	sodium channel, non--voltage--gated 1 alpha subunit
217463_s_at	2.06E--0	7.33E--0	27.757303	MYRF	myelin regulatory factor
217634_s_at	8.94E--0	2.13E--0	16.171844	SVIL	supervillin
217711_at	0.008267904	0.008246972	12.533059	TEK	TEK tyrosine kinase, endothelial
218186_at	1.24E--0	4.17E--0	47.26175	RAB25	RAB25, member RAS oncogene family
218261_at	4.62E--0	2.33E--0	15.115448	AP1M2	adaptor--related protein complex 1, mu 2 subunit
218368_s_at	1.26E--0	3.58E--0	10.663235	TNFRSF12A	tumor necrosis factor receptor superfamily, member 12A
218376_s_at	7.71E--0	4.71E--0	12.361067	MICAL1	microtubule associated monooxygenase, calponin and LIM domain containing 1
218445_s_at	5.77E--0	1.18E--0	10.151193	H2AFY2	H2A histone family, member Y2
218644_at	7.71E--0	4.72E--0	15.878833	PLEK2	pleckstrin 2
218677_at	1.50E--0	4.58E--0	10.461276	S100A14	S100 calcium binding protein A14
218885_s_at	1.39E--0	4.08E--0	42.876446	GALNT12	UDP--N--acetyl--alpha--D--galactosamine:polypeptide N--acetylglucosaminyltransferase 12 (GalNAc--T12)
218921_at	1.41E--0	4.18E--0	9.47954	SIGIRR	single immunoglobulin and toll--interleukin 1 receptor (TIR) domain
218963_s_at	2.24E--0	8.24E--0	24.063215	KRT23	keratin 23 (histone deacetylase inducible)
219077_s_at	0.002755151	0.002383147	10.308208	WWOX	WW domain containing oxidoreductase
219121_s_at	5.09E--0	9.78E--0	123.54625	ESRP1	epithelial splicing regulatory protein 1
219257_s_at	3.33E--0	5.11E--0	26.381027	SPHK1	sphingosine kinase 1
219304_s_at	2.68E--0	6.95E--0	30.03212	PDGFD	platelet derived growth factor D
219388_at	5.50E--0	2.94E--0	26.84399	GRHL2	grainyhead--like 2 (Drosophila)
219468_s_at	5.25E--0	2.74E--0	9.486332	CUEDC1	CUE domain containing 1
219476_at	0.002409247	0.002014822	11.878861	C1orf116	chromosome 1 open reading frame 116
219498_s_at	3.55E--0	1.56E--0	31.25175	BCL11A	B--cell CLL/lymphoma 11A (zinc finger protein)
219564_at	0.002237393	0.001840893	10.688598	KCNJ16	potassium inwardly--rectifying channel, subfamily I, member 16
219686_at	2.51E--0	9.81E--0	16.209522	STK32B	serine/threonine kinase 32B
219697_at	0.00187421	0.001478807	9.164882	HS3ST2	heparan sulfate (glucosamine) 3--O--sulfotransferase 2
219703_at	9.84E--0	2.51E--0	10.332835	MNS1	meiosis--specific nuclear structural 1
219752_at	0.001048873	7.02E--0	9.142463	RASAL1	RAS protein activator like 1 (GAP1 like)
219833_s_at	0.001526267	0.001128278	24.882479	EFHC1	EF--hand domain (C--terminal) containing 1
219850_s_at	2.67E--0	6.25E--0	36.943134	EHF	ets homologous factor
220120_s_at	8.18E--0	4.21E--0	21.260798	EPB41LA4	erythrocyte membrane protein band 4.1 like 4A
220218_at	0.005908871	0.005709415	9.823468	SPATA6L	spermatogenesis associated 6--like
220220_at	2.95E--0	1.22E--0	12.3678665	LRRC37A4P	leucine rich repeat containing 37, member A4, pseudogene
220272_at	0.001310307	9.31E--0	9.506173	BNC2	basonuclin 2
220298_s_at	1.31E--0	3.75E--0	11.074696	SPATA6	spermatogenesis associated 6
220299_at	6.85E--0	3.97E--0	12.385091	SPATA6	spermatogenesis associated 6
220303_at	1.86E--0	1.80E--0	28.486647	PDZD3	PDZ domain containing 3
220377_at	3.07E--0	1.29E--0	14.039273	KIAA0125	KIAA0125
220406_at	2.16E--0	2.66E--0	13.680102	TGFB2	transforming growth factor, beta 2
220446_s_at	5.24E--0	1.03E--0	40.805798	CHST4	carbohydrate (N--acetylglucosamine 6--O) sulfotransferase 4
220461_at	5.61E--0	3.01E--0	13.221404	PCNXL2	pecanex--like 2 (Drosophila)
220468_at	0.001082261	7.32E--0	9.871957	ARL14	ADP--ribosylation factor--like 14
220475_at	6.14E--0	1.31E--0	43.445732	SLC28A3	solute carrier family 28 (sodium--coupled nucleoside transporter), member 3
220484_at	1.70E--0	5.42E--0	20.476727	MCOLN3	mucopolip 3
220710_at	0.002059793	0.001653049	9.249805	ANP32A--IT1	ANP32A intronic transcript 1 (non--protein coding)
220806_x_at	0.003341766	0.002977979	13.853031	GNL3	guanine nucleotide binding protein (G protein), gamma 13
220919_s_at	5.87E--0	3.18E--0	17.356274	WDR96	WD repeat domain 96
221173_at	2.07E--0	2.28E--0	41.417828	USH1C	Usher syndrome 1C (autosomal recessive, severe)
221199_at	9.30E--0	6.04E--0	13.358225	GFRA4	GDNF family receptor alpha 4
221283_at	0.001427327	0.001035866	9.800603	RUNX2	runt--related transcription factor 2
221294_at	0.004372665	0.004062704	11.389156	GPR21	G protein--coupled receptor 21
221365_at	1.82E--0	6.02E--0	10.946323	MLNR	motilin receptor
221655_x_at	8.79E--0	5.57E--0	12.503999	EPSB1	EPSB--like 1
221665_s_at	8.90E--0	5.69E--0	12.4659815	EPSB1	EPSB--like 1
221696_s_at	2.91E--0	4.03E--0	12.197986	STYK1	serine/threonine/tyrosine kinase 1
221859_at	7.51E--0	4.50E--0	17.671015	SYT13	synaptotagmin XIII
221976_s_at	2.69E--0	1.08E--0	12.176625	HGFRP3	hepatoma--derived growth factor, related protein 3
222022_at	7.46E--0	4.45E--0	10.561483	DTX3	deltex homolog 3 (Drosophila)
222066_at	9.94E--0	2.55E--0	20.530214	EPB41L1	erythrocyte membrane protein band 4.1--like 1
222075_s_at	0.005195146	0.004949637	10.242946	OAZ3	ornithine decarboxylase antizyme 3
222234_s_at	1.92E--0	6.63E--0	13.257382	DBNDD1	dysbindin (dystrobrein binding protein 1) domain containing 1
222249_at	0.006122714	0.005962542	12.14773		
222298_at	0.00490055	0.004640014	24.68264		
222325_at	7.32E--0	4.32E--0	11.767524		
266_s_at	3.80E--0	6.06E--0	11.278719	CD24	CD24 molecule
40093_at	3.13E--0	4.46E--0	9.4559765	BCAM	basal cell adhesion molecule (Lutheran blood group)
49049_at	0.00186332	0.001462353	10.161979	DTX3	deltex homolog 3 (Drosophila)
91826_at	1.16E--0	8.22E--0	19.94288	EPSB1	EPSB--like 1
222449_at	4.55E--0	1.39E--0	10.032866	PMEP1	prostate transmembrane protein, androgen induced 1
222519_s_at	5.98E--0	3.24E--0	10.826259	IIFT57	intraflagellar transport 57 homolog (Chlamydomonas)
222694_at	9.88E--0	6.50E--0	11.163988	MGC2752	CENPB DNA--binding domains containing 1 pseudogene
222829_s_at	9.15E--0	2.22E--0	13.872188	IL20RA	interleukin 20 receptor, alpha
222853_at	3.99E--0	1.88E--0	10.075132	FLRT3	fibronectin leucine rich transmembrane protein 3
222860_s_at	1.77E--0	2.21E--0	30.570236	PDGFD	platelet derived growth factor D
222901_s_at	0.001329649	9.47E--0	10.114138	KCNJ16	potassium inwardly--rectifying channel, subfamily I, member 16
222932_at	1.01E--0	6.11E--0	31.07456	EHF	ets homologous factor
222933_at	0.002229078	0.001826528	12.554409	MORN1	MORN repeat containing 1
223698_at	0.006762901	0.006631638	14.540373	SLC25A36	solute carrier family 25 (pyrimidine nucleotide carrier), member 36
223748_at	0.001171411	8.16E--0	14.575098	SLCA11	solute carrier family 4, sodium borate transporter, member 11
223768_at	0.001101669	7.49E--0	9.42515	SSR4P1	signal sequence receptor, delta pseudogene 1
223915_at	5.10E--0	2.64E--0	9.634829	BCOR	BCL6 corepressor
223923_at	1.49E--0	4.52E--0	11.219766	C21orf62	chromosome 21 open reading frame 62
223974_at	0.00592491	0.005734913	10.329405	DLGAP1--AS2	DLGAP1 antisense RNA 2
224157_at	5.79E--0	1.20E--0	11.708758	KAAG1	kidney associated antigen 1
224168_at	0.001738483	0.001324768	9.604853	TXNDC2	thioredoxin domain containing 2 (spermatozoa)
224189_x_at	2.12E--0	2.51E--0	51.28004	EHF	ets homologous factor
224240_s_at	7.39E--0	4.39E--0	17.067583	CCL28	chemokine (C--C motif) ligand 28
224251_at	3.74E--0	1.71E--0	11.077557	WDR96	WD repeat domain 96
224277_at	0.002592308	0.002191977	9.423566	MOP--1	MOP--1
224355_s_at	1.48E--0	4.49E--0	53.31728	MS4A8	membrane--spanning 4--domains, subfamily A, member 8
225150_s_at	5.25E--0	2.75E--0	10.966467	RTKN	rotectin
225237_s_at	4.21E--0	7.35E--0	9.704395	MSI2	musashi RNA--binding protein 2
225238_at	2.06E--0	3.99E--0	9.259546	MSI2	musashi RNA--binding protein 2
225457_x_at	0.001569093	0.00116391	25.035736	LINC00263///PP7	long intergenic non--protein coding RNA 263///uncharacterized LOC25845
225500_x_at	0.001032017	6.87E--0	9.948278	SCAF1	SR--related CTD--associated factor 1
225617_at	7.88E--0	4.85E--0	12.052499	ODF2	outer dense fiber of sperm tails 2
225645_at	1.16E--0	8.28E--0	33.56338	EHF	ets homologous factor
225822_at	3.58E--0	1.60E--0	12.123997	TMEM125	transmembrane protein 125
225846_at	0.002394932	0.001998808	32.988415	ESRP1	epithelial splicing regulatory protein 1
225911_at	6.49E--0	3.68E--0	12.859749	NPNT	nephroretin
225996_at	0.002069784	0.001662814	20.385994	LONRF2	LON peptidase N--terminal domain and ring finger 2
226055_at	7.36E--0	1.65E--0	23.727343	ARRDC2	arrestin domain containing 2
226086_at	3.95E--0	1.83E--0	24.051788	SYT13	synaptotagmin XIII
226145_s_at	2.09E--0	7.49E--0	10.332328	FRS1	Fraser syndrome 1
226248_s_at	0.001863247	0.001459151	30.692993	KIAA1324	KIAA1324
226335_at	9.14E--0	5.90E--0	14.864879	ITGB6	integrin, beta 6
226560_at	5.79E--0	3.12E--0	16.011183		
226623_at	9.50E--0	6.19E--0	20.037853	PHYHIP1	phytanoyl--CoA 2--hydroxylase interacting protein--like
226869_at	0.003256794	0.002891263	10.027069	MEGF6	multiple EGF--like--domains 6
226961_at	0.002720583	0.002339472	11.100825	PRI15	proline rich 15
226980_at	0.004727106	0.004415955	9.902899	DEPDC1B	DEP domain containing 1B
227048_at	9.31E--0	6.05E--0	11.882622	LAMA1	laminin, alpha 1
227084_at	3.88E--0	6.54E--0	17.246822	DTNA	dystrobrein, alpha
227177_at	1.07E--0	2.84E--0	17.584064	CORO2A	coronin, actin binding protein, 2A
227194_at	2.67E--0	3.61E--0	73.305176	FAM3B	family with sequence similarity 3, member B

227399_at	0.006707925	0.006560747	10.608356	VGLL3	vestigial like 3 (Drosophila)
227720_at	5.52E--0	1.11E--0	9.543253	ANKRD13B	ankyrin repeat domain 13B
227747_at	4.48E--0	2.22E--0	19.23433	MPZL3	myelin protein zero--like 3
227812_at	2.91E--0	4.06E--0	14.7879305	TNFRSF19	tumor necrosis factor receptor superfamily, member 19
227992_s_at	0.007111583	0.007033566	10.940874	LINC00085	long intergenic non--protein coding RNA 85
228067_at	0.006000844	0.005823604	18.528948	KIAA1211L	KIAA1211--like
228241_at	4.31E--0	7.59E--0	101.49069	AGR3	anterior gradient 3 homolog (Xenopus laevis)
228491_at	8.10E--0	5.01E--0	15.700081	KRT19	keratin 19
228776_at	0.001584864	0.00117962	17.14341	GJC1	gap junction protein, gamma 1, 45kDa
228850_s_at	0.001164374	8.05E--0	13.435195	SLIT2	slit homolog 2 (Drosophila)
228860_at	2.16E--0	2.63E--0	11.596407	UBE3B	ubiquitin protein ligase E3B
228865_at	4.55E--0	8.38E--0	48.366005	C1orf116	chromosome 1 open reading frame 116
228956_at	9.15E--0	5.92E--0	36.14803	UGT8	UDP glycosyltransferase 8
229046_s_at	5.24E--0	1.02E--0	13.449312	PLEKHB1	pleckstrin homology domain containing, family B (evectins) member 1
229047_at	1.54E--0	4.76E--0	19.712955	PLEKHB1	pleckstrin homology domain containing, family B (evectins) member 1
229147_at	0.001427327	0.001035619	9.850531	RASSF6	Ras association (RalGDS/AF--6) domain family member 6
229190_at	0.001870152	0.001472449	10.758549	LOC100507376	uncharacterized LOC100507376
229242_at	2.28E--0	8.44E--0	17.85943	TNFSF15	tumor necrosis factor (ligand) superfamily, member 15
229263_at	0.001696633	0.001285719	11.0779295	IL17RD	interleukin 17 receptor D
229276_at	7.55E--0	4.53E--0	11.292273	IGSF9	immunoglobulin superfamily, member 9
229324_s_at	1.55E--0	4.81E--0	10.436306	ISYNA1	inositol--3--phosphate synthase 1
229627_at	8.79E--0	5.58E--0	17.603468	CDC180//LOC100507547	coiled--coil domain containing 180//LOC100499484--C9orf174 readthrough
229741_at	0.001623493	0.001219333	9.693807	MAVS	mitochondrial antiviral signaling protein
229759_s_at	7.29E--0	1.62E--0	108.406204	VEPH1	ventricular zone expressed PH domain--containing 1
229760_at	7.28E--0	4.29E--0	12.618239	VEPH1	ventricular zone expressed PH domain--containing 1
229782_at	0.004044001	0.003716386	9.917708	RMST	rhabdomyosarcoma 2 associated transcript (non--protein coding)
229890_at	3.99E--0	1.89E--0	9.671778	LOC100507547///	uncharacterized LOC100507547///proline--rich transmembrane protein 1
229990_at	2.40E--0	3.14E--0	17.448982	TSC22D1--AS1	TSC22D1 antisense RNA 1
230012_at	1.48E--0	4.45E--0	10.242456	LINC00324	long intergenic non--protein coding RNA 324
230054_at	0.002624435	0.002225787	9.260708	LOC100507547///	uncharacterized LOC100507547///proline--rich transmembrane protein 1
230100_x_at	0.002132909	0.001736926	11.014069	PAK1	p21 protein (Cdc42/Rac)--activated kinase 1
230252_at	6.12E--0	3.35E--0	9.53768	LPAR5	lysophosphatidic acid receptor 5
230280_at	6.72E--0	3.85E--0	32.819424	TRIM9	tripartite motif containing 9
230349_at	2.54E--0	1.00E--0	11.811716	KXRX	XK, Kell blood group complex subunit--related, X--linked
230378_at	0.001830152	0.001420263	11.9238	SCGB3A1	secretoglobulin, family 3A, member 1
230432_at	2.68E--0	7.12E--0	77.80164	LOC100422737	uncharacterized LOC100422737
230435_at	0.002344293	0.001942697	11.04161	FAM228B	family with sequence similarity 228, member 8
230495_at	0.001587587	0.001182987	10.673325	LOC150568	uncharacterized LOC150568
230585_at	2.74E--0	1.12E--0	22.075768		
230682_x_at	8.22E--0	1.90E--0	20.310078	ABCC3	ATP--binding cassette, sub--family C (CFTR/MRP), member 3
230746_s_at	1.40E--0	4.15E--0	9.145222		
230815_at	0.001967976	0.001567738	15.373846	LOC389765	kinesin family member 27 pseudogene
230876_at	8.89E--0	5.67E--0	20.749125	ZNF883	zinc finger protein 883
230894_s_at	1.04E--0	6.51E--0	10.114002		
230980_x_at	0.005171787	0.004918653	9.307927	MIR142	microRNA 142
231076_at	5.33E--0	2.81E--0	9.314831	C16orf82	chromosome 16 open reading frame 82
231084_at	9.03E--0	5.78E--0	14.054569	WDR96	WD repeat domain 96
231094_s_at	2.18E--0	2.73E--0	21.61475	LOC100996643///	monofunctional C1--tetrahydrofolate synthase, mitochondrial--like//methylene tetrahydrofolate dehydrogenase (NADP+ dependent) 1--like
231211_s_at	8.58E--0	4.65E--0	12.79827	YIF1B	Yip1 interacting factor homolog B (S. cerevisiae)
231270_at	6.21E--0	3.44E--0	15.24883	CA13//LOC10050	carbonic anhydrase XIII//uncharacterized LOC100507258
231339_at	0.002177355	0.001778633	11.464766	TSPYL6	TSPY--like 6
231361_at	0.005914654	0.005719995	12.056276	NLGN1	neuroligin 1
231888_at	4.33E--0	2.11E--0	11.880709		
231925_at	5.26E--0	2.02E--0	11.271834	OTTHUMG0000015	NULL//NULL
231966_at	3.07E--0	4.30E--0	11.354624	PPP1R9A	protein phosphatase 1, regulatory subunit 9A
231978_at	0.001031091	6.86E--0	9.192797	TPCN2	two pore segment channel 2
232058_at	0.005104645	0.004846182	9.557048		
232279_at	1.84E--0	6.13E--0	10.4553175	PHF15	PHD finger protein 15
232354_at	9.56E--0	6.24E--0	15.900315	OTTHUMG0000016	NULL//NULL
232360_at	9.15E--0	2.22E--0	17.802946	EHF	ets homologous factor
232361_s_at	1.02E--0	2.67E--0	71.544876	EHF	ets homologous factor
232406_at	2.05E--0	7.28E--0	17.65848		
232584_at	4.45E--0	8.04E--0	20.44557		
232656_at	0.00181753	0.001404943	10.094017		
232677_at	9.68E--0	6.33E--0	16.360933	SYT11	synaptotagmin XI
232684_at	1.25E--0	3.54E--0	9.979774	ZNF503--AS1	ZNF503 antisense RNA 1
232769_at	0.003346748	0.002985243	10.937857		
232816_s_at	0.001249628	8.81E--0	9.467244	DDX11	DEAD/H (Asp--Glu--Ala--Asp/His) box helicase 11
232944_at	0.002140281	0.00174595	19.498919		
232968_at	0.00479763	0.004498031	11.400988	FANK1	fibronectin type III and ankyrin repeat domains 1
232995_at	1.04E--0	2.76E--0	25.747149		
233318_at	0.00384227	0.003501816	9.587525		
233416_at	0.002537158	0.00213892	10.532397	CTB--12A17.2//C	NULL//NULL
233428_at	1.34E--0	7.92E--0	48.985233		
233449_at	2.46E--0	3.28E--0	12.611312		
233603_at	0.001085394	7.36E--0	12.739119		
233607_at	8.75E--0	5.52E--0	22.44843		
233682_at	0.004834679	0.004561326	13.275307		
233690_at	6.98E--0	4.08E--0	11.344979		
233731_at	3.21E--0	1.37E--0	17.43134		
233794_at	1.72E--0	5.51E--0	9.14928		
233891_at	0.002374042	0.001975363	13.613127	MUC3	intestinal mucin--like
233999_s_at	7.64E--0	4.61E--0	10.949024	TTC26	tetratricopeptide repeat domain 26
234222_at	0.002016266	0.001613013	11.153973		
234260_at	0.002234734	0.00183682	17.705086		
234465_at	7.42E--0	4.42E--0	17.413914	EME1	essential meiotic endonuclease 1 homolog 1 (S. pombe)
234484_s_at	0.001394233	0.001003613	9.374227	ACSS1	acyl--CoA synthetase short--chain family member 1
234547_at	1.70E--0	5.42E--0	11.485429		
234612_at	4.52E--0	2.26E--0	14.251362		
234613_at	9.39E--0	5.39E--0	45.064644		
234673_at	4.63E--0	1.63E--0	33.47462	HHLA2	HERV--H LTR--associating 2
234702_x_at	6.71E--0	3.83E--0	18.422346	CFTR	cystic fibrosis transmembrane conductance regulator (ATP--binding cassette sub--
234706_x_at	1.87E--0	6.34E--0	27.979406	AC000111.3//OT	NULL//NULL
234783_at	1.58E--0	4.93E--0	16.910969		
234794_at	0.002121273	0.00172566	11.047991		
234932_s_at	9.54E--0	2.38E--0	13.7294235	CDCP1	CUB domain containing protein 1
234940_s_at	1.63E--0	1.14E--0	86.07231	OTTHUMG0000015	NULL//NULL
234971_x_at	6.37E--0	3.55E--0	10.438281	PLCD3	phospholipase C, delta 3
235094_at	0.003847102	0.003522452	12.47159		
235213_at	0.003692318	0.003358003	9.387317	ITPKB	inositol--trisphosphate 3--kinase B
235247_at	3.14E--0	4.55E--0	21.734371		
235315_at	1.00E--0	2.58E--0	18.20525	TSC22D1	TSC22 domain family, member 1
235324_at	7.65E--0	4.63E--0	9.841036	SRSF3	serine/arginine--rich splicing factor 3
235329_at	0.004208155	0.00389565	9.186983	NOXO1	NADPH oxidase organizer 1
235515_at	0.00580131	0.00560059	18.300842	SYNE4	spectrin repeat containing, nuclear envelope family member 4
235525_at	0.003847102	0.003520892	12.7906		
235527_at	0.005976538	0.005790419	14.766477	DLGAP1	discs, large (Drosophila) homolog--associated protein 1
235546_at	0.003652867	0.003316865	11.080208	SPINT1	serine peptidase inhibitor, Kunitz type 1
235663_at	3.77E--0	1.73E--0	13.434085		
235736_at	0.003617597	0.003278733	13.466194	SMKR1	small lysine--rich protein 1
235774_at	4.62E--0	1.48E--0	27.906317	LOC100422737	uncharacterized LOC100422737
235775_at	0.003141942	0.002778697	14.969998	TMT2	transmembrane and tetratricopeptide repeat containing 2
235911_at	1.86E--0	6.24E--0	30.698381	MFI2	antigen p97 (melanoma associated) identified by monoclonal antibodies 133.2 and 96.5

235988_at	8.23E--0	5.12E--0	13.107081	GPR110	G protein--coupled receptor 110
235995_at	6.98E--0	4.07E--0	10.392147	PUM2	pumilio homolog 2 (Drosophila)
236075_s_at	0.00186792	0.001467539	12.555516	AC012146.7//OT	NULL//NULL
236083_at	6.07E--0	3.30E--0	23.068436	BCL2L15	BCL2--like 15
236085_at	1.81E--0	5.95E--0	36.803455	CAPSL	calyphosine--like
236414_at	0.00187421	0.001478021	13.7446785		
236489_at	0.003090063	0.002721716	15.787826	GPR110	G protein--coupled receptor 110
236513_at	4.26E--0	2.05E--0	40.926456		
236551_at	1.00E--0	2.59E--0	9.219437	ZNF311	zinc finger protein 311
236636_at	8.96E--0	2.14E--0	11.364258		
236637_at	2.12E--0	7.69E--0	10.598813	TAS2R14	taste receptor, type 2, member 14
236666_s_at	0.004834679	0.004559414	12.453005	LRRC10B	leucine rich repeat containing 10B
236909_at	5.26E--0	2.15E--0	50.203876	CCDC173	coiled--coil domain containing 173
236938_at	0.002517324	0.002113702	15.7298975		
236952_at	9.44E--0	5.50E--0	11.899035		
236960_at	9.31E--0	2.28E--0	9.659253		
237087_at	1.99E--0	6.95E--0	11.291783		
237137_at	0.001182302	8.26E--0	11.996122	SCARNA2	small Cajal body--specific RNA 2
237216_at	0.008027392	0.007993521	13.522857		
237238_at	0.001107518	7.54E--0	10.366672	WWC1	WW and C2 domain containing 1
237272_at	6.31E--0	1.36E--0	16.432991	LOC100506907	uncharacterized LOC100506907
237328_at	0.001524796	0.001124618	20.05386	C14orf105	chromosome 14 open reading frame 105
237369_at	6.76E--0	3.89E--0	20.56959		
237420_at	0.005182798	0.004933498	11.317534	ODF2L	outer dense fiber of sperm tails 2--like
237639_at	4.76E--0	2.42E--0	12.045369	TMEM207	transmembrane protein 207
237656_at	6.45E--0	3.62E--0	10.6296015	WWC2	WW and C2 domain containing 2
237697_at	5.48E--0	2.93E--0	10.465488	LOC100506403//	uncharacterized LOC100506403//runt--related transcription factor 1
237795_s_at	3.17E--0	1.35E--0	11.799117	SP2	Sp2 transcription factor
237804_at	4.08E--0	7.09E--0	51.122284	DNAH11	dynein, axonemal, heavy chain 11
237812_at	0.002317098	0.00191625	9.328435	AC004009.1//OT	NULL//NULL
237851_at	8.58E--0	5.38E--0	9.969121		
237860_at	0.002096211	0.001696428	16.415071	RBMS3	RNA binding motif, single stranded interacting protein 3
237888_at	7.56E--0	4.54E--0	47.585297	LOC100422737	uncharacterized LOC100422737
237889_s_at	2.39E--0	5.03E--0	70.900276	LOC100422737	uncharacterized LOC100422737
238157_at	6.60E--0	3.76E--0	30.747192		
238276_at	0.001849044	0.001443347	12.281342		
238344_at	3.99E--0	1.89E--0	13.018753		
238458_at	0.005432257	0.005184711	11.384384	MICU3	mitochondrial calcium uptake family, member 3
238470_at	9.08E--0	5.83E--0	12.180815	SYS1	SYS1 Golgi--localized integral membrane protein homolog (S. cerevisiae)
238567_at	0.004443804	0.00414005	19.26131	SGPP2	sphingosine--1--phosphate phosphatase 2
238584_at	0.004820192	0.004535455	11.090679	IQCA1	IQ motif containing with AAA domain 1
238626_at	0.00310773	0.002740572	10.041104	ANKS6	ankyrin repeat and sterile alpha motif domain containing 6
238689_at	0.001591397	0.001187169	10.182427	GPR110	G protein--coupled receptor 110
238718_at	0.005753064	0.005539448	10.997554		
238750_at	2.07E--0	2.34E--0	22.700378	CCL28	chemokine (C--C motif) ligand 28
238771_at	7.28E--0	4.28E--0	11.415668		
238786_at	8.31E--0	5.19E--0	20.096943	ANK3	ankyrin 3, node of Ranvier (ankyrin G)
238843_at	0.003485563	0.003135536	11.395241	NPHP1	nephronophthisis 1 (juvenile)
238844_s_at	0.002072633	0.001672098	21.439987	NPHP1	nephronophthisis 1 (juvenile)
238861_at	0.003612693	0.003268191	14.344231	SSBP2	single--stranded DNA binding protein 2
238986_at	0.008030324	0.008296233	12.274752	FLJ43663	uncharacterized LOC378805
239171_at	3.67E--0	1.66E--0	16.798512		
239192_at	0.005063573	0.004802917	10.344479	PARD3B	par--3 partitioning defective 3 homolog B (C. elegans)
239421_at	0.005029314	0.004766177	10.256429	DLGAP1--AS1	DLGAP1 antisense RNA 1
239464_at	1.86E--0	1.85E--0	35.63852		
239657_s_at	2.40E--0	3.13E--0	62.475414	FOXO6//FOXO6	forkhead box O6//NULL
239704_at	0.001435297	0.001042861	12.91507	RNF144B	ring finger protein 144B
239713_at	4.99E--0	2.57E--0	9.852018	CASC2	cancer susceptibility candidate 2 (non--protein coding)
239726_at	5.62E--0	2.42E--0	11.624519	ANK3	ankyrin 3, node of Ranvier (ankyrin G)
239746_at	0.008275781	0.008261813	11.113466	MESDC2	mesoderm development candidate 2
239837_at	2.04E--0	7.22E--0	11.898371	ADAM11	ADAM metalloproteinase domain 11
239924_at	1.99E--0	6.92E--0	10.768611	GUSBP11	glucuronidase, beta pseudogene 11
239928_at	0.004805443	0.004509412	11.189949	TCTN2	tectonic family member 2
239936_at	0.007574581	0.00751066	9.161222	DLEU2	deleted in lymphocytic leukemia 2 (non--protein coding)
239994_at	2.78E--0	3.80E--0	12.033568		
240072_at	0.003043942	0.002668908	11.132172	ASXL2	additional sex combs like 2 (Drosophila)
240112_at	2.30E--0	8.67E--0	11.6778555		
240245_at	0.001675668	0.001267003	10.643582		
240270_s_at	3.88E--0	1.79E--0	13.495025		
240356_s_at	0.001171411	8.15E--0	13.559552		
240365_at	0.005703221	0.00548183	10.683062	LINC00669	long intergenic non--protein coding RNA 669
240414_at	0.001987287	0.001584798	11.738828		
240471_at	9.23E--0	5.98E--0	9.18334		
240584_at	0.002728534	0.002350914	9.3332815	SHANK2--AS2//S	SHANK2 antisense RNA 2//NULL
240656_at	0.002806285	0.00243685	14.790627		
240828_at	0.003239705	0.002873359	10.234536	JARID2--AS1	JARID2 antisense RNA 1
240927_at	3.55E--0	1.58E--0	13.061043		
240935_at	2.04E--0	7.22E--0	31.853796		
241397_at	9.04E--0	5.80E--0	10.049128		
241481_at	0.00479763	0.004496902	9.346114	FAM81A	family with sequence similarity 81, member A
241628_at	0.003090063	0.002722385	9.4058275		
241631_at	0.001346301	9.60E--0	15.965557	ARHGEF40	Rho guanine nucleotide exchange factor (GEF) 40
241713_s_at	0.001185424	8.30E--0	56.11458	DYX1C1//DYX1C1	dyslexia susceptibility 1 candidate 1//DYX1C1--CCPC1 readthrough (NMD candidate)
241747_s_at	8.79E--0	5.59E--0	11.338421	CUL7	cullin 7
242013_at	0.001297293	9.20E--0	14.989882	BCL2L15	BCL2--like 15
242038_at	0.00228468	0.001824147	12.781484	LRRC8B	leucine rich repeat containing 8 family, member B
242045_at	0.006567651	0.006417054	12.8510685		
242057_at	0.001507134	0.001109047	9.150752		
242080_at	3.99E--0	1.88E--0	9.678622		
242098_at	8.38E--0	5.23E--0	9.346645	KIAA1244	KIAA1244
242228_at	0.00422257	0.003912558	10.050408		
242319_at	2.30E--0	8.63E--0	11.932533	DGKG	diacylglycerol kinase, gamma 90kDa
242322_at	1.52E--0	4.64E--0	15.300788		
242372_s_at	0.00162743	0.001233663	17.594627	MFSD4	major facilitator superfamily domain containing 4
242405_at	6.53E--0	3.00E--0	17.74782		
242544_s_at	0.00100579	6.65E--0	17.851545		
242572_at	0.00148059	0.001083267	11.694415		
242773_at	4.45E--0	8.04E--0	31.29685	SLC5A1	solute carrier family 5 (sodium/glucose cotransporter), member 1
242774_at	2.05E--0	2.21E--0	17.87066	SYNE2	spectrin repeat containing, nuclear envelope 2
242798_at	0.003784469	0.003445942	10.293033	AL773604.8//OT	NULL//NULL
242801_at	6.77E--0	3.92E--0	17.021389		
242820_at	0.007983767	0.007943342	9.325976		
242827_s_at	9.35E--0	5.29E--0	19.403103		
242874_at	5.61E--0	3.01E--0	11.065356	OTTHUMG0000017	NULL//NULL
242916_at	8.31E--0	5.18E--0	14.582943	CNTRL	centriolin
243010_at	4.26E--0	2.05E--0	9.827557	MSI2	musashi RNA--binding protein 2
243037_at	0.006839373	0.006729712	9.9949045		
243082_at	0.002882273	0.002517428	10.346411		
243198_at	0.003591908	0.003246358	12.311801	TEX9	testis expressed 9
243349_at	4.86E--0	2.49E--0	18.975801	KIAA1324	KIAA1324
243386_at	9.54E--0	2.35E--0	19.112347	CASZ1	castor zinc finger 1
243429_at	0.001525754	0.001126612	9.2018175		
243563_at	0.007286889	0.007219247	15.374826		
243579_at	4.53E--0	8.26E--0	12.4680805	MSI2	musashi RNA--binding protein 2

243693_at	3.59E--0	1.61E--0	10.243996		
243896_at	6.38E--0	3.56E--0	16.640202	WDR96	WD repeat domain 96
244050_at	0.002749993	0.002374044	11.038347	PTPLAD2	protein tyrosine phosphatase--like A domain containing 2
244240_at	0.004436554	0.004129552	12.601256		
244278_at	0.002599844	0.002202737	9.254769	OTTHUMG000001	NULL//NULL
244333_at	5.77E--0	3.10E--0	15.108922		
244363_at	0.001713679	0.001302975	9.870609	ROS1	c--ros oncogene 1, receptor tyrosine kinase
244469_at	0.001802416	0.00137805	10.895751		
244478_at	1.44E--0	4.30E--0	13.774608	LRRC37A3	leucine rich repeat containing 37, member A3
244527_at	0.002108302	0.001709771	11.138928	TRIO	trio Rho guanine nucleotide exchange factor
244568_at	0.002650978	0.002255009	14.348578		
244575_at	4.48E--0	2.22E--0	14.829588	POLA2	polymerase (DNA directed), alpha 2, accessory subunit
244593_at	2.76E--0	3.75E--0	17.163343	HID1	HID1 domain containing
244626_at	0.00211897	0.001721999	32.04564		
244646_at	0.003049827	0.002676641	15.314977		
244780_at	0.00573544	0.005517639	14.648462	SGPP2	sphingosine--1--phosphate phosphatase 2
244838_at	4.83E--0	9.09E--0	12.449867		
1552325_at	5.26E--0	2.09E--0	18.551413	CCDC11	coiled--coil domain containing 11
1552389_at	4.44E--0	7.95E--0	13.073278	Cborf47	chromosome 8 open reading frame 47
1552596_at	0.002643442	0.002244137	9.412173	GASL2	growth arrest--specific 2 like 2
1552769_at	0.001087635	7.39E--0	10.381464	ZNF625	zinc finger protein 625
1552848_a_at	1.11E--0	7.17E--0	9.857122	PTCHD1	patched domain containing 1
1552858_at	0.00693829	0.006838754	12.086302	MAGEB6	melanoma antigen family B, 6
1564757_a_at	7.39E--0	4.40E--0	11.056455	CDC148	coiled--coil domain containing 148
1553081_at	0.004766739	0.004461024	11.104801	WFDC12	WAP four--disulfide core domain 12
1553163_at	5.48E--0	2.92E--0	9.467901	ADPRHL1	ADP--ribosylhydrolase like 1
1553194_at	1.92E--0	6.62E--0	21.974987	NEGR1	neuronal growth regulator 1
1553574_at	2.43E--0	9.44E--0	11.379251	IFNE	interferon, epsilon
1553625_at	0.004173239	0.003856284	9.936452	FAM98B	family with sequence similarity 98, member B
1553710_at	0.001870152	0.001472342	15.143964	FAM218A	family with sequence similarity 218, member A
1553809_a_at	9.13E--0	5.88E--0	9.474896	TMEM252	transmembrane protein 252
1553812_at	1.63E--0	1.25E--0	30.923784	TLE6	transducin--like enhancer of split 6 (E(sp1) homolog, Drosophila)
1554113_a_at	6.46E--0	3.64E--0	13.40821	SLCA48	solute carrier family 4, sodium bicarbonate cotransporter, member 8
1554188_at	0.001497732	0.001099088	9.381889	C11orf53	chromosome 11 open reading frame 53
1554256_a_at	4.63E--0	1.62E--0	52.06049	PCNXL2	pecanex--like 2 (Drosophila)
1554261_at	5.16E--0	2.69E--0	10.428659	KLHL29	kelch--like family member 29
1554271_a_at	0.001180905	8.24E--0	21.225235	CENPL	centromere protein L
1554506_x_at	1.76E--0	5.75E--0	18.92844	NAALAD2	N--acetylated alpha--linked acidic dipeptidase 2
1554513_s_at	2.07E--0	2.37E--0	10.45751	CEP89	centrosomal protein 89kDa
1554522_at	0.002651433	0.00226153	10.004256	CNNM2	cyclin M2
1554547_at	7.72E--0	4.74E--0	9.325613	FAM13C	family with sequence similarity 13, member C
1554677_s_at	0.001227222	8.64E--0	10.969522	CTMT4	CKLF--like MARVEL transmembrane domain containing 4
1554694_at	0.00338032	0.003020894	11.21627	CCNY	cyclin Y
1554813_at	0.003847102	0.003513295	10.63067		
1554912_at	0.006235969	0.006078097	13.057538	ESYT3	extended synaptotagmin--like protein 3
1555002_at	0.001827313	0.00141449	14.612737	MGC39545	uncharacterized LOC403312
1555038_at	0.0028010376	0.002442774	18.860676	EPB41L4A	erythrocyte membrane protein band 4.1 like 4A
1555039_a_at	9.57E--0	2.41E--0	15.433027	ABCC4	ATP--binding cassette, sub--family C (CFTR/MRP), member 4
1555052_a_at	0.001439486	0.00104712	22.454824	SYT9	synaptotagmin IX
1555053_at	0.005642525	0.005409206	9.518323	SYT9	synaptotagmin IX
1555203_s_at	9.75E--0	6.38E--0	11.1498575	SLC44A4	solute carrier family 44, member 4
1555277_a_at	5.60E--0	1.13E--0	10.192579	SLC4A5	solute carrier family 4, sodium bicarbonate cotransporter, member 5
1555383_a_at	4.31E--0	7.61E--0	11.566774	POF1B	premature ovarian failure, 1B
1555392_at	7.16E--0	4.21E--0	15.874092		
1555397_at	0.001185424	8.30E--0	10.365807	MYO1D	myosin ID
1555400_at	0.006012787	0.005840269	9.693525	LOC645261	PP565
1555407_s_at	2.07E--0	2.38E--0	9.684505	FGD3	FYVE, RhoGEF and PH domain containing 3
1555650_at	1.50E--0	1.35E--0	17.823742	KLHL17	kelch--like family member 17
1555724_s_at	1.32E--0	3.82E--0	10.624196	TAGLN	transgelin
1555731_a_at	3.14E--0	4.52E--0	21.483456	AP1S3	adaptor--related protein complex 1, sigma 3 subunit
1555733_s_at	9.84E--0	2.51E--0	33.109776	AP1S3	adaptor--related protein complex 1, sigma 3 subunit
1555734_x_at	1.54E--0	4.75E--0	11.401026	AP1S3	adaptor--related protein complex 1, sigma 3 subunit
1556014_at	2.94E--0	1.22E--0	9.637482	MES2P2	mesoderm posterior 2 homolog (mouse)
1556017_at	0.001936153	0.001537485	10.015839	NBEAL2	neurobeachin--like 2
1556425_a_at	0.001465374	0.001068425	14.691621	LOC284219	uncharacterized LOC284219
1556653_at	0.001830152	0.00142135	12.376773	ANKAR	ankyrin and armadillo repeat containing
1556889_s_at	1.04E--0	2.76E--0	23.787687		
1556894_at	1.11E--0	7.23E--0	17.713064	NTSDC2	5'-nucleotidase domain containing 2
1556937_at	0.002802702	0.002431374	10.05778		
1557176_a_at	2.49E--0	9.72E--0	42.679096	C14orf37	chromosome 14 open reading frame 37
1557350_at	0.003017406	0.00264327	9.604865	G3BP1	GTPase activating protein (SH3 domain) binding protein 1
1557680_at	3.46E--0	1.51E--0	42.460666	SAMD15	sterile alpha motif domain containing 15
1557700_at	2.11E--0	7.65E--0	15.843484	POLH	polymerase (DNA directed), eta
1557803_at	0.002070559	0.001666931	11.420504		
1558195_at	0.002799675	0.002426385	14.641076	LINC00592	long intergenic non--protein coding RNA 592
1558392_at	5.03E--0	9.60E--0	46.307884	SYNE2	spectrin repeat containing, nuclear envelope 2
1558393_at	7.67E--0	4.67E--0	13.960542	KRT7	keratin 7
1558525_at	0.001911118	0.001512284	10.363566		
1558839_at	0.000065201	0.000077977	13.377173	MAPKBP1	mitogen--activated protein kinase binding protein 1
1558953_s_at	5.03E--0	9.60E--0	9.487525	CEP164	centrosomal protein 164kDa
1559109_a_at	3.71E--0	1.68E--0	15.283865	LOC100996816//	uncharacterized LOC100996816//vacuolar protein sorting 53 homolog (S. cerevisiae)
1559296_at	6.14E--0	3.38E--0	12.062514	ADAMTS9--AS2	ADAMTS9 antisense RNA 2
1559347_at	0.005547425	0.005313357	9.41536		
1559360_at	0.002660707	0.002276191	10.067954		
1559400_s_at	2.03E--0	7.15E--0	29.773304	PAPPA	pregnancy--associated plasma protein A, pappalysin 1
1559405_a_at	0.001038575	6.93E--0	10.002368	TRPV6	transient receptor potential cation channel, subfamily V, member 6
1559882_at	0.002230318	0.001829425	12.721977	SAMHD1	SAM domain and HD domain 1
1559990_at	0.002085611	0.001684329	12.545151		
1560019_at	2.19E--0	7.99E--0	12.08872	DLGAP1--AS2	DLGAP1 antisense RNA 2
1560063_a_at	0.003528022	0.003185641	13.579546	CTD--2540F13.2//	NULL//NULL
1560101_at	0.004051597	0.003730204	12.082341	SYDE2	synapse defective 1, Rho GTPase, homolog 2 (C. elegans)
1560149_at	0.002326381	0.00192589	9.593785	SLC29A2	solute carrier family 29 (nucleoside transporters), member 2
1560156_at	3.34E--0	1.44E--0	15.79455	OTTHUMG0000016	NULL//NULL
1560340_s_at	0.004117552	0.003801352	32.39228	RP9P	retinitis pigmentosa 9 pseudogene
1560419_at	4.02E--0	1.92E--0	10.623244	LOC100127974	uncharacterized LOC100127974
1560430_at	6.48E--0	3.66E--0	15.414474	NKPD1	NTPase, KAP family P--loop domain containing 1
1560458_s_at	1.04E--0	2.72E--0	13.319516	CAPS2	calyphosine 2
1560696_x_at	0.002655935	0.002268191	9.845674	QTRTD1	queuine tRNA--ribosyltransferase domain containing 1
1560834_a_at	5.44E--0	2.88E--0	13.623179	RMST	rhabdomyosarcoma 2 associated transcript (non--protein coding)
1560899_at	2.37E--0	3.06E--0	15.292304		
1560998_x_at	0.005703221	0.005477401	9.988319		
1561149_at	0.001505482	0.001106561	17.155903		
1561316_at	0.003917941	0.003593925	10.442309	GABRR3	gamma--aminobutyric acid (GABA) A receptor, beta 3
1561467_at	6.12E--0	3.36E--0	12.1520195		
1561504_s_at	0.003341766	0.002976238	12.441745	MYLK4	myosin light chain kinase family, member 4
1561633_at	6.77E--0	3.91E--0	9.989858	HMG2	high mobility group AT--hook 2
1561713_at	0.006750693	0.00661397	10.26809	CTD--2076M15.1//	NULL//NULL
1561867_at	5.10E--0	2.64E--0	11.134578		
1562019_at	0.007774426	0.007721941	9.414624	NTSDC4	5'-nucleotidase domain containing 4
1562022_s_at	0.0060990561	0.006896174	11.523403	LOC100130987//	uncharacterized LOC100130987//RAD9 homolog A (S. pombe)
1562049_at	1.37E--0	4.00E--0	21.877703	AC013275.2//OT	NULL//NULL
1562074_a_at	4.62E--0	2.32E--0	47.16255	UNC13C	unc--13 homolog C (C. elegans)
1562222_at	4.99E--0	2.56E--0	9.723425	OTTHUMG0000017	NULL//NULL
1562332_at	0.001997729	0.001596498	12.006876		

1562378_s_at	6.04E--0	1.28E--0	33.20028	PROM2	prominin 2
1566152_s_at	0.001911118	0.001512767	9.629547	AP000662.4//OT	NULL//NULL
1562632_at	3.88E--0	6.28E--0	10.105089	LOC285191	uncharacterized LOC285191
1562637_at	0.001382088	9.93E--0	16.084953	SAMD12	sterile alpha motif domain containing 12
1562788_at	0.001192286	8.36E--0	10.069833	LOC254099	uncharacterized LOC254099
1562970_at	0.003644211	0.00330593	10.097459		
1563092_at	0.001408882	0.001017724	16.658587	OTTHUMG000001	NULL//NULL
1563597_at	9.54E--0	2.37E--0	15.6376295		
1563776_at	3.43E--0	1.48E--0	10.463311	LOC100507283	uncharacterized LOC100507283
1563946_at	1.10E--0	2.97E--0	14.0125475		
1564000_at	6.49E--0	3.68E--0	12.908135	ANKRD31	ankyrin repeat domain 31
1564077_at	3.75E--0	1.71E--0	13.26066		
1564192_at	6.41E--0	3.59E--0	10.7572365		
1564276_at	4.63E--0	1.64E--0	17.425608	CSort56	chromosome 5 open reading frame 56
1564295_at	3.48E--0	1.52E--0	11.847257	FLJ25917	uncharacterized LOC401585
1564466_at	0.001578177	0.001173312	10.788683	FLJ37644	uncharacterized LOC400618
1564819_at	4.34E--0	2.12E--0	11.385895	OTTHUMG0000016	NULL//NULL
1565662_at	1.48E--0	4.42E--0	9.451534		
1565666_s_at	2.14E--0	2.55E--0	10.190565	MUC6	mucin 6, oligomeric mucus/gel--forming
1565685_at	4.32E--0	2.10E--0	17.00032	LOC400940	uncharacterized LOC400940
1565716_at	0.001171411	8.12E--0	9.432322	FUS	fused in sarcoma
1565737_at	0.002884027	0.002521394	9.52948	CTSR	secretin receptor
1565846_at	0.004814343	0.004525889	9.318266		
1565929_s_at	0.002650978	0.002254014	9.304388		
1566439_at	1.32E--0	3.82E--0	32.919643		
1566868_at	0.001830152	0.001425078	12.47608		
1566950_at	1.07E--0	2.86E--0	13.324545		
1567237_at	0.001132926	7.76E--0	12.237158	OR2L2	olfactory receptor, family 2, subfamily 1, member 2
1567361_at	0.004113578	0.00379074	13.852781	BDNF--AS	BDNF antisense RNA
1568574_x_at	2.06E--0	3.91E--0	47.452972	SPP1	secreted phosphoprotein 1
1568713_a_at	0.004884684	0.004616747	13.271148	TBC1D1	TBC1 (tre--2/USP6, BUB2, cdc16) domain family, member 1
1568720_at	1.36E--0	1.06E--0	26.150497	ZNF506	zinc finger protein 506
1568736_s_at	0.002440755	0.00204735	16.856682		
1569098_s_at	2.83E--0	3.89E--0	9.370172	TP53BP1	tumor protein p53 binding protein 1
1569128_at	4.43E--0	2.19E--0	23.810427	C3orf38	chromosome 3 open reading frame 38
1569230_at	0.001176654	8.20E--0	9.475482		
1569310_at	3.58E--0	1.60E--0	16.074282	IRGQ	immunity--related GTPase family, Q
1569512_at	8.69E--0	5.48E--0	21.998262		
1569596_at	7.56E--0	4.55E--0	25.480385		
1569652_at	0.002660707	0.002276757	12.115336	MLLT3	myeloid/lymphoid or mixed--lineage leukemia (trithorax homolog, Drosophila); translocated to, 3
1569794_at	7.39E--0	4.38E--0	13.14039	OTTHUMG0000003	NULL//NULL
1569818_at	2.09E--0	7.53E--0	14.949877		
1569916_at	0.002384406	0.001985999	13.731745		
1569980_x_at	0.001812842	0.001394	11.6297	HKR1//LOC10050	HKR1, GLI--Kruppel zinc finger family member//uncharacterized LOC100507342
1570050_at	0.002530895	0.002131505	12.0527		
1570057_x_at	4.99E--0	2.56E--0	23.865248		
1570181_a_at	2.06E--0	3.52E--0	56.839527		
1570284_x_at	0.001261955	8.91E--0	10.066106		
1570393_at	0.001214765	8.54E--0	32.806366	EML5	echinoderm microtubule associated protein like 5

Monkey liver zone I signature

Probe Set ID	Corrected p--value	p--value	FCAbsolute	Gene Symbol	Gene Title
201929_s_at	1.60E--0	1.16E--0	2.0226698	PKP4	plakophilin 4
202668_at	2.76E--0	5.53E--0	4.160641	EFNB2	ephrin--B2
203017_s_at	0.000132694	9.05E--0	3.1553092	SSX2IP	synovial sarcoma, X breakpoint 2 interacting protein
203238_s_at	0.00026628	2.39E--0	5.9945574	NOTCH3	notch 3
203355_s_at	1.09482E--0	1.62179E--0	2.4077823	PSD3	pleckstrin and Sec7 domain containing 3
203373_at	3.72E--0	1.65E--0	2.1142237	SOC2	suppressor of cytokine signaling 2
204608_at	1.55E--0	5.03E--0	2.2172706	ASL	argininosuccinate lyase
204836_at	4.74947E--0	1.22E--0	2.3754406	GLDC	glycine dehydrogenase (decarboxylating)
204948_s_at	0.000125069	8.42E--0	2.8610394	FST	folistatin
205502_at	6.94709E--0	4.93801E--0	2.5972629	CYP17A1	cytochrome P450, family 17, subfamily A, polypeptide 1
205531_s_at	4.24E--0	2.45E--0	11.614553	GLS2	glutaminase 2 (liver, mitochondrial)
205695_s_at	3.09E--0	1.25E--0	3.816197	SDS	serine dehydratase
206643_at	0.000224802	1.84E--0	7.8267226	HAL	histidine ammonia--lyase
206867_at	8.52004E--0	5.20E--0	2.1786163	GCKR	glucokinase (hexokinase 4) regulator
207076_s_at	6.09225E--0	3.77619E--0	2.339326	ASS1	argininosuccinate synthase 1
207192_at	1.81E--0	1.36E--0	3.3498814	DNASE1L2	deoxyribonuclease 1--like 2
207626_s_at	1.73E--0	5.92E--0	2.7783868	SLC7A2	solute carrier family 7 (cationic amino acid transporter, y+ system), member 2
207732_s_at	4.76252E--0	2.50E--0	3.903643	DLG3	discs, large homolog 3 (Drosophila)
208078_s_at	0.000114633	7.58E--0	2.3262808	SIK1	salt--inducible kinase 1
208234_x_at	5.40444E--0	3.01487E--0	5.290659	FGFR2	fibroblast growth factor receptor 2
208813_at	9.02E--0	2.68E--0	3.1203167	GOT1	glutamic--oxaloacetic transaminase 1, soluble
209641_s_at	1.78E--0	6.18E--0	4.128098	ABCC3	ATP--binding cassette, sub--family C (CFTR/MRP), member 3
209993_at	5.58686E--0	3.16E--0	4.7021565	ABCB1	ATP--binding cassette, sub--family B (MDR/TAP), member 1
210082_at	4.0781E--0	1.89E--0	3.1807747	ABCA4	ATP--binding cassette, sub--family A (ABC1), member 4
211357_s_at	2.75764E--0	1.09394E--0	2.129223	ALDOB	aldolase B, fructose--biphosphate
211401_s_at	6.61E--0	3.82E--0	2.1148927	FGFR2	fibroblast growth factor receptor 2
211652_s_at	4.61E--0	2.38E--0	2.853481	LBP	lipopolysaccharide binding protein
212729_at	9.62799E--0	5.93E--0	2.804292	DLG3	discs, large homolog 3 (Drosophila)
213363_at	0.000193519	1.52E--0	2.248653	CASBP1	carbonic anhydrase VB pseudogene 1
213380_x_at	3.23938E--0	3.61419E--0	2.0742316	LOC101060347//MST1//MST1L//MST1P2	hepatocyte growth factor--like protein--like//macrophage stimulating 1 (hepatocyte growth factor--like)//macrophage stimulating 1--like//macrophage stimulating 1 (hepatocyte growth factor--like) pseudogene 2
214423_x_at	6.09E--0	1.75E--1	2.4237053	ALDOB	aldolase B, fructose--biphosphate
214424_s_at	6.95E--0	5.17E--0	2.5824673	ALDOB	aldolase B, fructose--biphosphate
214535_s_at	0.000107263	6.91E--0	4.3361683	ADAMTS2	ADAM metalloproteinase with thrombospondin type 1 motif, 2
215387_x_at	5.17509E--0	1.35E--0	2.092774		
216320_x_at	2.45169E--0	2.63405E--0	2.0353086	MST1	macrophage stimulating 1 (hepatocyte growth factor--like)
216600_x_at	1.70E--0	7.03E--1	2.276072	ALDOB	aldolase B, fructose--biphosphate
217521_at	2.99E--0	2.94E--0	4.6426773	HAL	histidine ammonia--lyase
218330_s_at	0.000185705	1.44E--0	2.7302983	NAV2	neuron navigator 2
218510_x_at	2.63715E--0	1.00E--0	2.7069287	FAM134B	family with sequence similarity 134, member B
220491_at	1.68396E--0	2.71382E--0	6.357575	HAMP	hepcidin antimicrobial peptide
221008_s_at	4.01E--0	1.83E--0	3.2736363	ETNPPL	ethanolamine--phosphate phospho--lyase
221409_at	2.39E--0	2.02E--0	4.589332	OR2S2	olfactory receptor, family 2, subfamily S, member 2
37201_at	0.000175613	1.31E--0	2.928964	ITIH4	inter--alpha--trypsin inhibitor heavy chain family, member 4
223784_at	3.15504E--0	1.29E--0	2.4458632	TMEM27	transmembrane protein 27
223946_at	3.38329E--0	1.42602E--0	2.386193	MED23	mediator complex subunit 23
225949_at	1.41E--0	9.71E--0	2.4913821	NR8P2	nuclear receptor binding protein 2
226847_at	4.12E--0	1.93E--0	2.500492	FST	folistatin
227217_at	6.76147E--0	3.97E--0	12.520038	WNK2	WNK lysine deficient protein kinase 2
227311_at	0.000207654	1.66E--0	3.1206114	SNX25	sorting nexin 25
227411_at	0.00026628	0.000239835	2.3511484	WTIP	Wilms tumor 1 interacting protein
229148_at	2.62E--0	2.30E--0	3.9022493		
229596_at	1.70E--0	1.25E--0	2.458349	AMDHD1	amidohydrolase domain containing 1
229901_at	0.000141813	9.84E--0	3.8694465	ZNF488	zinc finger protein 488
230107_at	0.000147187	1.05E--0	2.6501658		
230602_at	0.000131435	8.90716E--0	3.3236809	ACMSD	aminocarboxymuconate semialdehyde decarboxylase
230603_at	2.65E--0	2.36E--0	2.9553885	COL27A1	collagen, type XXVII, alpha 1
230657_at	1.00E--0	6.39E--0	6.214824		
230658_at	9.80892E--0	6.08E--0	3.9699845	SLC7A2	solute carrier family 7 (cationic amino acid transporter, y+ system), member 2
231306_at	0.000272559	2.51E--0	4.062453	LYZL4	lysozyme--like 4

231662_at	2.86436E--0	5.95014E--0	3.561257	ARG1	arginase, liver
231663_s_at	3.19E--0	7.14E--0	3.8506296	ARG1	arginase, liver
231665_at	3.77E--0	8.88E--0	5.0547843	ARG1	arginase, liver
231691_at	4.00928E--0	1.84E--0	2.154672	C3P1	complement component 3 precursor pseudogene
232376_at	0.000254989	2.23E--0	5.6355305	PCCA	propionyl CoA carboxylase, alpha polypeptide
232573_at	0.000254989	0.000222918	4.594921		
233514_x_at	1.85E--0	1.43E--0	6.807696	TEX11	testis expressed 11
234296_s_at	6.30E--0	1.74E--0	17.898396	TEX11	testis expressed 11
234472_at	2.76246E--0	5.59E--0	8.569138	GALNT13	UDP--N--acetyl--alpha--D--galactosamine:polypeptide N--acetylgalactosaminyltransferase 13 (GalNAc--T13)
235453_at	0.000144341	1.03E--0	2.0961618	TOR1AIP2	torsin A interacting protein 2
235557_at	0.000272559	0.00025401	5.755047	GPAT2	glycerol--3--phosphate acyltransferase 2, mitochondrial
236708_at	2.90E--0	2.80E--0	4.3267956		
238259_at	2.74E--0	2.60E--0	3.0915186	ADSSL1	adenylosuccinate synthase like 1
238532_at	0.000184829	1.42E--0	2.1110234	DPF3	D4, zinc and double PHD fingers, family 3
238961_s_at	0.000218235	1.78E--0	2.047418	FNDC3A	fibronectin type III domain containing 3A
238984_at	0.000271766	0.00024706	4.584979	REG4	regenerating islet--derived family, member 4
239278_at	2.75E--0	2.62E--0	5.3486648		
239733_at	8.43E--0	5.12E--0	4.9863415	DYDC2	DPY30 domain containing 2
242168_at	0.000142078	9.92E--0	2.4522848	NDUFS7	NADH dehydrogenase (ubiquinone) Fe--S protein 7, 20kDa (NADH--coenzyme Q reductase)
242315_at	0.000234257	1.97E--0	6.2356443		
242668_x_at	0.000272559	0.000257917	2.5640159	SUN5	Sad1 and UNC84 domain containing 5
242972_at	3.72E--0	1.66E--0	2.2804952	HCG18	HLA complex group 18 (non--protein coding)
243691_at	2.65E--0	2.35E--0	3.895336		
1552390_a_at	0.000231353	1.91E--0	10.946081	C8orf47	chromosome 8 open reading frame 47
1555345_at	3.78679E--0	1.71E--0	2.068106	SLC38A4	solute carrier family 38, member 4
1555898_at	0.000229671	0.000188862	7.213749	ANKRD36C	ankyrin repeat domain 36C
1558449_at	2.55E--0	2.22E--0	3.7342243	OTTHUMG000001 77541///RP11-- 421E14.2	NULL//NULL
1559957_a_at	3.16E--0	1.32E--0	4.435049	LOC642852	uncharacterized LOC642852
1564706_s_at	8.53527E--0	2.47E--0	10.846187	GLS2	glutaminase 2 (liver, mitochondrial)
1564707_x_at	3.88026E--0	9.62E--0	5.3590403	GLS2	glutaminase 2 (liver, mitochondrial)
1564933_at	4.64099E--0	2.41638E--0	6.253354		
1566108_at	2.88E--0	2.76E--0	3.1932533	OTTHUMG000001 84028///RP11-- 362K14.5	NULL//NULL

Monkey liver zone III signature

Probe Set ID	Corrected p--value	p--value	FCAbsolute	Gene Symbol	Gene Title
1431_at	5.68E--0	1.52E--0	2.035073	CYP2E1	cytochrome P450, family 2, subfamily E, polypeptide 1
200648_s_at	4.63E--1	3.82E--1	14.877427	GLUL	glutamate--ammonia ligase
200762_at	4.33E--0	2.16E--0	2.0935678	DPYSL2	dihydropyrimidinase--like 2
200831_s_at	1.78E--0	6.34E--0	3.167257	SCD	stearoyl--CoA desaturase (delta--9--desaturase)
200832_s_at	2.67E--0	1.04E--0	3.0721378	SCD	stearoyl--CoA desaturase (delta--9--desaturase)
200974_at	2.73E--0	2.58E--0	3.3604124	ACTA2	actin, alpha 2, smooth muscle, aorta
201116_s_at	1.58E--0	1.37E--0	28.467802	CPE	carboxypeptidase E
201117_s_at	1.15E--0	7.70E--0	11.10634	CPE	carboxypeptidase E
201341_at	6.09E--0	1.76E--1	6.427483	ENC1	ectodermal--neural cortex 1 (with BTB domain)
201505_at	1.49E--0	4.74E--0	3.7487588	LAMB1	laminin, beta 1
201792_at	5.58E--0	7.38E--0	4.9137363	AEBP1	Af binding protein 1
201842_s_at	1.69E--0	1.24E--0	9.803346	EFEMP1	EGF containing fibulin--like extracellular matrix protein 1
201852_x_at	1.43E--0	1.00E--0	2.0042007	COL3A1	collagen, type III, alpha 1
201893_x_at	4.24E--0	2.38E--0	2.4181	DCN	decorin
202112_at	4.85E--0	2.61E--0	5.5790243	VWF	von Willebrand factor
202291_s_at	2.73E--0	2.52E--0	2.7271845	MGP	matrix Gla protein
202310_s_at	2.11E--0	1.69E--0	3.6278934	COL1A1	collagen, type I, alpha 1
202403_s_at	7.02E--0	4.15E--0	2.4008274	COL1A2	collagen, type I, alpha 2
202478_at	5.02E--0	2.74E--0	2.0922978	TRIB2	tribbles homolog 2 (Drosophila)
202728_s_at	6.65E--0	4.40E--0	4.3974094	LTBP1	latent transforming growth factor beta binding protein 1
202729_s_at	9.97E--0	6.29E--0	2.980554	LTBP1	latent transforming growth factor beta binding protein 1
202992_at	2.27E--0	8.36E--0	2.8978126	C7	complement component 7
203088_at	1.02E--0	3.10E--0	5.634558	FBIN5	fibulin 5
203300_x_at	3.11E--0	3.11E--0	2.1585739	API52	adaptor--related protein complex 1, sigma 2 subunit
203424_s_at	5.42E--0	3.04E--0	4.8441024	IGFBP5	insulin--like growth factor binding protein 5
203476_at	7.35E--0	2.10E--0	8.718351	TPBG	trophoblast glycoprotein
203666_at	3.46E--0	1.47E--0	2.1706047	CXCL12	chemokine (C--X--C motif) ligand 12
203887_s_at	1.59E--0	1.44E--0	20.653921	THBD	thrombomodulin
203888_at	2.66E--0	1.02E--0	8.692131	THBD	thrombomodulin
204271_s_at	2.71E--0	1.07E--0	2.0230274	EDNRB	endothelin receptor type B
204284_at	2.54E--0	2.19E--0	2.3123982	PPP1R3C	protein phosphatase 1, regulatory subunit 3C
204684_at	1.40E--0	1.74E--1	24.883291	NPTX1	neuronal pentraxin I
204971_at	1.80E--0	3.20E--0	5.0787926	CSTA	cystatin A (stefin A)
205243_at	1.55E--0	5.07E--0	11.223402	SLC13A3	solute carrier family 13 (sodium--dependent dicarboxylate transporter), member 3
205244_s_at	1.66E--0	2.61E--0	17.454174	SLC13A3	solute carrier family 13 (sodium--dependent dicarboxylate transporter), member 3
205430_at	4.78E--0	2.53E--0	2.2563703	BMP5	bone morphogenetic protein 5
205549_at	8.27E--0	2.73E--1	126.31053	PCP4	Purkinje cell protein 4
205648_at	1.80E--0	1.35E--0	6.2938004	WNT2	wingless--type MMTV integration site family member 2
205723_at	2.34E--0	1.96E--0	3.4714375	CNTRF	ciliary neurotrophic factor receptor
205923_at	1.60E--0	1.65E--0	2.535016	RELN	reelin
205935_at	2.76E--0	5.52E--0	5.5806346	FOXF1	forkhead box F1
205939_at	2.20E--0	1.04E--0	2.479733	CYP3A7	cytochrome P450, family 3, subfamily A, polypeptide 7
206049_at	4.28E--0	2.08E--0	5.6925597	SELP	selectin P (granule membrane protein 140kDa, antigen CD62)
206093_x_at	1.74E--0	3.02E--0	2.1962821	LOC101060681//TNXA//TNXB	tenascin--X--like//tenascin XA (pseudogene)//tenascin XB
206140_at	4.28E--0	2.05E--0	2.967638	LHX2	LIM homeobox 2
206170_at	6.50E--0	3.73E--0	2.471291	ADRB2	adrenoreceptor beta 2, surface
206214_at	2.73E--0	2.56E--0	5.6300383	PLA2G7	phospholipase A2, group VII (platelet--activating factor acetylhydrolase, plasma)
206354_at	1.03E--0	1.45E--0	4.642869	SLCO1B3	solute carrier organic anion transporter family, member 1B3
206440_at	3.19E--0	7.04E--0	2.840402	LIN7A	lin--7 homolog A (C. elegans)
206535_at	5.02E--0	2.73E--0	2.279424	SLC2A2	solute carrier family 2 (facilitated glucose transporter), member 2
207420_at	1.25E--0	3.93E--0	3.7526972	COLEC10	collectin sub--family member 10 (C--type lectin)
207486_x_at	2.73E--0	2.49E--0	2.1267917	CHN2	chimerin 2
207608_x_at	3.88E--0	9.78E--0	5.225593	CYP1A2	cytochrome P450, family 1, subfamily A, polypeptide 2
208131_s_at	4.82E--0	2.57E--0	5.4147186	PTGIS	prostaglandin I2 (prostaglycin) synthase
208335_s_at	2.90E--0	2.82E--0	4.168195	DARC	Duffy blood group, chemokine receptor
208963_x_at	8.12E--0	4.87E--0	2.7604668	FADS1//MIR1908	fatty acid desaturase 1//microRNA 1908
208964_s_at	2.16E--0	1.74E--0	2.63432	FADS1//MIR1908	fatty acid desaturase 1//microRNA 1908
208983_s_at	2.32E--0	1.93E--0	2.0008516	PECAM1	platelet/endothelial cell adhesion molecule 1
209014_at	5.35E--0	2.96E--0	2.4107947	MAGED1	melanoma antigen family D, 1
209047_at	2.39E--0	2.03E--0	3.70033	AQP1	aquaporin 1 (Colton blood group)
209070_s_at	9.02E--0	2.68E--0	3.274502	RGSS	regulator of G--protein signaling 5
209071_s_at	3.16E--0	1.31E--0	2.3304284	RGSS	regulator of G--protein signaling 5
209286_at	1.68E--0	5.69E--0	5.3740406	CDC42EP3	CDC42 effector protein (Rho GTPase binding) 3
209470_s_at	1.49E--0	1.07E--0	10.591253	GPMB6A	glycoprotein M6A
209505_at	4.33E--0	2.15E--0	2.9830382	NR2F1	nuclear receptor subfamily 2, group F, member 1
209687_at	1.60E--0	1.63E--0	4.0524507	CXCL12	chemokine (C--X--C motif) ligand 12
209763_at	6.67E--0	3.88E--0	7.5667996	CHRD1	chordin--like 1
209909_s_at	2.73E--0	2.55E--0	3.4340563	TFGR2	transforming growth factor, beta 2
209976_s_at	1.69E--0	2.79E--0	2.4294944	CYP2E1	cytochrome P450, family 2, subfamily E, polypeptide 1
210139_s_at	1.41E--0	9.67E--0	6.636576	PMP22	peripheral myelin protein 22
210353_s_at	5.68E--0	1.52E--0	14.1236	SLC6A2	solute carrier family 6 (neurotransmitter transporter, noradrenalin), member 2
211162_x_at	2.23E--0	7.48E--0	3.4691007	SCD	stearoyl--CoA desaturase (delta--9--desaturase)
211231_x_at	2.86E--0	6.04E--0	3.1054645	CYP4A11	cytochrome P450, family 4, subfamily A, polypeptide 11

211446_at	5.19E-0	2.85E-0	7.937799	RGSL1	regulator of G--protein signaling like 1
211651_s_at	6.85E-0	1.92E-0	2.5509596	LAMB1	laminin, beta 1
211696_x_at	1.64E-0	5.50E-0	2.8153446	HBB	hemoglobin, beta
211708_s_at	3.00E-0	6.45E-0	3.6494808	SCD	stearoyl--CoA desaturase (delta--9--desaturase)
211813_x_at	1.73E-0	2.93E-0	2.3402781	DCN	decorin
211820_x_at	5.67E-0	3.23E-0	3.717114	GYP A	glycophorin A (MNS blood group)
211896_s_at	2.36E-0	1.99E-0	2.3829098	DCN	decorin
212713_at	3.46E-0	1.49E-0	6.003065	MFAP4	microfibrillar--associated protein 4
213174_at	1.78E-0	6.34E-0	5.2318587	TTC9	tetratricopeptide repeat domain 9
213451_x_at	2.31E-0	4.29E-0	2.4910228	LOC101060681//TNXA//TNXB	tenascin--X--like//tenascin XA (pseudogene)//tenascin XB
213880_at	3.80E-0	9.27E-0	15.47983	LGR5	leucine--rich repeat containing G protein--coupled receptor 5
214460_at	1.98E-0	3.61E-0	14.667987	LSAMP	limbic system--associated membrane protein
214622_at	2.10E-0	7.54E-0	2.820437	CYP21A2	cytochrome P450, family 21, subfamily A, polypeptide 2
215001_s_at	6.62E-1	2.73E-1	5.6179895	GLUL	glutamate--ammonia ligase
215241_at	1.56E-0	1.12E-0	4.7711515	ANO3	anoctamin 3
216333_x_at	1.08E-0	7.04E-0	2.2600734	LOC101060681//TNXA//TNXB	tenascin--X--like//tenascin XA (pseudogene)//tenascin XB
216611_s_at	2.38E-0	4.52E-0	8.573141	SLC6A2	solute carrier family 6 (neurotransmitter transporter, noradrenalin), member 2
217202_s_at	2.41E-0	4.02E-1	18.476679	GLUL	glutamate--ammonia ligase
217213_at	4.40E-0	2.24E-0	9.983754	SLC6A2	solute carrier family 6 (neurotransmitter transporter, noradrenalin), member 2
217214_s_at	1.09E-0	1.63E-0	16.480368	SLC6A2	solute carrier family 6 (neurotransmitter transporter, noradrenalin), member 2
217232_x_at	3.19E-0	7.25E-0	2.806825	HBB	hemoglobin, beta
217621_at	8.12E-0	4.90E-0	6.3332825	SLC6A2	solute carrier family 6 (neurotransmitter transporter, noradrenalin), member 2
218084_x_at	9.81E-0	6.12E-0	2.1107783	FXD5	FXD domain containing ion transport regulator 5
218162_at	2.21E-0	8.02E-0	2.429233	OLFML3	olfactomedin--like 3
218332_at	3.25E-0	3.90E-0	2.5156305	BEX1	brain expressed, X--linked 1
218353_at	2.90E-0	2.80E-0	2.6854308	RG55	regulator of G--protein signaling 5
219087_at	1.14E-0	7.51E-0	2.048257	ASPN	asporin
219367_s_at	1.86E-0	1.46E-0	2.4363072	NRP2	neuropilin 2
219682_s_at	3.33E-0	4.13E-0	3.5890403	TBX3	T--box 3
219884_at	6.30E-0	1.74E-0	11.746349	LHX6	LIM homeobox 6
220510_at	1.17E-0	1.78E-0	6.8438015	RHBG	Rh family, B glycoprotein (gene/pseudogene)
222100_at	3.25E-0	3.78E-0	3.2986734	CYP2E1	cytochrome P450, family 2, subfamily E, polypeptide 1
32625_at	3.67E-0	1.61E-0	3.5482817	NPR1	natriuretic peptide receptor A/guanylate cyclase A (atrionatriuretic peptide receptor A)
222696_at	9.97E-0	6.30E-0	6.3932266	AXIN2	axin 2
223235_s_at	1.08E-0	7.04E-0	4.1362023	SMO2C	SPARC related modular calcium binding 2
223509_at	3.46E-0	1.50E-0	3.099317	CLDN2	claudin 2
223839_s_at	4.59E-0	5.88E-0	2.5346212		
224099_at	1.63E-0	1.19E-0	5.6362486	KCNH7	potassium voltage--gated channel, subfamily H (eag--related), member 7
224560_at	4.28E-0	2.07E-0	2.0329819	TIMP2	TIMP metalloproteinase inhibitor 2
224694_at	1.16E-0	3.60E-0	3.0481799	ANTXR1	anthrax toxin receptor 1
224847_at	3.78E-0	9.06E-0	11.888823	CDK6	cyclin--dependent kinase 6
225016_at	1.95E-0	1.54E-0	4.524202	APCDD1	adenomatous polyposis coli down--regulated 1
225241_at	2.52E-0	9.49E-0	9.486634	CDC80	coiled--coil domain containing 80
225242_s_at	1.60E-0	1.62E-0	8.755893	CDC80	coiled--coil domain containing 80
225367_at	1.81E-0	1.37E-0	2.3691063	PGM2	phosphoglucomutase 2
226016_at	2.18E-0	1.76E-0	2.443767	CD47	CD47 molecule
226237_at	2.94E-0	2.87E-0	7.0640454	COL8A1	collagen, type VIII, alpha 1
226303_at	1.81E-0	1.37E-0	3.7970037	PGM5	phosphoglucomutase 5
226425_at	2.03E-0	1.61E-0	3.0454032	CLIP4	CAP--GLY domain containing linker protein family, member 4
226769_at	2.42E-0	2.07E-0	2.894106	FIBIN	fin bud initiation factor homolog (zebrafish)
226939_at	9.08E-0	1.24E-0	2.506574	CPEB2	cytoplasmic polyadenylation element binding protein 2
226946_at	4.28E-0	2.09E-0	2.2867131	NADK2	NAD kinase 2, mitochondrial
227140_at	2.95E-0	2.89E-0	3.002679	INHBA	inhibin, beta A
227195_at	2.40E-0	8.92E-0	5.014571	ZNFS03	zinc finger protein 503
227235_at	2.73E-0	2.55E-0	2.8981478	GUCY1A3	guanylate cyclase 1, soluble, alpha 3
228186_s_at	7.62E-0	6.30E-0	9.02042	RSP03	R--spondin 3
228335_at	9.10E-0	2.75E-0	11.475331	CLDN11	claudin 11
228608_at	1.82E-0	1.39E-0	3.4475253	NALCN	sodium leak channel, non--selective
229477_at	4.25E-0	2.00E-0	4.5065765	THRSF	thyroid hormone responsive
230135_at	2.20E-0	1.09E-0	3.745248	HHIP	hedgehog interacting protein
231024_at	4.33E-0	2.18E-0	7.9859414	PGM5--AS1	PGM5 antisense RNA 1
231579_s_at	2.95E-0	1.18E-0	2.4674778	TIMP2	TIMP metalloproteinase inhibitor 2
231675_s_at	1.33E-0	4.95E-1	2.8346462	ADH4	alcohol dehydrogenase 4 (class II), pi polypeptide
231678_s_at	2.41E-0	4.98E-1	2.7749605	ADH4	alcohol dehydrogenase 4 (class II), pi polypeptide
231747_at	4.61E-0	2.36E-0	4.7382207	CYSLTR1	cysteinyl leukotriene receptor 1
233606_at	3.03E-0	3.01E-0	6.362521		
233882_s_at	1.64E-0	5.42E-0	2.7763536	SEMA6D	sema domain, transmembrane domain (TM), and cytoplasmic domain, (semaphorin) 6D
235111_at	7.97E-0	4.74E-0	8.813405	LSAMP	limbic system--associated membrane protein
235349_at	2.71E-0	2.45E-0	4.2362795	RMDN2	regulator of microtubule dynamics 2
237466_s_at	7.24E-0	5.68E-0	4.8819046	HHIP	hedgehog interacting protein
241789_at	2.66E-0	2.40E-0	2.6873555	RBMS3	RNA binding motif, single stranded interacting protein 3
242281_at	1.15E-0	7.73E-0	9.330574	GLUL	glutamate--ammonia ligase
1555316_a_at	4.33E-0	2.17E-0	10.405118	KCNH7	potassium voltage--gated channel, subfamily H (eag--related), member 7
1556167_at	1.43E-0	1.01E-0	7.835601	MROH2A	maestro heat--like repeat family member 2A
1556499_s_at	3.03E-0	3.01E-0	4.0777473	COL1A1	collagen, type I, alpha 1
1558254_s_at	1.02E-0	6.54E-0	3.0067284	SRPK2	SRSF protein kinase 2
1559921_at	2.48E-0	2.13E-0	3.5523612	PECAM1	platelet/endothelial cell adhesion molecule 1
1560291_at	3.06E-0	3.05E-0	4.2468786	RIPPLY1	rippl1 homolog (zebrafish)

Methapyrilene induced genes

Bile duct genes induced in treated animals vs. untreated animals at day 3

Probe Set ID	Gene Symbol	Gene Title
1367581_at	Spp1	secreted phosphoprotein 1
1367584_at	Anxa2	annexin A2
1367592_at	Tnnt2	troponin T type 2 (cardiac)
1367655_at	LOC100359493// LOC100359496/ LOC100361392 LOC10036159 LOC1003616 LOC100364 LOC10090 LOC1009 LOC1009 LOC1009	thymosin, beta 10---like//thymosin, beta 10--- like//thymosin, beta 10---like//hypothetical protein LOC100361596//thymosin, beta 10---like//thymosin, beta 10---like//thymosin beta---10---like//thymosin beta---10--- like//thymosin, beta 10
1368007_at	Dmbt1//LOC100 913031	deleted in malignant brain tumors 1//deleted in malignant brain tumors 1 protein---like
1368008_at	Prom1	prominin 1
1368013_at	Ddit4l//LOC1003 63484	DNA---damage---inducible transcript 4---like//DNA--- damage---
1368052_at	Tspan8	tetraspanin 8
1368097_a_at	Rtn1	reticulon 1
1368278_at	Lgals2	lectin, galactoside---binding, soluble, 2
1368374_a_at	Ggt1	gamma---glutamyltransferase 1
1368391_at	Slc7a1	solute carrier family 7 (cationic amino acid transporter, y+ system), member 1
1368392_at	Slc7a1	solute carrier family 7 (cationic amino acid transporter, y+ system), member 1
1368413_at	Abp1	amiloride binding protein 1 (amine oxidase, copper--- containing)
1368515_at	Epb41l3	erythrocyte membrane protein band 4.1---like 3
1368555_at	Cd37	CD37 molecule
1368921_a_at	Cd44	CD44 molecule
1369105_a_at	Pkib	protein kinase (cAMP---dependent, catalytic) inhibitor beta
1369513_at	Ccl28	chemokine (C---C motif) ligand 28
1369698_at	Abcc3	ATP---binding cassette, subfamily C (CFTR/MRP), member 3
1369953_a_at	Cd24	CD24 molecule
1369963_at	Pafah1b3	platelet---activating factor acetylhydrolase 1b, catalytic subunit 3
1370026_at	Cryab	crystallin, alpha B
1370269_at	Cyp1a1	cytochrome P450, family 1, subfamily a, polypeptide 1
1370379_at	Prss8	protease, serine, 8
1370594_at	Igslf1	immunoglobulin superfamily, member 1
1370894_at	Cldn7	claudin 7
1370902_at	Akr1b8	aldo---keto reductase family 1, member B8
1371256_at	Ptpn18	protein tyrosine phosphatase, non---receptor type 18
1371360_at	Ndrp1	N---myc downstream regulated 1
1371472_at		
1371883_at	Mmd	monocyte to macrophage differentiation---associated
1372064_at	Cxcl16	chemokine (C---X---C motif) ligand 16
1372179_at	Hpcal1	hippocalcin---like 1
1372256_at	Crip1	cysteine---rich protein 1 (Intestinal)
1372725_at	Plscr2	phospholipid scramblase 2
1373035_at		
1373458_at	Bex4	brain expressed, X---linked 4
1373631_at	Rap1gap	Rap1 GTPase---activating protein
1373908_at		
1374070_at	Gpx2	glutathione peroxidase 2
1374573_at	Dync2li1	dynein cytoplasmic 2 light intermediate chain 1
1374976_a_at	Soat1	sterol O---acyltransferase 1
1375170_at	S100a11	S100 calcium binding protein A11
1375267_at	Ppic	peptidylprolyl isomerase C
1375958_at	Tsc22d4	TSC22 domain family, member 4
1376292_at		
1376770_at	Efh1	EF---hand domain family, member D1
1376877_at	Cdcp1	CUB domain containing protein 1
1377008_at	RGD1566401	similar to GTL2, imprinted maternally expressed untranslated
1377018_at		
1377034_at	Serp1b1a	serine (or cysteine) proteinase inhibitor, clade B, member 1a
1379031_at	Gca	granulocytin
1382849_at		
1383935_at		
1386466_at		
1386862_at	Anxa5	annexin A5
1387195_at	St14	suppression of tumorigenicity 14 (colon carcinoma)
1387454_at	Fam129a	family with sequence similarity 129, member A
1387459_at	Pkib	protein kinase (cAMP---dependent, catalytic) inhibitor beta
1387671_at	Sctr	secretin receptor
1387952_a_at	Cd44	CD44 molecule
1388074_at	Krt20	keratin 20
1388152_at	Map2	microtubule---associated protein 2
1388199_at	Epcam	epithelial cell adhesion molecule
1388335_at	Tagln2	transgelin 2
1388547_at	Cldn4	claudin 4
1388557_at	C7//Tubb4b	complement component 7//tubulin, beta 4B class IVb
1388802_at	Bex1//LOC1009 12195	brain expressed, X---linked 1//protein BEX1---like
1388932_at	Lama5	laminin, alpha 5
1389360_at	Fxyd3	FXYD domain---containing ion transport regulator 3
1389409_at	Tes	testis derived transcript

1390070_at	LOC100911253	uncharacterized LOC100911253
1390557_at	Gca	grancalcin
1390659_at		
1393018_at	LOC100912649	uncharacterized LOC100912649
1398373_at	B3galnt1	beta---1,3---N---acetylgalactosaminyltransferase 1 (globoside blood group)
1377940_at	Fam101b	family with sequence similarity 101, member B
1378015_at	Ccl21	chemokine (C---C motif) ligand 21
1378168_at	Fam101b	family with sequence similarity 101, member B
1379008_at		
1379440_at	Fstl3	folliculin---like 3 (secreted glycoprotein)
1380086_at		
1380574_at		
1380909_at	Slc25a24	solute carrier family 25 (mitochondrial carrier, phosphate carrier), member 24
1381434_s_at	LOC100912349// /LOC302022	nidogen---2---like///similar to nidogen 2 protein
1382217_at		
1382291_at		
1382776_at	Mboat1	membrane bound O---acyltransferase domain containing 1
1382835_at		
1382882_x_at		
1383291_at	C7//Tubb4b	complement component 7//tubulin, beta 4B class IVb
1383311_at	Mtnr11	myotubularin related protein 11
1383401_at	Tes	testis derived transcript
1383668_at	Mmp15	matrix metalloproteinase 15
1383766_at	Sgcb	sarcoglycan, beta (dystrophin---associated glycoprotein)
1384000_at	Sox4	SRY (sex determining region Y)---box 4
1384468_at		
1384960_at	Cftr	cystic fibrosis transmembrane conductance regulator
1385472_at	Zbtb8a	zinc finger and BTB domain containing 8a
1385534_at	Ngfrap1	nerve growth factor receptor (TNFRSF16) associated protein 1
1385706_at		
1385716_at		
1385830_at	RGD1561507	similar to hypothetical protein FLJ31606
1385978_at		
1391063_at	Kif23	kinesin family member 23
1391162_at	Dcdc2	doublecortin domain containing 2
1391187_at	Ppl	periplakin
1392557_at		
1392813_at		
1393167_at		
1393234_at	LOC687105	hypothetical protein LOC687105
1393252_at		
1393337_at	Tfcg211	transcription factor CP2---like 1
1393584_at	Tnfrsf21	tumor necrosis factor receptor superfamily, member 21
1393641_at	Blink	B---cell linker
1395390_at		
1395966_at	Kctd14	potassium channel tetramerisation domain containing 14
1398716_at		

Bile duct genes induced in treated animals vs. untreated animals at day 7

Probe Set ID	Gene Symbol	Gene Title
1367581_a_at	Spp1	secreted phosphoprotein 1
1367584_at	Anxa2	annexin A2
1367592_at	Tnnt2	troponin T type 2 (cardiac)
1367655_at	LOC100359493// /LOC100359496/ //LOC100361392 //LOC10036159 6//LOC1003616 20//LOC100364 435//LOC10090 9821//LOC1009 11590//Tmsb10	thymosin, beta 10---like//thymosin, beta 10--- like//thymosin, beta 10---like//hypothetical protein LOC100361596//thymosin, beta 10---like//thymosin, beta 10---like//thymosin beta---10---like//thymosin beta---10--- like//thymosin, beta 10
1368007_at	Dmbt1//LOC100 913031	deleted in malignant brain tumors 1//deleted in malignant brain tumors 1 protein---like
1368008_at	Prom1	prominin 1
1368013_at	Ddit4//LOC1003 63484	DNA---damage---inducible transcript 4---like//DNA--- damage---
1368052_at	Tspan8	tetraspanin 8
1368097_a_at	Rtn1	reticulin 1
1368278_at	Lgals2	lectin, galactoside---binding, soluble, 2
1368374_a_at	Ggt1	gamma---glutamyltransferase 1
1368391_at	Slc7a1	solute carrier family 7 (cationic amino acid transporter, y+ system), member 1
1368392_at	Slc7a1	solute carrier family 7 (cationic amino acid transporter, y+ system), member 1
1368413_at	Abp1	amiloride binding protein 1 (amine oxidase, copper--- containing)
1368469_at	Aqp5	aquaporin 5
1368515_at	Epb413	erythrocyte membrane protein band 4.1---like 3
1368527_at	Ptgs2	prostaglandin---endoperoxide synthase 2
1368555_at	Cd37	CD37 molecule
1368921_a_at	Cd44	CD44 molecule
1369105_a_at	Pkib	protein kinase (cAMP---dependent, catalytic) inhibitor beta
1369513_at	Ccl28	chemokine (C---C motif) ligand 28
1369698_at	Abcc3	ATP---binding cassette, subfamily C (CFTR/MRP), member 3
1369953_a_at	Cd24	CD24 molecule

1369963_at	Pafah1b3	platelet---activating factor acetylhydrolase 1b, catalytic subunit 3
1370026_at	Cryab	crystallin, alpha B
1370218_at	Ldhb	lactate dehydrogenase B
1370269_at	Cyp1a1	cytochrome P450, family 1, subfamily a, polypeptide 1
1370379_at	Prss8	protease, serine, 8
1370594_at	Igsl1	immunoglobulin superfamily, member 1
1370894_at	Cldn7	claudin 7
1370902_at	Akr1b8	aldo---keto reductase family 1, member B8
1371256_at	Ptpn18	protein tyrosine phosphatase, non---receptor type 18
1371260_at	Mcpt2	mast cell protease 2
1371360_at	Ndrgr1	N---myc downstream regulated 1
1371472_at		
1371499_at	Cd9	CD9 molecule
1371883_at	Mmd	monocyte to macrophage differentiation---associated
1372064_at	Cxcl16	chemokine (C---X---C motif) ligand 16
1372179_at	Hpcal1	hippocalcin---like 1
1372256_at	Crip1	cysteine---rich protein 1 (intestinal)
1372725_at	Plscr2	phospholipid scramblase 2
1373035_at		
1373458_at	Bex4	brain expressed, X---linked 4
1373631_at	Rap1gap	Rap1 GTPase---activating protein
1373908_at		
1374070_at	Gpx2	glutathione peroxidase 2
1374573_at	Dync2ll1	dynein cytoplasmic 2 light intermediate chain 1
1374976_a_at	Soat1	sterol O---acyltransferase 1
1375170_at	S100a11	S100 calcium binding protein A11
1375267_at	Ppic	peptidylprolyl isomerase C
1375958_at	Tsc22d4	TSC22 domain family, member 4
1376292_at		
1376770_at	Efh1	EF---hand domain family, member D1
1376877_at	Cdec1	CUB domain containing protein 1
1376937_at	Filip1l	filamin A interacting protein 1---like
1377008_at	RGD1566401	similar to GTL2, imprinted maternally expressed untranslated
1377018_at		
1377034_at	Serp1b1a	serine (or cysteine) proteinase inhibitor, clade B, member 1a
1379031_at	Gca	granulosa cell
1382849_at		
1383935_at		
1386466_at		
1386862_at	Anxa5	annexin A5
1387195_at	St14	suppression of tumorigenicity 14 (colon carcinoma)
1387454_at	Fam129a	family with sequence similarity 129, member A
1387459_at	Pkib	protein kinase (cAMP---dependent, catalytic) inhibitor beta
1387671_at	Sctr	secretin receptor
1387952_a_at	Cd44	CD44 molecule
1388074_at	Krt20	keratin 20
1388152_at	Map2	microtubule---associated protein 2
1388199_at	Epcam	epithelial cell adhesion molecule
1388335_at	Tagln2	transgelin 2
1388433_at	Krt19	keratin 19
1388547_at	Cldn4	claudin 4
1388557_at	C7//Tubb4b	complement component 7//tubulin, beta 4B class IVb
1388802_at	Bex1//LOC100912195	brain expressed, X---linked 1//protein BEX1---like
1388902_at	Loxl1	lysyl oxidase---like 1
1388932_at	Lama5	laminin, alpha 5
1389360_at	Fxyd3	FXD domain---containing ion transport regulator 3
1389409_at	Tes	testis derived transcript
1390070_at	LOC100911253	uncharacterized LOC100911253
1390557_at	Gca	granulosa cell
1390659_at		
1393018_at	LOC100912649	uncharacterized LOC100912649
1398373_at	B3galnt1	beta---1,3---N---acetylgalactosaminyltransferase 1 (globoside blood group)
1377940_at	Fam101b	family with sequence similarity 101, member B
1378015_at	Ccl21	chemokine (C---C motif) ligand 21
1378168_at	Fam101b	family with sequence similarity 101, member B
1379008_at		
1379440_at	Fstl3	folliculin---like 3 (secreted glycoprotein)
1380086_at		
1380574_at		
1380909_at	Slc25a24	solute carrier family 25 (mitochondrial carrier, phosphate carrier), member 24
1381434_s_at	LOC100912349//LOC302022	nidogen---2---like//similar to nidogen 2 protein
1382217_at		
1382291_at		
1382776_at	Mboat1	membrane bound O---acyltransferase domain containing 1
1382835_at		
1382882_x_at		
1383137_at	Sox4	SRY (sex determining region Y)---box 4
1383291_at	C7//Tubb4b	complement component 7//tubulin, beta 4B class IVb
1383311_at	Mtmr11	myotubularin related protein 11
1383401_at	Tes	testis derived transcript
1383668_at	Mmp15	matrix metalloproteinase 15
1383766_at	Sgcb	sarcoglycan, beta (dystrophin---associated glycoprotein)
1383879_at	LOC688163	hypothetical protein LOC688163

1384000_at	Sox4	SRY (sex determining region Y)---box 4
1384468_at		
1384960_at	Cftr	cystic fibrosis transmembrane conductance regulator
1385472_at	Zbtb8a	zinc finger and BTB domain containing 8a
1385534_at	Ngfrap1	nerve growth factor receptor (TNFRSF16) associated protein 1
1385706_at		
1385716_at		
1385830_at	RGD1561507	similar to hypothetical protein FLJ31606
1385978_at		
1391022_at	Lamb3	laminin, beta 3
1391063_at	Kif23	kinesin family member 23
1391162_at	Dcdc2	doublecortin domain containing 2
1391187_at	Ppl	periplakin
1391331_at		
1392557_at		
1392813_at		
1393167_at		
1393234_at	LOC687105	hypothetical protein LOC687105
1393252_at		
1393337_at	Tfcp2l1	transcription factor CP2---like 1
1393584_at	Tnfrsf21	tumor necrosis factor receptor superfamily, member 21
1393641_at	Blnk	B---cell linker
1395390_at		
1395966_at	Kctd14	potassium channel tetramerisation domain containing 14
1398716_at		

Bile duct genes induced in treated animals vs. untreated animals at day 14

Probe Set ID	Gene Symbol	Gene Title
1367581_a_at	Spp1	secreted phosphoprotein 1
1367584_at	Anxa2	annexin A2
1367592_at	Tnnt2	troponin T type 2 (cardiac)
1367655_at	LOC100359493// LOC100359496// LOC100361392// LOC10036159 6//LOC1003616 20//LOC100364 435//LOC10090 9821//LOC1009 11590//Tmsb10	thymosin, beta 10---like//thymosin, beta 10--- like//thymosin, beta 10---like//hypothetical protein LOC100361596//thymosin, beta 10---like//thymosin, beta 10---like//thymosin beta---10---like//thymosin beta---10--- like//thymosin, beta 10
1368007_at	Dmbt1//LOC100 913031	deleted in malignant brain tumors 1//deleted in malignant brain tumors 1 protein---like
1368008_at	Prom1	prominin 1
1368013_at	Ddit4l//LOC1003 63484	DNA---damage---inducible transcript 4---like//DNA--- damage---
1368052_at	Tspan8	tetraspanin 8
1368097_a_at	Rtn1	reticulon 1
1368278_at	Lgals2	lectin, galactoside---binding, soluble, 2
1368374_a_at	Ggt1	gamma---glutamyltransferase 1
1368391_at	Slc7a1	solute carrier family 7 (cationic amino acid transporter, y+ system), member 1
1368392_at	Slc7a1	solute carrier family 7 (cationic amino acid transporter, y+ system), member 1
1368413_at	Abp1	amiloride binding protein 1 (amine oxidase, copper--- containing)
1368469_at	Aqp5	aquaporin 5
1368515_at	Epb41i3	erythrocyte membrane protein band 4.1---like 3
1368527_at	Ptgs2	prostaglandin---endoperoxide synthase 2
1368555_at	Cd37	CD37 molecule
1368921_a_at	Cd44	CD44 molecule
1369105_a_at	Pkib	protein kinase (cAMP---dependent, catalytic) inhibitor beta
1369513_at	Ccl28	chemokine (C---C motif) ligand 28
1369698_at	Abcc3	ATP---binding cassette, subfamily C (CFTR/MRP), member 3
1369953_a_at	Cd24	CD24 molecule
1369963_at	Pafah1b3	platelet---activating factor acetylhydrolase 1b, catalytic subunit 3
1370026_at	Cryab	crystallin, alpha B
1370218_at	Ldhb	lactate dehydrogenase B
1370269_at	Cyp1a1	cytochrome P450, family 1, subfamily a, polypeptide 1
1370379_at	Prss8	protease, serine, 8
1370594_at	Igslf1	immunoglobulin superfamily, member 1
1370894_at	Cldn7	claudin 7
1370902_at	Akr1b8	aldo---keto reductase family 1, member B8
1371164_at	Mcpt10//RGD15 65970	mast cell protease 10//similar to mast cell protease 8
1371256_at	Ptpn18	protein tyrosine phosphatase, non---receptor type 18
1371260_at	Mcpt2	mast cell protease 2
1371360_at	Ndrp1	N---myc downstream regulated 1
1371472_at		
1371499_at	Cd9	CD9 molecule
1371883_at	Mmd	monocyte to macrophage differentiation---associated
1372064_at	Cxcl16	chemokine (C---X---C motif) ligand 16
1372179_at	Hpcal1	hippocalcin---like 1
1372256_at	Crip1	cysteine---rich protein 1 (intestinal)
1372725_at	Plscr2	phospholipid scramblase 2
1373035_at		
1373458_at	Bex4	brain expressed, X---linked 4
1373631_at	Rap1gap	Rap1 GTPase---activating protein

1373908_at		
1374070_at	Gpx2	glutathione peroxidase 2
1374573_at	Dync2li1	dynein cytoplasmic 2 light intermediate chain 1
1374976_a_at	Soat1	sterol O---acyltransferase 1
1375170_at	S100a11	S100 calcium binding protein A11
1375267_at	Ppic	peptidylprolyl isomerase C
1375958_at	Tsc22d4	TSC22 domain family, member 4
1376292_at		
1376770_at	Efh1	EF---hand domain family, member D1
1376877_at	Cdcp1	CUB domain containing protein 1
1376937_at	Filip1l	filamin A interacting protein 1---like
1377008_at	RGD1566401	similar to GTL2, imprinted maternally expressed untranslated
1377018_at		
1377034_at	Serpib1a	serine (or cysteine) proteinase inhibitor, clade B, member 1a
1379031_at	Gca	grancalcin
1382849_at		
1383935_at		
1386466_at		
1386862_at	Anxa5	annexin A5
1387195_at	St14	suppression of tumorigenicity 14 (colon carcinoma)
1387454_at	Fam129a	family with sequence similarity 129, member A
1387459_at	Pkib	protein kinase (cAMP---dependent, catalytic) inhibitor beta
1387671_at	Sctr	secretin receptor
1387952_a_at	Cd44	Cd44 molecule
1388074_at	Krt20	keratin 20
1388152_at	Map2	microtubule---associated protein 2
1388199_at	Epcam	epithelial cell adhesion molecule
1388335_at	Tagln2	transgelin 2
1388433_at	Krt19	keratin 19
1388547_at	Cldn4	claudin 4
1388557_at	C7//Tubb4b	complement component 7//tubulin, beta 4B class IVb
1388802_at	Bex1//LOC100912195	brain expressed, X---linked 1//protein BEX1---like
1388902_at	Loxl1	lysyl oxidase---like 1
1388932_at	Lama5	laminin, alpha 5
1389360_at	Fxyd3	FXD domain---containing ion transport regulator 3
1389409_at	Tes	testis derived transcript
1390070_at	LOC100911253	uncharacterized LOC100911253
1390557_at	Gca	grancalcin
1390659_at		
1393018_at	LOC100912649	uncharacterized LOC100912649
1398373_at	B3galnt1	beta---1,3---N---acetylgalactosaminyltransferase 1 (globoside blood group)
1377940_at	Fam101b	family with sequence similarity 101, member B
1378015_at	Ccl21	chemokine (C---C motif) ligand 21
1378168_at	Fam101b	family with sequence similarity 101, member B
1379008_at		
1379440_at	Fstl3	folliculin---like 3 (secreted glycoprotein)
1380086_at		
1380574_at		
1380909_at	Slc25a24	solute carrier family 25 (mitochondrial carrier, phosphate carrier), member 24
1381434_s_at	LOC100912349//LOC302022	nidogen---2---like//similar to nidogen 2 protein
1382217_at		
1382291_at		
1382776_at	Mboat1	membrane bound O---acyltransferase domain containing 1
1382835_at		
1382882_x_at		
1383137_at	Sox4	SRY (sex determining region Y)---box 4
1383291_at	C7//Tubb4b	complement component 7//tubulin, beta 4B class IVb
1383311_at	Mtmr11	myotubularin related protein 11
1383401_at	Tes	testis derived transcript
1383668_at	Mmp15	matrix metalloproteinase 15
1383766_at	Sgcb	sarcoglycan, beta (dystrophin---associated glycoprotein)
1383879_at	LOC688163	hypothetical protein LOC688163
1384000_at	Sox4	SRY (sex determining region Y)---box 4
1384468_at		
1384960_at	Cftr	cystic fibrosis transmembrane conductance regulator
1385472_at	Zbtb8a	zinc finger and BTB domain containing 8a
1385534_at	Ngfrap1	nerve growth factor receptor (TNFRSF16) associated protein 1
1385706_at		
1385716_at		
1385830_at	RGD1561507	similar to hypothetical protein FLJ31606
1385978_at		
1391022_at	Lamb3	laminin, beta 3
1391063_at	Kif23	kinesin family member 23
1391162_at	Dcdc2	doublecortin domain containing 2
1391187_at	Ppl	periplakin
1391331_at		
1392557_at		
1392813_at		
1393167_at		
1393234_at	LOC687105	hypothetical protein LOC687105
1393252_at		
1393337_at	Tfcp2l1	transcription factor CP2---like 1
1393584_at	Tnfrsf21	tumor necrosis factor receptor superfamily, member 21

1393641_at	Blnk	B---cell linker
1395390_at		
1395966_at	Kctd14	potassium channel tetramerisation domain containing 14
1398716_at		

Appendix

Curriculum Vitae

CURRICULUM VITAE ET STUDIORUM

Dr. DIEGO CALABRESE

PhD in Clinical and Pathological Morphology

PhD in Molecular Toxicology

Place and date of birth:

Napoli (Italy) 03/03/1979

Address:

Missionsstrasse 15A, 4055, Basel

Telephone Number:

+41 767 000379

Mail Address:

diego.calabrese@unibas.ch

Working Experiences:

January 2018 - now

Review Editor of the Editorial Board of Pathology, a specialty of Frontiers in Medicine journal.

September 2015 - now

Responsible for the Department of Biomedicine Histology Core Facility.

Department of Biomedicine, Zentrum für Lehre und Forschung, University Hospital Basel.

As responsible for the Histology Core Facility my duty is to support the development of new histological assays in a multidisciplinary environment and in synergy with the Microscopy Core Facility. In addition I am personally involved in the training of new users, providing them with principle for the good laboratory practices (GLP), identify and propose new equipment and technologies to extend the experimental capabilities in the histology field and to supervise the laboratories, ensuring the proper functioning of the available equipment.

April 2012 - now

Senior Post-doc & Project leader

University Hospital Basel, Department of Biomedicine, Hepatology Laboratory.

Project aimed at establishing an innovative in-vitro system for HBV-host interaction and (innate) immune response study, taking advantage from the use of ex-vivo liver tissue culture and hepatocyte-like induced pluripotent stem cell (HL-iPSC) derived cells.

October 2013

Scientific fellowship at Scottish Centre for Regenerative Medicine (SCRM).

Scientific fellowship for learning the reprogramming and differentiation of iPSCs into hepatocyte-like cells. Guest of **Pluripotent Stem Cell Hepatocyte Development**, group lead by Dr. David Hay.

January 2009 – April 2012:

Ph.D. "Pharmaceutical Sciences - Molecular and System Toxicology".

Experimental work on liver molecular map profiling, across different species (Rat, Dog and Monkey), performed using laser capture microdissection to characterize the gene expression profile of morpho-functional liver parenchymal regions and the "portal triad" components. Gene signatures generated by this study have been validated by a preclinical study and are currently used for liver drug-induced injury detection, and drug safety assessment.

October 2008 – December 2008:

Instructor for the "Human Anatomy Laboratory" course. Inter-University School of Specialization for Secondary School Teaching (S.I.C.S.I.), Naples University "Federico II" (IT).

May 2008 – October 2008:

Scientific fellowship at Pathology Institute of University Hospital Basel (CH): "Analysis of apoptotic markers in cardiac ischemia by tissue microarray".

November 2005 – October 2008:

- ✓ **Teaching fellow and exam committee member for the Human Anatomy course** at Pharmacy and Biotechnology faculties. University of Naples "Federico II" (IT).
- ✓ **Tutor and master thesis supervisor** for students of Biotechnology, Pharmacy and Biology faculties. University of Naples "Federico II" (IT).

November 2005 – October 2008:

Ph.D. in "Clinical and Pathological Morphology - Normal Human Morphology"

Experimental work on cardiovascular diseases (aorta aneurysm and post-ischemic cardiac diseases).

May 2004 – July 2005:

Scientific fellowship at the Department of Structural and Functional Biology, Naples University "Federico II" (IT), for the development of master thesis.

Experimental work on the role of the p27^{BBP}/eIF6 protein during the *Xenopus* l. embryogenesis.

Education:

January 2009 – April 2012:

Ph.D. in "Pharmaceutical Sciences - Molecular and Systems Toxicology". University of Basel and Novartis Institute for Biomedical Research (NIBR/TS/PCS/iTox/ Mol.Pathology & Immunology), Basel (CH).

September 2005 – October 2008:

Ph.D. in "Clinical and Pathological Morphology – Normal Human Morphology". Anatomy Department of Medicine and Surgery School, Naples University "Federico II" (IT).

Thesis entitled *"Apoptosis markers analysis in cardiac ischemia by tissue microarray"*.

July 2005:

Master degree in Biological Sciences, Naples University "Federico II" (IT).

Thesis entitled *"p27^{BBP}/eIF6 expression during embryogenesis of *Xenopus laevis*"*.

Grants & Awards:

Winner of "**Research Fund Junior Researchers**", the University of Basel grant for promoting the academic careers of outstanding junior researchers, September 2015.

The long-term goals of the experiments proposed in this application was to build on the current state of the iPSC/HLC field and establish a physiologically relevant patient-specific in vitro liver model system. Specifically, I aimed at establishing iPSC-hepatocyte like cell (iPSC-HLC) cultures, paired with iPSC-sinusoidal endothelial cells (iPSC-SEC), mirroring the liver cell composition, intercellular interactions and paracrine signaling in a dynamic microenvironment resembling the liver lobules in terms of extracellular matrix and sinusoidal microcirculation.

Relevant courses:

Microscopy network Basel, **Microscopy Course** (32hrs). *University of Basel, Department of Biosystems Science and Engineering (D-BSSE), FMI, Basel, 2014.*

EASL, **Basic School of hepatology – course nr.8: Stem cells & the liver** (13hrs). *College of medicine and veterinary medicine, MRC Centre for regenerative medicine, Edinburgh (UK) 8th-9th February 2013.*

Introduction course in **Laboratory Animal Science (LTK Module 1)** (45 hrs). *Novartis Campus, Basel, October 2012.*

Molecular and Pathological Basis of Disease (90 hrs). *Pharmacenter, Basel University, Basel September – December 2011*

Advanced Biomicroscopy (40 hrs). *Leica Microsystem and FMI, Basel 7th – 11th September 2009*

Languages spoken:

Italian: native speaker

English: good reading, writing and verbal skills

REFERENCES available upon request

I hereby authorize the use of my personal details only on respect of the directive 95/46CE.

Diego Calabrese

----- 

PUBLICATION LIST

Papers in peer-reviewed Journals:

Authors highlighted in bold equally contributed

Campana B, Calabrese D, Matter MS, Terracciano LM, **Wieland SF, Heim MH**: **In vivo analysis at the cellular level reveals similar steatosis induction in both hepatitis C virus genotype 1 and 3 infections.** *J Viral Hepat* 2017.

Van Renne N, Roca Suarez AA, Duong FH, Gondeau C, **Calabrese D**, Fontaine N, Ababsa A, Bandiera S, Croonenborghs T, Pochet N *et al*: **miR-135a-5p-mediated downregulation of protein tyrosine phosphatase receptor delta is a candidate driver of HCV-associated hepatocarcinogenesis.** *Gut* 2017.

Rey S, Quintavalle C, Burmeister K, **Calabrese D**, Schlageter M, Quagliata L, Cathomas G, Diebold J, Molinolo A, Heim MH *et al*: **Liver Damage And Senescence Increases In Patients Developing Hepatocellular Carcinoma.** *Journal of gastroenterology and hepatology* 2017.

Planas-Paz L, Orsini V, Boulter L, Calabrese D, Pikiolek M, Nigsch F, Xie Y, Roma G, Donovan A, Marti P *et al*: **The RSPO-LGR4/5-ZNRF3/RNF43 module controls liver zonation and size.** *Nat Cell Biol* 2016, **18**(5):467-479.

Daster S, Amatruda N, **Calabrese D**, Ivanek R, Turrini E, Droeser RA, Zajac P, Fimognari C, Spagnoli GC, Iezzi G *et al*: **Induction of hypoxia and necrosis in multicellular tumor spheroids is associated with resistance to chemotherapy treatment.** *Oncotarget* 2016.

Andreozzi M, Quintavalle C, Benz D, Quagliata L, Matter M, **Calabrese D**, Tosti N, Ruiz C, Trapani F, Tornillo L *et al*: **HMGA1 Expression in Human Hepatocellular Carcinoma Correlates with Poor Prognosis and Promotes Tumor Growth and Migration in in vitro Models.** *Neoplasia* 2016, **18**(12):724-731.

Mailly L, Xiao F, Lupberger J, Wilson GK, Aubert P, Duong FH, **Calabrese D**, Leboeuf C, Fofana I, Thumann C *et al*: **Clearance of persistent hepatitis C virus infection in humanized mice using a claudin-1-targeting monoclonal antibody.** *Nat Biotechnol* 2015, **33**(5):549-554.

Groppa E, Brkic S, Bovo E, Reginato S, Sacchi V, Di Maggio N, Muraro MG, **Calabrese D**, Heberer M, Gianni-Barrera R *et al*: **VEGF dose regulates vascular stabilization through Semaphorin3A and the Neuropilin-1+ monocyte/TGF-beta1 paracrine axis.** *EMBO Mol Med* 2015, **7**(10):1366-1384.

Wieland S, Makowska Z, Campana B, **Calabrese D**, Dill MT, Chung J, Chisari FV, Heim MH: **Simultaneous detection of hepatitis C virus and interferon stimulated gene expression in infected human liver.** *Hepatology* 2014, **59**(6):2121-2130.

Mele V, Muraro MG, **Calabrese D**, Pfaff D, Amatruda N, Amicarella F, Kvinlaug B, Bocelli-Tyndall C, Martin I, Resink TJ *et al*: **Mesenchymal stromal cells induce epithelial-to-mesenchymal transition in human colorectal cancer cells through the expression of surface-bound TGF-beta.** *Int J Cancer* 2014, **134**(11):2583-2594.

Duong FH, Trincucci G, Boldanova T, Calabrese D, Campana B, Krol I, Durand SC, Heydmann L, Zeisel MB, Baumert TF *et al*: IFN-lambda receptor 1 expression is induced in chronic hepatitis C and correlates with the IFN-lambda3 genotype and with nonresponsiveness to IFN-alpha therapies. *J Exp Med* 2014, 211(5):857-868.

Duong FH, Dill MT, Matter MS, Makowska Z, Calabrese D, Dietsche T, Ketterer S, Terracciano L, Heim MH: **Protein phosphatase 2A promotes hepatocellular carcinogenesis in the diethylnitrosamine mouse model through inhibition of p53. *Carcinogenesis* 2014, 35(1):114-122.**

Dill MT, Makowska Z, Trincucci G, Gruber AJ, Vogt JE, Filipowicz M, Calabrese D, Krol I, Lau DT, Terracciano L *et al*: **Pegylated IFN-alpha regulates hepatic gene expression through transient Jak/STAT activation. *J Clin Invest* 2014, 124(4):1568-1581.**

Bernsmeier C, Calabrese D, Heim MH, Duong HT: **Hepatitis C virus dysregulates glucose homeostasis by a dual mechanism involving induction of PGC1alpha and dephosphorylation of FoxO1. *J Viral Hepat* 2014, 21(1):9-18.**

Postiglione L, Santo LD, Spigna GD, Castaldo C, Guerra G, Ladogana P, Arcucci A, Calabrese D, Covelli B, Vitale S *et al*: **Cardiac remodeling in postischemic end-stage human hearts: Involvement of extracellular matrix and angiogenesis-related molecules. *World Journal of Cardiovascular Diseases* 2013, 03(01):91-99.**

Kratschmar DV, Calabrese D, Walsh J, Lister A, Birk J, Appenzeller-Herzog C, Moulin P, Goldring CE, Odermatt A: **Suppression of the Nrf2-dependent antioxidant response by glucocorticoids and 11beta-HSD1-mediated glucocorticoid activation in hepatic cells. *PLoS One* 2012, 7(5):e36774.**

Sconocchia G, Zlobec I, Lugli A, Calabrese D, Iezzi G, Karamitopoulou E, Patsouris ES, Peros G, Horcic M, Tornillo L *et al*: **Tumor infiltration by FcgammaRIII (CD16)+ myeloid cells is associated with improved survival in patients with colorectal carcinoma. *Int J Cancer* 2011, 128(11):2663-2672.**

Book chapters:

Calabrese D, Wieland SF: **Highly Sensitive Detection of HBV RNA in Liver Tissue by In Situ Hybridization. *Methods Mol Biol* 2017, 1540:119-134.**

Participation at conferences and symposia:

Speaker at:

Annual Meeting of the Swiss Society of Gastroenterology (SGG-SSG), the Swiss Society of Visceral Surgery (SGVC-SSCV), the Swiss Association for the Study of the Liver (SASL) and the Swiss Society of Endoscopy Nurses and Associates (SVEP-ASPE)

“Autologous differentiation of liver derived iPSC into hepatocyte-like cells”
Lausanne, September 14th – 15th 2017

16th Surgical and Gastrointestinal Research Retreat

“Autologous differentiation of liver derived iPSC into hepatocyte-like cells”

Stoos / Switzerland, January 13th – 15th, 2017

14th Surgical and Gastrointestinal Research Retreat

“Induced pluripotent stem cells: a step forward towards personalized medicine? Application in the hepatology field”

January 9th – 11th, 2015, Vulpera Switzerland

Invited speaker at:

Swiss Centre for Applied Human Toxicology (SCAHT) Research Retreat 2016

“Molecular analysis of phenprocoumon induced liver disease”

Hotel l’Aubier, Les Murailles 5, 2037 Montezillon, December 2nd, 2016

Annual meeting of Swiss Association of Veterinary Pathologist (S.V.T.P.).

“Contribution of laser capture microdissection to molecular histology”

F. Hoffmann-La Roche Ltd, Basel, July 5th 2013

Novartis Institute for Biomedical Research (NIBR), Preclinical Safety Townhall.

“Towards a translational molecular map of the liver”

NIBR, Basel, December 2011